Survival and recovery of *Escherichia coli* O157:H7 during starvation at sub-optimal temperatures

A thesis

submitted in fulfilment

of the requirements for the degree

of

Doctor of Philosophy in Biological Sciences

at

The University of Waikato

by

Ron Neo Xavier

THE UNIVERSITY OF
WAIKATO
Te Whare Wānanga o Waikato

2014

Abstract

Escherichia coli O157:H7 is an important foodborne pathogen with a dual lifestyle of growth within a host and persistence in non-host environments. Environmental survival of *E. coli* O157:H7 is particularly important in New Zealand due to the increasing trend in notified clinical cases, with most being associated with rural environments rather than contaminated regulated foods. Starvation and a decrease in temperature are characteristic of the conditions encountered by bacteria during transition from a reservoir host, normally a ruminant, to the environment; cf. feast to famine. These conditions are known to induce bacterial entrance into the viable but non-culturable (VBNC) state where cell viability can only be detected using culture-independent methods with the number of colonies recovered decreasing over the duration of the starvation period. Findings from this study showed that formation of a VBNC sub-population can be induced by starving *E. coli* O157:H7 at sub-optimal temperatures.

Five *E. coli* O157:H7 strains were used in this study; NCTC12900 as a reference strain, three New Zealand clinical isolates and a New Zealand bovine isolate. Cells were starved in phosphate buffered saline for 84 days at sub-optimal temperatures. Cell viability was determined using the SYTO 9-PI staining system coupled with a haemocytometer counting method developed in this study. Cell culturability was assessed using the nutrient-rich tryptic soy agar (TSA), nutrient-limited plate count agar (PCA), and PCA with additional supplements. The distribution of colony size provided information on the population dynamics of starved cells and their ability to recover on agar. The role of quorum sensing (LuxS/autoinducer-2) on starved cell recovery was investigated by supplementing PCA with quorum sensing molecules and using a mutant strain deficient in *luxS*, a gene encoding the synthase of autoinducer-2. The ability of starved and non-starved cells to metabolise single carbon sources were compared using the Biolog MicroPlates™.

When held at 4°C, a three- to six-log reduction in culturability on PCA was observed after 84 days of starvation. The reduction in culturability observed for

cells starved at 15°C was between one to two logs on PCA. Despite the decline in culturability on PCA, the number of viable cells as determine by LIVE/DEAD® *Bac*Light™ staining remained within one log of the initial viable count. Supplementation of PCA with 0.2% sodium pyruvate resulted in a significant increase in the number of colonies recovered from 4°C-starved cultures for all *E. coli* O157:H7 strains tested. Recovery on TSA was consistently at least two-logs higher than recovery on PCA for *E. coli* O157:H7 cells after 84 days of starvation at 4°C. The distribution of colony diameter was markedly wider for 4°C-starved cells compared to non-starved cells when recovered under aerobic conditions. In addition to the strain variation observed, culturability of starved *E. coli* O157:H7 was found to be dependent on the starvation temperature, the nutrient level of recovery media, and the presence of specific resuscitation factors such as pyruvate. While the culturability phenotype was similar between reference, clinical and bovine *E. coli* O157:H7 strains, metabolic profiles determined using carbon source MicroPlates™ differed. Analysis of the carbon utilisation kinetics allowed comparison of carbon metabolism between exponential phase, stationary phase and starved *E. coli* O157:H7. The duration of lag in substrate utilisation was significantly different between starved and non-starved cells. Supplementing PCA with quorum sensing molecules and using a mutant strain deficient in *luxS*, a gene encoding the synthase of autoinducer-2, did not result in a significant improvement in the recovery of starved VBNC cells.

Based on current knowledge, models for the change in *E. coli* O157:H7 population dynamics during its lifecycle, the role of pyruvate resuscitation of VBNC cells, and factors involved in *E. coli* O157:H7 infection of bovine and human hosts were proposed. The ability of New Zealand clinical and bovine isolates to enter the VBNC state, which was demonstrated in this study, highlighted the potential for culture-based assessment methods to underestimate the number of viable *E. coli* O157:H7. While reports of the use of pyruvate for resuscitating VBNC cells are in the literature, this study is the first to propose a mechanism of pyruvate resuscitation. By understanding the physiology of VBNC cells and mechanism of their resuscitation, it may be possible to eliminate the potential for underestimation of viable *E. coli* O157:H7 in the environment and in food by tailoring culture methods to promote their growth.

Acknowledgement

This work is dedicated to Yu-Chin (Steffi) Mao, whose faith in me inspired me to aim higher, push harder and, most importantly, not give up.

A very special thank you to Dr Helen Withers, who mentored me in academia and in life for the past eight year; and through laughs and tears taught me what it means to be a scientist and helped me find my future path.

I would like to thank Professor Hugh Morgan and Associate Professor Ian McDonald for their continual support and their contribution along the way.

To Shelly Ulrich, Adam Stuart and Tanushree Gupta, thank you for being there for me over the past years. Knowing you are there to catch me when I fall gives me great strength and encouragement to carry on and get things done.

I would also like to thank the past and present members of the Food Assurance and Meat Quality team for their help and input in this project.

Finally, I would like to acknowledge the Ministry of Business, Innovation and Employment for funding the project, University of Waikato Doctoral Scholarship for funding of the three-year stipend, and AgResearch for funding a six-month stipend. Travel costs for conference attendance and presentation that contributed to this work were funded by AgResearch, the University of Waikato Thesis in 3 Competitions, the University of Waikato School of Biological Sciences Special Purpose Fund, and the American Society for Microbiology.

Table of contents

Abstract **2**

Acknowledgement **4**

Table of contents **5**

Chapter 1 Introduction **8**

1.1 *Escherichia coli* 8

1.1.1 Enterohaemorrhagic *E. coli* (EHEC) and Shiga-toxin producing *E. coli* (STEC) 9

1.2 Quorum sensing in Gram-negative bacteria 16

1.2.1 *N*-acyl-homoserine lactone (AHL) 17

1.2.2 Autoinducer-2 (AI-2) 22

1.2.3 Quorum sensing in *E. coli* 27

1.3 Viable but non-culturable (VBNC) state 29

1.3.1 Induction, detection and resuscitation of VBNC cells 34

1.3.2 VBNC state as a survival strategy 35

1.3.3 VBNC state in *E. coil* 37

1.4 *E. coli* central metabolism 39

1.4.1 Regulation of central metabolism by the phosphoenolpyruvate: phosphotransferase system (PEP:PTS) 39

1.4.2 PEP-pyruvate-oxaloacetate (PPO) node 43

1.5 *E. coli* stress response 45

1.5.1 RpoS-mediated stress response 46

1.5.2 Regulation of *E. coli* response to nutrient starvation 49

1.6 Aims and hypothesis 50

Chapter 2 Material and methods **51**

2.1 Bacterial strains and plasmids 51

2.2 Media and chemical solutions 51

2.2.1 Media 51
2.2.2 Chemicals 54
2.3 Bacterial starvation in phosphate buffered saline 55
2.3.1 Culture preparation 55
2.3.2 Starvation conditions 56
2.3.3 Sampling 56
2.4 Determination of cell viability 56
2.5 Determination of culturability on solid media 59
2.5.1 Colony diameter measurement 59
2.6 Growth analysis of culturability in broth 60
2.7 Phenotype microarray 60
2.7.1 Inoculum preparation 60
2.7.2 Plate preparation and incubation conditions 60
2.7.3 Measurements from kinetic curve 61
2.7.4 Statistical analyses 64
2.8 Preparation of autoinducer-2 (AI-2)-containing conditioned media (CM) and CM agar 64
2.8.1 Preparation of conditioned media 64
2.8.2 *Vibrio harveyi* bioluminescence assay (VHBA) 65
2.8.3 Preparation of conditioned media (CM) agar 65
Chapter 3 Phenotypic analysis of starved cells 66
3.1 Introduction 66
3.2 Results 66
3.2.1 Detection of viability and phenotypic changes 67
3.2.2 Viability and culturability of starved *E. coli* K-12 and O157:H7 72
3.2.3 Viability and culturability of New Zealand clinical and bovine isolates 93
3.3 Discussion 107
Chapter 4 Metabolic analysis of starved *E. coli* O157:H7 113

4.1 Introduction 113

4.2 Results 114

4.2.1 Sole substrate use profiles for NCTC12900 114

4.2.2 Substrate utilisation by clinical and bovine isolates of *E. coli* O157:H7 130

4.3 Discussion 155

Chapter 5 Involvement of LuxS during starvation and recovery 160

5.1 Introduction 160

5.2 Results 161

5.2.1 Viability and colony recovery of starved NCTC12900 *luxS*$^{-}$ compared with the parental NCTC12900 161

5.2.2 Growth comparison between NCTC12900 and NCTC12900 *luxS*$^{-}$ during broth recovery 169

5.2.3 Comparison of metabolic activities between NCTC12900 and NCTC12900 *luxS*$^{-}$ mutant during recovery after starvation 171

5.3 Discussion 187

Chapter 6 Discussion 191

Chapter 7 Conclusion 204

Chapter 8 References 207

Appendices 229

Chapter 1 Introduction

1.1 *Escherichia coli*

Escherichia coli is a non-sporulating Gram-negative facultative anaerobe belonging to the Enterobacteriaceae family (Williams *et al.*, 2010). It is found in the avian (Amit-Romach *et al.*, 2004; Gordon & Cowling, 2003), reptilian (Gordon & Cowling, 2003), and mammalian gut microbiota (Arumugam *et al.*, 2011; Gordon & Cowling, 2003). In humans, *E. coli* is among the first facultative anaerobes to colonise the infant intestine after birth (Mackie *et al.*, 1999). The source of the colonising bacteria is either from the maternal faecal flora or the birthing environment (Penders *et al.*, 2006). *E. coli* along with other commensal bacteria that colonise the human gut have a metabolic function within the host of fermenting non-digestible carbohydrates, resulting in the production of short-chain fatty acids that stimulate the proliferation and differentiation of epithelial cells in the intestinal tract (Guarner & Malagelada, 2003). In addition, establishment of appropriate commensal bacteria exposes the immature infant immune system to bacterial antigens that may induce immunological tolerance and promote the development of both innate and adaptive immunity (Kelly *et al.*, 2007; Sears, 2005).

Although virulence traits are generally absent in commensal strains of *E. coli*, they have the potential to cause infections in immune compromised hosts upon disruption of the gastrointestinal barrier, or cross-contamination to extraintestinal locales (Russo & Johnson, 2003). In addition to the commensal strains, there are strains of *E. coli* with specific virulence factors capable of establishing infection that result in one of three clinical syndromes: urinary tract infections, sepsis or meningitis, and enteric or diarrhoeal diseases (Kaper *et al.*, 2004). Extraintestinal pathogenic *E. coli* (ExPEC) do not generally cause gastroenteritis, but can cause infections of the urinary tract, abdomen, pelvis and surgical sites as well as pneumonia, bacteraemia and sepsis (Russo & Johnson, 2003). Diarrheagenic *E. coli* (DEC) are responsible for gastrointestinal infections (Kaper *et al.*, 2004). There are six recognised broad categories of DEC based on their pathotypes: diffusely adherent *E. coli* (DAEC), enteroinvasive *E. coli* (EIEC), enterotoxigenic *E. coli* (ETEC), enteroaggregative *E. coli* (EAEC), enteropathogenic *E. coli* (EPEC), and enterohaemorrhagic *E. coli* (EHEC) (Nataro & Kaper, 1998). In

addition, a new pathotype, enteroaggregative haemorrhagic *E. coli* (EAHEC) had recently been described (Brzuszkiewicz *et al.*, 2011).

Clonal groups of *E. coli* can be characterised by their serotype; based on the combination of O (somatic) and H (flagellar) surface antigen profiles (Kaper *et al.*, 2004; Orskov *et al.*, 1977). Adhesins are expressed to allow the initial attachment of DEC onto the enterocytes and the colonisation of intestinal mucosa (Kaper *et al.*, 2004). Although the ability to colonise intestinal mucosa is highly conserved among DEC pathotypes, genetic variability is reflected by the variety of post-colonisation pathogenic strategies (Kaper *et al.*, 2004). Once established on the intestinal mucosa, enterotoxins may be produced, as in the case of ETEC and EAEC infection; invasion of enterocytes may occur, such as during EIEC infections; and intimate adherence may be initiated, for example, the formation of attaching and effacing (A/E) lesions formed by EPEC and EHEC during infection (Nataro & Kaper, 1998). Virulence genes of DEC are carried predominately on plasmids and pathogenicity islands within the chromosome (Nataro & Kaper, 1998). Clinical manifestations of DEC infections range from asymptomatic carriage to severe systemic involvement, such as haemolytic uraemic syndrome (HUS) associated with the O157:H7 serotype of EHEC (Pennington, 2010).

1.1.1 Enterohaemorrhagic *E. coli* (EHEC) and Shiga-toxin producing *E. coli* (STEC)

Enterohaemorrhagic *E. coli* (EHEC) was first recognised as a human pathogen in 1982 following sporadic cases of severe haemolytic colitis in the United States linked to the consumption of undercooked beef patties (Centers for Disease Control, 1982; Riley *et al.*, 1983b). *E. coli* O157:H7 was isolated from 9 of the 12 stool samples of patients in the outbreak in Oregon and Michigan in 1982 (Riley *et al.*, 1983a). Shiga toxin, produced by *E. coli* O157:H7, was also detected from the stool samples of the outbreak patients who had developed HUS (Karmali *et al.*, 1983; O'Brien *et al.*, 1983). By 2010, over 380 different STEC serotypes had been isolated from patients with gastrointestinal illness, with *E. coli* O157:H7 being the major serotype with the most frequent association with severe disease (Karmali *et al.*, 2010). Although the incidence of STEC infection in New Zealand is relatively low compared to other foodborne and water-borne pathogens, the number of notified cases has increased from below 20 in 1997 to 147 cases in

2012 with *E. coli* O157:H7 accounting for 83.8% of the reported cases (The Institute of Environmental Science and Research Ltd., 2013).

In humans, *E. coli* O157:H7 can cause a wide spectrum of illnesses ranging from non-specific diarrhoea and haemorrhagic colitis (HC), to potentially life-threatening haemolytic uraemic syndrome (HUS) (Griffin & Tauxe, 1991; Karmali, 1989). The infectious dose has been estimated to be below 24 colony forming units (cfu) (Strachan *et al.*, 2001). In most cases of diagnosed *E. coli* O157:H7 infections, non-specific diarrhoea progresses to haemorrhagic colitis and, with supportive treatment, most patients recover fully (Karmali *et al.*, 2010). Approximately 10 to 15% of diagnosed patients, most commonly children under the age of five, develop HUS, which is defined by the triad of features: acute renal failure, thrombocytopenia, and microangiopathic haemolytic anaemia (Scheiring *et al.*, 2008; Tarr *et al.*, 2005). While most patients with HUS recover from the acute episode, approximately 30% suffer a range of long-term sequelae including renal abnormalities, neurological deficits, and hypertension (Scheiring *et al.*, 2008; Tarr *et al.*, 2005).

E. coli O157:H7 is able to survive passage through the acidic conditions of the stomach and colonise the gastrointestinal epithelium (Benjamin & Datta, 1995). The formation of attaching and effacing (A/E) lesions is characteristic of EHEC colonisation in the colon (Schmidt, 2010). Initial attachment of the bacteria onto the surface of enterocytes is facilitated by the interaction of long polar fimbriae, Lpf1 and Lpf2, with the extracellular matrix proteins on the surface of eukaryotic epithelial cells (Farfan & Torres, 2012). Effector proteins, including Tir, are injected from the bacterium into the host cell via the type III secretion system (Kenny *et al.*, 1997). Upon phosphorylation, Tir inserts into the eukaryotic membrane where it interacts with intimin, an *E. coli* membrane protein encoded by *eaeA* (Tree *et al.*, 2009). The intimin-Tir complex promotes additional Tir insertion and further interaction with intimin resulting in the intimate attachment of EHEC onto host cells (Farfan & Torres, 2012). Tir is also involved in the modulation of eukaryotic actin cytoskeleton assembly which results in the formation of A/E lesions (Campellone, 2010). The bacterial genes required for the formation of A/E lesions are mainly encoded in the locus of enterocyte effacement

(LEE), including genes encoding the structural components of TTSS, *tir* and *eaeA* (Nataro & Kaper, 1998).

The production of Shiga toxins (Stx) by EHEC strains is key to the pathogenesis of HC and HUS (Ethelberg *et al.*, 2004). Stx is an AB_5 toxin. The B pentamer attaches to the glycolipid globotriaosylceramide (Gb3) receptors expressed on renal glomerular endothelial, mesangial and tubular epithelial cells, and delivers the A subunit to the cytoplasm where it inhibits protein synthesis which leads to cytokine release and apoptosis of the host cell (O'Brien *et al.*, 1992). There are two forms of Stx, Stx1 and Stx2, which are produced and share approximately 60% amino acid similarity, but are not immunologically cross-reactive (Fuller *et al.*, 2011; O'Brien & Holmes, 1987). An EHEC strain may produce one or more types of Stx and the type of Stx produced by the strain is related to its degree of pathogenicity (Kawano *et al.*, 2008). In addition to differences in amino acid sequences, the potency of Stx2 was found to be 100 times higher than Stx1 in mouse models (Tesh *et al.*, 1993). Of the subtypes of Stx2, Stx2a and Stx2d were the more potent to human renal proximal tubule epithelial cells. Stx2a, Stx2c and Stx2d are often associated with the more severe clinical outcomes, including HC and HUS (Boerlin *et al.*, 1999; Fuller *et al.*, 2011; Kawano *et al.*, 2008; Orth *et al.*, 2007).

Vero toxin (VT), isolated from the stools of children presenting with sporadic cases of post-diarrhoeal HUS in 1983 (Karmali *et al.*, 1983), was found to be structurally and antigenically similar to the Shiga toxin (Stx) produced by *Shigella dysenteriae* serotype 1, and was referred to as Shiga-like toxins (SLT) (O'Brien *et al.*, 1983). Since then, VT and SLT had become synonyms of Stx, and Shiga toxin-producing *E. coli* (STEC) or VT-producing *E. coli* (VTEC) are commonly used to classify *E. coli* strains capable of producing Stx, while EHEC is used to describe a subset of strains associated with human disease, with serotype O157:H7 being the most common EHEC serotype (Meng *et al.*, 2007).

In 2011, a new variant of EHEC, serotype O104:H4, was found to be responsible for 3816 cases of infection in Germany, where 845 (22%) patients developed HUS, resulting in 54 deaths (Frank *et al.*, 2011). This serotype lacked the typical STEC virulence factors *eae* and *ehx*, and is believed to have acquired *stx2a* by

horizontal gene exchange (Bezuidt *et al.*, 2011; Frank *et al.*, 2011). Analysis of two strains isolated from patients revealed a combination of EHEC and EAEC characteristics, and a new pathotype, EAHEC, was proposed (Brzuszkiewicz *et al.*, 2011).

Outbreaks and sporadic cases of *E. coli* O157:H7 have been attributed to both foodborne and environmental sources. Contaminated meat products are the predominant vehicle for foodborne *E. coli* O157:H7 infections (Rangel *et al.*, 2005). Other food sources such as dairy products (Morgan *et al.*, 1993; Rey *et al.*, 2006) and salad greens (Erickson & Doyle, 2007; Ferguson *et al.*, 2005) are also vectors for *E. coli* O157:H7 transmission. Although contaminated food products remained the major source of *E. coli* O157:H7 infections in the US, UK and Argentina (Etcheverría & Padola, 2013; Gormley *et al.*, 2011; Rangel *et al.*, 2005), environmental transmissions via municipal drinking water (Licence *et al.*, 2001), recreation water (Paunio *et al.*, 1999), farm visits (Strachan *et al.*, 2001) and petting zoos (Control, 2009) are increasingly recognised as important sources particularly in Scotland (Strachan *et al.*, 2006) and New Zealand (Institute of Environmental Science and Research Limited, 2004).

Cattle are major reservoirs of *E. coli* O157:H7 and exposure to faecal matter in farm environments, contact with animals or cross-contamination of food products with faeces or agricultural runoff all contribute to the dissemination of the bacteria (Chase-Topping *et al.*, 2008). The site of *E. coli* O157:H7 colonisation within bovine hosts is the lymphoid follicle-dense mucosa of the terminal rectum (Naylor *et al.*, 2003). Transmission of *E. coli* O157:H7 is facilitated by shedding from ruminant reservoirs, environmental persistence external to the host, and finally survival through the gastrointestinal tract of the host (Russell & Jarvis, 2001).

E. coli O157:H7 has been detected in a range of environmental settings such as soil, water, plant matter and even farm equipment, where it may encounter competition from other organisms, varying organic matter content, extreme pH, desiccation, and/or fluctuating temperature (Money *et al.*, 2010) (Figure 1-1). *E. coli* O157 has been found to survive in soil for up to 105 days (Ogden *et al.*, 2002), up to 7 days on spinach shoots (Patel *et al.*, 2010), up to 28 days on wood (Williams *et al.*, 2005), up to 9 days on cattle hides (Arthur *et al.*, 2011), and up to

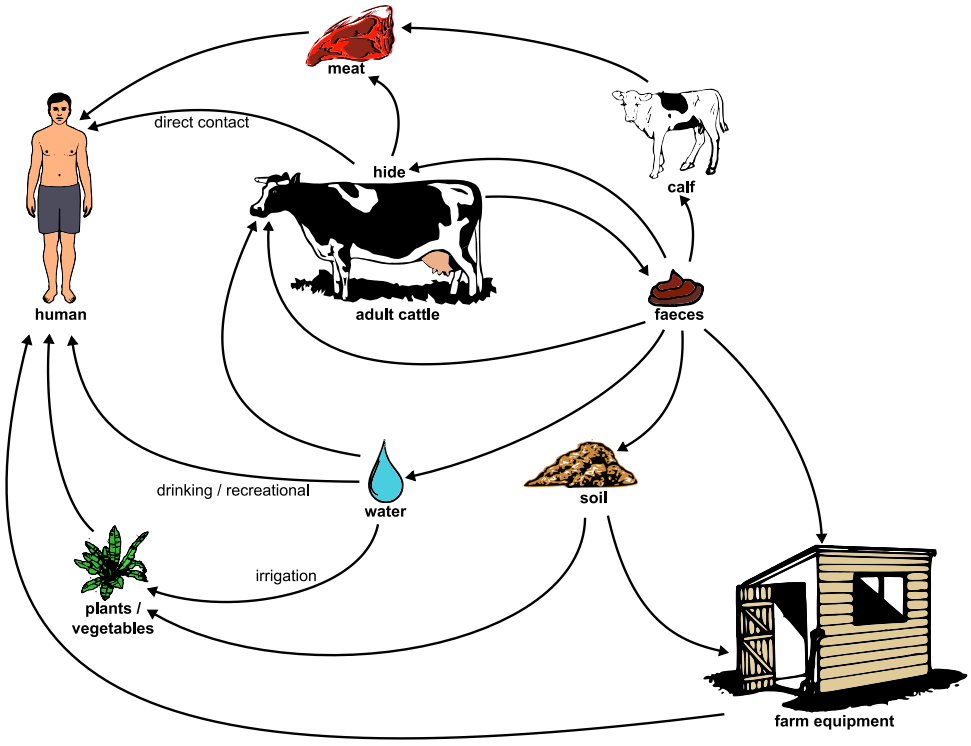

Figure 1-1 Schematic representation of the transmission routes of *E. coli* O157:H7 from cattle to human.

245 days in water troughs (LeJeune *et al.*, 2001). In addition, persistent subtypes of *E. coli* O157:H7 in faecal samples from feedlot cattle have been found on commercial feedlot pens where rapid turnover of large cattle populations had occurred over a six-month period (LeJeune *et al.*, 2004).

In 2002, an outbreak involving 20 scouts in the United Kingdom was found to be associated with environmental contact with contaminated pasture (Ogden *et al.*, 2002). An area that was not exposed to water run-off or sheep faeces was fenced off to investigate the duration of *E. coli* O157 persistence in soil. Soil samples were tested using culture-based methods involving enrichment in selective medium, immunomagnetic separation (IMS), and plating on selective media. *E. coli* O157 was isolated from soil samples for 105 days.

Patel *et al.* (2010) tested the ability of *E. coli* O157:H7 to survive on spinach leaves in a growth chamber. Four-week old spinach plants were inoculated using *E. coli* O157:H7 mixed with sterile manure extracts. Survival was assessed by enumeration using the most probable number (MPN) method in selective media. Of the five *E. coli* O157:H7 strains tested, two were detected on spinach leaves after seven days.

Williams *et al.* (2005) tested *E. coli* O157:H7 survival on wood and metal surfaces under different temperature and moisture conditions. Surfaces were inoculated with cattle faeces spiked with *E. coli* O157:H7. Survival was assessed by plating on selective media. At least two logs of *E. coli* O157:H7 were recovered after 28 days on wooden surfaces kept at 20 and 5°C.

Arthur *et al.* (2011) segregated 36 cattle carrying *E. coli* O157:H7 on their hides in holding pens and recontamination was minimised by regular cleaning of the holding environment. *E. coli* O157:H7 was detected from sponge samples of cattle hides for up to 9 days using a combination of IMS, enrichment and plating methods.

LeJeune *et al.* (2001) used continuous-flow chambers to study the survival of *E. coli* O157 in water trough sediment. Feedlot water trough sediment inoculated with the bovine *E. coli* O157 isolate was transferred to the chambers which was

filled with either chlorinated or unchlorinated water. *E. coli* O157 in sediment samples was detected by plating onto selective media. Culturable *E. coli* O157 was detected in sediments for up to 183 days in chlorinated microcosms and up to 245 days in unchlorinated microcosms.

The human 'gastric bactericidal barrier' against enteric pathogens is dependent on the pH of gastric acid in the stomach which is comprised of hydrochloric acid at pH below 2.5 (Lin *et al.*, 1996). Once in the intestine, the pH rises to between 4.5 and 7 with increased presence of weak organic acids (Lin *et al.*, 1996). In ruminants, the pH of the reticulorumen, abomasum, small intestine and colon varies depending on the diet (Wheeler & Noller, 1977). In a study by Wheeler and Noller (1977), the pH of the gastrointestinal tract of cattle and sheep fed on a range of corn-based diets were measured. The abomasum was the most acidic environment within the bovine and ovine gut with pH ranging from 2.27 to 4.16 in cattle and 2.74 to 2.94 in sheep. The pH of the reticulorumen, small intestine and colon ranged from 5.38 to 6.58, 5.75 to 6.78 and 5.65 to 6.80, respectively.

E. coli O157:H7 can survive acid challenge at pH 2.5 for at least 2 hours in Luria-Bertani (LB) broth (Lin *et al.*, 1996). An estimated 20 to 80% of ingested *E. coli* O157 survived the acidic environment in a human gastric model (Takumi *et al.*, 2000). While the pH of gastric acids produced by a mammalian stomach can be as low as 0.9, the actual pH in the stomach can be as high as 6.0, depending on the amount and type of food ingested (Russell & Jarvis, 2001). In addition, *E. coli* O157:H7 pre-exposed to sub-lethal pH, such as lactic acid treatment at pH 3.48, can be acid-adapted resulting in enhanced survival in acidic foods, such as salami (pH 5.0) and apple cider (pH 3.4) (Leyer *et al.*, 1995).

Three acid resistance (AR) systems have been described in *E. coli* (Foster, 2004). Acid resistance system 1 (AR1) requires both RpoS (σ^S) and cAMP receptor protein (CRP). *E. coli* mutants lacking σ^S, a stress response global regulator activated upon the onset of stationary phase, showed significantly higher sensitivity to acid challenge at pH 2.5 (Small *et al.*, 1994). The addition of glucose during stationary phase resulted in the repression of CRP as well as AR1 (Castanie-Cornet *et al.*, 1999). The acid resistance systems 2 and 3 (AR2 and AR3) are dependent on the intracellular conversion of glutamate and arginine to γ-

amino butyric acid and agmatine, respectively (Foster, 2004). These reactions replace the α-carboxyl groups of glutamine and arginine with a proton through the action of decarboxylases (Foster, 2004). AR2 was found to be the most effective in protecting *E. coli* O157:H7 against acid challenge at pH 2.5 for two and six hours as well as weak acid challenge with volatile fatty acids (VFAs) and benzoic acid (Lin *et al.*, 1996). In addition, after acid challenged cells had been stored at 4°C in pH neutral media for 28 days, the acid resistance mechanisms, particularly AR2 and AR3, remained active during subsequent acid challenges where cells were able to survive up to two hours at pH 2.0 (Lin *et al.*, 1996). Since the infectious dose of *E. coli* O157:H7 was estimated to be below 24 (Strachan *et al.*, 2001), the acid resistance mechanisms are important virulence traits that contribute to its survival in the mammalian stomach.

1.2 Quorum sensing in Gram-negative bacteria

Bacterial behaviour is influenced by both physical and biological factors. In complex microbial communities where multiple species are present, appropriate population-wide responses to changes in the environment and to the presence of other microbes can be competitively advantageous and may be crucial for survival (Atkinson & Williams, 2009). A range of chemically distinct signalling molecules have been found to facilitate intra- and inter-species communication for prokaryotes. These were first found to regulate competence in *Streptococcus pneumoniae* (Tomasz, 1965) and contribute to the maintenance of bacteria-host symbiosis between *Vibrio fischeri* and *Euprymnascolopes*, a marine squid (Nealson *et al.*, 1970). The term "quorum sensing" (QS) was proposed (Fuqua *et al.*, 1994) to describe the phenomena of density-dependent coordinated population responses mediated by signalling molecules. Since then, three major classes of QS signals, or autoinducers have been described (West *et al.*, 2012). These are peptide autoinducers used by Gram-positive bacteria, *N*-acyl-L-homoserine lactones (AHLs) used by Gram-negative bacteria, and 3-(2H)-furanones also known as autoinducer-2 (AI-2) used by both Gram-positive and Gram-negative bacteria (Tarighi & Taheri, 2011).

Fully functional QS systems require the presence of a signal synthase and a signal receptor (Turovskiy *et al.*, 2007). Depending on the size and composition, QS

signals may either diffuse or be actively transported across the cell membrane to the extracellular environment (Boyer & Wisniewski-Dyé, 2009). QS signals are constitutively produced at low levels and as the population of signal producing bacteria expands, the extracellular QS signal accumulates proportionally (Bassler & Losick, 2006). Once a threshold is reached, transcriptional regulators are activated within the cells eliciting a population-wide response in gene expression (Bassler & Losick, 2006). Bacteria with QS capabilities are thus able to regulate gene expression according to the population density. Competence, bioluminescence, sporulation, biofilm formation, antimicrobial production and virulence factor production have been found to be regulated by QS systems in both Gram-positive and Gram-negative bacteria (Bassler & Losick, 2006; Schauder & Bassler, 2001; Turovskiy *et al.*, 2007).

1.2.1 *N*-acyl-homoserine lactone (AHL)

The AHL quorum sensing system, first described in *V. fischeri* (Nealson *et al.*, 1970) for the regulation of the luciferase operon, is composed of LuxI and LuxR, the AHL synthase and receptor, respectively (Engebrecht & Silverman, 1984; Turovskiy *et al.*, 2007). All AHLs share a common homoserine lactone (HSL) ring, and an acyl chain varying in the degree of saturation and length of the carbon chain (R^2, Figure 1-2a) with either -O, -H or -OH on the third carbon of the chain (R^1, Figure 1-2a) (Tarighi & Taheri, 2011). Acyl chains range from four to 18 carbons in length with the majority having an even number of carbon atoms in the chain (Whitehead *et al.*, 2001; Williams *et al.*, 2007).

LuxI catalyses the synthesis of AHL through the formation of the amide bond between *S*-adenosylmethionine (SAM), the donor of the conserved homoserine lactone ring, and the acyl side chain of a specific acyl carrier protein (ACP) (Figure 1-2a and b) (Hanzelka & Greenberg, 1996; Moré *et al.*, 1996; Parsek *et al.*, 1999; Val & Cronan Jr, 1998). SAM is regenerated by the cells via the activated methyl cycle (AMC) (Figure 1-2b). Over 100 AHL synthases of the LuxI family have been documented in genomic databases (Atkinson & Williams, 2009). Mutational analysis of *V. fischeri* LuxI revealed that the N-terminal is highly conserved while the C-terminal is more variable (Hanzelka *et al.*, 1997). It

has been hypothesized that recognition of variable acyl chains carried by specific ACP is via interaction with the C-terminal (Hanzelka *et al.*, 1997). Many of the

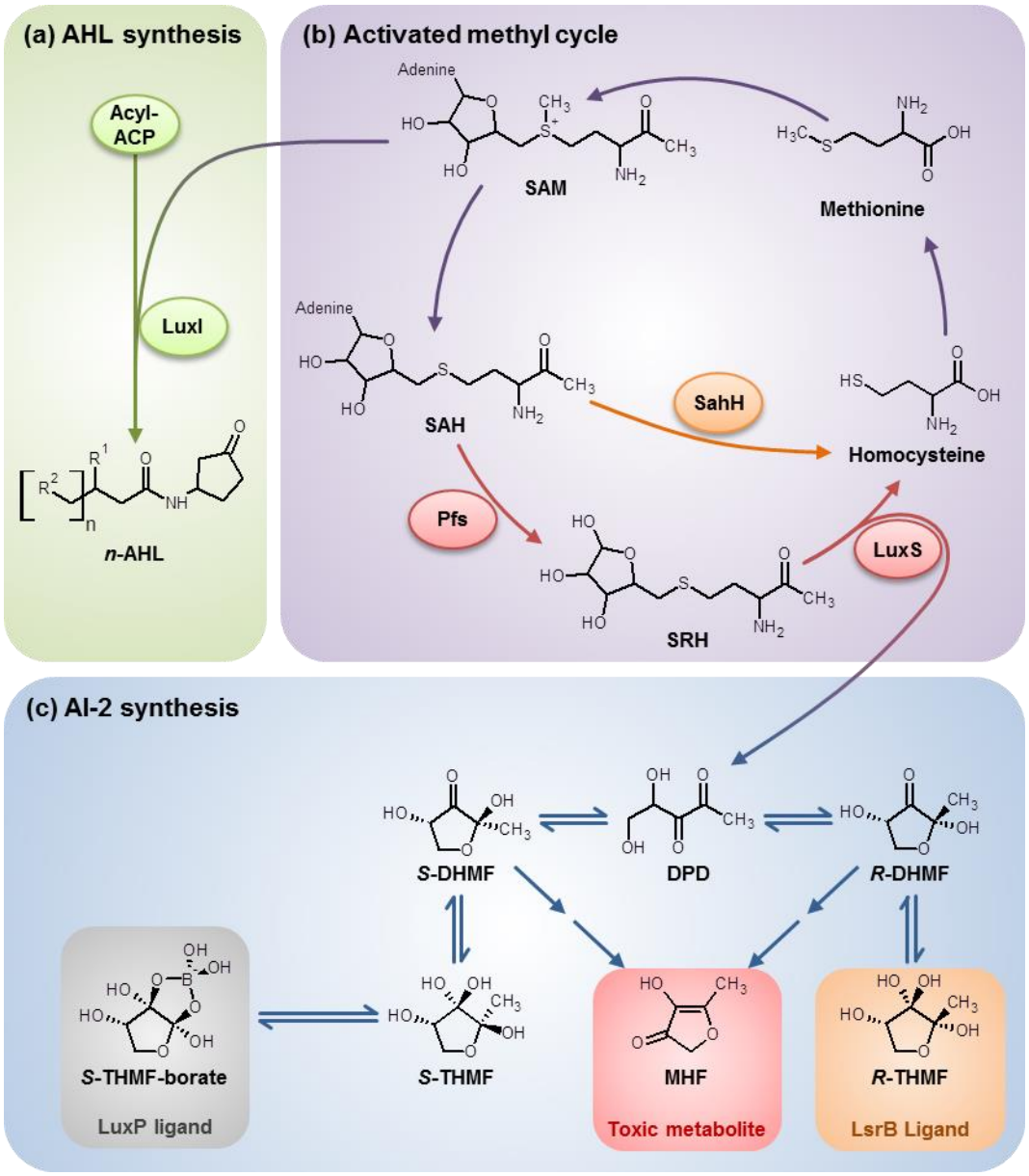

Figure 1-2 Synthesis of *N*-acyl-L-homoserine lactone (AHL) and autoinducer-2 (AI-2) via the activated methyl cycle. (a) AHL synthesis from *S*-adenosylmethionine (SAM) of the (b) activated methyl cycle, which is also involved in (c) AI-2 synthesis. Conversion of *S*-adenosylhomocysteine (SAH) to homocysteine is either completed via a one-step reaction using SahH (orange arrow), or a two stage reaction using Pfs and LuxS (red arrows). Key enzymes are shown in ovals. *n*, number of carbon in the acyl chain; R^1, either -O, -H or -OH; R^2, acyl side chain; SRH, *S*-ribosyl-homocysteine; DPD, 4,5-dihydroxy-2,3-pentanedione; DHMF, 2,4-dihydroxy-2-methyldihydro-3-furanone; *R*-THMF, (*2R,4S*)-2-methyl-2,3,3,4-tetrahydroxytetrahyrofuran; *S*-THMF, (*2S,4S*)-THMF. Modified from Vendeville *et al.* (2005).

LuxI homologues are able to produce AHLs with different chain sizes by accepting ACP with different chain lengths (Parsek *et al.*, 1999; Schaefer *et al.*, 1996). However, sequence comparison did not reveal any correlation between the sequence of LuxI homologues and the type of AHL synthesised (Eberl, 1999). While short-chain AHLs are able to diffuse across bacterial membranes, active transport is required for long-chain AHLs (Pearson *et al.*, 1999). The N-terminal of AHL receptors, LuxR, bind to their cognate AHLs while the C-terminal bind to *lux* boxes located up-stream of QS-regulated genes resulting in a population-density dependent response (Egland & Greenberg, 2000; Stevens *et al.*, 1999).

Quorum sensing in *Pseudomonas aeruginosa* is a well-studied system where population-density regulates virulence and persistence via multiple signalling networks including two AHL-dependent QS systems, Las and Rhl, for the hierarchical expression of virulence factors (Figure 1-3) (Schauder & Bassler, 2001). *N*-3-oxododecanoyl homoserine lactone (3-oxo-C12-HSL) and *N*-butanoyl homoserine lactone (C4-HSL) are produced by LuxI homologues, LasI and RhlI, respectively (Whitehead *et al.*, 2001). The signals are recognised by their cognate LuxR homologue receptors, LasR and RhlR. The concentration of 3-oxo-C12-HSL increases as the population expands. Once a threshold of 3-oxo-C12-HSL is reached, the signal receptor, LasR, is activated. The LasR/3-oxo-C12-HSL complex increases 3-oxo-C12-HSL production by up-regulating LasI expression and activating the expression of exofactors (Figure 1-3 pink box). LasR/3-oxo-C12-HSL complex also activates the RhlR/RhlI system by inducing the production of RhlR (Figure 1-3). C4-HSL is synthesised by RhlI and binds to RhlR, the RhlR/C4-HSL complex induces the production of C4-HSL and the expression of a second set of virulence factors (Figure 1-3 light blue box) (Whitehead *et al.*, 2001). It is hypothesised that cell density dependent temporal regulation mediated by the LasR/LasI and RhlR/RhlI systems allows sequential control of the expression of different virulence factors to cause maximum impact on the host (Schauder & Bassler, 2001).

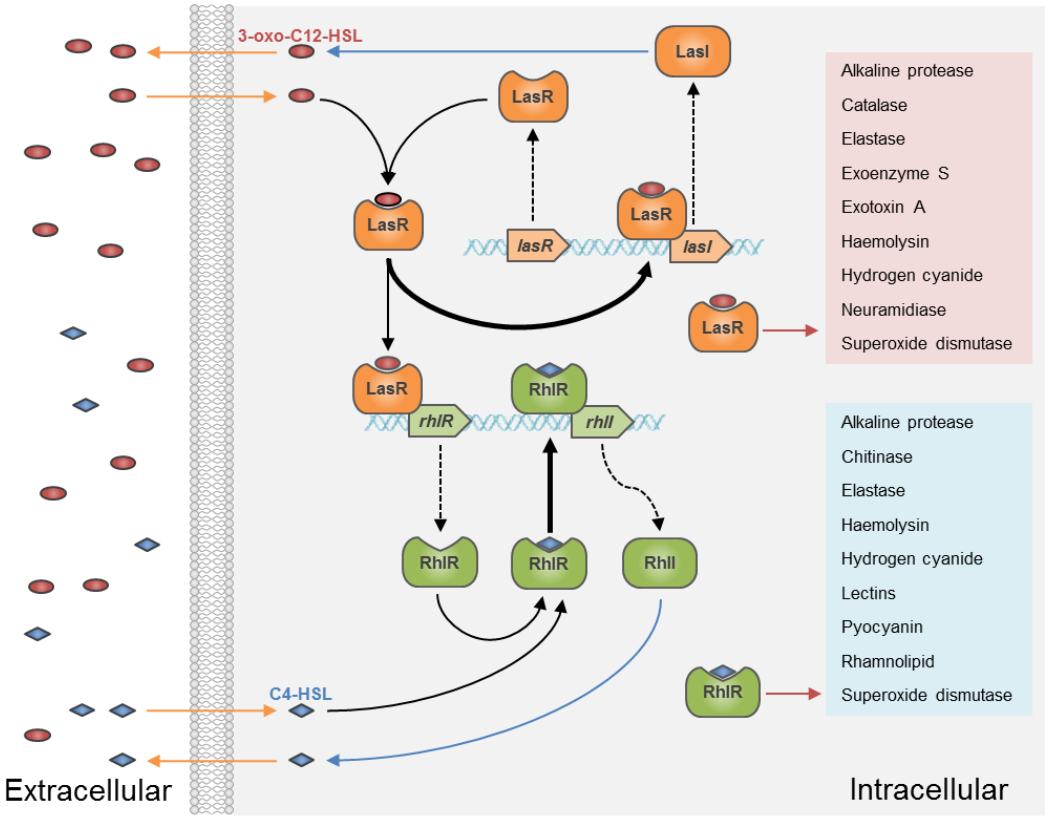

Figure 1-3 Schematic representation of the hierarchical AHL regulation of *P. aeruginosa* virulence. Orange arrows indicate diffusion and transport across cell membrane, black arrows indicate interactions, dashed arrows indicate protein expression, bold arrows indicate autoinduction, blue arrows indicate signal production and red arrows indicate induction of virulence gene expression. Virulence factors regulated by the LasR/LasI system are boxed in pink and those regulated by RhlR/RhlI system are boxed in light blue. Modified from Whitehead *et al.* (2001).

1.2.2 Autoinducer-2 (AI-2)

The autoinducer-2 (AI-2) quorum sensing system was first discovered as an inter-species signalling system in *Vibrio* species, where the addition of cell-free supernatant, or conditioned media, from nonluminous *Vibrio* strains induced light production in *Vibrio harveyi* (Greenberg *et al.*, 1979). Contrary to the AHL QS system, where the signalling molecules produced are specific to each species, the same AI-2 molecule is recognised by multiple species (Bassler *et al.*, 1997). The AI-2 QS system was proposed to mediate universal "language" between bacteria species (Bassler, 1999). At present, homologues of the AI-2 synthase LuxS have been identified in at least 537 sequenced bacterial genomes (Pereira *et al.*, 2013).

AI-2 is a by-product of a central metabolic pathway, the activated methyl cycle (AMC) (Figure 1-2b) (Pereira *et al.*, 2013). AMC is involved in the regeneration of *S*-adenosylmethionine (SAM), the main methyl donor in archaebacteria and eubacteria (Chiang *et al.*, 1996). The conversion of SAM to *S*-adenosylhomocysteine (SAH) occurs during methylation reactions essential for cellular processes including growth, chemotaxis, and the synthesis of phospholipids and vitamins (Figure 1-2b) (Fontecave *et al.*, 2004; Parveen & Cornell, 2011). SAH is a toxic end-product of the reaction and depending on the organism, detoxification of SAH to homocysteine is either by the direct conversion catalysed by SahH, or a two-step conversion using Pfs and LuxS (Figure 1-2b) (Pereira *et al.*, 2013). Bacteria can have either the SahH system or the Pfs/LuxS system (Pereira *et al.*, 2013).

Bacteria using the Pfs/LuxS pathway produce 4,5-dihydroxy-2,3-pentanedione (DPD), the linear form of AI-2, as the by-product of *S*-ribohomocysteine (SRH) conversion to homocysteine (Figure 1-2c) (Pei & Zhu, 2004; Winzer *et al.*, 2002a). DPD is unstable and spontaneously cyclises into *S* or *R* isomers of 2,4-dihydroxy-2-methyldihydro-3-furanone (DHMF) (Figure 1-2c) (Nedvidek *et al.*, 1992). Different enantiomers of DPD are recognised by different bacteria (Pereira *et al.*, 2013). The hydrated and borated form of *S*-DHMF, *S*-2-methyl-2,3,3,4-tetrahydroxytetrahyrofuran-borate (*S*-THMF-borate) is recognised by LuxP in *V. harveyi*, and was the first structure of AI-2 characterised in its receptor-ligand form (Chen *et al.*, 2002; Vendeville *et al.*, 2005). The hydrated form of *R*-DHMF, *R*-2-methyl-2,3,3,4-tetrahydroxytetrahyrofuran (*R*-THMF), was identified as the

ligand of LsrB in *Salmonella typhimurium* ssp. *enterica* serovar Typhimurium (Miller *et al.*, 2004). Despite the similarities in the fold of LuxP and LsrB, the sequence homology between the two proteins is low and the AI-2 binding sites differ in polarity and overall charge (Vendeville *et al.*, 2005). Since the chemically distinct forms of AI-2 are capable of inter-conversion, it has been suggested that the chemical structure of the active AI-2 signal may depend on the niche in which the bacteria resides (Vendeville *et al.*, 2005).

AI-2 is hydrophilic and is relatively impermeable to the cell membrane (Kamaraju *et al.*, 2011). TqsA in *E. coli* belongs to the AI-2 exporter superfamily of putative membrane transporters proposed to be involved in the export of AI-2, but it is not the sole export mechanism (Pereira *et al.*, 2013; Rettner & Saier Jr, 2010). Two main families of AI-2 receptors have been identified, LuxP and LsrB (Pereira *et al.*, 2013). In addition, the ribose binding protein family, RbsB, in *Haemophilus influenzae* and *Aggregatibacter actinomycetemcomitans*, has also shown affinity to AI-2 (Armbruster *et al.*, 2011; Shao *et al.*, 2007a). Although the presence of AI-2 cannot be directly detected using a biochemical assay, detection is possible using specific reporter strains, such as *V. harveyi* BB170, that lack the ability to produce AI-2 but remain capable of detecting AI-2 and produce luminescence in response (Bassler *et al.*, 1997; Bassler *et al.*, 1994; Winzer *et al.*, 2003). AI-2 accumulates during bacterial growth, and is not detectable during the early exponential phase (Winzer *et al.*, 2003). Depending on the strain, maximal levels of AI-2 can be detected during mid- to late-exponential phase, the transition to stationary phase, or during the stationary phase (Winzer *et al.*, 2003). The function of AI-2 or LuxS has been studied in more than 50 bacterial strains. Phenotypes affected by *luxS* mutation in pathogenic bacteria are summarised in Table 1-1.

Since LuxS is required for both AI-2 production and SAM metabolism, phenotypes observed for *luxS* mutants could be the result of the lack of AI-2 signalling, metabolic defects, or the combination of both (Pereira *et al.*, 2013; Winzer *et al.*, 2003) (Table 1-1). Complementation of *luxS* mutants can be achieved by either gene complementation or addition of either conditioned media (the supernatant of AI-2 producing bacterial culture) or purified synthetic AI-2 (Kadirvel *et al.*, 2010; Pereira *et al.*, 2013). Gene complementation alone is

Table 1-1 Phenotype caused by the loss of LuxS function in pathogenic bacteria.[a]

Species	AI-2 receptor	Phenotype associated with the loss of LuxS function	Complementation			References
			Gene	CM	AI-2[b]	
Aggregatibacter actinomycetemcomitans	LsrB and RbsB	Decreased leukotoxin expression and decreased activity of putative iron transport protein	NS	Yes	NS	James *et al.* (2006b); Fong *et al.* (2001); Fong *et al.* (2003); Shao *et al.* (2007b)
		Growth deficiencies under iron-limiting conditions	Yes	NS	NS	
		Impaired biofilm formation	Yes	Yes[c]	NS	
Bacillus anthracis	Unknown	Growth deficiencies	Yes	NS	NS	Jones & Blaser (2003); Jones *et al.* (2010)
Bacillus subtilis	Unknown	Decreased swarming phenotype, impaired colony architecture and biofilm formation	NS	Yes	NS	Lombardia *et al.* (2006)
Campylobacter jejuni	Unknown	Impaired Biofilm formation	NS	Yes	NS	Reeser *et al.* (2007); Plummer *et al.* (2012)
		Inability to colonise chicken and guinea pig intestines and decreased virulence in the pregnant guinea pig model	Yes	NS	NS	
Clostridium perfringens	Unknown	Decreased toxin expression	NS	Yes	NS	Ohtani *et al.* (2002)
EHEC	LsrB	Increased growth rate	Yes	Yes	NS	Sperandio *et al.* (2001); Sperandio *et al.* (2002a); Sperandio *et al.* (2002b); Sperandio *et al.* (1999)
		Decreased motility	Partial	Partial	NS	
		Activation of quorum sensing *E. coli* regulator A (*qseA*) transcription, a regulator of LEE-encoded regulator (Ler)	Yes	Yes	NS	
		Down-regulation of *qseB* and *qseC* transcription, putative regulators of genes involved in motility and flagella assembly	Yes	Yes	NS	
		Decreased type III secretion	Yes	No	NS	

Table 1-1 Phenotype caused by the loss of LuxS function in pathogenic bacteria (*continued*).

Species	AI-2 receptor	Phenotype associated with *luxS* mutation	Complementation			References
			Gene	CM	AI-2	
EPEC	LsrB	Decreased protein secretion	Yes	NS	NS	Sperandio *et al.* (1999); Sircilli *et al.* (2004)
		Decreased expression of plasmid-encoded regulator (*per)*, a regulator of virulence genes	Yes	NS	NS	
		Decreased type III secretion	Yes	NS	NS	
		Decreased motility	Yes	NS	NS	
		Decreased adherence to HeLa cells	Yes	NS	NS	
Haemophilus influenza	RbsB	Impaired biofilm formation	NS	NS	Yes	Armbruster *et al.* (2009); Armbruster *et al.* (2011)
Helicobacter pylori	Unknown	Decreased motility	Yes	Partial	Yes	Loh *et al.* (2004); Rader *et al.* (2007); Rader *et al.* (2011)
Neisseria meningitidis	Unknown	Defective for bacteraemia	Yes	NS	NS	Winzer *et al.* (2002b); Heurlier *et al.* (2009)
		Growth deficiencies	Yes	NS	No	
Porphyromonas gingivalis	Unknown	Altered expression of iron acquisition genes	Yes	Yes[c]	NS	James *et al.* (2006a)
Salmonella enterica ssp. serovar Typhimurium	LsrB	Decreased expression of AI-2 transporter, LuxS regulated proteins (*lsr*) operon	Yes	Yes	Yes	Miller *et al.* (2004); Taga *et al.* (2001); Taga *et al.* (2003); Choi *et al.* (2007); Choi *et al.* (2012)
		Impaired invasion into eukaryotic cells	Yes	NS	NS	
		Decreased flagella gene expression	Yes	No	NS	
Serratia marcescens	unknown	Decreased haemolysin and carbapenem antibiotic productions	Yes	NS	NS	Coulthurst *et al.* (2004)
		Decrease prodigiosin production	Yes	Yes	NS	
Staphylococcus aureus	Unknown	Increased transcription of capsular polysaccharide synthesis genes and increased survival rate in human blood and microphages	Yes	NS	Yes	Zhao *et al.* (2010); Doherty *et al.* (2006)
		Growth deficiencies in sulphur-limited medium	Yes	No	NS	

Table 1-1 Phenotype caused by the loss of LuxS function in pathogenic bacteria (*continued*).

Species	AI-2 receptor	Phenotype associated with *luxS* mutation	Complementation			References
			Gene	CM	AI-2	
Staphylococcus epidermidis	Unknown	Increased expression of intercellular adhesin	Yes	NS	NS	Xu *et al.* (2006); Li *et al.* (2008)
		Increased biofilm formation	Yes	Yes	NS	
		Alteration in metabolism and decreased expression of phenol-soluble modulins, acetoin dehydrogenase, glucokinase, apoptosis protein LrgB, and fructose specific phosphoenolpyruvate phosphotransferase system. Increased expression of nitrite extrusion protein.	NS	NS	Yes	
Streptococcus pneumoniae	Unknown	Impaired biofilm formation	Yes	Yes	Yes	Vidal *et al.* (2011); Trappetti *et al.* (2011)
		Decrease iron uptake during early exponential phase	Yes	NS	NS	
		Reduced competence	Yes	NS	NS	
Streptococcus pyogenes	Unknown	Media-dependent growth deficiencies	Yes	NS	NS	Lyon *et al.* (2001); Marouni & Sela (2003); Siller *et al.* (2008)
		Enhanced haemolytic activity and decreased cysteine protease activity	Yes	NS	NS	
		Increased acid tolerance and increased internalisation and survival in human pharyngeal epithelial cells	Yes	NS	NS	
Vibrio cholerae	LuxP	Decreased competence	NS	Yes	Yes	Miller *et al.* (2002); Antonova & Hammer (2011)
Vibrio vulnificus	LuxP	Increased production of haemolysin	Yes	Yes	NS	Kim *et al.* (2003);
		Delayed and decreased production of protease	Yes	Yes	NS	
		Decreased cytotoxicity to HeLa cells	Yes	NS	NS	

[a] Only studies where *luxS* mutants were used and the mutant phenotype was rescued by complementation are included in this table. [b] Purified AI-2. [c] Partially purified. CM, conditioned media; NS, not shown; partial, partial complementation achieved.

not sufficient to determine whether the change of phenotype is due to the lack of AI-2 signal or intracellular metabolic changes; hence, both gene and signal complementation are required to demonstrate AI-2 QS function (Pereira *et al.*, 2013) (Table 1-1).

1.2.3 Quorum sensing in *E. coli*

E. coli can detect AHLs but cannot synthesise the signalling molecule. Detection of AHL in *E. coli* is mediated by an orphan AHL receptor LuxR homologue, SdiA (Kanamaru *et al.*, 2000; Michael *et al.*, 2001; Wang *et al.*, 1991). AI-2 is detected and synthesised in *E. coli* by LsrB and LuxS, respectively (Pereira *et al.*, 2009).

SdiA, or suppressor of cell division inhibitor A, was originally identified as a positive regulator of the *ftzQAZ* cluster involved in *E. coli* cell division (Wang *et al.*, 1991). Over-expression of plasmid-encoded *sdiA* in *E. coli* up-regulated cell division through the activation of *ftzQAZ* (Wang *et al.*, 1991) and increased resistance to mitomycin C and quinolones through the up-regulation of the multidrug efflux, *acrAB* (Rahmati *et al.*, 2002; Wei *et al.*, 2001b). In addition, microarray analysis showed that over-expression of plasmid-encoded SdiA led to changes in the expression of 75 genes, including up-regulation of genes involved in cell division, DNA modification, metabolism and drug sensitivity; and, down-regulation of 40 genes involved in cell surface structure and motility (Wei *et al.*, 2001a). Dyszel *et al.* (2010) reported discrepancies between the effect of SdiA over-expression from plasmids, and chromosomal *sdiA*. *ftzQAZ* and *acrAB*, genes previously found up-regulated, did not respond to chromosomal SdiA expression or to the addition of *N*-(3-oxo-hexanoyl)-L-homoserine lactone. However, genes involved in glutamate-dependent acid resistance were up-regulated in both *E. coli* K-12 strain MG1655 and EHEC strain ATCC 700927 (Dyszel *et al.*, 2010). Since AHL is present in the bovine rumen and absent in other areas of the gastrointestinal tract, Hughes *et al.* (2010) proposed that EHEC detection of AHL via SdiA in the bovine rumen activates acid resistance and down-regulates flagellar function. Once EHEC cells enter the bovine intestine, where AHL is absent, flagella and genes in the LEE locus is expressed, allowing EHEC colonisation of the anal-rectal junction (Hughes *et al.*, 2010).

The *luxS*-dependent quorum-sensing system in *E. coli* is one of the most extensively studied among non-*Vibrio* species (Pereira *et al.*, 2009; Surette & Bassler, 1998; Surette *et al.*, 1999; Xavier & Bassler, 2005b). Maximum accumulation of AI-2 occurs during late exponential phase (Surette & Bassler, 1998). AI-2 production increases with cell density and is stimulated by increased glucose levels, high osmolarity and iron pulses; and decreases as a result of exposure to RpoS-inducers, such as heat shock and ethanol treatment (DeLisa *et al.*, 2001a, 2001b). The shift in metabolic activity of stressed cells was proposed to be the cause of the lowered AI-2 production observed (DeLisa *et al.*, 2001a). *E. coli* has, within its genome, homologues of the *Salmonella* AI-2 receptor, LsrB, responsible for the recognition of AI-2 (Pereira *et al.*, 2009). Internalisation of signal is mediated by the LuxS regulated (Lsr) transport system encoded by *lsrACDB* (Pereira *et al.*, 2012). In addition to the transport system, the *lsr* operon also encodes the proposed AI-2 phosphorylation kinase LsrK, repressor Lsr, and proposed AI-2-phosphate degradation proteins LsrF and LsrG (Marques *et al.*, 2011; Pereira *et al.*, 2009; Taga *et al.*, 2003; Taga *et al.*, 2001; Xavier & Bassler, 2005b). Recently, the phosphoenolpyruvate (PEP) phosphotransferase system (PTS), responsible for the transport of carbohydrates, was also found to be involved in the initial uptake of AI-2 in *E. coli* (Pereira *et al.*, 2012).

The current model of AI-2 signalling in *E. coli* proposed by Pereira *et al.* (2013) suggested that *luxS* transcription increases during the exponential phase of bacterial growth. The gradual accumulation of extracellular AI-2 peaks during the late-exponential phase. PTS-dependent transport is required for the initial internalisation of AI-2 in the absence of LsrACDB. Internalised AI-2 is then phosphorylated by LsrK, and interacts with LsrR leading to the de-repression of the *lsr* operon. Transcription of genes within the operon leads to the production of LsrACDB and additional LsrK and LsrR. This results in a positive feedback loop which would account for the observed decline in the level of extracellular AI-2 during stationary phase. Because of the hydrophilic nature of AI-2 and its low affinity for lipid, it is not likely to be membrane permeable and therefore an export system is required (Kamaraju *et al.*, 2011). Despite the advancement in the knowledge of AI-2 detection, transport and regulation, the mechanism of AI-2 export in *E. coli* remains elusive.

The LuxS/AI-2 system affects a number of cellular processes (Table 1-1), including the transcription of 242 genes in *E. coli* (DeLisa *et al.*, 2001c). Over-expression of LuxS resulted in altered expression of genes involved in cell division, DNA processing, cell morphology, biofilm formation and motility in *E. coli* K-12 (DeLisa *et al.*, 2001c). Although AI-2 cannot be metabolised by *E. coli* as the sole carbon source, it acts as a chemoattractant (Hegde *et al.*, 2011; Taga *et al.*, 2001). This chemoattraction was also observed in EHEC in a concentration-dependent manner in *luxS* mutants (Bansal *et al.*, 2008). Motility, flagella assembly, activation of LEE-encoded regulator (Ler), and type III secretion have also been associated with AI-2/LuxS regulation in EHEC (Sperandio *et al.*, 2002a; Sperandio *et al.*, 1999; Sperandio *et al.*, 2001; Sperandio *et al.*, 2002b) (Table 1-1).

1.3 Viable but non-culturable (VBNC) state

For readily culturable bacteria such as *E. coli*, it has been a long-held belief that colony count corresponds to bacterial viability (Postgate, 1969). However, discrepancies between the number of colony forming units (cfu) and the number of viable cells determined using microscopy were reported for both *E. coli* and *Vibrio cholerae* cell suspensions maintained in salt water at 4 to 6°C (Xu *et al.*, 1982). While viability of the starved cells determined by fluorescent antibody and acridine orange direct counts (AODC) remained unchanged for the 14 day period, the number of colonies recovered on agar decreased over time. For example, the number of *V. cholerae* cfu decreased from an initial 5.5 logs to undetectable levels within nine days (Xu *et al.*, 1982). The term "viable but non-culturable" (VBNC) was coined to describe this phenomenon of long-term bacterial dormancy in aquatic systems (Grimes & Colwell, 1986; Rollins & Colwell, 1986; Roszak *et al.*, 1984). Since the discovery of VBNC in *Vibrio* spp., a diverse range of bacteria, including plant, marine and human pathogens, were found to enter into VBNC under specific conditions (Oliver, 2010). A summary of studies of VBNC for human pathogens are summarised in Table 1-2.

Table 1-2 Published studies of VBNC for human bacterial pathogens. The summary excludes studies where culture independent determination of viability, resuscitation from the VBNC state or virulence retention was not shown.

Species	VBNC inducing condition	Viability monitoring method	Resuscitation or virulence assessment	References
Aeromonas hydrophilia	filter-sterilized seawater at 23 and 5°C	CTC, and SYBR Green II-PI double staining	incubation at 23°C	Maalej *et al.* (2004)
	SDW at 4°C	AODC, passive dye exclusion method and LIVE/DEAD *Bac*Light staining	supplementing recovery media with catalase or sodium pyruvate	Wai *et al.* (2000)
Campylobacter jejuni	filter-sterilized surface water	CTC and DAPI staining	colonisation in embryonated eggs following incubation at 37°C for up to 96 hours	Cappelier *et al.* (1999)
	acidified MH broth (pH4) at 37°C	CTC and DAPI staining	colonisation in embryonated eggs following incubation at 37°C for up to 96 hours	Chaveerach *et al.* (2003)
	ASW at 4°C	CTC and DAPI staining	establishment of infection in mice	Baffone *et al.* (2006)
	acidified MH broth (pH4) at 42°C	CTC and DAPI staining	passage through chicken intestine prior to recovery on MH agar	Gangaiah *et al.* (2009)
	Ringer solution (5 mM KH_2PO_4) at 42°C	LIVE/DEAD *Bac*Light staining	intracellular survival in Caco-2 cells	Klančnik *et al.* (2009)
	Campylobacter selective nutrient media at 4°C	LIVE/DEAD *Bac*Light staining	intracellular survival in Caco-2 cells	Chaisowwong *et al.* (2012)
Enterococcus faecalis	filter -sterilized lake water at 7 or 4°C	AODC, DAPI and uptake of [^{3}H]-leucine	incubation in 50% BHI at room temperature	Lleò *et al.* (1998)
	filter-sterilized lake water at 4°C	uptake of [^{3}H]-leucine	incubation under optimal growth conditions	Lleò *et al.* (2000)
	filter-sterilized lake water at 4°C	LIVE/DEAD *Bac*Light staining	incubation at 37°C for four days in TSB	Lleò *et al.* (2001)
Enterococcus hirae	filter -sterilized lake water at 4°C	LIVE/DEAD *Bac*Light staining	incubation at 37°C for four days in TSB	Lleò *et al.* (2001)
Enteroaggregative haemorrhagic *Escherichia coli*	saline with 500 µM $CuSO_4$ and tap water at 4 or 23°C	LIVE/DEAD *Bac*Light staining	chelation of Cu^{2+} using EDTA	Aurass *et al.* (2011)

Table 1-2 Published studies of VBNC for human bacterial pathogens. The summary excludes studies where culture independent determination of viability, resuscitation from the VBNC state or virulence retention was not shown (*continued*).

Species	VBNC inducing condition	Viability monitoring method	Resuscitation or virulence assessment	References
Enterohaemorrhagic *Escherichia coli*	SDW at 4°C	AODC and LIVE/DEAD *Bac*Light staining	supplementing recovery media with catalase, sodium pyruvate, α-ketoglutaric acid or 3,3'-thiodiproprionic acid	Mizunoe *et al.* (1999)
	13% NaCl at 37°C	LIVE/DEAD *Bac*Light staining	lethality in mice	Makino *et al.* (2000)
	PBS with 5% NaCl at 37°C	direct microscopic counting of Löfer's alkali methylene blue solution stained cells	relief from saline stress and supplementation with nalidixic acid	Ohtomo and Saito (2001)
	13% NaCl or 0.05% H_2O_2 at 37°C	LIVE/DEAD *Bac*Light staining	supplementing recovery media with sodium pyruvate	Asakura *et al.* (2005)
	PBS at 4°C	LIVE/DEAD *Bac*Light staining	co-culture with eukaryotic cells	Senoh *et al.* (2012)
Enteropathogenic *Escherichia coli*	PBS at 4°C	LIVE/DEAD *Bac*Light staining	co-culture with eukaryotic cells	Senoh *et al.* (2012)
Enterotoxigenic *Escherichia coli*	Chesapeake Bay water	AODC, DVC, radiolabelled direct viable count	incubation in ligated rabbit ileal loops prior to recovery	Roszak & Colwell (1987a)
	PBS at 4°C	LIVE/DEAD *Bac*Light staining	co-culture with eukaryotic cells	Senoh *et al.* (2012)
Helicobacter pylori	pre-filtered and sterilized seawater at 37°C	LIVE/DEAD *Bac*Light staining	co-culture with marine copepod, *Tigriopus fulvus*	Cellini *et al.* (2005)
Legionella pneumophila	SDW at 25°C	flow cytometry of LIVE/DEAD *Bac*Light-stained cells	intracellular growth in *Acanthamoeba polyphaga*	Myoung *et al.* (2006)
	SDW with 0.05 ppm chlorine at 37°C	real-time PCR and flow cytometry of cells stained with AES-Chemunex Detection of Legionella pneumophila kit	intracellular growth in *A. polyphaga*	Dusserre *et al.* (2008)
Listeria monocytogenes	filtered sterilised distilled water at 4 or 20°C	DVC and DAPI	injection of VBNC cells into chicken embryos and incubated for 2 and 6 days at 37°C	Cappelier *et al.* (2007)
Mycobacterium tuberculosis	Sauton's medium supplemented with albumen, glucose and NaCl at 37°C	CTC, rhodamine 123 and propidium iodide	addition of resuscitation-promoting factor or supernatant of late-exponential phase *M. tuberculosis*	Shleeva *et al.* (2002)

Table 1-2 Published studies of VBNC for human bacterial pathogens. The summary excludes studies where culture independent determination of viability, resuscitation from the VBNC state or virulence retention was not shown (*continued*).

Species	VBNC inducing condition	Viability monitoring method	Resuscitation or virulence assessment	References
Pseudomonas aeruginosa	SDW at 25°C	flow cytometry of LIVE/DEAD *Bac*Light-stained cells	intracellular growth in *A. polyphaga*	Myoung (2006)
	filter-sterilized drinking water with 0.01 µM to100 µM of copper sulfate at 20°C	DAPI and LIVE/DEAD *Bac*Light staining	recovery in sterile distilled water with sodium diethyldithiocarbamate trihydrate (copper chelator) and cytotoxicity assay in CHO cells	Dwidjosiswojo (2011)
	PBS at 4°C	LIVE/DEAD *Bac*Light staining	co-culture with eukaryotic cells	Senoh *et al.* (2012)
Salmonella enterica serovar Enteritidis	sterile Potomac River water microcosms	AODC, DVC and fluorescent antibody direct count	recovery in BHI	Roszak *et al.* (1984)
	Chesapeake Bay water	AODC, DVC, radiolabelled direct viable count	incubation in ligated rabbit ileal loops prior to recovery	Roszak & Colwell (1987a)
Salmonella enterica serovar Typhimurium	Butterfield phosphate solution at 5 and 21°C	LIVE/DEAD *Bac*Light and CTC staining	temperature upshift to 56°C	Gupte *et al.* (2003)
	sewage effluent water and SDW with peracetic acid treatment kept at 15°C	AODC and DVC	virulence to HeLa cells	Jolivet-Gougeon *et al.* (2006)
	dehydration (40 to 50 % relative humidity) and 4°C incubation	LIVE/DEAD *Bac*Light staining	LB, TSB, or BHI at 25 and 37°C	Gruzdev *et al.* (2012)
Shigella dysenteriae	SDW at 30 or 37°C	modified DVC using INT and AODC	cytotoxicity to HeLa cells	Rahman *et al.* (1994)
		modified DVC using INT	adherence to Henle 407 cells	Rahman *et al.* (1996)
Shigella flexneri	PBS at 4°C	LIVE/DEAD *Bac*Light staining	co-culture with eukaryotic cells	Senoh *et al.* (2012)
Staphylococcus aureus	filter-sterilized seawater at 4 or 22°C	DAPI and DVC	incubation at 22°C	Masmoudi *et al.* (2010)
Vibrio alginolyticus	ASW at 5°C	CTC and DAPI	establishment of infection in mice, reactivation of adhesion to HEp-2 cells and cytotoxicity to CHO cells following passage through rat ileal loops	Baffone *et al.* (2003)
	filter-sterilized seawater at 4°C	AODC and DVC	incubation at 26°C with or without yeast extract	Du *et al.* (2007a)

Table 1-2 Published studies of VBNC for human bacterial pathogens. The summary excludes studies where culture independent determination of viability, resuscitation from the VBNC state or virulence retention was not shown (*continued*).

Species	VBNC inducing condition	Viability monitoring method	Resuscitation or virulence assessment	References
Vibrio cholerae	estuarine water secured to a sunken barge offshore in Nixon's Harbor, Bahamas	AODC, DVC and fluorescent antibody count	establishment of infection in rabbits	Colwell *et al.* (1985)
	ASW at 4°C	AODC and DVC	incubation at 30°C for three days	Ravel *et al.* (1995)
	ASW at 4°C	DVC	incubation in thiosulfate-citrate-bile saults-sucrose broth for up to five days	Berlin *et al.* (1999)
	ASW at 4°C	LIVE/DEAD *Bac*Light staining	co-culture with CHO cells at 37°C for four days	Chaiyanan *et al.* (2001)
Vibrio mimicus	ASW at 4°C	DVC	incubation at room temperature for two days	Berlin *et al.* (1999)
Vibrio parahaemolyticus	ASW at 4°C	DVC	incubation in thiosulfate-citrate-bile saults-sucrose broth for up to five days	Berlin *et al.* (1999)
	modified PBS containing 0.04% NaCl, 0.01% KCl, 0.145% Na_2HPO_4 and 0.01% KH_2PO_4	LIVE/DEAD *Bac*Light staining	supplementing recovery media with catalase or sodium pyruvate	Mizunoe *et al.* (2000)
	ASW at 5°C	CTC and DAPI	establishment of infection in mice, reactivation of adhesion to HEp-2 cells and cytotoxicity to CHO cells following passage through rat ileal loops	Baffone *et al.* (2003)
	ASW at 4°C	DVC	22°C incubation overnight	Bates & Oliver (2004)
	Morita mineral salt-0.5% NaCl medium at 4°C	LIVE/DEAD *Bac*Light staining	cytotoxicity to HEp-2 cells and enteropathogenicity and lethality in mice	Wong *et al.* (2004)
	PBS at 4°C	LIVE/DEAD *Bac*Light staining	co-culture with eukaryotic cells	Senoh *et al.* (2012)
Vibrio vulnificus	ASW microcosm at 5°C	AODC with INT assay	incubation at room temperature overnight	Nilsson *et al.* (1991)
	ASW microcosm at 5°C	AODC, DAPI, CTC and DVC	establishment of infection in mice	Oliver & Bockian (1995)

AODC, acridine orange direct count
ASW, artificial seawater
PBS, phosphate buffered saline
SDW, sterile distilled water
CTC, 5-cyano-2,3-ditolyl tetrazolium chloride
DAPI, 2-(4-amidinophenyl)-1H -indole-6-carboxamidine
DVC, direct viable count
INT, *p*-iodonitrotetrazolium violet
BHI, brain heart infusion broth
LB, Luria-Bertani broth
MH, Mueller-Hinton
TSB, tryptic soy broth
CHO, Chinese hamster ovary

1.3.1 Induction, detection and resuscitation of VBNC cells

There has been some debate surrounding the use of the "viable but non-culturable" terminology (Barcina & Arana, 2009; Nyström, 2003; Oliver, 2010). Although numerous studies document the entry of bacteria into VBNC, few demonstrate the ability of bacteria to resuscitate after a period of dormancy.

Chemical and physical stress factors, including nutrient limitation, salinity, low-pH and sub-optimal incubation temperatures, have been shown to induce VBNC in bacteria (Table 1-2). While exposed to VBNC inducers, the number of cells culturable on routine media decreases until the entire population enters the VBNC state. Viability of cells during this time can be determined by microscopy or flow cytometry of fluorescent stained cells (Oliver, 2010). Commonly used fluorescent dyes (e.g. the LIVE/DEAD *Bac*Light STYO 9-PI dual staining system, 5-cyano-2,3-ditolyl tetrazolium chloride (CTC) and rhodamine 123) determine cell viability by testing cytoplasmic membrane integrity, respiration and membrane potential (Breeuwer & Abee, 2000). Detection of continual expression of *pbp5*, a gene encoding penicillin binding protein, using reverse transcriptase (RT)-PCR was found to correlate with the metabolic activity of *Enterococcus faecalis* and was used as a measure of viability (Lleò *et al.*, 2000).

In addition to changes in culturability, morphological, physiological and metabolic characteristics of VBNC cells may differ from pre-VBNC actively metabolising cells. Reduction in cell size from rod to coccoid forms has been documented for VBNC *V. cholerae*, *Vibrio vulnificus*, *Campylobacter jejuni* and *Campylobacter coli* (Beumer *et al.*, 1992; Chaiyanan *et al.*, 2001; Höller *et al.*, 1998; Oliver *et al.*, 1991). Su *et al.* (2013) described budding and bulging morphology of *Vibrio parahaemolyticus* when in the VBNC state and suggested that the formation of such irregular shaped cells was due to increased cell wall thickness. Similar irregular-shaped cell morphology was also described for VBNC *V. cholerae*, *Vibrio alginolyticus* and *V. parahaemolyticus* (Albertini *et al.*, 2006; Chaiyanan *et al.*, 2001; Chen *et al.*, 2009). In addition, protein profiles of VBNC *Enterococcus faecalis* and *V. parahaemolyticus* cultures were found to be different to the culturable state (Heim *et al.*, 2002; Lai *et al.*, 2009). Expression of specific proteins in the VBNC state, such as fibrils, differed between VBNC and pre-VBNC *Salmonella enterica* serovar Typhimurium (Gupte *et al.*, 2003). In

addition, the outer membrane subproteome in *E. coli*, as well as the membrane fatty acid composition in *V. vulnificus*, were found to differ between pre-VBNC and VBNC cells (Day & Oliver, 2004; Muela *et al.*, 2008). Reissbrodt *et al.* (2002) noted that the size of colonies recovered from *S. enterica* serovar Typhimurium became smaller and more irregular in margin as the cells age in starvation before whole population eventually becoming VBNC. Rahman *et al.* (1994) showed that VBNC *S. dysenteriae* were capable of the uptake and incorporation of ^{35}S-labelled methionine into newly synthesised proteins despite the loss of culturability. Höller *et al.* (1998) found that in addition to a reduction in culturability, the pattern of organic acid production by *C. coli*, particularly succinate and fumarate excretion, differed between cells starved at 4, 10 and 20°C, suggesting a temperature-dependent variation in the phenotypic presentation of VBNC cells.

Although it is not clear whether VBNC cells can directly cause infections, a number of species were found to cause infections once resuscitated from the VBNC state, including *Edwardsiella tarda*, *V. harveyi*, *V. cholerae*, *V. vulnificus*, *V. parahaemolyticus*, *V. alginolyticus*, *S. enterica* serovar Typhimurium, *C. jejuni* and *E. coli* (Baffone *et al.*, 2006; Baffone *et al.*, 2003; Du *et al.*, 2007b; Grimes & Colwell, 1986; Sun *et al.*, 2008). Cappelier *et al.* (2005; 2007) found that VBNC *Listeria monocytogenes* was unable to either form plaques in HT-29 cell monolayers, or colonise mouse spleens unless first resuscitated in embryonated egg at 37°C for two to six days. Resuscitation of VBNC cells has been achieved by the removal of stress, nutrient addition, supplementation with catalase or pyruvate, passage through animal, or incubation with eukaryotic or protozoan cells (Table 1-2).

1.3.2 VBNC state as a survival strategy

The maintenance of low metabolic activity as a strategy to survive starvation was postulated in the 1970s (Ensign, 1970; Kurath & Morita, 1983; Nelson & Parkinson, 1978; Novitsky & Morita, 1978). Roszak and Colwell (1987b) further proposed that entrance into the VBNC state may be a survival mechanism employed by bacteria in natural environments. Opponents of this view argued that the phrase "viable but non-culturable" is an oxymoron since the definition of the

VBNC state requires that the bacteria eventually "resuscitate" (Barer, 1997). Furthermore, it is difficult to attribute the source of the cells recovered to either the remaining culturable cells within the population or resuscitation of VBNC cells (Bogosian & Bourneuf, 2001). Reduced bacterial culturability associated with exposure to cell stress could be due to the irreversible damage caused by the stressor, and that the associated growth arrest of individual cells would result in their death (Nyström, 2001, 2003).

The involvement of RpoS, a global stress response regulator, in the formation of VBNC cells supports the hypothesis that VBNC may be a bacterial survival strategy in natural environments (Oliver, 2010). Mutant *E. coli* and *S. enterica* strains lacking *rpoS* were found to enter the VBNC state faster than the wild type strains, suggesting that RpoS may be a regulator of the VBNC response (Boaretti *et al.*, 2003; Kusumoto *et al.*, 2012). Cross-protection of VBNC state with other stresses has been described for a number of bacteria, including *E. coli*, *S. enterica* serovar Enteritidis, *S. enterica* serovar Typhimurium, *V. vulnificus*, *V. parahaemolyticus*, *C. jejuni* and *Mycobacterium smegmatis* (Jenkins *et al.*, 1990).

Within a genetically homogeneous microbial population, phenotypic heterogeneity may exist (Balaban *et al.*, 2004). This inherent heterogeneity had been found to be associated with the observation of persister subpopulations that do not respond to antibiotic treatment (Avery, 2006). Persisters form rapidly during exponential phase and constitute a maximum of 1% of the post-stationary phase population (Balaban *et al.*, 2004; Lewis, 2007). Balaban *et al.* (2004) suggested that slow-growing dormant subpopulations, such as persister cells, may have been evolutionarily selected to increase the chance of population survival in fluctuating environments. Buerger *et al.* (2012) hypothesised that slow-growing cells, such as VBNC or other persisting subpopulations, within a heterogenic bacterial population may stochastically exit the non-growing state acting as scouts for favourable growth conditions. The nonculturable subpopulations may have implications on the accuracy of bacteria detection in the food industry (Buerger *et al.*, 2012; Dinu *et al.*, 2009). Since VBNC-inducing conditions may occur during food production or in food processing environment; there is a risk of underestimation of pathogen detection, which may also hinder epidemiological identification of outbreak origins (Dinu *et al.*, 2009).

Bacterial injury has also been associated with cells' inability to grow on selective media, particularly following exposure to sublethal stress associated with food processing and handling procedures (Wu, 2008). Injury usually refers to damage to cellular components caused by physical or chemical treatment, such as temperature and/or osmotic shock, but the term has also been used loosely to describe stressed cells, particularly in the food context (Wesche *et al.*, 2009). In contrast, the VBNC state is typically used to describe the non-culturable phenomenon of population adaptation to stress (Oliver, 2010). Entrance into the VBNC state had been considered by some authors as a survival mechanism used by severely injured but metabolically active cells (Wesche *et al.*, 2009). Others define injured cells as cells that survived sublethal stress with the capability to regain growth on selective media following resuscitation, which is similar to the definition of VBNC cells (Wu, 2008).

1.3.3 VBNC state in *E. coil*

E. coli was among the first species discovered to enter the VBNC state (Xu *et al.*, 1982). Sub-optimal temperature, nutrient-starvation, presence of copper ions, or salinity were found to induce *E. coli* into the VBNC state (Table 1-2). The time for the entire cell population to enter the VBNC state, where the number of culturable cells declined to undetectable levels, varies depending on the strain and VBNC inducing conditions. Asakura *et al.* (2005) examined the VBNC response of *E. coli* O157:H7 strains isolated from an outbreak linked to contaminated salted salmon roe. *E. coli* O157:H7 isolates from both the food and the patients were subjected to a range of stress factors, such as osmotic and oxidative stresses. The decline in culturability differed between the strains isolated from food and patients. Exposure to 0.5% hydrogen peroxide induced entry into VBNC by the clinical isolate after 6 hours while 144 hours were required to for the food isolate. Mouse passage of *E. coli* O157:H7 isolates from food also resulted in the formation of VBNC cells within a shorter period of time. The results showed that *in vivo* passage reduced the time required for VNBC induction.

In addition to the observed decline in culturability of *E. coli* population entering VBNC, changes such as the modification to peptidoglycan and expression of outer membrane proteins have been observed (Lai *et al.*, 2004; Muela *et al.*, 2008;

Signoretto *et al.*, 2002). Analysis of penicillin-binding proteins (PBPs) of exponentially growing and VBNC *E. coli* KN126 showed that PBPs 1A, 1B, 2 and 3 were absent from cells in VBNC (Signoretto *et al.*, 2002). Diaminopimelic acid (DAP)-DAP cross-linking of the cell wall peptidoglycan, and autolytic capability, were higher than that observed for exponential and stationary phase cells (Signoretto *et al.*, 2002). Proteomic analysis of the outer membrane sub-proteome of *E. coli* strain Spanish Type Culture Collection 416, using two-dimensional electrophoresis, revealed that 106 proteins differed between stationary phase and starvation-induced VBNC cells, although expression of proteins exclusive to the VBNC cells were not identified (Muela *et al.*, 2008).

A number of ETEC strains were found to remain virulent while in the VBNC state (Grimes & Colwell, 1986; Lothigius *et al.*, 2010; Pommepuy *et al.*, 1996). ETEC strain H10407 kept in membrane chambers at semitropical ocean water temperature (25°C) entered the VBNC state within 13 hours and remained capable of producing exotoxins (Grimes & Colwell, 1986). The production of exotoxin was confirmed using ganglioside-enzyme-linked immunosorbent assay (GM1-ELISA) (Pommepuy *et al.*, 1996). Lothigius *et al.* (2010) found that clinical isolates of ETEC were able to survive in both seawater and freshwater. The cell population reached VBNC state within 12 weeks in freshwater at room temperature. Although production of exotoxin by VBNC cells was not detected using the GM1-ELISA, real-time reverse transcriptase PCR of cDNA derived from VBNC cells revealed that genes encoding the ETEC toxins and colonising factors were expressed.

Reissbrodt *et al.* (2002) showed that *E. coli* O157:H7 kept in distilled-water microcosms at room temperature could be resuscitated during starvation for up to 455 days by the addition of purified enterobacterial autoinducer, secreted by a enterobacterial species in the presence of mammalian norepinephrine. Using the *E. coli* O157:H7 *luxS* deletion mutant, VS94, Soni et al (2008), showed that the number of culturable cells remained higher in PBS supplemented with AI-2 conditioned media compared to PBS supplemented with autoclaved conditioned media or PBS, suggesting a potential role of AI-2 signalling in promoting culturability of cells that would otherwise enter the VBNC state. Liu *et al.* (2010) found that VBNC *E. coli* O157:H7 cells starved for up to 19 months could

produce Shiga toxins (Stx). In addition, bovine VBNC isolates produced higher levels of Stx than clinical VBNC cells. The ability of *E. coli* O157:H7 to enter the VBNC state and retain virulence has major implications for food safety and public health in regard to detection and control of this zoonotic pathogen (Dinu *et al.*, 2009).

1.4 *E. coli* central metabolism

E. coli is a chemotroph that utilises organic compounds as the carbon, electron and energy source (Voet & Voet, 2011). Carbon sources are transported into the cell via facilitated diffusion, symport, antiport, active transport, or the phosphotransferase system (PTS) (Dills *et al.*, 1980) (Figure 1-4). Biochemical pathways including PTS, glycolysis, pentose monophosphate bypass, tricarboxylic acid (TCA) cycle and gluconeogenesis form the central metabolism of *E. coli* (Maciag *et al.*, 2012). Of the central metabolic pathways, glycolysis and the TCA cycle are major catabolic pathways that generate energy from carbon sources (Madigan *et al.*, 2012) (Figure 1-5).

1.4.1 Regulation of central metabolism by the phosphoenolpyruvate: phosphotransferase system (PEP:PTS)

Transport systems for substrates form an integral part of carbon metabolism regulation in bacteria (Deutscher *et al.*, 2006; Dills *et al.*, 1980; Görke & Stülke, 2008). In *E. coli*, activities of PEP:PTS regulate the expression of proteins that leads to carbon catabolite repression (CCR), where the expression of enzymes required for transport and metabolism of less favourable substrates is repressed by the presence of preferred carbon sources, such as glucose and fructose (Görke & Stülke, 2008). The mechanisms of glucose uptake via PEP:PTS and CCR are schematically represented in Figure 1-6.

In the presence of preferred carbon sources, such as glucose, PTS is driven by PEP conversion to pyruvate and the subsequent phosphorylation cascade via enzyme I (EI), phosphohistidine carrier protein (HPr), and the A, B and C subunits of enzyme II (EII). Glucose is transported into the cell in its phosphorylated form, where it enters the glycolytic pathway for catabolism (Escalante *et al.*, 2012) (Figure 1-6). Dephosphoryated $EIIA^{Glc}$ inhibits the

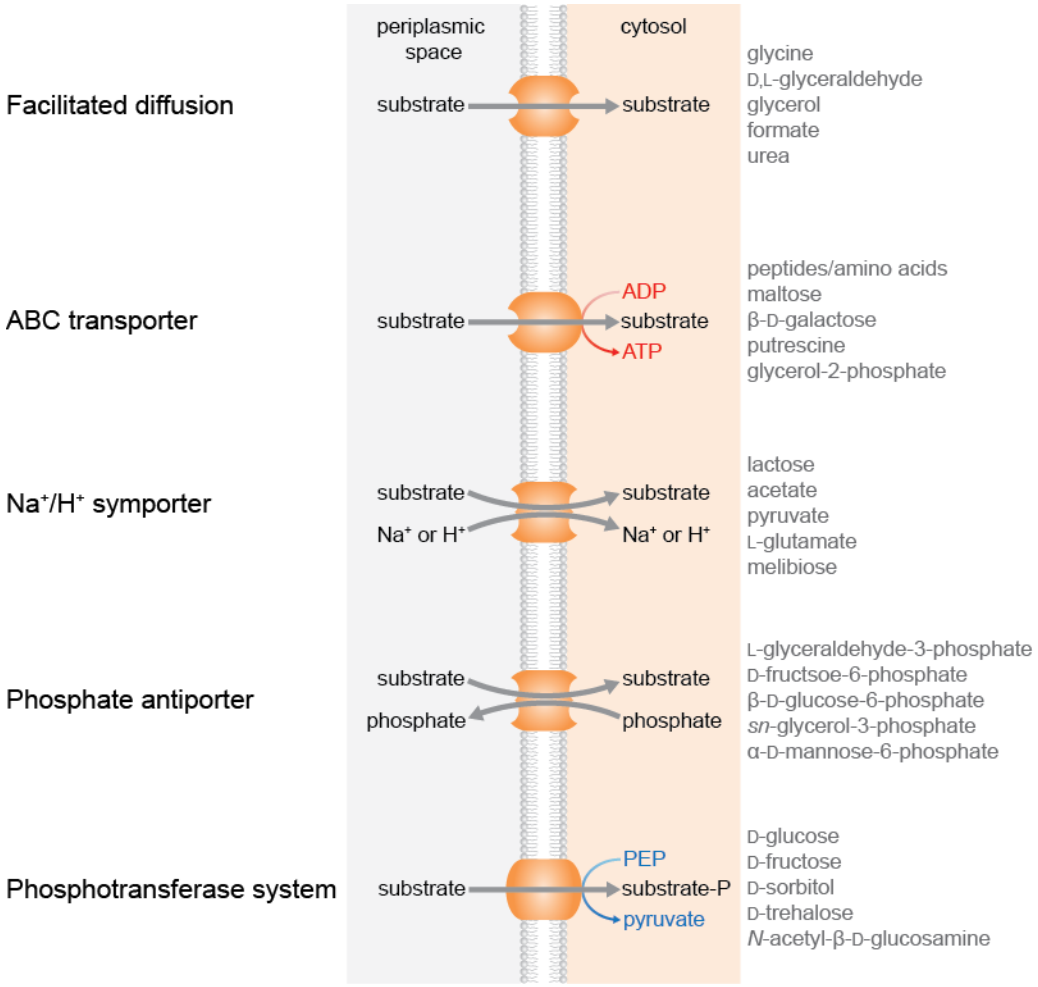

Figure 1-4 Summary of the *E. coli* carbon transport systems and examples of substrates transported from the periplasmic space to the cytosol via these systems. Example substrates for each transport system are shown in grey. ABC, ATP-binding cassette transporter; PEP, phosphoenolpyruvate. Modified from Dills *et al.* (1980). Substrate association with specific transport systems was drawn based on information from the BioCyc Database (Caspi *et al.*, 2014).

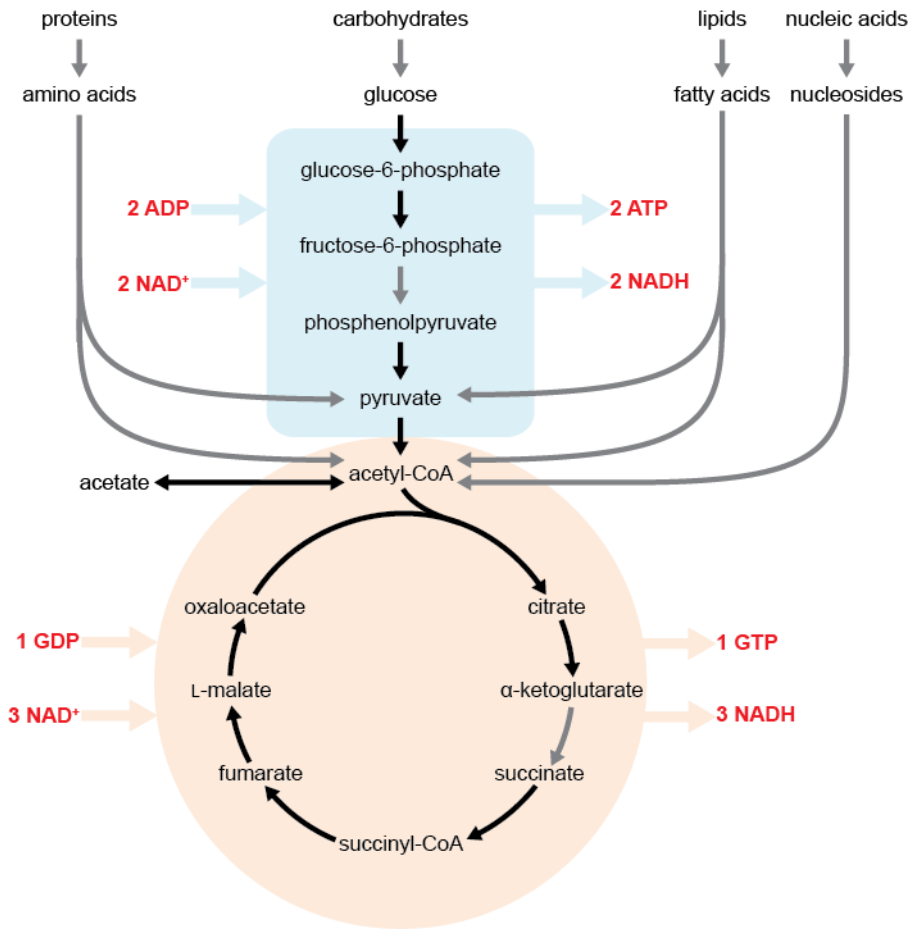

Figure 1-5 Schematic representation of the *E. coli* central metabolic pathways and the net energy gain from substrate catabolism. Glycolytic processes are boxed in blue and the tricarboxylic acid (TCA) cycle is shaded in pink. Black arrows indicate direct conversion and grey arrows indicate indirect conversions where intermediary processes are not shown. Modified from Holms (1996) with information from the BioCyc Database (Caspi *et al.*, 2014).

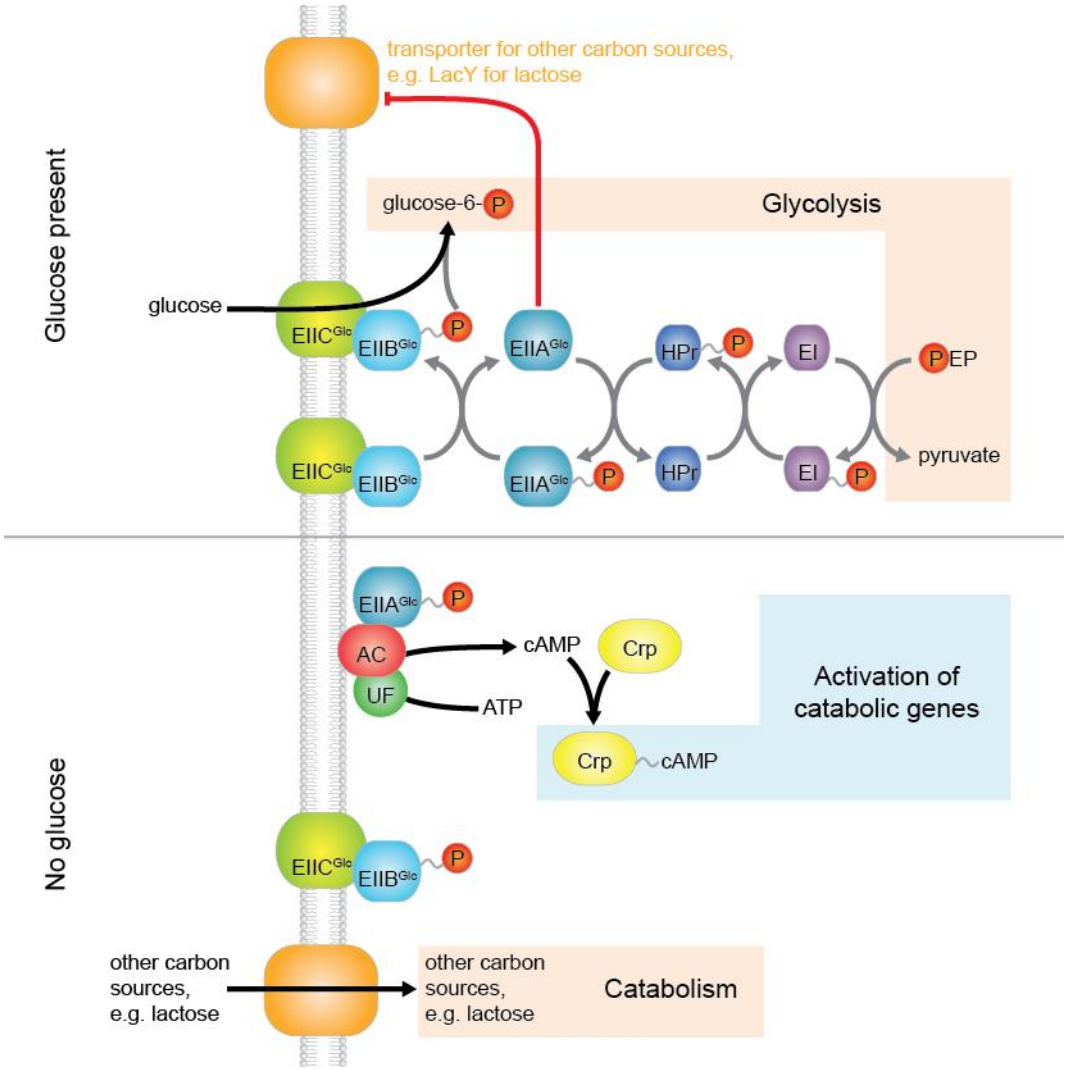

Figure 1-6 The phosphoenolpyruvate: phosphotransferase system (PEP:PTS) in *E. coli* in the presence and absence of glucose. Phosphorylation cascades are shown by grey arrows and inducer exclusion on non-PTS transporters is shown by the red line. Phosphorylated forms of proteins are shown by ~P. EI, enzyme I; EII, enzyme II; HPr, phosphohistidine carrier protein; AC, adenylate cyclase; UF, unidentified co-factor; cAMP, cyclic AMP; Crp, cAMP receptor protein. Cellular processes are boxed in pink or blue. Modified from Notley-McRobb *et al.* (1995), Kotrba *et al.* (2001) and Park *et al.* (2006).

activity of the transport of non-PTS substrates through allosteric regulation and/or inhibits the formation of inducers required to catabolise non-PTS substrates resulting in inducer exclusion (Görke & Stülke, 2008) (Figure 1-6).

In the absence of glucose, or other PTS carbon sources, transport and catabolism of non-PTS carbon occur without inhibition from the PTS system. In addition, phosphorylated $EIIA^{Glc}$ binds to adenylate cyclase (AC) leading to increased conversion of ATP to cAMP (Escalante *et al.*, 2012) (Figure 1-6). The increased intracellular cAMP level results in the increased formation of cAMP-bound cAMP receptor protein (Crp), which activates the catabolic genes required for the metabolism of non-PTS substrates such as lactose (Görke & Stülke, 2008) (Figure 1-6). Genomic screening identified 378 promoters as the target of cAMP-CRP regulation, including 70 transcription factor genes (Shimada *et al.*, 2011). The functions of these transcription factors include regulators for carbon metabolism, nitrogen metabolism, nucleoid proteins, and the stress response gene RpoS (Shimada *et al.*, 2011).

1.4.2 PEP-pyruvate-oxaloacetate (PPO) node

The ratio of PEP and pyruvate determines the function of PTS and subsequently, the intracellular cAMP level (Gabor *et al.*, 2011). While carbohydrates are catabolised via the glycolytic pathway, other carbon sources enter the central metabolic pathways via pyruvate, acetyl-CoA or TCA cycle intermediates such as L-malate and oxaloacetate (Sauer & Eikmanns, 2005) (Figure 1-5). Growth on substrates that enter central metabolism through non-glycolytic pathways results in the reversal of glycolysis and gluconeogenesis of sugar phosphates. The PEP-pyruvate-oxaloacetate (PPO) node serves as the metabolic switch where glycolysis, gluconeogenesis and the TCA cycle converge (Sauer & Eikmanns, 2005) (Figure 1-7).

The direction of the reactions within PPO depends on the carbon source (Holms, 2001; Sauer & Eikmanns, 2005). Flux analysis, the measurement of the conversion of single carbon sources to biomass and by-products, is an established method for the deduction of the route of substrate metabolism (Holms, 1996, 2001). Metabolism of PTS substrates, such as glucose and fructose, follow the

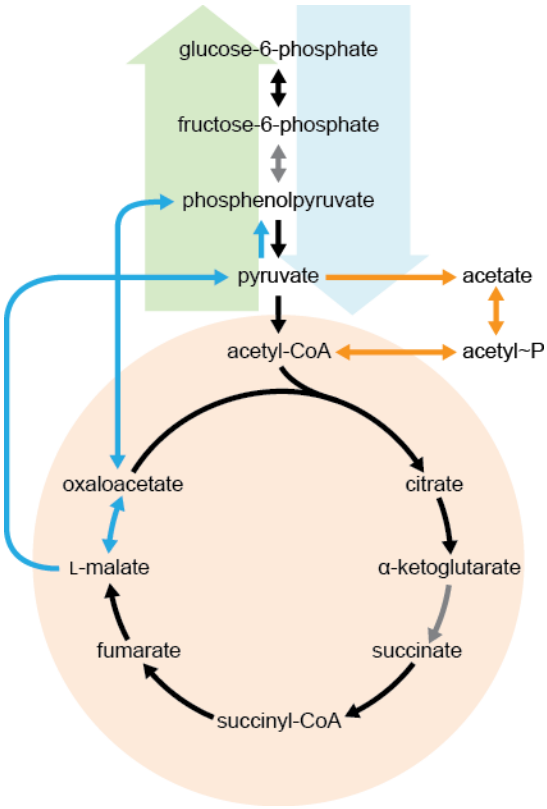

Figure 1-7 The phosphoenolpyruvate-pyruvate-oxaloacetate (PPO) node in *E. coli*. Direction of glycolysis is shown by the light blue block arrow and the direction of gluconeogenesis is shown by the light green block arrow. Black arrows indicate direct conversion and grey arrows indicate indirect conversions where intermediary processes are not shown. The PPO reactions are shown by the blue arrows and the acetate activation pathway is shown by the orange arrows. Modified from Wolfe (2005) and Castaño-Cerezo *et al.* (2011).

glycolytic pathway (Figure 1-5). However, growth on other carbon sources such as pyruvate and acetate follow different routes in the central metabolic pathways (Holms, 1996; Liao *et al.*, 1994; Wolfe, 2005).

Pyruvate is transported into the cell via the proton symport (Holms, 2001) (Figure 1-4). Increased intracellular pyruvate concentration lowers the PEP: pyruvate ratio and metabolism of pyruvate occurs either by entry into the TCA cycle via acetyl-CoA, or by conversion to PEP followed by gluconeogenesis (Gabor *et al.*, 2011; Holms, 2001) (Figure 1-7). Acetate is transported into the cell by ActP, a sodium symporter (Stenberg *et al.*, 2005). Acetate is a toxic by-product of central metabolism excreted during growth in excess glucose, and is one of the least efficient carbon sources for supporting *E. coli* growth (Holms, 2001; Wolfe, 2005). However, short-chain fatty acids such as acetate, propionate and butyrate are major energy sources for organisms in the human colon, an important niche for *E. coli* (Wolfe, 2005). Intracellular acetate is converted to acetyl-P and the majority enters the TCA cycle via acetyl-CoA (Holms, 2001). The intermediary acetyl-P is a global regulator of two-component signal transduction pathways such as flagella synthesis (Wolfe, 2005).

1.5 *E. coli* stress response

Bacteria encounter changing environments and need to respond appropriately to ensure survival (Battesti *et al.*, 2011; Kolter *et al.*, 1993). These changes in environmental conditions may result in cellular stress, which requires the translation of specific proteins to counteract the negative impact of the stress(es) (Battesti *et al.*, 2011). Further, initiation of the appropriate response for damage repair and/or re-establishment of homeostasis is important for adaptation to a new environment and ensure the bacterial survival (Battesti *et al.*, 2011).

Growth during optimal conditions and response to stress both require the transcription of appropriate genes (Nyström, 2004). For *E. coli* and other γ-proteobacteria, transcription of housekeeping genes during growth and expression of stress response-related genes are dependent on the promoter specificity of the RNA polymerase (RNAP) (Battesti *et al.*, 2011; Nyström, 2004). *E. coli* RNAP

consists of a core enzyme (E) and one of the seven sigma factors which controls promoter specificity of E (Table 1-3). Of the seven sigma factors, σ^{38} (RpoS) is responsible for the global stress response and is triggered under a variety of stress conditions (Battesti *et al.*, 2011). In addition to RpoS, five other alternative sigma factors exist in *E. coli*, each controls a specific set of genes in response to different stressors and supplements the housekeeping sigma factor σ^{70} (RpoD) (Loewen *et al.*, 1998) (Table 1-3).

1.5.1 RpoS-mediated stress response

RpoS was initially found to be involved in the resistance to near-UV challenge (Tuveson & Jonas, 1979), regulation of catalase (Loewen & Triggs, 1984), exonuclease III (Sak *et al.*, 1989) and acid phosphatase production (Touati *et al.*, 1986). In addition, RpoS was identified as a central regulator for stationary phase-inducible genes (Lange & Hengge-Aronis, 1991). More recently, RpoS-mediated stress response has been found to be induced by a number of other stress factors including nutrient starvation (Mandel & Silhavy, 2005), osmotic stress (Hengge-Aronis *et al.*, 1993), oxidative stress (Sammartano *et al.*, 1986), low temperature (White-Ziegler *et al.*, 2008), and low pH (Cheville *et al.*, 1996).

Depending on the type of stress involved, detection of stress factors and thereby the induction of RpoS rely on specific signalling mechanisms such as guanosine 3',5'-bis(diphosphate) (ppGpp), guanosine 3'-diphosphate, 5'-triphosphate (pppGpp), collectively known as (p)ppGpp, and two component regulatory systems such as PhoP/PhoQ, and ArcB/ArcA (Battesti *et al.*, 2011). Expression of RpoS is tightly controlled, with regulation at transcriptional, translational and proteolytic levels involving several mediators of stress signals (Table 1-4). While signalling mechanisms involved in RpoS activation under specific stress conditions are well defined for *E. coli*, the signalling cascade involved in RpoS-dependent resistance to low pH, high pH, high osmolarity and oxidative stress is less well understood (Battesti *et al.*, 2011).

Regulation of gene expression during exponential phase and upon exposure to stress is dependent on the regulation of the level of sigma factors within the cell

and competition of sigma factors for E binding (Nyström, 2004). During exponential growth, σ^{70} binding to E results in the expression of the majority of

Table 1-3 Sigma factors in *E. coli*, the genes and the cellular processes they control.

Sigma Factor	Gene	Control	Reference
σ^{70} (σ^{D})	*rpoD*	Regulation of house-keeping genes during exponential growth	Helmann & Chamberlin (1988)
σ^{19} (σ^{FecI})	*fecI*	Regulation of the ferric citrate transport system; transcriptional regulation of extracytoplasmic functions	Angerer *et al.* (1995); Crosa (1995)
σ^{24} (σ^{E})	*rpoE*	Heat shock response	Rouviére *et al.* (1995)
σ^{28} (σ^{F})	*rpoF*	Flagella expression	Helmann (1991)
σ^{32} (σ^{H})	*rpoH*	Heat shock response	Newlands *et al.* (1993)
σ^{38} (σ^{S})	*rpoS*	Stationary phase; starvation; global stress response	Tanaka *et al.* (1993); Battesti *et al.* (2011)
σ^{54} (σ^{N})	*rpoN*	Response to nitrogen deficiency	Merrick (1993)

Table 1-4 Mediators of stressors and their involvement in RpoS expression.

Mediators	Regulation of RpoS expression	Stressor	References
RelA/(p)ppGpp	Inhibit proteolysis	Amino acid starvation	Wendrich *et al.* (2002)
SpoT/(p)ppGpp	Inhibit proteolysis	Phosphate starvation	Bougdour & Gottesman (2007)
		Carbon starvation	Xiao *et al.* (1991)
		Fatty acid starvation	Battesti & Bouveret (2006)
		Iron limitation	Vinella *et al.* (2005)
		Oxidative stress	Chang *et al.* (2002)
PhoQ/PhoP	Inhibit proteolysis	Magnesium starvation	Bougdour *et al.* (2008)
DsrA	Increase translation	Low temperature	Sledjeski *et al.* (1996); Kandror *et al.* (2002)
ArcB/ArcA	Increase transcription, increase translation, and decrease proteolysis	Low energy and high oxygen levels	Mika & Hengge (2005)
RprA	Increase translation	Osmotic shock	Majdalani *et al.* (2001)

housekeeping genes controlling cell growth, with low cellular levels of σ^{38} maintained by reduced synthesis and rapid degradation (Battesti *et al.*, 2011). Upon starvation or exposure to stress, σ^{38} synthesis is induced while σ^{38} proteolysis is down-regulated, resulting in increased cellular concentration of RpoS (Battesti *et al.*, 2011). σ^{38} out competes σ^{70} and other alternative σ factors for binding to E, leading to increased formation of $E\sigma^{38}$ complex which results in RpoS-dependent gene expression and cross protection to a wide range of stress treatments (Battesti *et al.*, 2011; Hengge, 2009).

Genome-wide analysis of the *E. coli* K-12 strain MC4100 stress response network showed that RpoS controlled the expression of 481 genes (Weber *et al.*, 2005). Comparison of *E. coli* O157:H7 EDL933 wild type and the *rpoS* mutant showed that the expression of more than 1000 genes differed between the two strains by at least two-fold (Dong & Schellhorn, 2009b). Decreased expression of genes involved in acid resistance, hyperosmotic resistance, ethanol tolerance, and decreased survival under UV, heat and oxidative stress were observed for the *rpoS* mutant compared to the wild type. In addition, RpoS was found to regulate the expression of genes involved in substrate use, amino acid utilisation, and genes located on the LEE pathogenic island (Dong & Schellhorn, 2009b). Up-regulation of the expression of genes involved in different stress responses is likely to be responsible for RpoS-mediated cross protection (Battesti *et al.*, 2011).

1.5.2 Regulation of *E. coli* response to nutrient starvation

During the transition from feast to famine, transcription of *E. coli* stress-response proteins by RNAP activity is modulated by RpoS (Sharma & Chatterji, 2010). Regulation of RpoS levels during nutritional stress is primarily through (p)ppGpp which is synthesised by RelA or SpoT (Kanjee *et al.*, 2012). RelA synthesis of (p)ppGpp from ATP and GTP is induced by amino acid starvation. Induction of SpoT activity by other stress factors such as carbon, amino acid and phosphorus starvation results in the synthesis of (p)ppGpp and the inhibition of (p)ppGpp degradation (Kanjee *et al.*, 2012).

The nutrient availability of the environment is reflected by intracellular level of (p)ppGpp which regulates RpoS activity as well as Lrp (leucine responsive

protein)-regulon (Traxler *et al.,* 2011). Lrp is a global regulator of *E. coli* metabolism, for example, amino acid metabolism, nutrient transport and nitrogen metabolism (Newman & Lin, 1995). Traxler *et al.* (2011) proposed that the concentration of (p)ppGpp have differential effects on RpoS activation and the activities of Lrp regulon. Limited amino acid levels induces low level accumulation of (p)ppGpp activates the Lrp regulon which induces the synthesis of amino acids. In the absence of nutrients, (p)ppGpp accumulates to a high level, inducing both RpoS activity and the Lrp regulon. The mechanisms of ppGpp modulation of Lrp regulon and RpoS activity are yet to be identified (Gummesson *et al.,* 2009; Traxler *et al.,* 2011), however, Gummesson *et al.* (2009) proposed that ppGpp, together with DksA, an RNAP-binding protein, cause RNAP instability and thus promote RNAP-RpoS association. In addition, RpoS expression was found to be affected by other metabolic components such as $EIIA^{Glc}$ of the phosphoenolpyruvate: phosphotransferase system (PEP:PTS), where phosphorylation of $EIIA^{Glc}$ during nutrient transport repressed *rpoS* expression (Ueguchi *et al.,* 2001).

1.6 Aims and hypothesis

Although the gene(s) and pathway(s) responsible for the VBNC phenotypes have yet to be identified, resistance of VBNC cell to other stresses, as well as the detection of VBNC cells in foodstuffs and natural environments, support the hypothesis that VBNC is a survival strategy, and that these cells are a risk to human health and food safety (Dinu *et al.,* 2009; Oliver, 2010). This study aimed to characterise the impact of prolonged carbon starvation at both refrigeration and environmental temperatures on the recovery of *E. coli* O157:H7, and the impact of changes in metabolic potential during starvation on recovery. In addition, the potential role of *luxS*-mediated quorum sensing in starved-cell recovery was also investigated. We hypothesise that the phenotypic and metabolic characteristics identified form part of the adaptive behaviour of the *E. coli* O157:H7 in response to the changing environment encountered during their lifecycle in and around their mammalian hosts.

Chapter 2 Material and methods

2.1 Bacterial strains and plasmids

All bacterial strains were stored long-term in 25% glycerol at -80°C. Bacteria were cultured on tryptic soy agar (TSA) and in Luria-Bertani broth (LB). The bacterial strains used in this study are listed in Table 2-1. Two plasmids were used in this study: pCR®2.1-TOPO (Life Technologies; referred to as pCR2.1 in subsequent text) and pSS03. pSS03 was constructed by inserting a 874bp PCR fragment containing the coding region of *luxS* from *E. coli* E2348/69 into pCR2.1 (constructed by T. Gupta).

2.2 Media and chemical solutions

All media and chemical solutions were prepared in reverse osmosis filtered water (RO H_2O), autoclaved at 121°C for 20 minutes, or filter sterilised using a Stericup filter system with 0.22 μm GP Millipore Express® PLUS membrane (Millipore Corporation), and stored at 4°C (if required) unless otherwise stated.

2.2.1 Media

2.2.1.1 Luria-Bertani broth (LB)

10 g Bacto™ tryptone (Becton, Dickinson and Company), 5 g Bacto™ yeast extract (Becton, Dickinson and Company) and 5 g sodium chloride (BDH Laboratory Supplies) were added to 1 L RO H_2O and pH adjusted to 6.8. The broth was autoclaved and stored at 4°C.

2.2.1.2 Luria-Bertani broth agar (LA)

15 g Bacto™ agar (Becton, Dickinson and Company) was added to 1 L LB and pH adjusted to 6.8. Agar was dissolved by boiling for one minute prior to autoclaving and tempered at 50°C for pouring. Supplements were added immediately prior to pouring. Plates were stored at 4°C.

Table 2-1 Bacterial strains used in this study.

Strains	Source
E. coli MG1655	Jensen (1993)
E. coli MG1655 *luxS*$^-$	Helen Withers
E. coli MG1655 *sdiA*$^-$	Helen Withers
E. coli MG1655 *tnaA*$^-$	Helen Withers
E. coli O157:H7 NCTC12900	ATCC® 700728
E. coli O157:H7 NCTC12900 *luxS*$^-$	Katy Enfield (2004)
E. coli O157:H7 EDL933 *stx*$^-$	Helen Withers
E. coli O157:H7 Sakai *stx*$^-$	Helen Withers
E. coli O157:H7 N427	Faecal calf sample MIRINZ culture collection
E. coli O157:H7 N635	Calf hide sample MIRINZ culture collection
E. coli O157:H7 H11	Calf hide sample MIRINZ culture collection
E. coli O157:H7 ERL10780	Environmental Science & Research
E. coli O157:H7 ERL10630	Environmental Science & Research
E. coli O157:H7 ERL10621	Environmental Science & Research
Escherichia fergusonii H11	Calf hide sample MIRINZ culture collection
Vibrio harveyi MM32	Wong *et al*. (2009)

2.2.1.3 M9 minimal broth

5× M9 minimal salt solution was prepared by dissolving 56.4 g M9 minimal salts (Sigma-Aldrich, Co.) in 1 L RO H_2O. The stock solution was autoclaved and stored at 4°C. 1× M9 minimal broth was prepared by mixing 200 mL 5× M9 minimal salt solution, 1 mL 10 mg/mL thiamine (Sigma-Aldrich, Co.), 0.5 (w/v) casamino acids (Difco) and RO H_2O made up to 1 L. Carbon supplements were added as required to a final concentration of 0.2% (w/v).

2.2.1.4 Plate count agar broth (PCB)

5 g Bacto™ yeast extract (Becton, Dickinson and Company) and 2 g glucose (BDH Laboratory Supplies) were dissolved in 1 L RO H_2O (Atlas, 1995), and the pH adjusted to 7.0. The broth was autoclaved and stored at 4°C.

2.2.1.5 Plate count agar (PCA)

23.5 g Difco™ plate count agar powder (Becton, Dickinson and Company) was dissolved in 1 L RO H_2O and the pH adjusted to 7.0. The mixture was boiled for one minute, autoclaved and tempered to 50°C prior to pouring. Supplements were added as required immediately prior to pouring. Plates were stored at 4°C.

2.2.1.6 Tryptic soy broth (TSB)

30 g Bacto™ tryptic soy broth powder (Becton, Dickinson and Company) was dissolved in 1 L RO H_2O and the pH adjusted to 7.0. The broth was autoclaved and stored at 4°C.

2.2.1.7 Tryptic soy agar (TSA)

Pre-poured tryptic soy agar plates were supplied by Fort Richard.

2.2.1.8 Dulbecco's modified eagle medium (DMEM)

GIBCO® DMEM (Life Technologies) with 4.5 g/mL D-glucose, 4mM L-glutamine and 25 mM HEPES (4-(2-Hydroxyethyl) piperazine-1-ethanoesulfonic acid)

buffer was supplemented with 10% foetal bovine serum (FBS) (Life Technologies).

2.2.1.9 Marine agar (MA)

55.1 g Difco™ marine agar 2216 powder (Becton, Dickinson and Company) was dissolved in 1 L RO. The mixture was boiled for one minute, autoclaved and tempered to 50°C prior to pouring. Plates were stored at 4°C.

2.2.1.10 Autoinducer bioassay (AB) medium

Autoinducer bioassay (AB) medium was made according to Greenberg *et al*. (1979). AB base consisted of 0.3 M NaCl (BDH Laboratory Supplies), 0.05 M $MgSO_4$ (Sigma) and 0.2% (w/v) vitamin-free casamino acids (Bacto™, Difco) in RO H_2O adjusted to pH 7.5. AB base was autoclaved and kept at 4°C. Prior to use, 100 mL of AB base was supplemented with 1 mL of 1 M potassium phosphate buffer (1 M K_2HPO_4 and 1 M KH_2PO_4; BDH Laboratory Supplies), 1 mL of 0.1 M L-arginine (SERVA) and 2 mL of 50% glycerol (BDH Laboratory Supplies).

2.2.2 Chemicals

2.2.2.1 1× phosphate buffered saline (PBS)

Phosphate buffered saline (PBS) was prepared by dissolving one PBS tablet (Lorne Laboratory) in 1 L of RO H_2O and autoclaved once dissolved. PBS was stored at 4°C and allowed to warm up to room temperature prior to use.

2.2.2.2 20% glucose solution

20% w/v D-glucose (BDH Laboratory Supplies) was dissolved in RO H_2O, filter sterilised and stored at room temperature.

2.2.2.3 20% sodium pyruvate solution

20% w/v sodium pyruvate (Sigma-Aldrich, Co.) was dissolved in RO H_2O, filter sterilised and stored at room temperature.

2.2.2.4 20% sodium acetate solution

20% w/v sodium acetate (BDH Laboratory Supplies) was dissolved in RO H_2O, filter sterilised and stored at room temperature.

2.2.2.5 *N*-acyl-homoserine lactones (AHLs)

Dehydrated *N*-dodecanoyl-D,L-homoserine lactone (C12-HSL) (Sigma-Aldrich, Co.) and *N*-(3-oxohexanoyl)-L-homoserine lactone (3-oxo-C6-HSL) (University of Nottingham) were dissolved in ethyl acetate (BDH Ltd). Stock solutions were prepared at 10 μM and used at a final concentration of 5 nM.

2.3 Bacterial starvation in phosphate buffered saline

Changes in bacterial physiology during carbon starvation in PBS were monitored for 84 days using both culture-independent analysis of cell viability and culture-based assessment of recoverability. Where comparisons were made, *p* values less than 0.05 were considered statistically significant unless otherwise stated.

2.3.1 Culture preparation

Bacteria from -80°C frozen stock were streaked onto TSA and incubated at 37°C for 16 hours. Overnight cultures were prepared by inoculating 10 mL LB with several colonies. Cultures were incubated at 37°C with shaking at 200 rpm for 16 hours. The overnight culture was sub-cultured in LB at 1-in-100 dilution and incubated at 37°C with shaking at 200 rpm for 16 hours. The OD_{600} (NanoPhotometer, IMPLEN) of the sub-cultured broth culture was measured and adjusted to 1.0. A 4-mL inoculum with an OD_{600} of 1.0 was used to inoculate 400mL LB. Cultures were grown for 2 hours for exponential cultures, 3 hours for mid-exponential cultures, 4 hours for late-exponential cultures, and 8 hours for stationary phase cultures. Once grown to the desired growth phase, the cultures were divided into *a* and *b* biological replicates, and cells harvested 50 mL at a time by centrifugation at 3261 ×*g* for 10 minutes in a swing bucket rotor (Multifuge 3 S-R, Heraeus). The total volume harvested per replicate was 200 mL. The resulting cell pellet was washed twice in PBS at room temperature. After

the final wash, the cell pellet of each biological replicate was resuspended in 200 mL PBS.

2.3.2 Starvation conditions

Cell suspensions in PBS were held at either 4, 15 or 25°C for up to 84 days. When testing multiple starvation temperatures, the cultures were divided into smaller volumes and kept in sterile plastic containers of the same size. If only one starvation temperature was used, the entire 200 mL cell suspension was stored.

2.3.3 Sampling

Samples of starved cells were taken on the first day to establish Day 0 viability and recoverability baselines. Samples were taken every 14 or 28 days for the duration of the 84-day starvation period. Prior to sampling, the larger cell suspension volumes were mixed five times by gentle inversion, while the smaller volumes were mixed by gentle swirling.

2.4 Determination of cell viability

Cell viability was determined by epi-fluorescent microscopy using the LIVE/DEAD® *Bac*Light™ Bacterial Viability Kit (Molecular Probes). The dye mixture was prepared according to manufacturer's instructions. 0.15 µL of SYTO 9 and PI mixture was used per 50 µL of cell suspension. Cells were incubated for 15 minutes in the dark at room temperature. Once stained, the number of live cells was determined by counting green-fluorescent cells using a Helber counting chamber with Thoma ruling (Hawksley) using a fluorescent microscope viewed under oil immersion at 1000× magnification (Olympus BX60). The green-fluorescent cells were visualised using the U-MWIB filter (Table 2-2), and photographed using Nikon DS-5Mc and software Nikon NIS-Element Basic Research. The same field was photographed under both phase contrast and fluorescence. Two slides were prepared for each sample and a total of 16 squares were photographed per slide. Image analysis was performed using Adobe® Photoshop CS3 extended. The phase contrast photo of the slide was overlaid onto the fluorescence photograph of the same field, showing the location of the rulings

and a pre-drawn grid was overlaid on top of the rulings. Once the location of the rulings was defined, the phase contrast layer was hid and the number of green fluorescent cells counted. Cells located on the left and top borders of each square were counted but those on the right and bottom borders were not. The number of green fluorescent cells in the 16 squares photographed for each slide was tallied and the number of viable cells per mL was calculated.

Validation of this method was carried out using 100% live, 50% live/dead and 100% dead cell suspensions. For the 100% live culture, 10 mL fresh LB was inoculated with 100 µL of overnight culture and incubated at 37°C for 3 hours with shaking at 200 rpm. OD_{600} of the cultures was measured and adjusted to an OD_{600} of 1.0 using fresh LB. The live cell preparations were held on ice to prevent further growth. The dead cell suspension was prepared by mixing 300 µL of the live cell preparation with 700 µL of 100% ethanol. The ethanol/cell mixture was left at room temperature for one minute before dead cells were harvested by centrifugation at 1559 ×*g* for 10 minutes (Multifuge 3 S-R, Heraeus). The supernatant was removed and the pellet resuspended in 300 µL PBS. The 50% live/dead cell mixture was prepared by mixing equal volume of 100% live and 100% dead cells prior to staining. The number of culturable cells from the three cell suspensions was determined by plating a dilution series on TSA. Plates were incubated at 37°C for 24 hours.

To assess cell morphology of LIVE/DEAD-stained cells, cells were immobilised on agarose slides prepared by boiling 1% w/v agarose (GIBCO® agarose) in RO H_2O. The molten agarose was immediately filter sterilised using a MILLEX®-GP PES 0.22 µm syringe driven filter unit (Millipore Ireland Ltd.) to remove any particulate material that might interfere with imaging. 1 mL of sterile molten agarose was spread onto a glass slide and quickly covered with a coverslip. The coverslip was removed once the agarose had set, and 20 µL of stained cell suspension was spread onto the agarose surface. The slide was allowed to air dry in the dark at 30°C for 15 minutes before covering with a fresh coverslip and imaging. Cells were visualised using both phase contrast and fluorescent microscopy (Table 2-2). The same field was photographed under oil immersion at 1000× magnification phase contrast and both fluorescence filters using Nikon DS-5Mc and software Nikon NIS- Element Basic Research. Image analysis was

Table 2-2 Olympus fluorescence filter cubes used in this study.

Filter cube	Excitation filter (nm)	Dichroic mirror (nm)	Barrier filter
U-MWIB	460 – 490	505	420*
U-MWG	330 – 385	400	515*

*long pass filter

performed using Adobe® Photoshop CS3 extended. The fluorescent image was overlaid onto the phase contrast image.

2.5 Determination of culturability on solid media

Culturability of starved cells was determined by plating 50 μL of undiluted and/or serial-diluted sample onto each half of the divided PCA, TSA or supplemented agar plates. To allow comparison of colony development, all plates were incubated for 24 hours at 37°C, 48 hours at 37 or 25°C. All plates were counted immediately after incubation, or stored at 4°C for a maximum of 24 hours before counting. The concentration of culturable cells in each sample was calculated as cfu/mL. Anaerobic growth was tested by anaerobic incubation in a chamber (Whitley H35 Hypoxystation) with an atmospheric mixture of 5% H_2, 10% CO_2 and 85% N_2 by adding CO_2 to 5% H_2 in N_2 gas mix (BOC New Zealand).

2.5.1 Colony diameter measurement

During the pilot stage of starvation studies, the size of colonies recovered noticeably reduced and the variability in colony size increased during the course of starvation. A protocol was developed to standardise measurements of colony diameter. Selected plates from each starvation experiment were photographed using the same settings on the Alliance 4.7 (UVitec). The width, length and circularity of all colonies present was measured using Adobe® Photoshop CS3 extended. Appropriate thresholds were applied to the image to separate the colonies from background. A pre-made black mask was used to block the petri dish outline in the background. The improved contrast allowed selection of colonies using the 'Color Range…' selection function to select for the light coloured colonies with a fuzziness setting of 50. Selections were manually inspected before the 'Circularity', 'Height' and 'Width' measurements in pixels were recorded using the 'Ruler Tool' in Adobe® Photoshop CS3 extended. Data was analysed using Microsoft Excel®. Measurements of single colonies were distinguished from clusters of colonies by excluding measurements with unacceptable circularity of less than 0.80. The smaller of the width or height measurements was used as a measure of colony diameter to prevent measurements of doublet colonies appearing to be circular.

2.6 Growth analysis of culturability in broth

Growth kinetics of cells were assessed in a 96-well microtitre plate by inoculating 2× broth with inoculums adjusted to an OD_{600} of 0.02. The final OD_{600} of 0.01 was achieved in each well by mixing 100 µL inoculum with 100 µL 2× broth media. The microtitre plate was sealed with a Breathe-Easy™ gas permeable sealing membrane (Diversified Biotech) and incubated at 37°C for 24 hours in a VersaMax™ Microplate Reader (Associates of Cape Cod). OD_{600} readings were taken every 15 minutes with no shaking at time 0 sampling, and 10 second shaking between subsequent samplings.

2.7 Phenotype microarray

The metabolic activity of cells was assessed using the Phenotype MicroArrays™ (PM) plates (Biolog, Inc.). PM1 and PM2A MicroPlates™ Carbon Sources plates were used to test the ability of cells to utilise different substrates as the sole carbon source. Where comparisons are made, *p* values less than 0.05 were considered statistically significant unless otherwise stated.

2.7.1 Inoculum preparation

Broth cultures were centrifuged at 3261 ×*g* for 10 minutes in a swing bucket rotor (Multifuge 3 S-R, Heraeus). The supernatant was removed and cell pellet resuspended in 1× PBS.

Plate inoculums were prepared by mixing 12.5 mL of 1.2× PM IF-0a GN/GP Base (Biolog), 150 µL of 100× Biolog Redox Dye Mix A (Biolog), the volume of cell suspension in PBS required to achieve a final OD_{600} of 0.07 (85% transmittance), and the volume of sterile RO H_2O required to make a final volume of 15 mL. The final OD_{600} of the inoculums was checked prior to use.

2.7.2 Plate preparation and incubation conditions

Plates were prepared by dispensing 100 µL of inoculum into each well of the 96-well plate. A Breathe-Easy™ gas permeable sealing membrane (Diversified

Biotech) was used to seal the plate. The plate was incubated at 37°C for 24 hours in a VersaMax^{TM} Microplate Reader. Optical density measurements at 590 and 750 nm were taken every 15 minutes with no shaking at time 0 sampling, and 10 second shaking between subsequent samplings. The difference between OD_{590} and OD_{750} ($OD_{590-750}$) was calculated to determine the level of tetrazolium violet reduction in each well. $OD_{590-750}$ readings of substrates were normalised by subtracting the $OD_{590-750}$ reading of the negative control. The normalised value was used to determine the ability of cells to utilise a specific substrate as a carbon source ($A_{activity}$).

2.7.3 Measurements from kinetic curve

The kinetic data collected was plotted and features of the curves measured (Figure 2-1). All measurements were performed on individual replicates and the results averaged.

2.7.3.1 Endpoint ($A_{endpoint}$)

Endpoint substrate use ($A_{endpoint}$) was defined as the $A_{activity}$ at 24 hour time point.

2.7.3.2 Rate of exponential utilisation (μ_{exp})

A semi-automated system was used to determine the rate of exponential $A_{activity}$ (μ_{exp}). To avoid background noise, hourly data points were used to determine μ_{exp}. Automated modelling of the curves was performed using the grofit package developed by Kahm *et al.* (2010) in R (version 2.15.1). Input data was prepared in Microsoft Excel®, imported into R, and the program was run using the standard workflow described by Kahm *et al.* (2010). A comparison of best parametric and model-free spline fits on each data curve was shown as part of the standard workflow. Visual inspection of the fits was carried out, and the best fit, if any, was recorded.

A summary of the parameters was exported to an Excel worksheet. Based on visual inspections, if neither the parametric or model-free spline fit were appropriate, μ_{exp} was determined manually (Figure 2-2) using Equation 2-1:

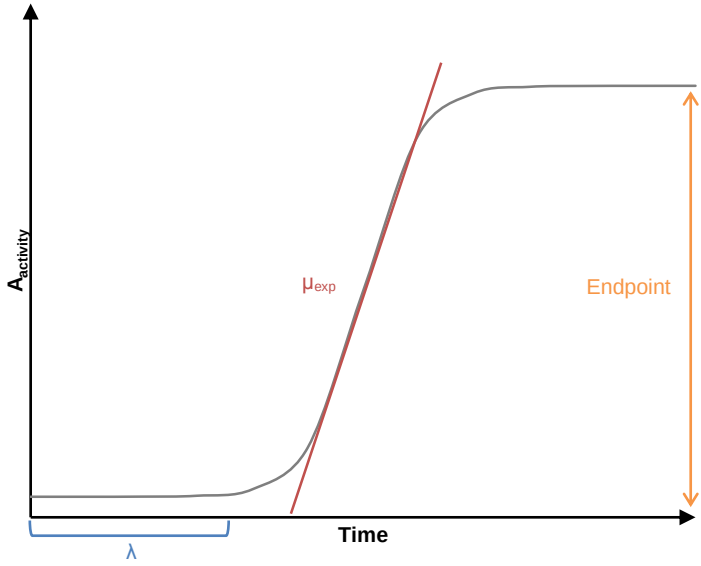

Figure 2-1 Measurements from the substrate utilization ($A_{activity}$) kinetic curve with data collection points indicated. Features of a typical sigmoid substrate utilization curve include the lag time (λ), the rate of exponential activity (μ_{exp}) and the endpoint activity ($A_{endpoint}$).

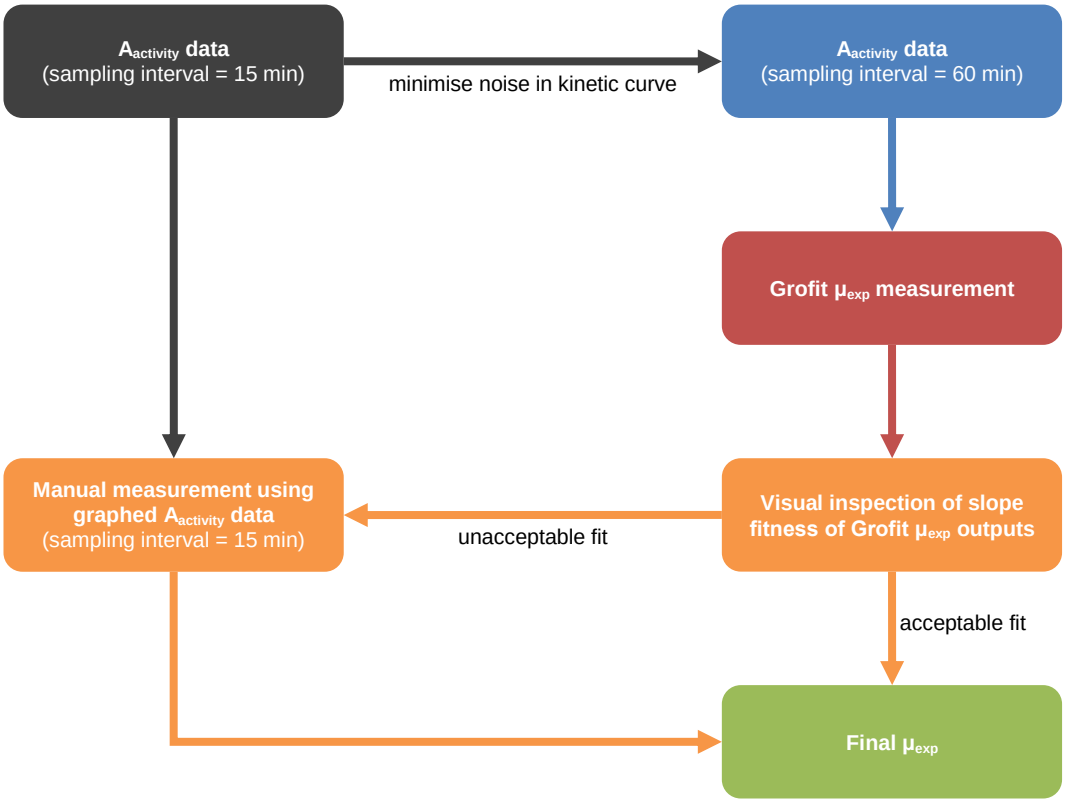

Figure 2-2 Schematic representation of the process involved in the determination of exponential rate (μ_{exp}).

$$\mu_{exp} = \left|\frac{A_1 - A_2}{T_1 - T_2}\right|$$

Equation 2-1 Formula for the determination of rate of exponential $A_{activity}$ (μ_{exp}), where: A_1 is the $A_{activity}$ value corresponding to time point 1 (T_1), and A_2 is the $A_{activity}$ value corresponding to time point 2 (T_2).

2.7.3.3 Lag time (λ)

The time point at which the corresponding $A_{activity}$ value became larger than the threshold of 0.01 was deemed the lag time (λ). Visual determination of λ was performed where the standard deviation between the λ of duplicates was larger than 2 or where the $A_{endpoint}$ was less than 0.250.

2.7.4 Statistical analyses

Phenotype MicroArrays™ assays for each test condition were performed in duplicate. Endpoint results from repeat experiments were combined and single factor analysis of variance (ANOVA) was performed using the Analysis ToolPak in Microsoft Excel®. The 'within group' mean square (MS) and degrees of freedom (df) values were used to calculate the least significant difference with 95% confidence ($LSD_{95\%}$). A carbon source was considered to be utilised if the difference between averaged $A_{endpoint}$ of the substrate and the negative control was larger than $LSD_{95\%}$. Where pairwise comparisons were made, the difference in average values must be larger than the $LSD_{95\%}$ to be deemed statistically significant.

2.8 Preparation of autoinducer-2 (AI-2)-containing conditioned media (CM) and CM agar

Conditioned media (CM) were prepared from NCTC12900 and NCTC12900 *luxS*$^-$ cultures grown in LB. The presence of AI-2 in NCTC12900 CM and the absence of AI-2 in NCTC12900 *luxS*$^-$ CM were determined using the *Vibrio harveyi* bioluminescence assay (VHBA).

2.8.1 Preparation of conditioned media

Conditioned media (CM) were made by growing NCTC12900 and NCTC12900 *luxS*$^{-}$ in LB for 8 hours at 37°C, followed by centrifugation of the culture at 3261 ×*g* for 10 minutes in a swing bucket rotor (Multifuge 3 S-R, Heraeus). The supernatant was filter-sterilised and the resulting CM was stored at -20°C until required.

2.8.2 *Vibrio harveyi* bioluminescence assay (VHBA)

The presence or absence of AI-2 in CM was determined using *V. harveyi* MM32 as described by Miller *et al.* (2004). *V. harveyi* MM32 was grown on MA from frozen stocks for 48 hours at 30°C. AB was inoculated with three freshly isolated colonies and incubated for 16 hours at 30°C with shaking at 200 rpm to an OD_{600} of 1.7. The *V. harveyi* MM32 culture was diluted 1:5000 in fresh AB and 10% (v/v) of test CM added. The mixture was incubated at 30°C with shaking at 200 rpm. Hourly samples of 200µL were dispensed into a black µClear® bottom 96-well microtitre plate (Greiner Bio-one). OD_{600} and light emission were measured using Wallac 1420 VICTOR^{2TM} (PerkinElmer Inc.)

2.8.3 Preparation of conditioned media (CM) agar

Equal volumes of CM and autoclaved 3% (w/v) Bacto™ agar held at 45°C were mixed and poured.

Chapter 3 Phenotypic analysis of starved cells

3.1 Introduction

E. coli O157:H7 maintains a dual lifestyle within the host and in the environment. Survival of *E. coli* O157:H7 has been documented in a wide variety of environments, including water, soil as well as the hide of animals (Arthur *et al.*, 2011; Avery *et al.*, 2005; Ibekwe *et al.*, 2004). LeJeune *et al.* (2001) showed that *E. coli* O157:H7 was able to survive in water troughs for up to 245 days and remain infectious. Starvation in aquatic environments outside the optimal growth temperatures is known to induce a physiological state in at least 20 human pathogens where the number of cells able to recover on routine bacteriological media declines over time while remaining viable (Oliver, 2010). This phenomenon, termed the viable but non-culturable (VBNC) state, has been proposed to be a physiological adaptation where bacterial species, including *E. coli* O157:H7, persist in unfavourable conditions for long periods of time by maintaining low metabolic activity while retaining the ability to resume growth upon encounter of favourable conditions (Dinu *et al.*, 2009). While carbon limitation is one of the main inducers of VBNC, the viability and culturability of starved cells also depends on the starvation temperature and the growth phase of cells prior to VBNC induction (Na *et al.*, 2006; Navarro Llorens *et al.*, 2010; Rigsbee *et al.*, 1996; Zhao & Matthews, 2000).

3.2 Results

Nutrient deprivation and decreased temperatures were hypothesized to be the major stresses encountered by *E. coli* O157:H7 in aqueous environments outside of mammalian hosts. *E. coli* O157:H7 cells were harvested and resuspended in PBS at pH 6.8 to mimic carbon starvation. Cells were held at either 15°C to mirror the average water temperature of New Zealand freshwater in warmer months; or at 4°C to simulate the freshwater temperature in winter as well as the refrigeration temperature of food storage (National Institute of Water and Atmospheric Research, 2011). In addition, starvation was carried out at the intermediary temperature of 25°C, which is at the lower end of the optimal growth temperature range for *E. coli* O157:H7. Viability and culturability of starved cells

were monitored over 84 days. Definition of viability and culturability in the context of this study is shown in Figure 3-1.

3.2.1 Detection of viability and phenotypic changes

Since the culturability of cell populations is expected to decline over the duration of starvation, a method for culture-independent quantification of viable cells was required to assess bacterial survival. In this study, viability was determined using live/dead staining (LIVE/DEAD® *Bac*Light™ Bacterial Viability Kit) and quantified in a counting chamber. To monitor changes in colony recovery during starvation, a standardised culturing method was developed to quantitatively compare the number of culturable cells as well as the diameter of colonies recovered.

3.2.1.1 Quantitative analysis of cells with intact membranes using live/dead fluorescent microscopy

The effectiveness live/dead fluorescent microscopy as a culture-independent viability test was determined by assessing the correlation of colony recovery on TSA and the number of SYTO 9 and PI-stained cells for 100% live, 100% dead and 50% live/dead cell suspensions (Figure 3-2).

The average number of viable cells determined by live/dead analysis from the 100% live cell suspension was significantly higher (19%, $p<0.05$) than the average number of colonies recovered on TSA for MG1655. While live/dead analysis detected a higher number of viable NCTC12900 cells than colony recovery on TSA, the difference was not statistically significant due to the large standard deviation observed for TSA recovery.

From the 50% live/dead cell suspension, the average viability and colony counts were expected to be 50% of that observed for 100% live cell suspensions. Colony counts on TSA averaged 48 and 51% of that observed for 100% live cell suspensions for MG1655 and NCTC12900, respectively; which were not significantly different than expected. SYTO 9 staining detected the expected number of live cells for MG1655 and NCTC12900, averaged 50 and 49% of that observed for 100% live cell suspension, respectively. However, the number of

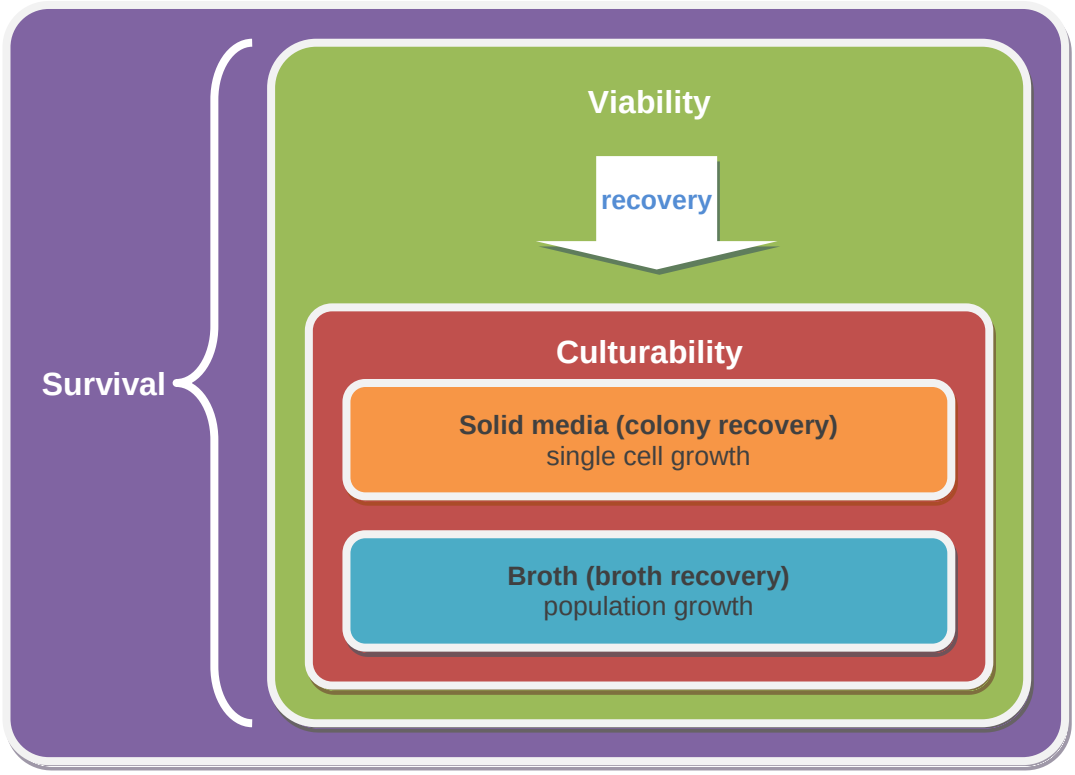

Figure 3-1 Summary of the terms used in the starvation studies presented. Survival was defined as the maintenance both viability and culturability. The viable cell population includes nonculturable cells and culturable cells able to recover on either solid media or in broth.

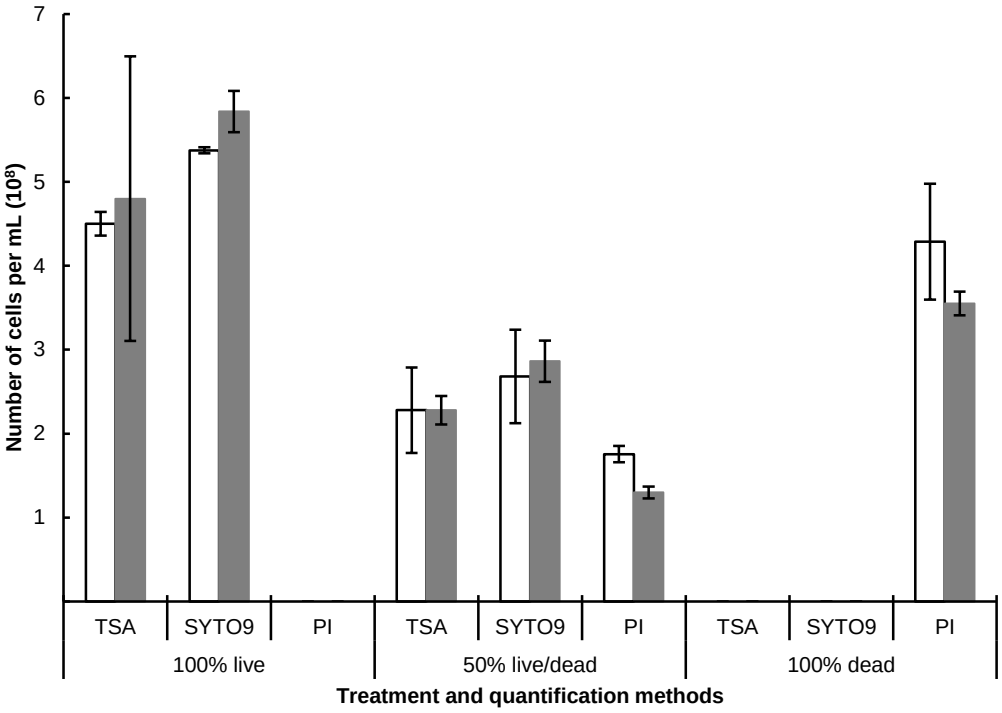

Figure 3-2 Comparison of the number of viable cells detected using culture-dependent and culture-independent methods. Growth on TSA MG1655 (hollow bars) and NCTC12900 (grey bars) after 24 hours of incubation at 37°C was used as the culture-dependent method of viable cell detection. Culture-independent detection was performed using SYTO 9 (viable cell stain) and PI (dead cell stain). Results are the average of two technical replicates and the standard deviation is indicated by the error bars.

dead cells detected by PI staining was significantly lower than expected ($p<0.05$), where the average was 17 and 28% lower than expected for MG1655 and NCTC12900, respectively.

No colonies were recovered from the ethanol-treated 100% dead cell suspension and no SYTO 9-stained cells were observed. While the number of PI-stained cells in the 100% dead cell suspension was expected to be the same as the number of SYTO 9-stained cells in the 100% live cell suspension, the actual number observed was significantly lower ($p<0.05$) than expected. The average number of PI-stained cells was 20 and 39% lower than expected for MG1655 and NCTC12900, respectively.

The inconsistency observed between the number of PI-stained cells and the expected number of dead cells in the 50% live/dead and 100% dead cell suspensions may be due to the dissipation of DNA from dead cells with damaged membrane. To test this hypothesis, the morphology of EDL933 prior to starvation and after 28 days of starvation at 4°C was compared by immobilising SYTO 9 and PI-stained cells on 1% agarose slides. Prior to starvation, the location of SYTO 9 fluorescence in the field was within the cell outlines observed under phase contrast (Day 0, Figure 3-3). Similarly, fluorescence detected from SYTO 9-stained day 28 cells was confined within the cell outline observed under phase contrast (Day 28, Figure 3-3). While most PI-stained DNA located in the centre of the day 0 cells observed under phase contrast, some smears of PI staining were observed without any corresponding intact cell outline. By day 28, the majority of the PI-stained cells were smears of DNA located outside of cell outlines under phase contrast or (white arrows; Figure 3-3).

Results confirmed the hypothesis that DNA dissipated from cells with damaged membranes, which meant PI-staining of dead cells underestimated the true number of dead cells. Therefore, determination of viable count was based on the quantification of SYTO 9-stained cells in cell suspension stained with both SYTO 9 and PI. PI staining was used to discount the dead cells at the time of sampling.

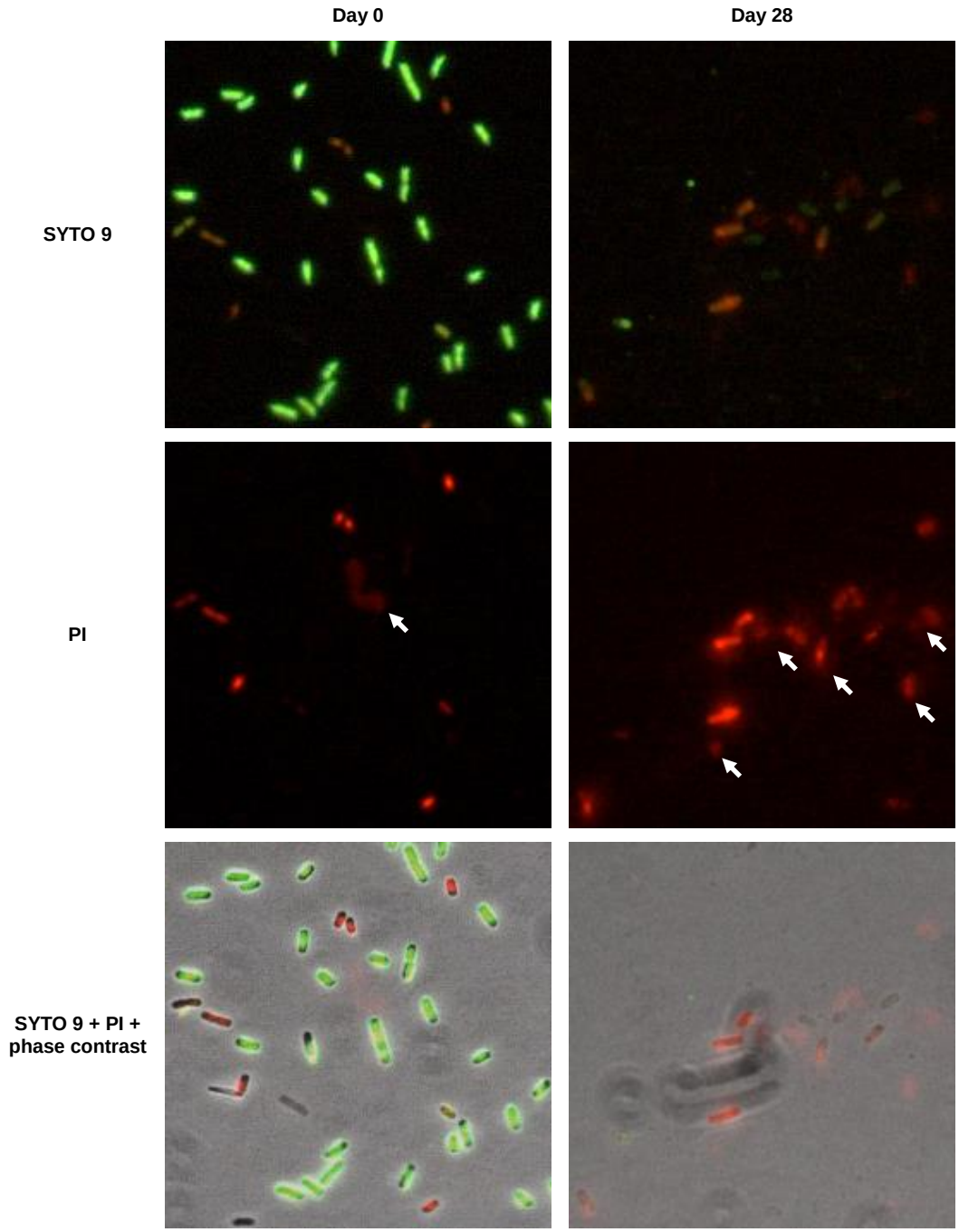

Figure 3-3 Live/dead stained cells sampled from non-starved (Day 0) and starved (Day 28) EDL933 cultures. The same field of view was photographed under phase contrast, 460 to 490 nm excitation for SYTO 9 and 330 to 385 nm excitation for PI. White arrows indicate areas within the field where PI-stained DNA smears were observed.

3.2.1.2 Assessment of culturability on solid media

Culturability of individual cells within a population was determined based on the ability of each cell to form a colony on solid media after 24 hours of incubation at 37°C, or 48 hours at 25°C. By standardising the duration of incubation and the method of photography, the number of colonies and their diameters from different plates and different sampling day were made comparable. To ensure accuracy in the colony size measurements, the circularity, vertical and horizontal widths of the colonies were measured by a semi-automated program designed in this study using the Adobe Photoshop platform. The colony diameter was measured in pixels; each pixel is equivalent to 0.09901 mm, or 20.2 pixels in 1 mm.

To determine the effect of nutrient concentration on colony growth prior to starvation, late-exponential cells were plated onto both PCA and TSA (Table 3-1). TSA has a higher concentration of available nutrients compared to PCA, however, no significant difference in the number of colonies recovered was observed. This suggested that nutrient concentration did not affect colony growth of late-exponential cells on solid media. The effect of nutrient concentration on the size of colonies developed was assessed by measuring the diameter of colonies formed on plates without visible colony crowding (Figure 3-4). The distributions of colony diameters were narrow. The diameter of the majority of colonies measured was between 40 and 60 pixels for MG1655, EDL933, Sakai and NCTC12900; and between 30 and 50 pixels for the bovine (H11- and H11+) and clinical strains (ERL10621, ERL10630 and ERL10780). In all cases, no significant difference in mean diameter was observed for colonies recovered on PCA and TSA.

3.2.2 Viability and culturability of starved *E. coli* K-12 and O157:H7

Viability and culturability of MG1655, an *E. coli* K-12 strain often used in cell physiology studies, NCTC12900, the *E. coli* O157:H7 reference strain, and the toxin-minus derivatives of the clinical strains EDL933 and Sakai were assessed by starving cells in PBS at 4, 15 and 25°C. Viability, as determined by live/dead analysis and culturability on solid media were monitored every 28 days for 84 days. Culturability in broth was also assessed for non-starved (day 0) cells and cells starved at 4°C for 28 to 34 days.

Table 3-1 Colony counts of cells harvested from late-exponential cultures of different *Escherichia* strains on PCA and TSA at 37°C for 24 hours. The colony counts are the average of four technical replicates and the standard deviations are shown in brackets.

	Colony counts (log_{10} cfu mL^{-1})	
Strains	**PCA**	**TSA**
EDL933	8.63 (0.03)	8.76 (0.12)
Sakai	8.67 (0.02)	8.78 (0.09)
ERL10621	8.53 (0.07)	8.62 (0.11)
ERL10630	8.57 (0.09)	8.64 (0.18)
ERL10780	8.57 (0.07)	8.60 (0.10)
H11-	8.60 (0.06)	8.64 (0.07)
H11+	8.62 (0.08)	8.63 (0.07)
MG1655	8.80 (0.05)	8.85 (0.08)
NCTC12900	8.49 (0.06)	8.59 (0.07)

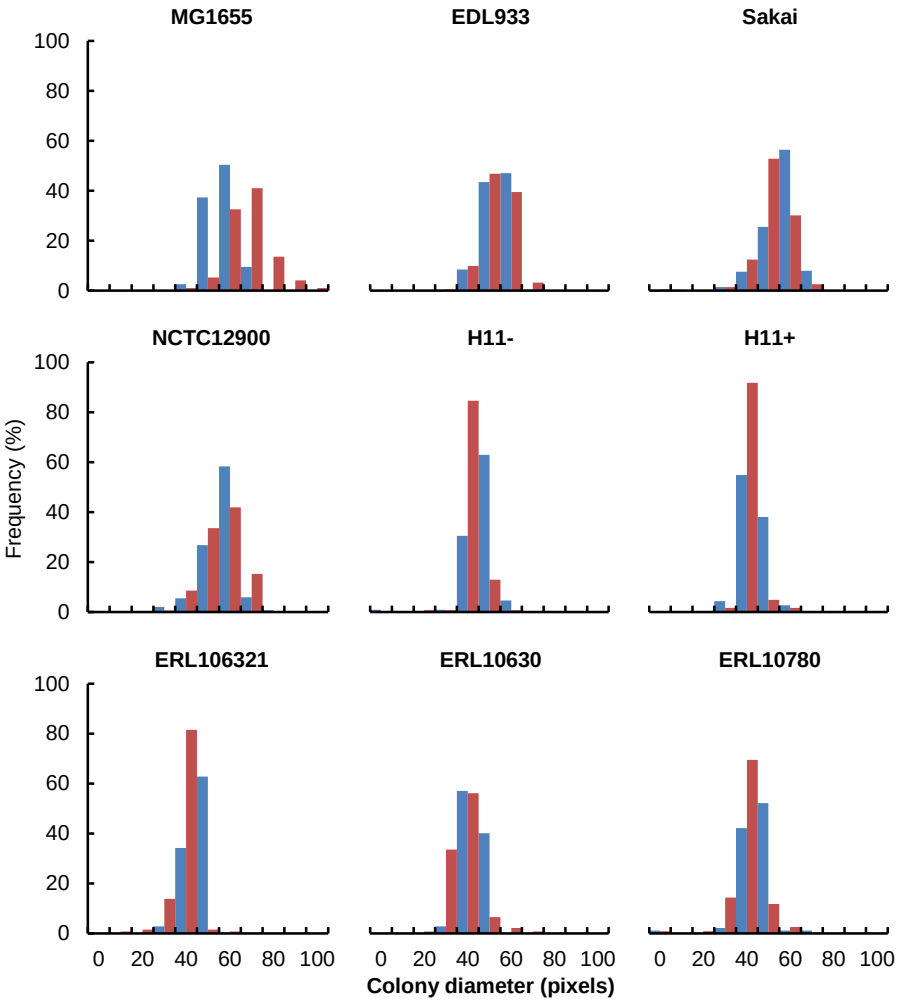

Figure 3-4 Distribution of the diameters of colonies formed by late-exponential cells on PCA and TSA following incubation at 37°C for 24 hours. The blue and red bars represent the percentage of colonies within each diameter category on PCA and TSA, respectively. Data obtained from the measurement of a minimum of 50 colonies.

3.2.2.1 The effect of growth phase prior to starvation at 4°C on the viability and colony recovery of NCTC12900

The length of time required to achieve early-, mid-, late-exponential and stationary phase cultures was determined (Figure 3-5). Cells harvested from each of the four growth phases indicated were used to examine the effect of growth phase and cell metabolic activity prior to starvation on viability and colony recovery of cells after starvation in PBS at 4°C.

Despite the slight decreases in viable count, the number of viable cells in the starved culture remained high for 84 days. For cells harvested during early-exponential phase, a significant decrease ($p<0.05$) of 0.58 logs in viability was observed within the initial 28 days of starvation. The number of viable cells, however, remained between 7.28 and 7.36 logs for the remainder of starvation period. A gradual decline in viable count was observed for the mid-exponential cell cultures over 84 days (Figure 3-6). Viable count on day 56 and 84 were 0.58 and 0.73 logs lower than day 0, respectively; all of which were statistically significant ($p<0.05$). Similar to those harvested during early-exponential phase, a statistically significant ($p<0.05$) decrease in viable count was observed within 28 days of starvation for stationary phase cell cultures, which then remained between 8.8 and 8.92 logs for the remainder of the assessment period. No significant change in viable count during the 84-day starvation period was observed for the late-exponential phase cell cultures (Figure 3-6).

Colony recovery of early-, mid-, late-exponential and stationary phase NCTC12900 cells starved at 4°C was assessed using PCA and TSA. In all cases, colony count was lower than the viable count (Figure 3-6). The growth phase during which the cells were harvested prior to starvation affected the pattern of recovery on both TSA and PCA during the 84-day starvation. In general, lower recovery was observed for early growth phase cell cultures compare to cells harvested during later phases, especially on TSA (Figure 3-6). In addition, the difference between the number of colonies recovered on PCA and TSA increased during the course of starvation, with the exception of early-exponential phase cell cultures (Figure 3-6).

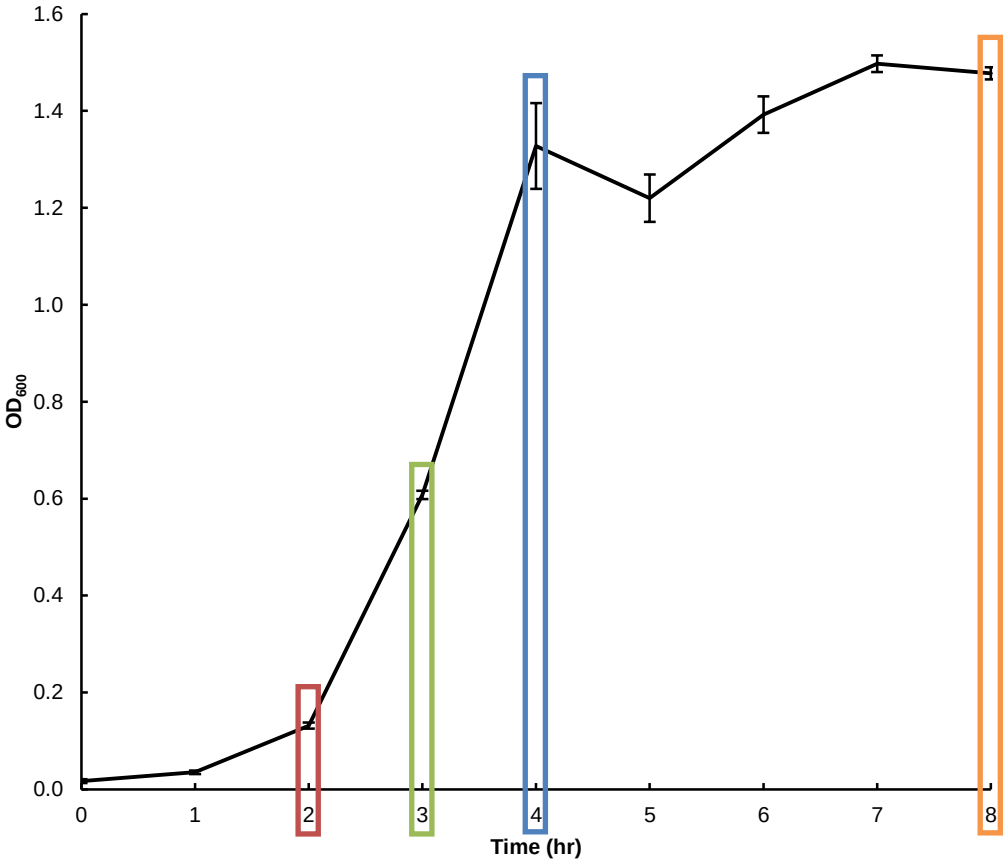

Figure 3-5 Growth curve of NCTC12900 in TSB incubated at 37°C with shaking at 150 rpm. Cells collection points at early- (□), mid- (□), late-exponential (□) and the stationary (□) phases are indicated by coloured rectangles. Data points represent the average of two repeats. Standard deviations are indicated by the error bars.

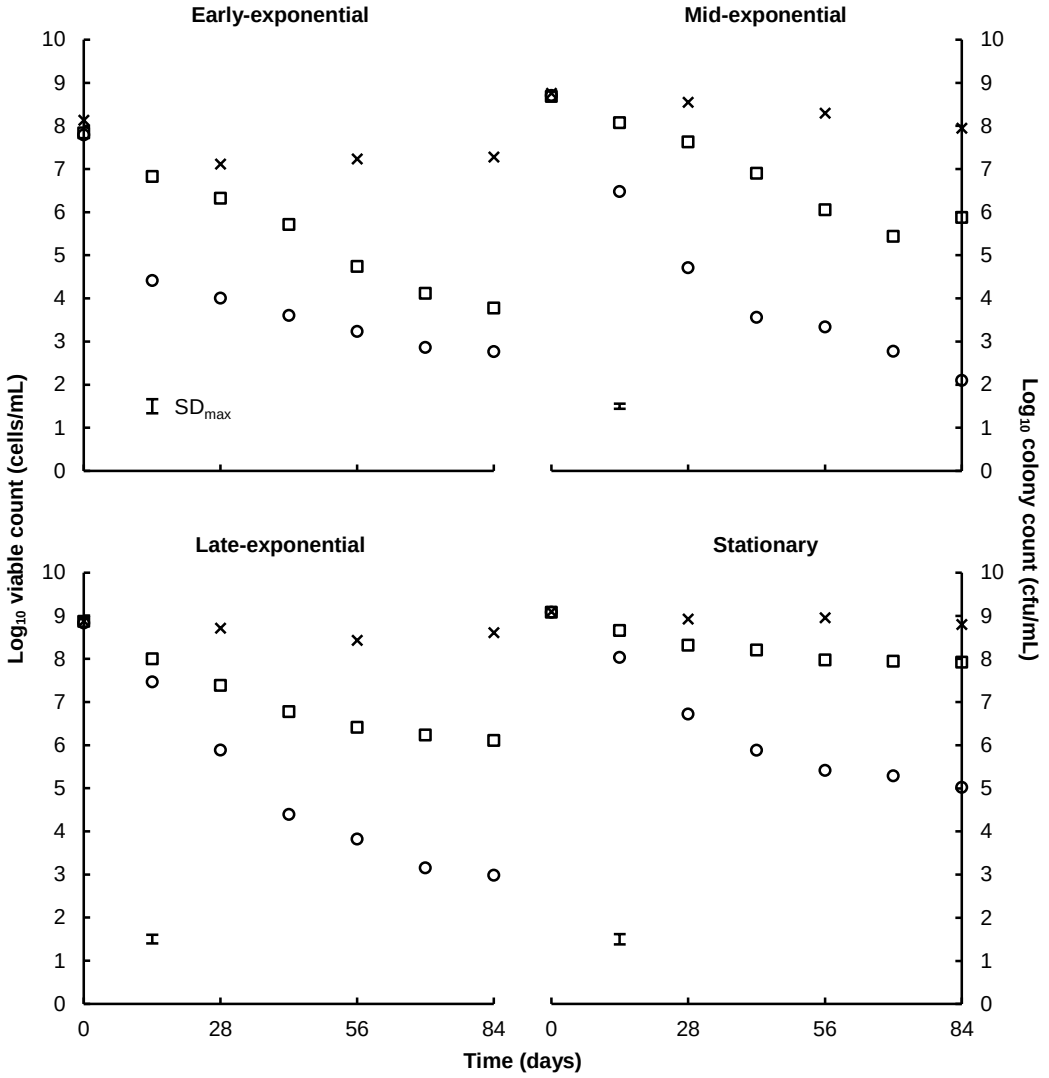

Figure 3-6 Viability and colony recovery of early-, mid-, late-exponential and stationary phase NCTC12900 cell cultures starved in PBS at 4°C for 84 days. Viable count (×) and the number of colonies present after incubation at 37°C for 24 hours on TSA (□) and PCA (○) are shown. Each viable count data point shows the average of two technical repeats. Each colony count data point is the average of four technical replicates. The maximum standard deviation (SD_{max}) is indicated by the error bar on each graph. Data shown are representative of two biological repeats.

Recovery on PCA for early- and mid-exponential phase cell cultures decreased by 2 logs within 28 days of starvation; followed by a gradual decline in recovery for the remainder of the assessment period (Figure 3-6). Interestingly, the number of colonies recovered on day 84 from early-exponential phase cell cultures was 0.64 logs higher than that from mid-exponential phase cell cultures; a difference that was statistically significant ($p<0.05$). Statistically significant ($p<0.05$) and gradual decreases in recovery were observed for late-exponential and stationary phase cell cultures during the 84-day starvation, with stationary phase cell cultures maintaining the highest level of colony recovery on PCA and TSA.

The level of recovery on TSA was consistently higher than PCA, and gradual declines were observed for all cultures (Figure 3-6). By day 84, recovery on TSA was 3 to 4 logs higher than PCA for mid-, late-exponential and stationary phase cell cultures, while a one-log difference was observed for early-exponential cell cultures. In addition, the difference in viable count and recovery on TSA on day 84 was statistically significant for all cultures, with the greatest difference observed for early-exponential phase cells and the least difference for stationary phase cells.

Since the greatest proportion of viable cells were detected from late-exponential phase cell cultures with the most significant difference in colony recovery on PCA and TSA observed, late-exponential phase cell cultures were used for investigation into changes of viability and culturability of other *E. coli* strains during starvation in PBS.

3.2.2.2 Viability and colony recovery of late-exponential cells starved at 4°C

To investigate whether the viability and colony recovery phenotypes observed for NCTC12900 during starvation differed to that for other *E. coli* strains, MG1655, EDL933 and Sakai, cells were harvested during late-exponential phase and starved in PBS at 4°C (Figure 3-7). Trends in viable count and colony count on TSA and PCA were similar for NCTC12900, EDL933 and Sakai. However, while the change in viable count and recovery on TSA during the 84-day starvation was similar for MG1655 and NCTC12900, the level of MG1655 recovery on PCA was significantly higher ($p<0.05$) than NCTC12900, EDL933 and Sakai.

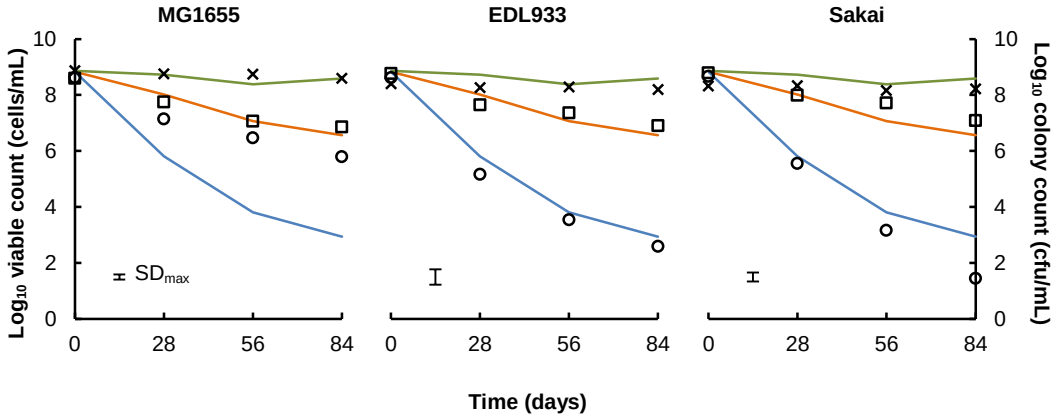

Figure 3-7 Viability and colony recovery of late-exponential MG1655, EDL933 and Sakai starved in PBS at 4°C for 84 days. Viable count (×) and the number of colonies present after incubation at 37°C for 24 hours on TSA (□) and PCA (○) are shown. For reference, the trends of viable count (–) and recovery on TSA (–) and PCA (–) for 4°C-starved late-exponential NCTC12900 (Figure 3-6) are shown on each graph. Each viable count data point shows the average of two technical repeats. Each colony count data point is the average of four technical replicates. The maximum standard deviation (SD_{max}) is indicated by the error bar on each graph. Data shown are representative of two biological repeats.

No significant difference in viable count was observed for MG1655 or EDL933 during 84 days of starvation at 4°C (Figure 3-7). A slight but statistically significant (p<0.05) decrease in viable count was observed for Sakai, where viable count declined by 0.16 logs within 56 days of starvation, and remained above 8 logs for the remainder of the assessment time. Gradual decreases in recovery on PCA and TSA were observed for MG1655, EDL933 and Sakai (Figure 3-7). By day 84, MG1655 recovery on PCA and TSA had declined by 2.8 and 1.7 logs, respectively. For EDL933 and Sakai, recovery on PCA decreased by 6.0 and 7.2 logs during the 84-day starvation, respectively; and the decrease in recovery observed on TSA was 1.9 and 1.7 logs, respectively.

3.2.2.3 Effect of starvation temperature on viability and colony recovery of MG1655 and NCTC12900

To investigate the effect of starvation temperature on the viability and colony recovery of starved cells, MG1655 and NCTC12900 were harvested during late-exponential phase and starved at 15 and 25°C. The viability and recovery on PCA and TSA of cells held at 15 and 25°C were compared to observations made for cells starved 4°C (Figure 3-8).

The change in viable count for MG1655 and NCTC12900 during the 84-day starvation at 15 and 25°C was similar to that observed for cells held at 4°C. No significant change in viability was observed for 15°C-starved MG1655 over 84 days. For MG1655 starved at 25°C, no significant change in viable count was observed during the first 56 days, however, the number of viable cells detected on day 84 was 0.45 logs lower than day 0, a difference that was statistically significant (p<0.05). For NCTC12900, starvation at 25°C did not result in any change in viable count over 84 days. A statistically significant (p<0.05) decrease in viability was observed for NCTC12900 starved at 15°C, where the viable counts on day 56 and 84 were 0.20 and 0.37 logs lower than day 0.

While recovery on TSA for both strains starved at 15 and 25°C was similar to that observed from 4°C-starved cells, recovery on PCA was significantly higher (p<0.05) for 15 and 25°C-starved cultures compared to 4°C-starved cultures (Figure 3-8). In general, gradual declines in culturability were observed for

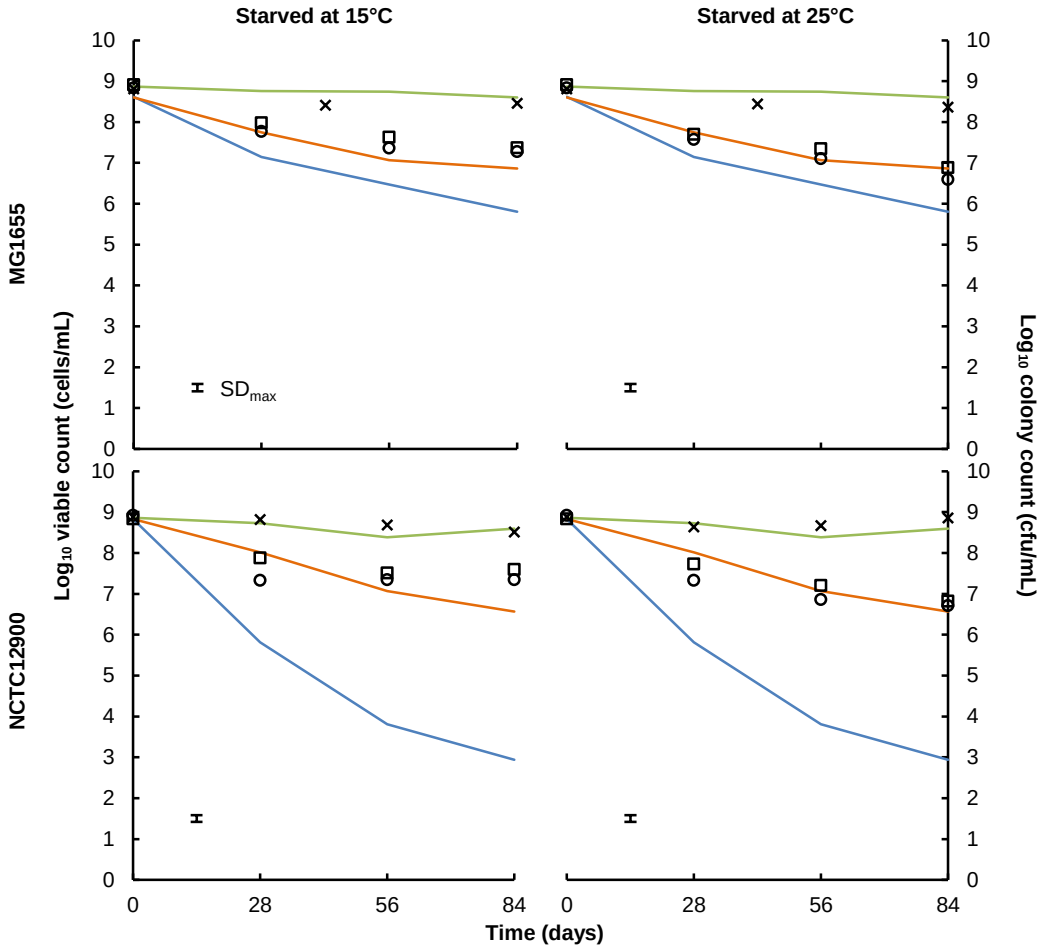

Figure 3-8 Viability and colony recovery of MG1655 and NCTC12900 starved at 15 and 25°C compared to cells starved at 4°C. Viable count (×) and the number of colonies present after incubation at 37°C for 24 hours on TSA (□) and PCA (○) are shown. For reference, the trends of viable count (–) and recovery on TSA (–) and PCA (–) for 4°C-starved late-exponential MG1655 (Figure 3-7) and NCTC12900 (Figure 3-6) are shown on each graph. Each viable count data point shows the average of two technical repeats. Each colony count data point is the average of four technical replicates. The maximum standard deviation (SD_{max}) is indicated by the error bar on each graph. Data shown are representative of two biological repeats.

cultures starved at 15 and 25°C, and there was very little difference between recovery on PCA and TSA. The decline in colony recovery was greater for the 25°C-starved cultures compared to the 15°C-starved cultures. By day 84, recovery on PCA and TSA were significantly lower than at the start of the assessment in all cases. For cultures starved at 15°C, a maximum decline of 1.5 logs was observed on PCA and TSA; a decline of 2.2 and 2.0 logs was observed on PCA and TSA for cultures starved at 25°C, respectively. No significant difference in recovery on PCA and TSA was observed for cultures starved at 15 and 25°C (Figure 3-8), with the exception of day 28 where recovery on TSA was significantly higher ($p<0.05$) than on PCA.

3.2.2.4 Effect of recovery temperature on the colony recovery

The standard incubation temperature and time for colony recovery used in this study was 37°C for 24 hours. To test the effect of different incubation conditions on the number of colonies recovered, plates inoculated with 4°C-starved EDL933 and Sakai were incubated at 37 or 25°C for 48 hours. Incubation at 37°C for an extended period of 48 hours did not result in any significant change in recovery (data not shown). A sharper decrease in starved-cell recovery was observed for plates incubated at 25°C for 48 hours compared to plates incubated at 37°C for 24 hours during 84 days of starvation. The observed differences in recovery were statistically significant from day 14 to day 84 (Figure 3-9). On day 84, recovery on PCA incubated at 25°C was 0.5 logs lower than plates incubated at 37°C for EDL933, and was below the limit of detection for Sakai. The difference in recovery between TSA incubated 25 and 37°C on day 84 was 2.3 and 1.9 logs for EDL933 and Sakai, respectively.

3.2.2.5 Effect of supplements on recovery

For cultures starved at 4°C, differences in recovery on nutrient-rich TSA and the nutrient-limited PCA had been observed for all strains tested. To further test the hypothesis that recovery is dependent on the metabolic status of the starved cells, a range of carbon sources associated with glycolysis and the TCA cycle were tested on late-exponential phase EDL933 and Sakai after 49 days of starvation at 4°C (Table 3-2).

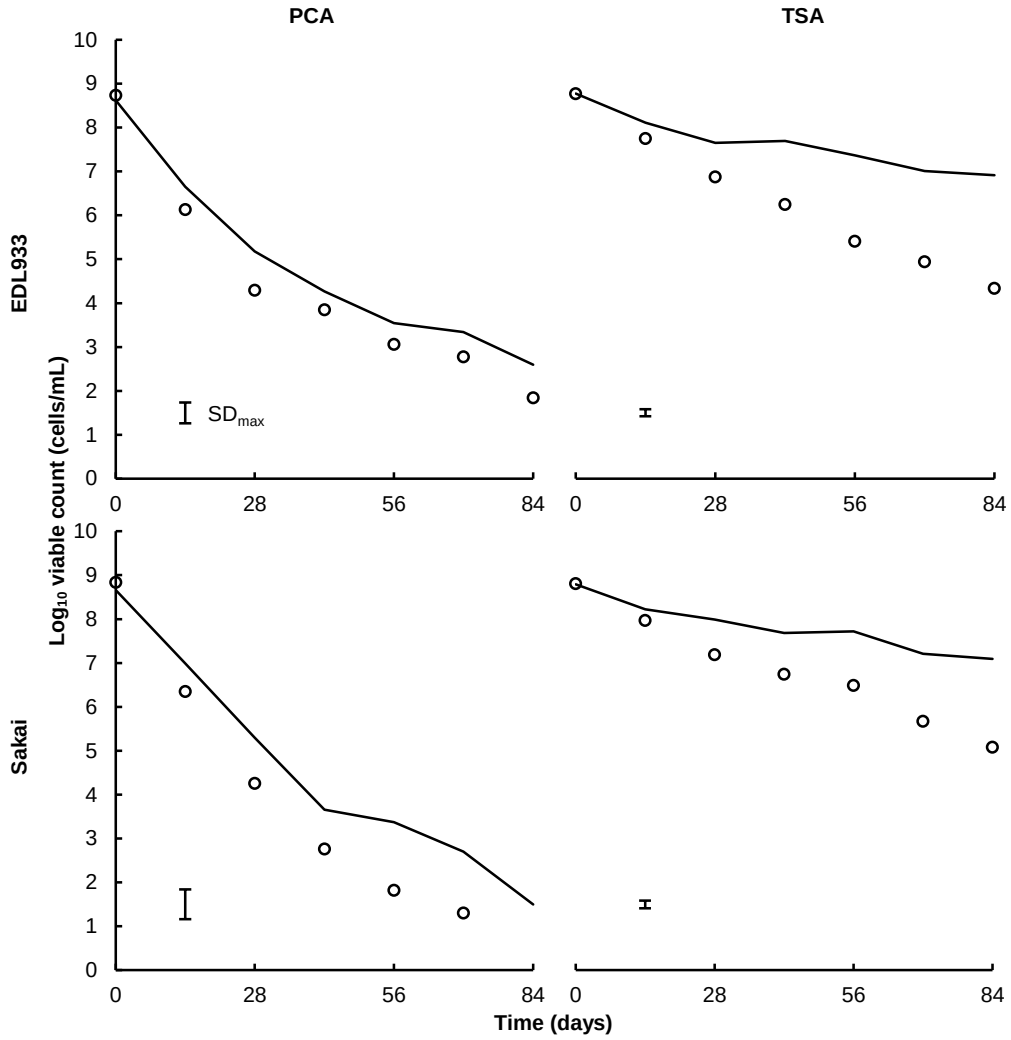

Figure 3-9 Recovery of EDL933 and Sakai starved at 4°C for 84 days on PCA and TSA incubated at 25°C for 48 hours. For reference, the trends of recovery on plates incubated at 37°C for 24 hours (–) (Figure 3-7) are shown on each graph. Each colony count data point is the average of four technical replicates. The maximum standard deviation (SD_{max}) is indicated by the error bar on each graph. Data shown are representative of two biological repeats.

Table 3-2 Recovery of starved EDL933 and Sakai harvested on day 49 on PCA, supplemented PCA and TSA after incubation at 37°C for 24 hours. The colony counts are the average of four technical replicates and the standard deviations are indicated in brackets.

	Colony counts (cfu/mL)	
Media	**EDL933**	**Sakai**
PCA	3.31 (0.32)	3.25 (0.24)
PCA with 0.2% casamino acids	4.70* (0.18)	4.68* (0.39)
PCA with 0.2% glucose	4.24* (0.34)	3.99* (0.51)
PCA with 0.2% glycerol	4.26* (0.18)	4.05* (0.18)
PCA with 0.2% sodium acetate (PCAace)	4.09* (0.17)	3.45 (0.21)
PCA with 0.2% sodium pyruvate (PCApyr)	5.20* (0.08)	6.27* (0.06)
PCA with 0.2% sodium succinate	4.27* (0.14)	3.63 (0.29)
PCA with 0.2% trisodium citrate	4.02* (0.15)	4.28* (0.03)
TSA	7.30 (0.04)	7.36* (0.11)

* Supplementations resulting in statistically higher recovery on PCA

Abbreviations of media indicated in brackets.

In general, supplementing PCA with additional carbon sources resulted in an increase in colony recovery, except for addition of sodium acetate and sodium succinate (Table 3-2). Of the carbon sources tested, supplementation with 0.2% sodium pyruvate (PCApyr) resulted in the highest increase in recovery, where a 1.9 and 3.0 log increase was observed for EDL933 and Sakai, respectively. However, recovery on PCApyr did not reach the level of recovery observed on TSA. Supplementation with sodium acetate (PCAace) had the least impact on the number of colonies recovered for both EDL933 and Sakai. Visual inspection of colony morphologies revealed that colonies recovered on PCAace appeared smaller than those observed on PCA without supplementation while colonies recovered on PCApyr appeared larger.

To test the effect of pyruvate and acetate supplementation on recovery during starvation at 4°C, the number of MG1655, NCTC12900, EDL933 and Sakai colonies recovered on PCApyr and PCAace was monitored over 84 days. No significant difference was observed in the number of colonies recovered on PCApyr and PCA for MG1655 (Figure 3-10). On day 84, the colony count on PCApyr for NCTC12900, EDL933 and Sakai was 3.1, 1.9 and 4.0 logs higher (p<0.05) than unsupplemented PCA, respectively (Figure 3-10). Increasing the concentration of sodium pyruvate to 0.5% did not result in any additional improvements in recovery (data not shown). Supplementing TSA with 0.2% and 0.5% sodium pyruvate had no significant effect on colony count (data not shown). In all cases, supplementing PCA with sodium acetate did not have any significant effect on the number of colonies recovered.

The effect of incubation temperature on starved-cell recovery on PCApyr and PCAace was tested by incubating plates at 25°C for 48 hours. Similar to the observation made on PCA and TSA, the number of EDL933 and Sakai colonies recovered on PCApyr and PCAace after incubation at 25°C was significantly lower (p<0.05) than plates incubated at 37°C; and the difference in recovery was greater on PCApyr (Figure 3-11). Colony count on PCApyr incubated at 25°C was 1.5 and 2.4 logs lower than plates incubated at 37°C for 84 day-starved EDL933 and Sakai, respectively. Recovery on PCAace for day 84 EDL933 was 0.5 logs lower when incubated at 25°C compared to 37°C incubation. For Sakai,

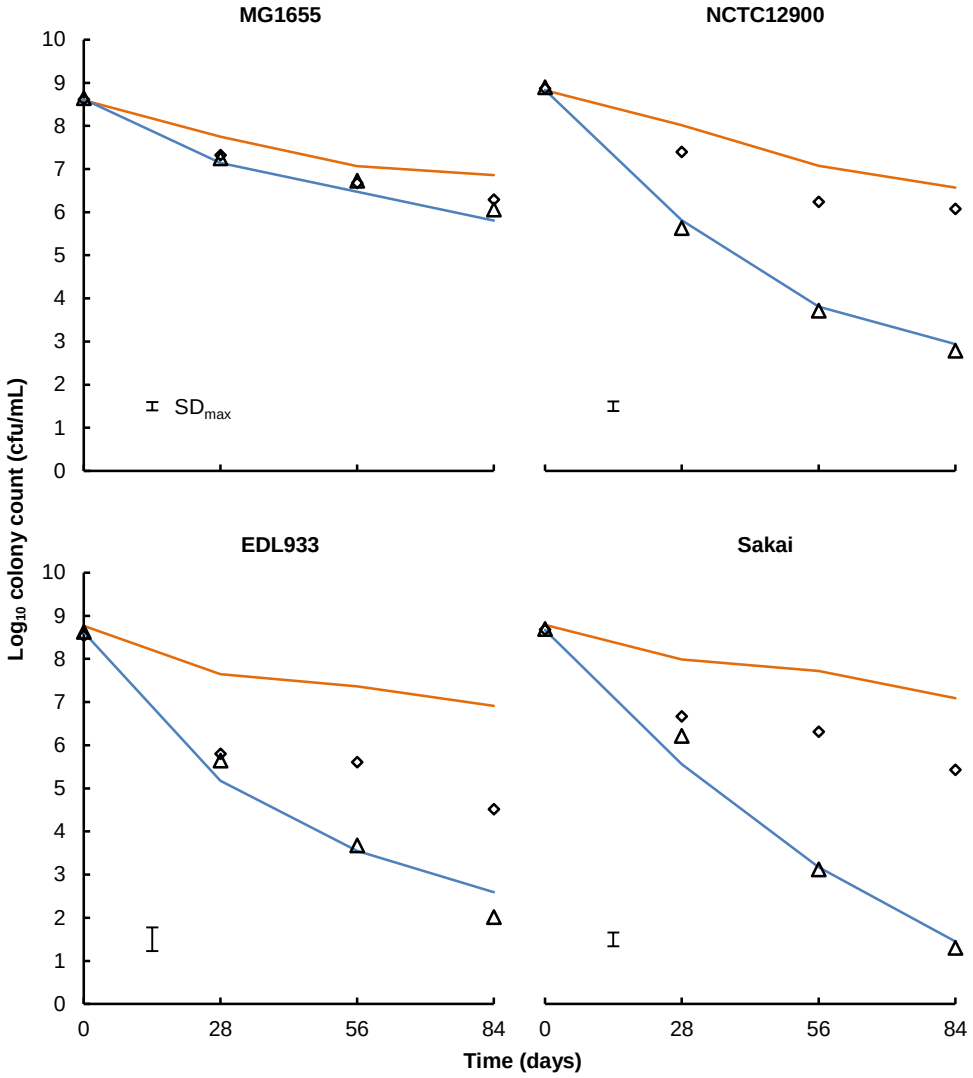

Figure 3-10 Effect of pyruvate and sodium supplementations on the recovery of MG1655, NCTC12900, EDL933 and Sakai starved in PBS at 4°C for 84 days. The number of colonies recovered on PCApyr (◇) and PCAace (△) are shown. For reference, the trends of recovery of late-exponential cells starved at 4°C on TSA (–) and PCA (–) (Figure 3-6 and Figure 3-7) are shown on each graph. Each colony count data point is the average of four technical replicates. The maximum standard deviation (SD_{max}) is indicated by the error bar on each graph. Data shown are representative of two biological repeats.

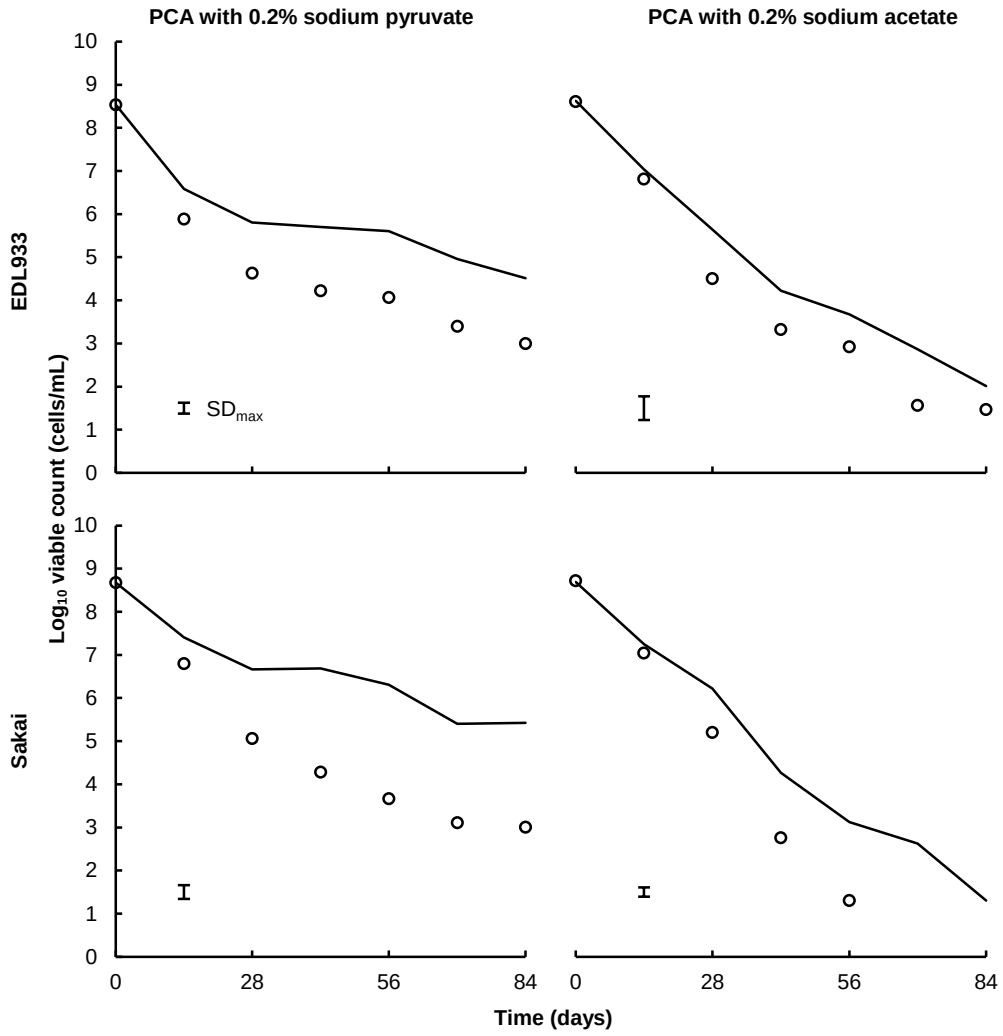

Figure 3-11 Recovery of EDL933 and Sakai starved at 4°C for 84 days on pyruvate and acetate supplemented PCA incubated at 25°C for 48 hours. Each colony count data point is the average of four technical replicates. For reference, the trends of EDL933 and Sakai recovered on plates incubated at 37°C for 24 hours (–) (Figure 3-10) are shown on each graph. The maximum standard deviation (SD_{max}) is indicated by the error bar on each graph. Data shown are representative of two biological repeats.

recovery on PCAace at 25°C was below the limit of detection on day 70 and 84.

The potential role of quorum sensing molecules on recovery was tested using AHL supplemented PCA. C12-HSL and 3-oxo-C6-HSL were two AHLs found to alter motility phenotypes in EPEC and EHEC at 5 nM (B. S. Govan, personal communication, March 1, 2011). These were used to supplement PCA to a final concentration of 5 nM and since AHLs were dissolved in ethyl acetate, ethyl acetate supplemented PCA was used as the negative control. Late-exponential NCTC12900 starved at 4°C were harvested on days 0 and 42 and the colony count on AHL supplemented plates were compared to unsupplemented PCA. Supplementation of PCA with ethyl acetate, C12-HSL or 3-oxo-C6-HSL had no significant effect on colony count on neither day 0 nor day 42 (Figure 3-12).

3.2.2.6 Change in the diameter of colonies recovered during starvation

In addition to the decline in colony count, the diameter of colonies recovered also changed with starvation. By standardising the duration of incubation as well as the method of photography, variations in colony diameter of late-exponential NCTC12900 on PCA, PCApyr, PCAace and TSA during starvation at 4 and 15°C were made comparable.

In general, diameter of colony formed was dependent on the starvation temperature. No significant change in colony diameter was observed during the 84-day starvation period at 15°C (Figure 3-13). For cells starved at 4°C, the distribution of colony diameter widened and shifted toward the left (diameter decreased) as the cells aged in PBS. On day 0, a narrow distribution in colony diameter was observed for 4°C colonies on PCA, TSA, PCApyr and PCAace (Figure 3-13). By day 42, the distribution of colony diameters on all media had widened and shifted toward the left. In addition, the mean colony diameter on all media was significantly lower ($p<0.05$) than on day 0. After 84 days, the mean colony diameter on PCApyr and TSA had decreased by 38 and 41%, respectively. Greater decline in mean colony diameter was observed for PCA and PCAace, with average reductions of 58 and 66% observed after 84 days, respectively. In addition, the distribution of colony diameter on PCAace was narrower than

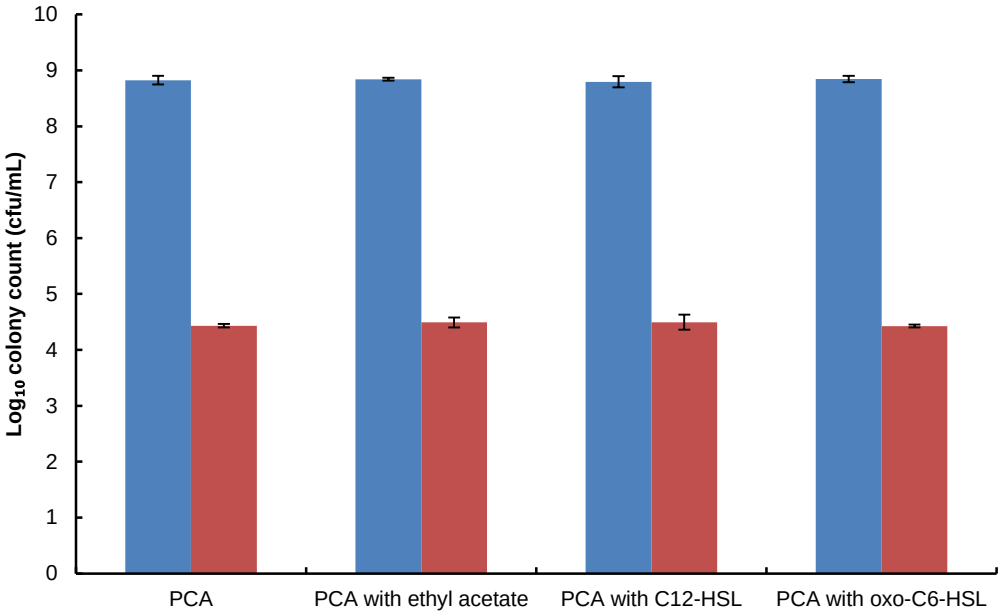

Figure 3-12 Effect of AHL supplementations on the recovery of for NCTC12900 starved in PBS at 4°C for 0 and 42 days. The average colony counts of four technical replicates are shown from day 0 (blue) and day 42 (red) cultures. The standard deviation is indicated by the error bar. Data shown are representative of two biological repeats.

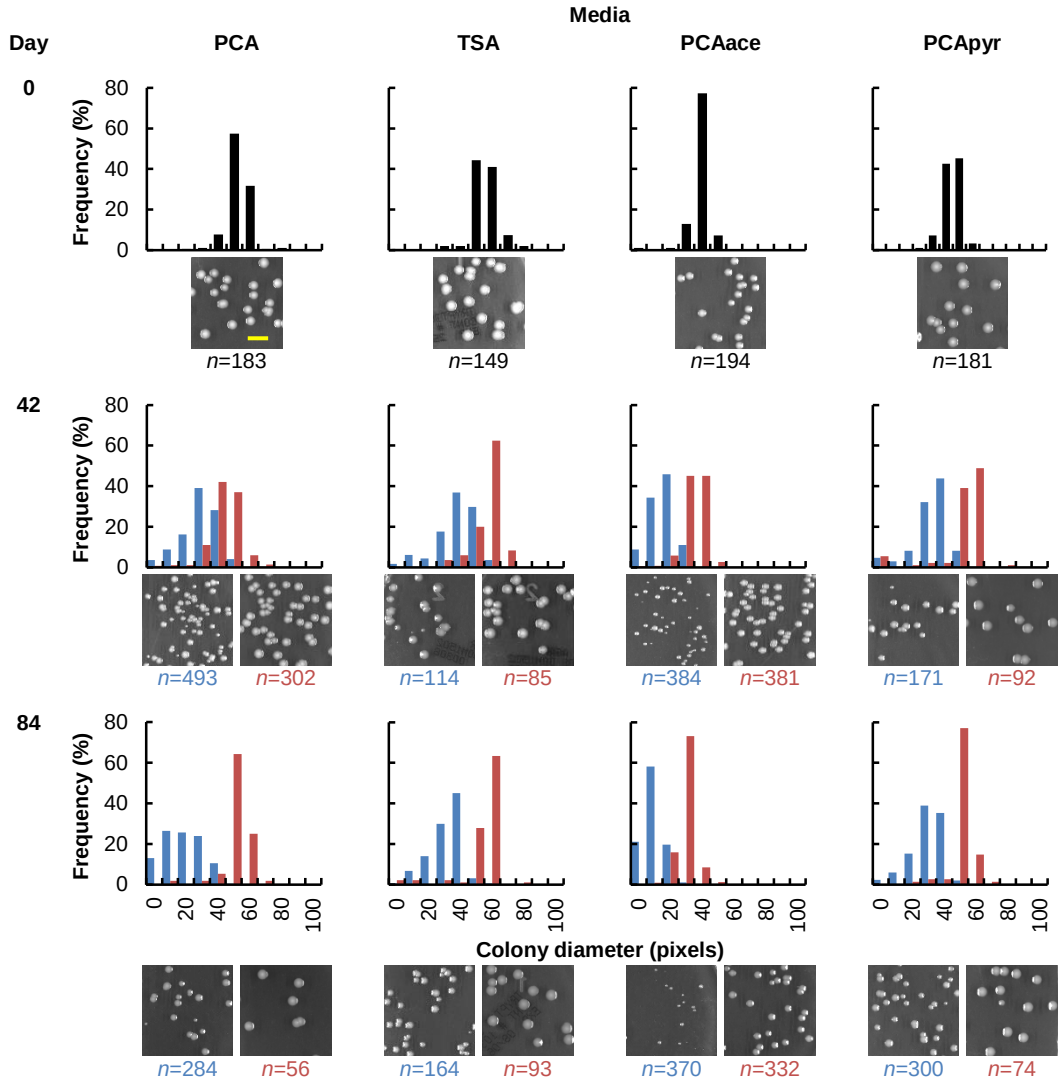

Figure 3-13 Distribution of the diameter of NCTC12900 colonies recovered on different media during starvation. The distribution of colony diameter measured prior to starvation is indicated by the black bars, and that of those held at 4 and 15°C are shown by the blue and red bars, respectively. The number of colonies measured is indicated in their respective colours below their respective images. Representative photographs of colonies starved at 4 (left) and 15°C (right) are shown at the same scale; a scale of 5 mm is shown in yellow in the top left photograph.

unsupplemented PCA, PCApyr and TSA; with 58% of colonies recovered on day 84 measuring between 10 and 20 pixels.

3.2.2.7 Culturability of starved cells in broth

To test the ability of starved cells to recover in broth, starved NCTC12900 cells were harvested and used to inoculate plate count broth (PCB), tryptic soy broth (TSB), PCB supplemented with 0.2% sodium acetate (PCBace) and PCB with 0.2% sodium pyruvate (PCBpyr). Late-exponential NCTC12900 cells grown to an OD_{600} of 1.0 were used as the pre-starvation control. The endpoint OD_{600}, the duration of lag and the rate of exponential growth were measured and compared. For cells grown in PCB-based media, growth had plateaued by 12 hours of incubation, and no significant difference in endpoint OD_{600} was observed between the pre-starvation control, cells starved at 4 and 15°C. While the stationary phase was reached after 12 hours of incubation in TSB, OD_{600} continued to increase between 12 and 24 hours (data not shown). No significant difference in the rate of exponential growth was observed between the pre-starvation control and cells starved at 4 and 15°C (Figure 3-14). Similarly, no significant difference was observed in endpoint OD_{600} after 24 hours of growth. One major difference observed between the starved and the pre-starvation control was the lag in growth, the length of which was dependent on the temperature at which the cells were starved (Figure 3-14).

The duration of lag observed for the pre-starvation control was 0.5 and 1.0 hours in PCB and TSB, respectively. For cells starved at 4°C for 34 days, the lag observed was 4.1 hours in PCB and 6.0 hours in TSB. The lag was shorter for those starved at 15°C, where a 1.6 and 1.9 hour lag was observed in PCB and TSB, respectively. A similar association of lag time and starvation was observed for cells grown in supplemented PCB (Figure 3-14). In PCBace, the duration of lag for the pre-starvation control, cells starved at 15°C and those starved at 4°C was 0.6, 2.1 and 5.0 hours, respectively. A lag of 0.5 hours was observed for the pre-starvation control grown in PCBpyr, and 1.5 and 3.4 hours for cells starved at 15 and 4°C, respectively.

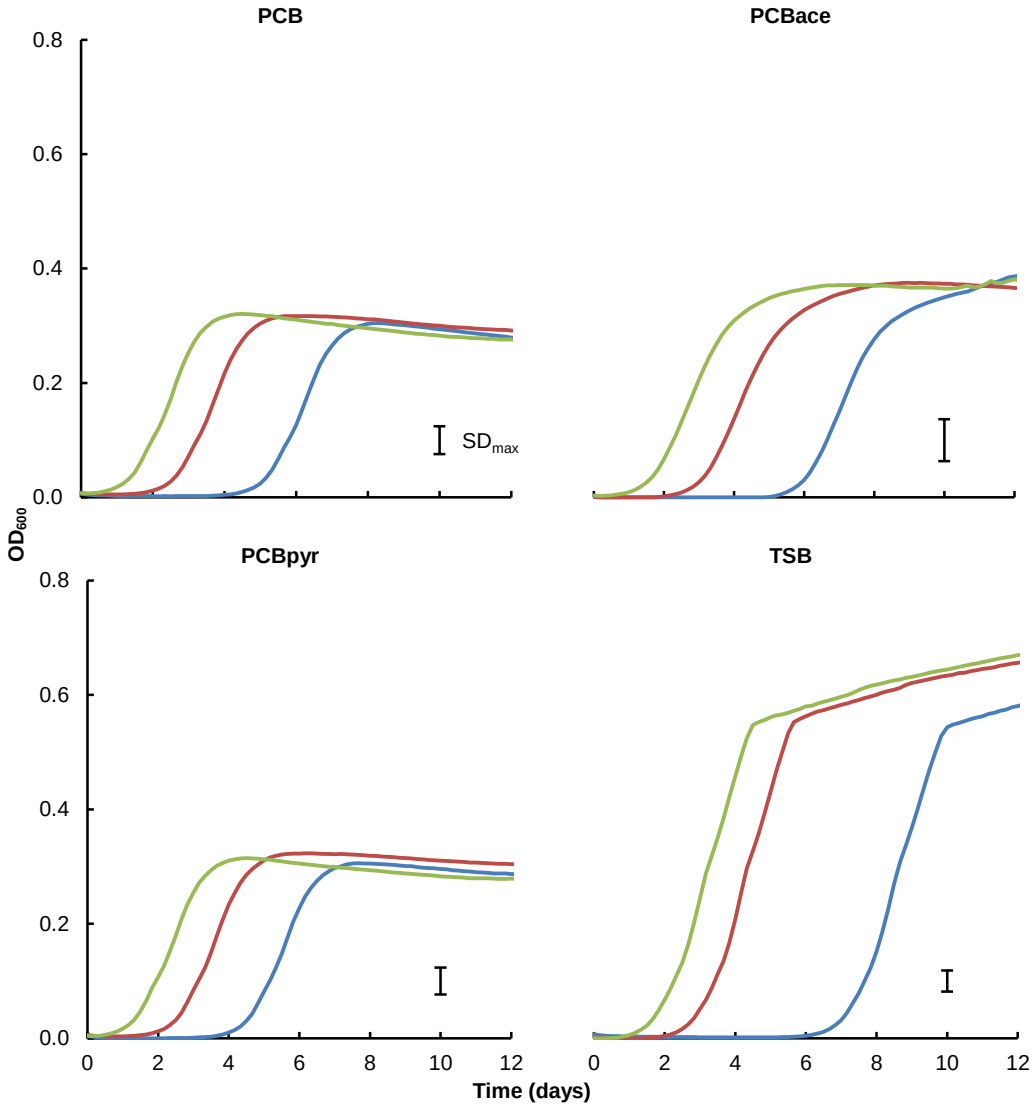

Figure 3-14 Comparison of growth kinetics of late-exponential pre-starvation control and starved NCTC12900. Following inoculation with pre-starvation control (green), 4°C day 34-starved cells (blue) or 15°C day 34-starved cells (red), cultures were incubated at 37°C for 24 hours. Plates were shaken and OD_{600} were recorded every 15 minutes. Data shown are the average of three technical repeats from the first 12 hours of incubation. The maximum standard deviation (SD_{max}) is indicated by the error bar on each graph.

3.2.3 Viability and culturability of New Zealand clinical and bovine isolates

Observations thus far were made on laboratory reference strains. To investigate whether New Zealand clinical and bovine isolates can survive and recover from starvation, strains were grown in LB and harvested during late-exponential phase, starved in PBS at 4 and 15°C, and monitored over 84 days.

3.2.3.1 Viability and colony recovery of clinical and bovine isolates starved at 4 and 15°C

The change in viable count was similar for clinical and bovine strains starved at 4 and 15°C. In all cases, no significant change in viability was observed during 84 days of starvation at either 4 or 15°C. Higher recovery was observed for cells starved at 15°C compared to cells starved at 4°C. In general, a gradual decline in recovery was observed for cells starved at 4°C, and recovery on TSA remained higher than on PCA-based media from day 14.

When starved at 4°C, recovery on nutrient-rich TSA decreased over 84 days by 2.4, 2.3 and 2.3 logs for ERL10621, ERL10630 and ERL10780, respectively (Figure 3-15). For the bovine isolates, a 1.7 log decrease was observed for H11- and 2.3 log for H11+ (Figure 3-16). Recovery of 4°C-starved cultures on nutrient-restricted PCA was significantly lower ($p<0.05$) than that observed on TSA. To investigate the role of specific nutrients on recovery of starved clinical and bovine strains, recovery on PCApyr and PCAace were assessed every 28 days. No significant difference in colony count was observed on PCAace and PCA, however, colony count on PCApyr was significantly higher than on PCA for all strains ($p<0.05$; Figure 3-15 and Figure 3-16).

For 15°C-starved cultures, no significant change in recovery was observed for ERL10630, ERl10621, H11- and H11+ during the 84-day period regardless of the media used (Figure 3-15 and Figure 3-16). For ERL10780, recovery on TSA was significantly higher than on PCA from day 28 till day 84 ($p<0.05$; Figure 3-15). By day 84, the number of ERL10780 colonies recovered on PCApyr was 0.9 logs higher on PCA and PCAace ($p<0.05$) and was the same as the level of recovery on TSA. No significant difference was observed between recovery on PCA and PCAace for the duration of the starvation period at 15°C.

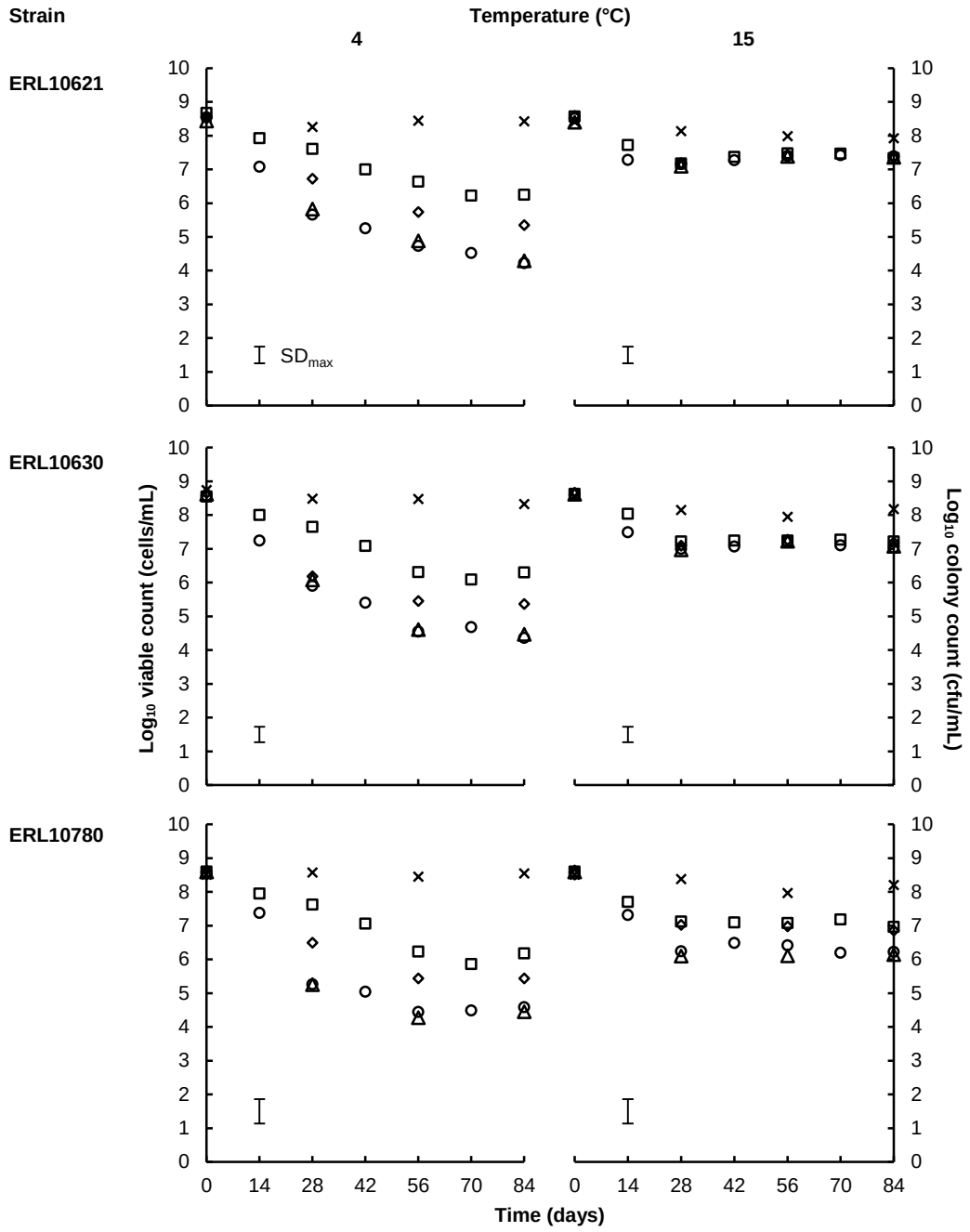

Figure 3-15 Viability and colony recovery of clinical O157:H7 strains, ERL10780, ERL10630 and ERL10621, harvested during late-exponential phase and starved in PBS at 4 and 15°C for 84 days. Viable count (×) and the number of colonies present after incubation at 37°C for 24 hours on TSA (□), PCA (○), PCApyr (◇) and PCAace (△) are shown. Each viable count data point shows the average of two technical repeats. Each colony count data point is the average of four technical replicates. The maximum standard deviation (SD_{max}) is indicated by the error bar on each graph. Data shown are representative of two biological repeats.

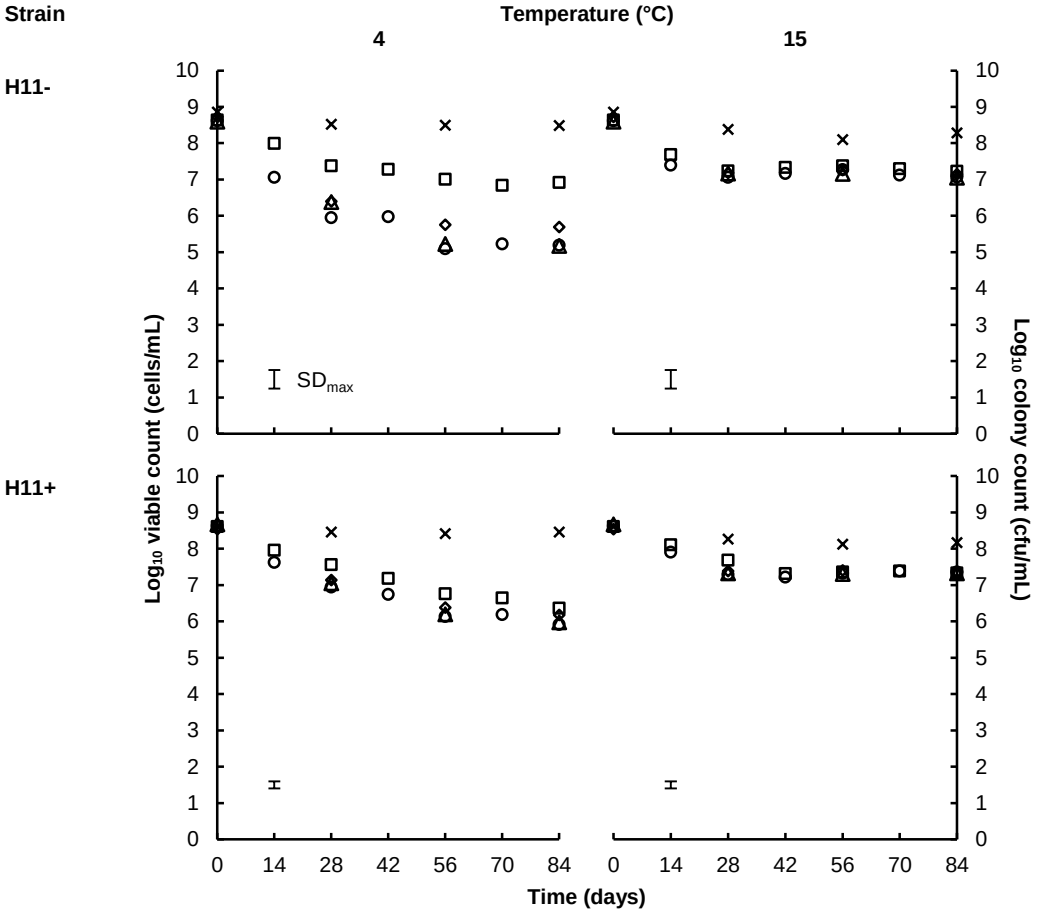

Figure 3-16 Viability and colony recovery of bovine O157 strains, H11- and H11+, harvested during late-exponential phase and starved in PBS at 4 and 15°C for 84 days. Viable count (×) and the number of colonies present after incubation at 37°C for 24 hours on TSA (□), PCA (○), PCApyr (◇) and PCAace (△) are shown. Each viable count data point shows the average of two technical repeats. Each colony count data point is the average of four technical replicates. The maximum standard deviation (SD_{max}) is indicated by the error bar on each graph. Data shown are representative of two biological repeats.

In summary, viability of late-exponential clinical and bovine cell cultures did not change during 84 days of starvation, however, their culturability on solid media decreased with time, and the decline in recoverability was dependent on the nutrient concentration of the media, as well as the starvation temperature.

3.2.3.2 Change in the size of colony recovered during starvation

Similar to NCTC12900, a change in the diameter of colonies recovered during starvation was observed for the clinical and bovine strains tested. The change in colony diameter and distribution was dependent on the media used and the starvation temperature. No significant change in colony diameter was observed for 15°C-starved cultures at over the course of starvation (data not shown). For 4°C-starved cultures, a gradual decrease in colony diameter was observed during aerobic recovery.

The distributions of colony diameter for ERL0780, ERL10630 and ERL10621 on day 0, and after 84 days of starvation at 4°C, are shown in Figure 3-17. Bimodal distribution in colony diameter was observed for colonies recovered aerobically on PCA on day 0 with the majority of cells forming colonies between 40 and 60 pixels in diameter. The average diameter of day 0 colonies on PCA was 49, 48 and 49 pixels for ERL10780, ERL10630 and ERL10621, respectively (Table 3-3). The diameter of day 0 colonies grown on PCApyr and TSA averaged between 42 and 50 pixels for all three strains. In comparison, the average colony diameter observed on PCAace was significantly lower ($p<0.05$), averaging between 20 and 25 pixels (Table 3-3). By day 84, the average diameter of colonies recovered on all PCA-based media for all three clinical strains was significantly lower than day 0 colonies ($p<0.05$; Table 3-3). No significant difference in diameter was observed between day 0 and day 84 colonies for ERL10621 and ERL10780 on TSA. This was mainly due to the large standard deviation observed for aerobic recovery on day 84 (Table 3-3). For ERL10630, the average diameter of day 84 colonies on TSA was significantly lower ($p<0.05$) than day 0 colonies. The variance in the distribution of colony diameter on PCA, PCApyr and TSA increased for all strains tested during starvation at 4°C (Figure 3-17). For PCAace, increased variance was observed for ERL10621 and ERL10780, but not ERL10630.

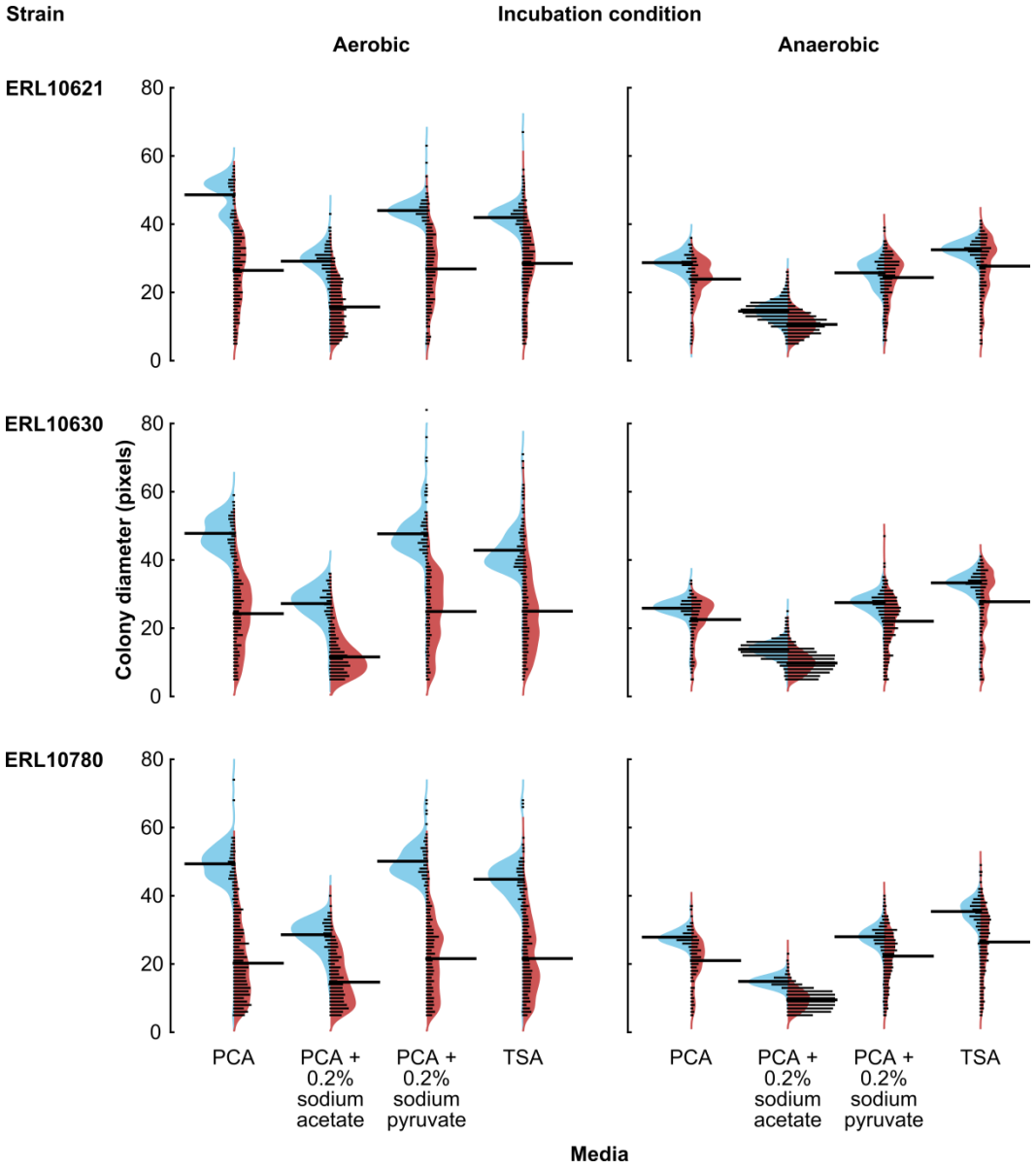

Figure 3-17 Distribution and mean colony diameter of clinical isolates recovered prior to starvation (day 0), and after 84 days of starvation at 4°C. Plates were incubated at 37°C for 24 hours under aerobic or anaerobic conditions. Diameters of colonies recovered on PCA, PCAace, PCApyr, and TSA, from day 0 (blue) and day 84 (red) cells were measured. The beanlines for each half of a bean are vertical histograms of the data distribution; the thicker long bean lines indicate the mean of each distribution. The shape of each half of the asymmetric bean represents the Gaussian density estimation of the distribution.

Table 3-3 Mean diameter of colonies recovered on day 0 and day 84 of starvation at 4°C grown under aerobic and anaerobic conditions. The means are the average of at least 50 colonies. The standard deviations are indicated in brackets.

Day	Strain	PCA		PCAace		PCApyr		TSA	
		ae[a]	an[b]	ae	an	ae	an	ae	an
0	**ERL10621**	*49* (5.3)	*29* (3.6)	*29* (4.7)	*14* (3.0)	*44* (5.3)	*26* (4.3)	42 (5.0)	32 (2.3)
	ERL10630	*48* (4.8)	*26* (3.5)	*27* (5.0)	*14* (2.5)	*48* (8.2)	*28* (2.8)	43 (6.5)	33 (3.2)
	ERL10780	*49* (7.1)	*28* (2.1)	*29* (4.4)	*15* (1.3)	*50* (5.0)	*28* (3.2)	*45* (6.7)	*35* (3.6)
	H11-	*51* (6.2)	*26* (2.8)	*31* (3.4)	*14* (1.8)	*49* (4.4)	*26* (2.7)	*46* (4.5)	*33* (2.9)
	H11+	*49* (4.7)	*33* (4.1)	*35* (3.8)	*16* (1.7)	*47* (6.2)	*27* (2.7)	*46* (3.7)	*35* (3.3)
84	**ERL10621**	26* (9.7)	24 (5.5)	16* (6.8)	11 (3.0)	27* (9.7)	24 (6.5)	29 (10.4)	28 (7.9)
	ERL10630	24* (9.8)	23 (5.9)	12* (5.2)	10 (2.8)	25* (10.1)	22 (7.1)	25 (11.7)	28 (9.2)
	ERL10780	20* (10.5)	21 (6.3)	15* (7.0)	9 (2.7)	22* (10.4)	22 (7.3)	22* (10.6)	26 (9.1)
	H11-	20* (8.3)	21 (5.7)	11* (4.6)	10 (2.7)	25* (9.2)	24 (6.0)	30 (11.9)	26 (8.9)
	H11+	28* (9.1)	28 (7.5)	16* (6.1)	10 (2.9)	29 (10.5)	20 (5.4)	39 (10.6)	29 (8.8)

[a] ae, aerobic recovery

[b] an, anaerobic recovery

* mean colony diameter on day 84 significantly lower than on day 0 ($p<0.05$)

Numbers are in italic where a statically significant ($p<0.05$) difference in mean colony diameter exists between the aerobic and anaerobic recovery

The distribution of colony diameter of H11- and H11+ grown aerobically on day 0 and after 84 days of starvation at 4°C are shown in Figure 3-18. Unimodal distributions in diameter were observed for day 0 H11- and H11+ colonies grown on PCA, PCAace, PCApyr or TSA. No significant difference in average diameter was observed between colonies grown on PCA, TSA and PCApyr for both H11- and H11+. In contrast, the average diameter of H11- and H11+ colonies grown on PCAace was significantly lower than colonies recovered on PCA, TSA and PCApyr (p<0.05; Table 3-3). By day 84, colony diameter on all PCA-based media was significantly smaller compared to day 0 (p<0.05; Table 3-3) with the greatest decreased observed on PCAace. No significant difference in average colony diameter was observed on TSA. In addition, greater variance in the distribution of diameters was observed for colonies grown on PCA, TSA and PCApyr. No significant difference in variance was observed between day 0 and day 84 colonies recovered on PCAace for both strains. Despite the difference in variance observed, no significant difference in average diameter was observed between day 84 colonies grown on PCA, PCAace, PCApyr and TSA.

3.2.3.3 Anaerobic recovery of starved clinical and bovine isolates

E. coli are facultative anaerobes. To assess the effect of anaerobic incubation conditions on the number and diameter of colonies recovered from starved cultures, ERL10780, ERL10630, ERL10621, H11- and H11+ starved at 4 and 15°C were harvested on day 0 and day 84, and grown anaerobically at 37°C for 24 hours on PCA, PCAace, PCApyr and TSA. No significant difference in colony count was observed between aerobic and anaerobic recovery for cultures starved at 4 (Table 3-4) or 15°C (Table 3-5) regardless of the media used.

In all cases, no significant difference in average diameter was observed between anaerobically recovered day 0 and day 84 colonies (Table 3-3). The average diameters of anaerobically recovered day 0 colonies on PCA, PCAace and PCApyr were significantly smaller (p<0.05) than aerobically recovered colonies for all strains tested (Table 3-3, Figure 3-17 and Figure 3-18). On TSA, the average diameter of anaerobically recovered da 0 ERL10621, H11- and H11+ (p<0.05) colonies were significantly smaller than aerobically recovered colonies; no significant difference was observed for ERL10780 and ERL10630 (Table 3-3,

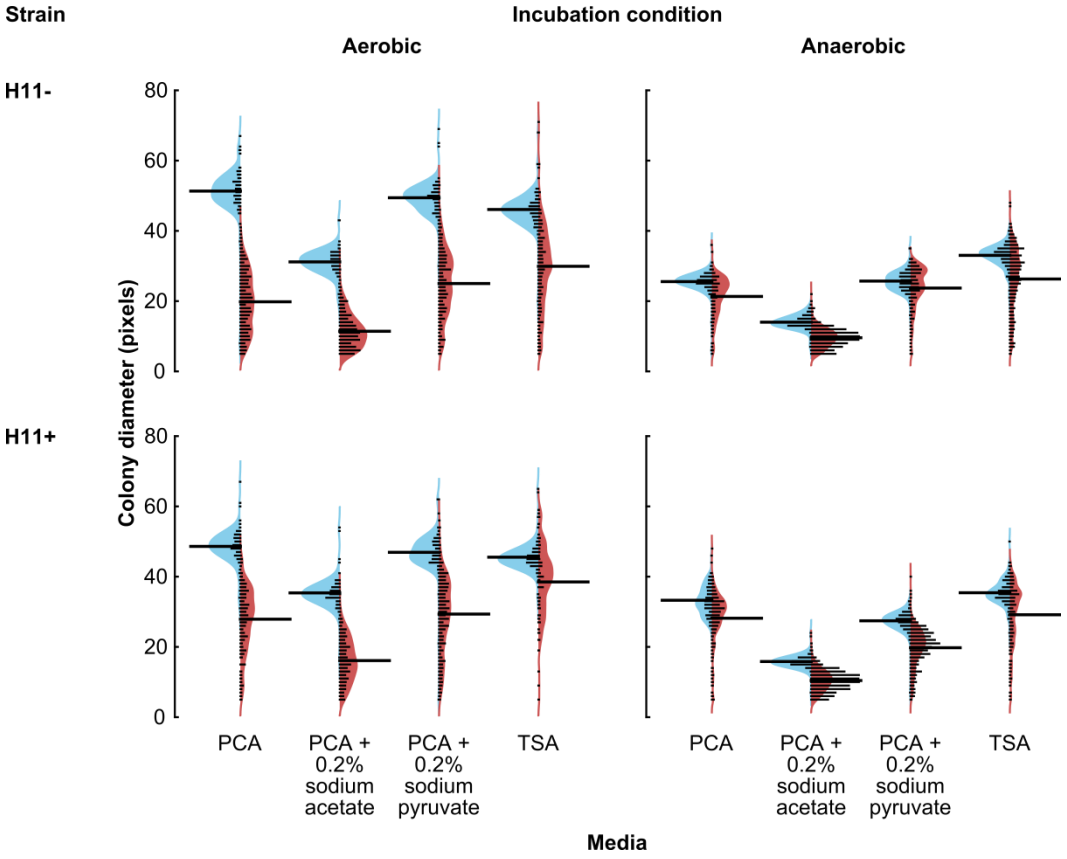

Figure 3-18 Distribution and mean of colony diameter of bovine O157 isolates recovered prior to starvation (day 0) and after 84 days of starvation at 4°C. Plates were incubated at 37°C for 24 hours under aerobic or anaerobic conditions. Diameters of colonies recovered on PCA, PCAace, PCApyr and TSA from day 0 (blue) and day 84 (red) cells were measured. The beanlines for each half of a bean are vertical histograms of the data distribution; the thicker long bean lines indicate the mean of each distribution. The shape of each half of the asymmetric bean represents the Gaussian density estimation of the distribution.

Table 3-4 Colony count clinical and bovine strains starved at 4°C recovered under aerobic and anaerobic conditions. The colony counts are the average of four technical replicates and the standard deviations are indicated in brackets.

Day	Strain	PCA		PCAace		PCApyr		TSA	
		ae[a]	an[b]	ae	an	ae	an	ae	an
0	**ERL10621**	8.54 (0.082)	8.40 (0.066)	8.44 (0.042)	8.41 (0.032)	8.53 (0.052)	8.66 (0.104)	8.67 (0.120)	8.57 (0.099)
	ERL10630	8.57 (0.083)	8.55 (0.069)	8.62 (0.118)	8.45 (0.062)	8.66 (0.041)	8.67 (0.024)	8.55 (0.171)	8.63 (0.072)
	ERL10780	8.58 (0.048)	8.41 (0.027)	8.59 (0.098)	8.46 (0.314)	8.52 (0.034)	8.57 (0.11)	8.60 (0.131)	8.59 (0.029)
	H11-	8.62 (0.061)	8.64 (0.141)	8.60 (0.021)	8.60 (0.082)	8.73 (0.043)	8.63 (0.075)	8.64 (0.092)	8.70 (0.083)
	H11+	8.63 (0.098)	8.66 (0.056)	8.67 (0.05)	8.58 (0.075)	8.54 (0.059)	8.66 (0.091)	8.61 (0.094)	8.70 (0.092)
84	**ERL10621**	4.22 (0.081)	4.46 (0.097)	4.30 (0.036)	4.34 (0.029)	5.35 (0.106)	6.00 (0.053)	6.25 (0.056)	6.62 (0.121)
	ERL10630	4.37 (0.095)	4.74 (0.009)	4.47 (0.033)	4.50 (0.084)	5.37 (0.293)	6.25 (0.057)	6.30 (0.036)	6.76 (0.112)
	ERL10780	4.59 (0.023)	4.67 (0.033)	4.45 (0.107)	4.25 (0.023)	5.44 (0.338)	6.39 (0.073)	6.18 (0.055)	7.13 (0.033)
	H11-	5.19 (0.122)	5.58 (0.088)	5.17 (0.103)	5.42 (0.069)	5.7 (0.353)	6.88 (0.174)	6.92 (0.072)	7.27 (0.021)
	H11+	5.91 (0.189)	5.85 (0.111)	5.98 (0.041)	5.84 (0.078)	6.18 (0.057)	6.27 (0.051)	6.36 (0.032)	6.40 (0.031)

[a] ae, aerobic recovery

[b] an, anaerobic recovery

Table 3-5 Colony counts clinical and bovine strains starved at 15°C recovered under aerobic and anaerobic conditions. The colony counts are the average of four technical replicates and the standard deviations are indicated in brackets.

Day	Strain	PCA		PCAace		PCApyr		TSA	
		ae[a]	an[b]	ae	an	ae	an	ae	an
0	**ERL10621**	8.54 (0.082)	8.40 (0.066)	8.44 (0.042)	8.41 (0.032)	8.53 (0.052)	8.66 (0.104)	8.67 (0.120)	8.57 (0.099)
	ERL10630	8.61 (0.025)	8.55 (0.069)	8.62 (0.118)	8.45 (0.062)	8.66 (0.041)	8.67 (0.024)	8.63 (0.063)	8.63 (0.072)
	ERL10780	8.58 (0.048)	8.41 (0.027)	8.59 (0.098)	8.61 (0.096)	8.52 (0.034)	8.57 (0.110)	8.60 (0.131)	8.59 (0.029)
	H11-	8.62 (0.061)	8.64 (0.141)	8.60 (0.021)	8.60 (0.082)	8.73 (0.043)	8.63 (0.075)	8.64 (0.092)	8.70 (0.083)
	H11+	8.63 (0.098)	8.66 (0.056)	8.67 (0.050)	8.58 (0.075)	8.54 (0.059)	8.66 (0.091)	8.61 (0.094)	8.70 (0.092)
84	**ERL10621**	7.39 (0.084)	7.43 (0.034)	7.39 (0.053)	7.34 (0.022)	7.44 (0.098)	7.43 (0.026)	7.58 (0.087)	7.63 (0.109)
	ERL10630	7.03 (0.031)	6.84 (0.102)	7.08 (0.060)	6.77 (0.177)	7.19 (0.054)	7.22 (0.032)	7.22 (0.049)	7.26 (0.094)
	ERL10780	6.22 (0.037)	6.09 (0.044)	6.15 (0.070)	5.74 (0.101)	6.86 (0.044)	6.79 (0.054)	6.96 (0.071)	6.95 (0.071)
	H11-	7.07 (0.051)	6.91 (0.169)	7.05 (0.122)	6.82 (0.033)	7.15 (0.089)	7.17 (0.081)	7.23 (0.026)	7.23 (0.054)
	H11+	7.36 (0.049)	7.34 (0.048)	7.33 (0.047)	7.23 (0.056)	7.36 (0.028)	7.29 (0.060)	7.34 (0.032)	7.40 (0.062)

[a] ae, aerobic recovery

[b] an, anaerobic recovery

Figure 3-17 and Figure 3-18). On day 84, no significant difference in average colony diameter was observed between aerobically and anaerobically recovered colonies on all media for all strains tested (Table 3-3).

3.2.3.4 Recovery of starved clinical and bovine cells in broth

The ability of clinical and bovine cells to recover in broth prior to and after 28 to 29 days of starvation at 4 or 15°C was tested by growing harvested cells in PCB, PCBace, PCBpyr and TSB at 37°C. Late-exponential cells grown to an OD_{600} of 1.0 were harvested and used to establish the growth potential of each strain as the pre-starvation control. The endpoint OD_{600} following 24 hours of incubation, the lag and the rate of exponential growth were measured.

Overall, no significant difference in endpoint OD_{600} and rate of exponential growth was observed between the pre-starvation controls of the strains tested (Table 3-6 and Table 3-7). In contrast, significant variation ($p<0.05$) in lag time was observed; the shortest lag in growth was observed for ERL10630 and the longest from H11- (Table 3-8). When starved, the variations in lag between the strains were also significant ($p<0.05$). Among the 4°C-starved cells, ERL10780 exhibited the shortest lag time and H11+ the longest, while the lag in ERL10630 growth was the shortest among the 15°C-starved cells and H11- the longest (Table 3-8).

In all cases, no significant difference in endpoint OD_{600} was observed between the pre-starvation control and cells starved at 4 or 15°C grown in PCApyr, PCAace and TSA (Table 3-6). For ERL10630 grown in PCB, the endpoint OD_{600} for 4°C-starved cells was significantly lower ($p<0.05$) than the pre-starvation control; no significant difference was observed for ERL10621, ERL10780, H11- or H11+ (Table 3-6). For all strains tested, no significant difference in the rate of exponential growth was observed between the pre-starvation control and cells starved at 4 or 15°C (Table 3-7). The lag time of cells starved 4 and 15°C was significantly longer ($p<0.05$) than the pre-starvation control for all strains, regardless of the growth media (Table 3-8). In addition, the lag time for 4°C-starved cells was significantly longer ($p<0.05$) than cells starved at 15°C (Table 3-8).

Table 3-6 OD_{600} of pre-starvation and starved clinical and bovine strains grown in PCB, PCBace, PCBpyr and TSB following 24 hours of incubation at 37°C. OD_{600} shown are the average of technical triplicates. The standard deviations are shown in brackets.

Media	ERL10621			ERL10630			ERL10780			H11+			H11-		
	LE[a]	15°C[b]	4°C[c]	LE	15°C	4°C	LE	15°C	4°C	LE	15°C	4°C	LE	15°C	4°C
PCB	0.34 (0.017)	0.32 (0.024)	0.31 (0.011)	0.34 (0.013)	0.31 (0.02)	0.30 (0.007)	0.33 (0.012)	0.32 (0.009)	0.33 (0.014)	0.36 (0.006)	0.36 (0.006)	0.36 (0.004)	0.35 (0.023)	0.34 (0.02)	0.33 (0.018)
PCBace	0.42 (0.009)	0.41 (0.023)	0.41 (0.01)	0.42 (0.025)	0.38 (0.038)	0.38 (0.015)	0.42 (0.012)	0.40 (0.037)	0.40 (0.009)	0.44 (0.04)	0.41 (0.007)	0.41 (0.003)	0.35 (0.007)	0.43 (0.029)	0.35 (0.012)
PCBpyr	0.35 (0.011)	0.34 (0.027)	0.34 (0.011)	0.35 (0.013)	0.33 (0.028)	0.32 (0.007)	0.34 (0.017)	0.34 (0.028)	0.34 (0.012)	0.41 (0.034)	0.39 (0.008)	0.39 (0.008)	0.37 (0.033)	0.34 (0.012)	0.33 (0.018)
TSB	0.83 (0.029)	0.86 (0.109)	0.78 (0.019)	0.79 (0.026)	0.85 (0.116)	0.75 (0.017)	0.82 (0.021)	0.93 (0.098)	0.79 (0.03)	0.78 (0.018)	0.79 (0.03)	0.78 (0.026)	0.76 (0.025)	0.76 (0.024)	0.78 (0.102)

[a] LE, late-exponential pre-starvation control

[b] cells starved at 15°C in PBS harvested on day 29

[c] cells starved at 4°C in PBS harvested on day 28

Table 3-7 Growth curve rate (OD_{600} hr^{-1}) of pre-starvation and starved clinical and bovine strains grown in PCB, PCBace, PCBpyr and TSB following 24 hours of incubation at 37°C. The rates were measured in minutes and are shown are the average of technical triplicates. The standard deviations are shown in brackets.

Media	ERL10621			ERL10630			ERL10780			H11+			H11-		
	LE[a]	15°C[b]	4°C[c]	LE	15°C	4°C	LE	15°C	4°C	LE	15°C	4°C	LE	15°C	4°C
PCB	0.17 (0.005)	0.17 (0.007)	0.17 (0.003)	0.16 (0.002)	0.15 (0.008)	0.15 (0.007)	0.19 (0.003)	0.19 (0.005)	0.18 (0.005)	0.20 (0.002)	0.20 (0.001)	0.21 (0.003)	0.15 (0.004)	0.15 (0.007)	0.15 (0.001)
PCBace	0.16 (0.003)	0.15 (0.005)	0.16 (0.004)	0.14 (0.001)	0.14 (0.007)	0.14 (0.005)	0.16 (0.003)	0.15 (0.004)	0.16 (0.003)	0.15 (0.009)	0.16 (0.004)	0.16 (0.003)	0.13 (0.001)	0.14 (0.005)	0.14 (0.004)
PCBpyr	0.17 (0.003)	0.17 (0.007)	0.17 (0.004)	0.16 (0.008)	0.16 (0.013)	0.15 (0.004)	0.18 (0.002)	0.19 (0.011)	0.18 (0.001)	0.21 (0.017)	0.21 (0.008)	0.21 (0.005)	0.15 (0.011)	0.15 (0.003)	0.15 (0.002)
TSB	0.29 (0.003)	0.28 (0.020)	0.27 (0.005)	0.25 (0.005)	0.25 (0.013)	0.24 (0.014)	0.28 (0.003)	0.28 (0.000)	0.28 (0.011)	0.30 (0.006)	0.30 (0.005)	0.31 (0.009)	0.25 (0.005)	0.25 (0.001)	0.25 (0.010)

[a] LE, late-exponential pre-starvation control

[b] cells starved at 15°C in PBS harvested on day 29

[c] cells starved at 4°C in PBS harvested on day 28

Table 3-8 Lag of pre-starvation and starved clinical and bovine strains grown in PCB, PCBace, PCBpyr and TSB following 24 hours of incubation at 37°C. The lag times were measured in minutes and are shown are the average of technical triplicates. The standard deviations are shown in brackets.

Media	ERL10621			ERL10630			ERL10780			H11+			H11-		
	LE[a]	15°C[b]	4°C[c]	LE	15°C	4°C	LE	15°C	4°C	LE	15°C	4°C	LE	15°C	4°C
PCB	1.6 (0.029)	3.8 (0.040)	4.9 (0.029)	1.4 (0.044)	3.4 (0.006)	4.6 (0.029)	1.6 (0.018)	3.4 (0.055)	4.5 (0.008)	1.8 (0.013)	3.4 (0.013)	5.0 (0.015)	1.7 (0.065)	3.9 (0.08)	4.7 (0.029)
PCBace	1.5 (0.023)	4.1 (0.059)	5.5 (0.017)	1.3 (0.048)	3.6 (0.042)	5.1 (0.009)	1.6 (0.009)	4.0 (0.032)	4.9 (0.027)	1.8 (0.017)	3.7 (0.019)	5.5 (0.017)	1.8 (0.071)	4.3 (0.067)	5.2 (0.049)
PCBpyr	1.5 (0.020)	3.6 (0.013)	4.6 (0.047)	1.3 (0.064)	3.2 (0.044)	4.4 (0.024)	1.5 (0.006)	3.3 (0.009)	4.3 (0.038)	1.7 (0.035)	3.2 (0.008)	4.5 (0.035)	1.6 (0.050)	3.7 (0.010)	4.4 (0.011)
TSB	2.0 (0.019)	4.3 (0.050)	5.6 (0.030)	1.8 (0.023)	3.9 (0.021)	5.5 (0.069)	2.0 (0.018)	3.9 (0.028)	5.2 (0.037)	2.2 (0.022)	3.9 (0.034)	5.7 (0.055)	2.4 (0.035)	4.5 (0.049)	5.9 (0.044)

[a] LE, late-exponential pre-starvation control

[b] cells starved at 15°C in PBS harvested on day 29

[c] cells starved at 4°C in PBS harvested on day 28

3.3 Discussion

As a zoonotic pathogen, maintaining a dual lifestyle within animal hosts and the environment is crucial for the survival of *E. coli* O157:H7. A number of variables that impact on both bacterial survival and growth are likely to differ between the gastrointestinal tract of an animal host and the external environment, including temperature and nutrient availability. Conditions in non-host environments, such as nutrient limitation and sub-optimal temperatures, are known inducers of the viable but non-culturable (VBNC) state. Therefore, we hypothesised that VBNC may be a survival mechanism adopted by *E. coli* O157:H7 upon transition from feast to famine. Investigation into the effect of starvation at low temperatures on *E. coli* requires both culture-dependent and culture-independent measures of survival, as well as resuscitation factors to restore growth of non-culturable cells.

To understand how *E. coli* O157:H7 responds to the transition from its niche within an animal, a nutrient rich environment at optimal growth temperature, to the external environment where nutrient levels and temperatures are likely to be relatively lower, cells were harvested from early-, mid-, late-exponential or stationary phase, starved in PBS to mimic the low nutrient environment and incubated at 25, 15 and 4°C to simulate room temperature, New Zealand freshwater temperatures and the refrigeration temperature of foodstuffs, respectively.

Colony recovery was determined using growth on TSA and PCA media. The culture-independent viable count was determined using a combination of the LIVE/DEAD® *Bac*Light™ staining system and a quantification protocol developed in this study. One major advantage of the viability assay used in this study was the direct quantification of SYTO 9-stained cells instead of the widely used method of expressing the SYTO 9- and PI-stained cells as a percentage. The PI-stained cells were not quantified in this study since DNA of the dead or injured cells with membranes permeable to PI are likely to degrade and dissipate over time (Figure 3-3).

Strains chosen for this study included three *E. coli* O157:H7 reference strains, three New Zealand clinical *E. coli* O57:H7 isolates, and two New Zealand bovine

O157-positive strains. The hypothesis was that VBNC response of strains from different origins may reflect the evolution pressures in each environment. *E. fergusonii* H11+ was included in this study because it was initially identified as a sorbitol-fermenting *E. coli* O157 strain from bovine hide. In an on-farm study, anti-O157 immunomagnetic separation (IMS) assays were used as part of the isolation protocol for *E. coli* O157 (H. L. Withers, personal communication, June 12, 2012). Further investigation of H11+ revealed that this strain, as well as a number of other *E. fergusonii* isolated using IMS from the same study, cross-reacted with the anti-O157 immunomagnetic beads during IMS isolation (H. L. Withers, personal communication, June 12, 2012). As this discovery was made after starvation studies had commenced, H11+ was included in this study to explore the behaviour of non-*E. coli* but O157-positive bovine strain during starvation in PBS and whether there is any relationship between the phenotypes observed and the source of isolation.

Less than one log difference in viable count was observed for the duration of the 84-day starvation regardless of the strain, starvation temperature, or the physiological state of the bacteria prior to starvation. For the late-exponential cell cultures starved at 15 or 25°C, statistically significant declines in viable count were observed for some strains. These declines, however, were less than half a log and viability remained high during the 84-day assessment period. When starved at 4°C, the viable count of the late-exponential cell cultures of all strains tested remained high for 84 days with no significant decline. Interestingly, for NCTC12900 harvested during the early-, mid-exponential and stationary phase, statistically significant declines in viable count were observed during starvation at 4°C. Overall, maximum maintenance of viability, as defined by membrane integrity, was observed for late-exponential cell cultures starved at 4°C compared to other conditions tested. The late-exponential phase marks the transition from exponential to the stationary phase, where RpoS-mediated stress response initiates (Lange & Hengge-Aronis, 1991). The higher viable cells counts observed from late-exponential phase cells suggest that long-term survival of *E. coli* during starvation at 4°C may be dependent on RpoS stress response.

Viable count was reflective of the number of cells with intact membranes in the population, and colony count reflected the number of cells able to grow under

culturing conditions. Culture-based estimation of survival has been an integral part of microbiology for over a century, and the assumption is that each colony was formed by a single bacterium (Breed & Dotterrer, 1916). Colony count is the fundamental tool used for growth analysis. Measurement of colony diameter in addition to colony count provided additional information about the physiology and fitness of the cells recovered. The method developed in this study allowed such measurement to be carried out accurately; capturing the population distribution of the colony size formed on plates under different conditions.

While viability remained largely unchanged, colony recovery of cultures declined during starvation at 4, 15 and 25°C. This was consistent with the characteristics of VBNC cells where cell viability is maintained while colony recovery declines (Oliver, 2010). In addition, results from this study showed that the extent of decrease in culturability was dependent on the physiological state of the cells prior to starvation, the starvation temperature, and the nutrient level of the recovery medium.

A sharp decline in recovery on PCA was observed for NCTC12900 harvested from the early-exponential phase during the first 28 days of starvation at 4°C while gradual declines over time were observed for those harvested from the mid-, late-exponential and stationary phases (Figure 3-6). When starved at 15 or 25°C, recovery of all strains remained high, with a maximum of two-log decline observed over 84 days. Nutrient composition had no effect on the recovery of most strains starved at 15 or 25°C, except for ERL10780 on TSA where recovery was 1 log higher than on PCA after 84 days of starvation at 15°C (Figure 3-15). For cells starved at 4°C, recovery decreased progressively over 84 days of starvation on both TSA and PCA, and the number of colonies recovered on TSA was consistently higher than on PCA, except for H11+.

For *E. coli* O157:H7 cells starved at 4°C for 84 days, the mean colony size observed on PCA-based media following aerobic recovery was significantly smaller than that observed prior to starvation (Table 3-3). Interestingly, no significant difference in mean colony diameter was observed between day 0 and day 84 starved cells following anaerobic recovery (Table 3-3). This may be due to the difference in oxidative and fermentative pathways used during aerobic and

anaerobic growth, respectively. Results suggest that energy generation via the oxidative pathway was impaired by pro-longed starvation at 4°C, while growth via the fermentative pathway was not affected.

When recovered in broth, there was no significant difference in the final OD_{600} for 4°C- and 15°C-starved cells compared to the pre-starvation control for all strains tested. Similarly, no significant difference was observed for the rate of exponential growth. However, the lag in growth was significantly longer for starved cells compared to the control (Figure 3-14 and Table 3-8). Moreover, the lag of cells starved at 4°C was significantly longer than cells starved at 15°C for all strains.

Similar trends in viability, colony count and colony diameter during starvation at both 4 and 15°C were observed for the *E. coli* O157:H7 strains tested. In addition, greater decrease in colony count during starvation at 4°C was observed for *E. coli* O157:H7 strains compared to *E. coli* MG1655. While trends in viability and colony diameter were similar between the bovine isolates tested, nutrient level had less impact on the number of colonies recovered for H11+ compared to H11- (Figure 3-16). These results showed that the nutrient requirements for colony formation during starvation, particularly at 4°C, differed between *E. coli* MG1655, *E. coli* O157:H7 strains and *E. fergusonii* H11+ while changes in membrane integrity and thereby viability were similar between all strains tested.

Sodium pyruvate has been shown to "resuscitate" cells from the VBNC state (Bjergbæk & Roslev, 2005; Mizunoe *et al.*, 1999; Na *et al.*, 2006). We hypothesised that the supplementation of sodium pyruvate to PCA would improve recovery of starved cells. Supplementing PCA with 0.2% sodium pyruvate resulted in higher recovery for all strains starved at 4°C. The diameter of NCTC12900 colonies recovered was also significantly larger than unsupplemented PCA (Figure 3-13); however, this difference in colony size was not observed for the clinical or bovine strains tested. Interestingly, supplementation with sodium acetate resulted in the formation of smaller colonies for all strains while having no significant effect on the number of colonies recovered. As neither pyruvate or acetate were the sole available nutrient in PCA,

the effect of these two substrates on colony formation was likely due to their role as metabolic regulators rather than the main source of carbon or energy.

The mammalian gastrointestinal tract is the habitat for a number of bacterial species, and cell-to-cell signalling is likely to occur in these environments. Reissbrodt *et al*. (Reissbrodt *et al.*, 2002) suggested that cell-to-cell signalling may have been involved in the resuscitation of *E. coli* by supplementation of enterobacterial autoinducers to the recovery media. However, supplementation of 5 nM C12-HSL or 3-oxo-C6-HSL to PCA did not result in any significant change in colony count. Results from this study showed that C12-HSL and 3-oxo-C6-HSL, as supplements, had no effect on starved-cell recovery, however, the possible role of cell-to-cell communication in the resuscitation of VBNC cells could not be eliminated based on these results.

Since the gastrointestinal tracts of *E. coli* O157:H7 hosts are anaerobic environments, the effect of anaerobic incubation on the recovery of clinical and bovine strains starved at 4 and 15°C was tested. Anaerobic incubation did not have any significant effect on the number of colonies recovered compared to aerobic recovery (Table 3-4 and Table 3-5), however, the size of colonies recovered was markedly different. The size of colonies recovered anaerobically was smaller than aerobically recovered colonies for non-starved cells. While the mean diameter of the colonies recovered aerobically decreased during starvation at 4°C, no significant difference was observed for anaerobically recovered colonies from day 0 and day 84 of starvation (Figure 3-17 and Figure 3-18).

In summary, nutrient limitation and incubation at sub-optimal temperatures had no effect on the maintenance of *E. coli* or *E. fergusonii* H11+ membrane integrity for up to 84 days. Colony recovery of the starved cells was most affected by the starvation temperature, followed by the nutrient level of the media.

The data presented here suggest that the VBNC state may be a stress response mechanism for *E. coli* O157:H7 against nutrient limitation at the refrigeration temperature of 4°C. This may contribute to lower detection of the organism during winter months (Money *et al.*, 2010). The elevation in temperature during recovery combined with high nutrient level is likely to be the triggers that rescue

E. coli O157:H7 from the dormant VBNC state, regardless of oxygen availability. Since pyruvate is a mammalian salivary component (Silwood *et al.*, 2002), this may act as an important resuscitation factor for VBNC cells upon entry into the host.

Chapter 4 Metabolic analysis of starved *E. coli* O157:H7

4.1 Introduction

Starvation at low temperatures can induce *E. coli* O157:H7 into a viable but nonculturable (VBNC) state, where the number of colonies recovered on solid media decreases during starvation while the number of viable cells detected by microscopy remains unchanged (Oliver, 2010). Nutrient starvation also induces RpoS-mediated stress responses in *E. coli*, which result in alterations in metabolic gene expression (Dong & Schellhorn, 2009a; Sharma & Chatterji, 2010). In this study, the number of *E. coli* O157:H7 colonies recovered after starvation decreased significantly over 84 days of starvation in PBS, particularly for cultures held at 4°C compared to those held at 15 or 25°C (see Chapter 3). Nutrient levels and key metabolic substrates such as pyruvate and acetate altered the number of colonies recovered from starved cultures and/or the diameter of colonies recovered (see Chapter 3).

The dependency of starved-cell colony recovery on the nutrient level of recovery media or the presence of pyruvate suggested that carbon requirements and/or carbon utilisation kinetics during recovery differed between the starved and non-starved *Escherichia* O157 strains. The decline in colony recovery observed during starvation at 4°C was likely to be the result of decreasing energy levels within the starved cell, such as cAMP accumulation, that may lead to changes in substrate catabolism during recovery (Escalante *et al.*, 2012). The growth phase of cells prior to recovery may also affect carbon utilisation during recovery, since RpoS-mediated expression of metabolic genes is dependent on the growth phase of *E. coli* (Rahman *et al.*, 2006). The atmospheric environment in which *Escherichia* O157 strains recover from starvation during passage through the host gastrointestinal tract may be anaerobic (Jones *et al.*, 2011). As facultative anaerobes, *Escherichia* strains can grow under anaerobic conditions using respiratory pathways different to aerobic growth (Ingledew & Poole, 1984). We hypothesise that the growth stage of the cells prior to recovery, such as growth phase or starvation, affects substrate catabolism during recovery. In addition, carbon source utilisation is likely to differ between starved and non-starved cells during anaerobic growth.

4.2 Results

Biolog PM1 and PM2A Phenotype MicroArrays™ Carbon Sources MicroPlates™ were used to measure the metabolic activity of six *Escherichia* O157 strains during recovery. The full list of substrates tested and their respective chemical classes are shown in Appendix 1. Exponential phase cells were harvested after 1.5 hours of growth in LB at 37°C to an OD_{600} of 0.2, stationary phase cells were harvested after 24 hours of growth in LB at 37°C and starved cells were harvested between day 37 and day 59 of starvation at 4°C. Cells tested under anaerobic incubation (5% H_2, 10% CO_2 and 85% N_2) were harvested during stationary phase or on day 81 to 90 of starvation at 4°C. The duration of lag (λ), the rate of exponential substrate utilisation (μ_{exp}) and the endpoint level of substrate use after 24 hours ($A_{endpoint}$), were used to create metabolic profiles. These profiles were used to compare carbon source utilisation between strains and between cells harvested during different growth stages. Interpretation of scatter plot for pairwise comparisons of $A_{endpoint}$, λ and μ_{exp} is schematically represented in Figure 4-1.

4.2.1 Sole substrate use profiles for NCTC12900

NCTC12900 substrate utilisation during aerobic incubation was tested using Biolog PM1 and PM2A plates. Of the 190 substrates tested, 67 were metabolised by NCTC12900. $A_{endpoint}$, λ and μ_{exp} for NCTC12900 harvested during exponential, stationary, and after 56 to 59 days of starvation at 4°C were compared using ANOVA. Substrates not utilised were omitted.

4.2.1.1 $A_{endpoint}$ of substrate use by NCTC12900

A statistically significant difference (p<0.05) in $A_{endpoint}$ between exponential phase, stationary phase and starved NCTC12900 was observed for 16 substrates (Table 4-1 numbered and Figure 4-2). $A_{endpoint}$ of five substrates (SS 4, 7, 11, 12 and 16) differed significantly (p<0.05) between exponential and stationary phase cells; seven (SS 1, 3, 4, 6, 8, 10 and 14) differed between exponential phase and starved cells; and twelve (SS 1, 2, 4, 5, 7 to 10 and 12 to 15) differed between stationary phase and starved cells (Figure 4-2). Supplementation of PCA with sodium pyruvate and sodium acetate altered colony recovery from starved cultures

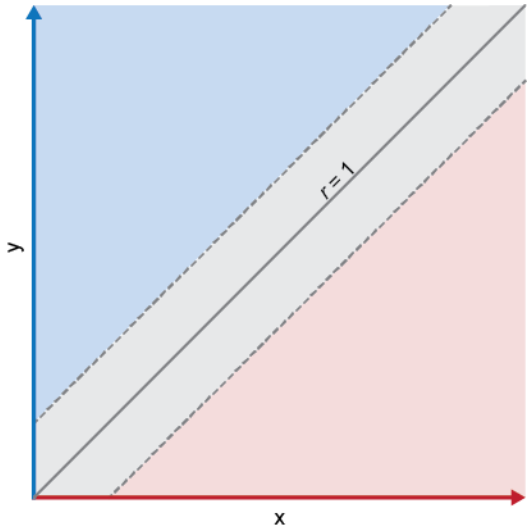

Figure 4-1 Interpretation of pairwise comparison using scatter plots. Data points on the line of correlation coefficient (r) = 1 were considered to be equivalent between the x and y variables. Boundaries of the 95% least significant difference ($LSD_{95\%}$) are marked by dotted grey lines. Data points within the grey area marked by the $LSD_{95\%}$ lines are considered to be used to the same levels by x and y. Data points located in the blue area represent substrates with higher y values than x values. Data points located in the pink area represent substrates with higher x values being greater than y values. Data points on the x-axis (red) represent substrates used by x but not y, and those on the y-axis (blue) represent substrates used by y but not x.

Table 4-1 $A_{endpoint}$ for substrates used by NCTC12900 harvested during exponential phase, stationary phase and starved state. Dash (–) indicates substrates tested but not utilised. Results are the average of duplicates. Substrates where a significantly different (p<0.05) average $A_{endpoint}$ was observed between any of the pairwise comparisons between exponential phase, stationary phase and starved cells are in bold and the highest value underlined.

Chemical sub-class	Substrates	*SS	Endpoint ($A_{endpoint}$)		
			[1]EP	[2]SP	Starved
Glycosides	α-methyl-D-glucoside		0.661	0.656	0.552
	β-methyl-D-galactoside		0.548	0.536	0.516
Monosaccharides	**D-fructose**	1	**<u>0.703</u>**	**0.679**	**0.515**
	D-galactose		0.539	0.592	0.520
	D-galacturonic acid		0.806	0.686	0.791
	D-gluconic acid		0.850	0.795	0.801
	Dihydroxy acetone		0.099	–	–
	D-mannose		0.649	0.592	0.576
	D-ribose	2	**0.437**	**<u>0.567</u>**	**0.392**
	D-xylose		0.426	0.437	0.492
	L-arabinose		0.280	0.389	0.282
	L-fucose	3	**<u>0.635</u>**	**0.524**	**0.468**
	L-rhamnose		0.388	0.395	0.315
	N-acetyl-D-galactosamine		0.555	0.456	0.421
	N-acetyl-D-glucosamine		0.410	0.507	0.432
	N-acetyl-neuramic acid		0.368	0.299	0.262
	N-acetyl-β-D-mannosamine		–	–	0.115
	α-D-glucose		0.471	0.460	0.497
Oligosaccharides	**3-O-β-D-galactopyranosyl-D-arabinose**	4	**0.271**	**<u>0.650</u>**	**–**
	D-melibiose		0.578	0.533	0.506
	D-raffinose		0.626	0.559	0.508
	D-trehalose	5	**0.584**	**0.498**	**<u>0.707</u>**
	Lactulose	6	**0.131**	**0.238**	**<u>0.389</u>**
	Maltose		0.487	0.514	0.459
	Maltotriose		0.550	0.515	0.610
	Melibionic acid		0.689	0.611	0.614
	α-D-lactose		0.412	0.363	0.451
Polysaccharides	**Dextrin**	7	**0.226**	**<u>0.630</u>**	**0.267**
Sugar alcohols	D-mannitol		0.523	0.456	0.483
	Glycerol	8	**0.388**	**<u>0.406</u>**	**0.222**
Sugar phosphates	D,L-α-glycerol-phosphate		0.375	0.330	0.324
	Fructose-6-phosphate		0.817	0.805	0.706
	Glucose-1-phosphate	9	**0.625**	**0.605**	**<u>0.774</u>**
	Glucose-6-phosphate		0.708	0.666	0.713
Acetic acids	Acetic acid		0.173	0.264	0.228
Dicarboxylic acids	Bromo succinic acid		0.258	0.245	0.248
	D,L-malic acid		0.331	0.355	0.313
	Dihydroxy fumaric acid	10	**0.570**	**<u>0.689</u>**	**–**
	D-malic acid		0.243	0.344	0.289
	Fumaric acid		0.335	0.320	0.324

Chemical sub-class	Substrates	*SS	Endpoint ($A_{endpoint}$)		
			[1]EP	[2]SP	Starved
	L-malic acid		0.403	0.517	0.427
	Mono methyl succinate	11	**–**	**0.160**	**0.118**
	Succinic acid		0.362	0.332	0.286
Hydroxy acids	L-lactic acid		0.545	0.435	0.438
Keto acids	Methyl pyruvate		0.706	0.647	0.670
	Pyruvic acid		0.620	0.648	0.655
Propionates	Propionic acid		–	0.150	–
Sugar acids	D-glucuronic acid		0.695	0.777	0.634
	L-galactonic acid-γ-lactone		0.509	0.474	0.555
	Mucic acid		0.300	0.450	0.428
Nucleosides	**2-deoxy adenosine**	12	**0.727**	**0.444**	**0.627**
	Adenosine		0.752	0.635	0.607
	Inosine		0.634	0.604	0.676
	Thymidine		0.611	0.519	0.562
	Uridine		0.584	0.501	0.534
Amino acids	D-alanine		0.224	0.206	0.176
	L-alanine		0.250	0.308	0.185
	L-asparagine	13	**0.508**	**0.623**	**0.367**
	L-aspartic acid		0.438	0.487	0.440
	L-glutamic acid	14	**0.108**	**0.126**	**0.286**
	L-glutamine		0.259	0.279	0.257
	L-proline		0.499	0.443	0.424
	L-serine	15	**0.511**	**0.588**	**0.435**
	L-threonine	16	**–**	**0.160**	**0.134**
Other amino acids	Glycyl-L-aspartic acid		0.117	–	–
	Glycyl-L-proline		0.165	0.185	0.133
	L-alanyl-glycine		0.337	0.372	0.259

*SS, significant substrates correspond to the numbered substrates in Figure 4-2.

[1]EP, exponential phase

[2]SP, stationary phase

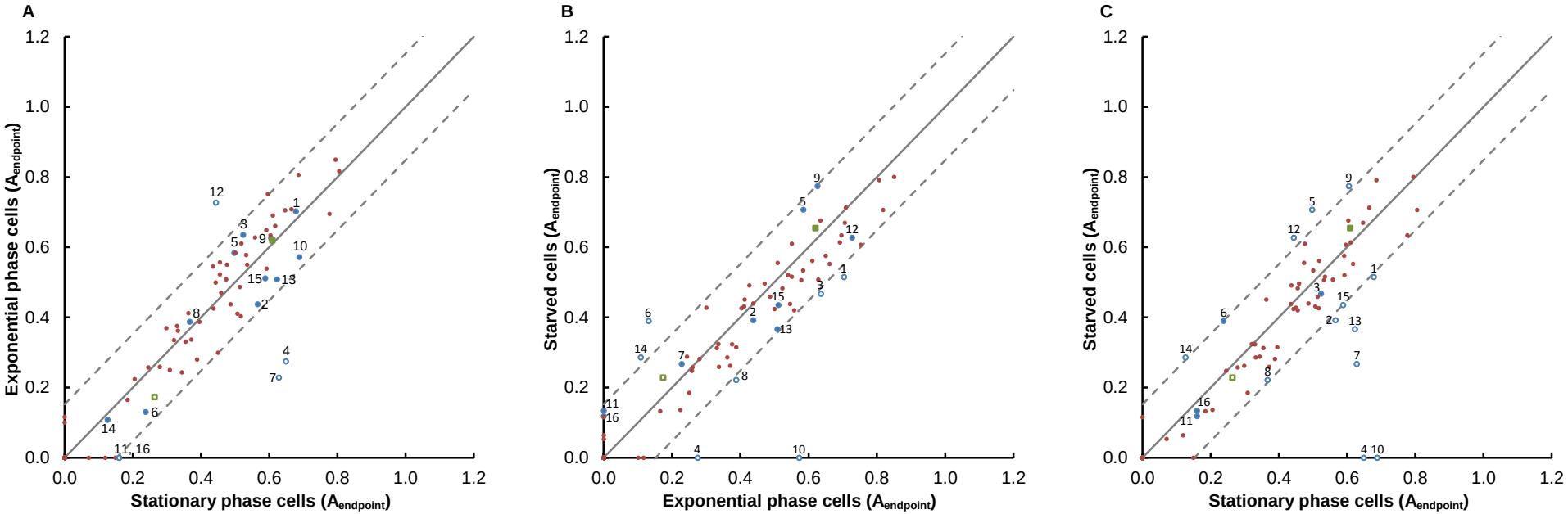

Figure 4-2 Scatter plot comparisons of average $A_{endpoint}$ for substrates used by NCTC12900 harvested during exponential phase (exponential), stationary phase (stationary), and after starvation at 4°C (starved). Pairwise comparisons of $A_{endpoint}$ between exponential and stationary phase (A), starved and exponential phase (B), and starved and stationary phase (C) are shown. The 95% LSD boundaries are marked by dash lines and correlation coefficient (r) = 1 is indicated by the solid line on each graph. Numbered data points marked by blue dots (solid or hollow) correspond to the numbered substrates in Table 4-1; hollow dots mark data points where statistically significant (p<0.05) difference was observed in the pairwise comparison. Pyruvic acid data points are marked by solid green squares and acetic acid data points marked by hollow green squares. Each data point represents the average of duplicates.

(see Chapter 3), which suggested that utilisation of these substrates by starved cells may be different to the non-starved cells. However, no significant difference in $A_{endpoint}$ was observed for pyruvic acid or acetic acid utilisation between exponential phase, stationary phase and starved NCTC12900 (Table 4-1 and Figure 4-2, green squares).

Of the 32 carbohydrates metabolised by NCTC12900, $A_{endpoint}$ of nine substrates differed significantly between exponential phase, stationary phase and starved cells (SS 1 to 9, Table 4-1). $A_{endpoint}$ for the majority of these substrates were significantly higher (p<0.05) for either exponential or stationary phase cells compared to starved cells, except for D-trehalose, lactulose and glucose-1-phosphate (SS 5, 6 and 9, Table 4-1 and Figure 4-2). $A_{endpoint}$ for D-trehalose (SS 5) and glucose-1-phosphate (SS 9) was significantly higher (p<0.05) for starved cells compared to stationary phase cells. No significant difference in $A_{endpoint}$ was observed between exponential phase and starved cells for either substrate.

For 2-deoxy adenosine (SS 12), $A_{endpoint}$ of utilisation was significantly lower for stationary phase cells compared to exponential phase and starved cells. Four of the 12 amino acids (SS 13 to 16) utilised by NCTC12900 were metabolised to significantly different (p<0.05) endpoint levels by exponential phase, stationary phase and starved cells. $A_{endpoint}$ for L-asparagine (SS 13) and L-serine (SS 15) were significantly lower (p<0.05) for starved cells compared to stationary phase cells. The highest L-glutamic acid (SS 15) $A_{endpoint}$ was observed for starved cells. 3-O-β-D-galactopyranosyl-D-arabinose (SS 4) and dihydroxy fumaric acid (SS 10) were utilised by both exponential and stationary phase cells but not starved cells (Table 4-1). Mono methyl succinate (SS 11) and L-threonine (SS 16) were utilised by stationary phase and starved cells while no detectable utilisation was observed for exponential phase cells (Table 4-1).

4.2.1.2 Lag in substrate utilisation by NCTC12900

Of the 67 substrates utilised by exponential phase, stationary phase or starved NCTC12900, λ varied significantly for 52 substrates (p<0.05). Substrates not utilised by exponential phase, stationary phase or starved cells within the duration of the 24-hour assay were considered to have a greater than 24 hour lag and were

omitted from statistical comparisons. The differences between λ observed for the majority of substrates utilised by exponential and stationary phase cells were less than six hours and were not statistically significant (Figure 4-3 A, orange square).

Overall, data points were observed to cluster for each of the three comparisons (Figure 4-3 A, B and C). For exponential to stationary phase, the majority of data points clustered around the r=1 line within the $LSD_{95\%}$ boundaries on the scatter plot (Figure 4-3 A). For both the starved to exponential phase and starved to stationary phase comparisons, the clusters located to the left of the r=1 line outside of the $LSD_{95\%}$ boundary, indicating a significantly longer λ for the majority of the substrates used by the starved cells compared to the exponential and stationary phase cells (Figure 4-3 B and C).

The observed difference in λ between exponential, stationary phase and starved cells was greater than six hours for nine substrates (SS 1 to 9, Table 4-2 and Figure 4-3). λ for 3-O-β-D-galactopyranosyl-D-arabinose (SS 5) was significantly longer (p<0.05) for exponential phase cells compared to stationary phase cells, while λ for L-glutamine (SS 9) was significantly longer (p<0.05) for stationary phase cells. λ for the majority of the numbered substrates were significantly longer (p<0.05) for starved cells compared to exponential phase or stationary phase cells (SS 1 to 8), except for L-glutamine (SS 9). λ for L-glutamine (SS 9) for stationary phase cells was significantly longer (p<0.05) than starved cells (Figure 4-3 C) and no significant difference was observed between starved and exponential phase cells (Figure 4-3 B).

Interestingly, λ for all three pentose sugars tested, D-ribose (SS 1), D-xylose (SS 2) and L-arabinose (SS 3), was at least six hours longer for starved cells compared to exponential and stationary phase cells (Figure 4-3 B and C). A significantly longer (p<0.05) λ in sugar phosphate utilisation was also observed for starved cells compared to exponential and stationary phase cells, with the greatest difference observed for fructose-6-phosphate (SS 6). λ for acetic acid and pyruvic acid utilisation was significantly longer (p<0.05) for starved NCTC12900 cells compared to exponential and stationary phase cells, with approximately a four hour difference observed in both cases (Figure 4-3 B and C and Table 4-2).

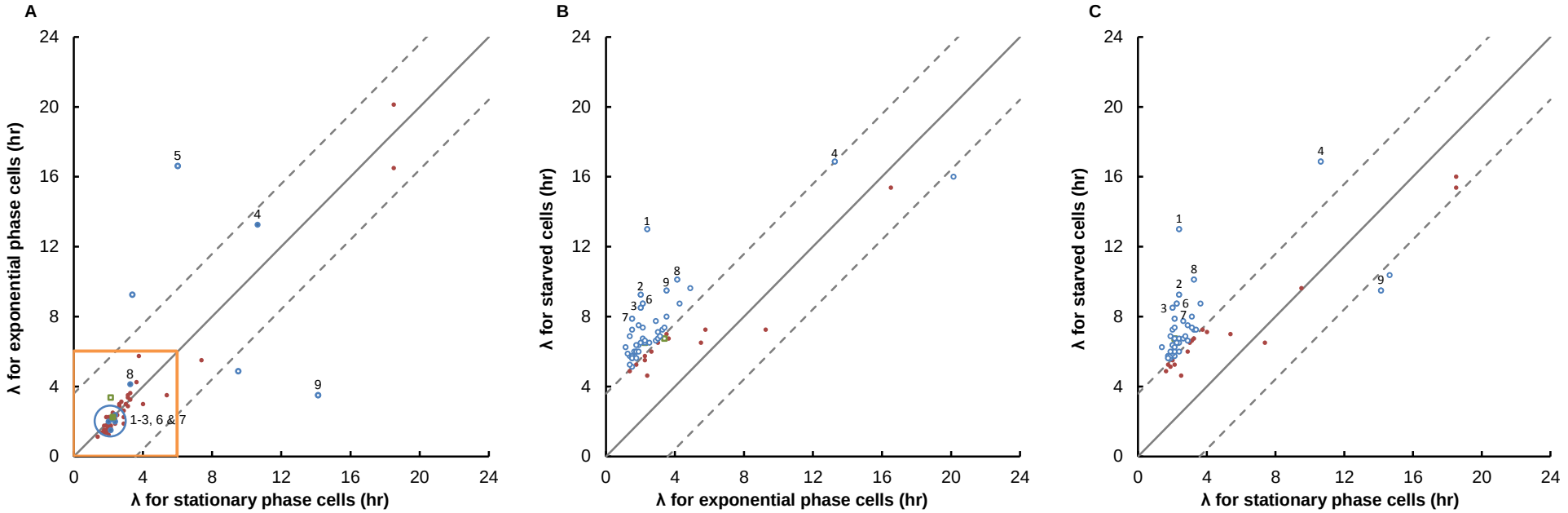

Figure 4-3 Scatter plot comparison of average lag (λ) in substrate utilisation by NCTC12900 harvested during exponential phase, stationary phase, and after starvation at 4°C. Pairwise comparisons of λ between exponential and stationary phase cells (A), starved and exponential phase cells (B), and starved and stationary phase cells (C) are shown. The 95% LSD boundaries are marked by dash lines and correlation coefficient (r) = 1 is indicated by the solid line. Numbered substrates marked by blue dots (solid or hollow) correspond to the numbered substrates in Table 4-2; hollow dots mark data points where statistically significant (p<0.05) difference was observed in the pairwise comparison. Pyruvic acid is marked by solid green squares and acetic acid is marked by hollow green squares. The orange square marks the six-hour difference boundary of the cluster observed in A. Each data point represents the average of duplicates.

Table 4-2 Lag time (λ) for substrates utilised by exponential phase, stationary phase and starved NCTC12900 cells. Results are the average of duplicates. Substrates where a significant different (p<0.05) average lag time was observed between exponential, stationary and starved cells are in bold and are numbered.

Chemical sub-class	Substrates	*SS	λ (hr)		
			[1]EP	[2]SP	Starved
Glycosides	**α-methyl-D-glucoside**		**2.3**	**2.9**	**6.6**
	β-methyl-D-galactoside		3.5	5.4	7.0
Monosaccharides	**D-fructose**		**1.4**	**1.8**	**5.8**
	D-galactose		**1.9**	**2.9**	**7.5**
	D-galacturonic acid		**2.0**	**2.4**	**6.5**
	D-gluconic acid		**1.5**	**1.9**	**5.6**
	Dihydroxy acetone		16.9	>24	>24
	D-mannose		**1.5**	**1.8**	**5.6**
	D-ribose	1	**2.4**	**2.4**	**13.0**
	D-xylose	2	**2.0**	**2.4**	**9.3**
	L-arabinose	3	**2.0**	**2.0**	**8.5**
	L-fucose		**4.3**	**3.6**	**8.8**
	L-rhamnose	4	**13.3**	**10.6**	**16.9**
	***N*-acetyl-D-galactosamine**		**1.9**	**2.4**	**6.0**
	N-acetyl-D-glucosamine		1.4	1.6	4.9
	N-acetyl-neuramic acid		2.4	2.5	4.6
	N-acetyl-β-D-mannosamine		>24	>24	21.8
	α-D-glucose		**1.4**	**1.8**	**5.3**
Oligosaccharides	**3-O-β-D-galactopyranosyl-D-arabinose**	5	**16.6**	**6.0**	**>24**
	D-melibiose		**2.9**	**2.6**	**7.8**
	D-raffinose		**2.1**	**2.4**	**6.8**
	D-trehalose		**1.5**	**1.9**	**5.6**
	Lactulose		**20.1**	**18.5**	**16.0**
	Maltose		**1.8**	**1.9**	**6.0**
	Maltotriose		**1.5**	**1.9**	**5.1**
	Melibionic acid		5.5	7.4	6.5
	α-D-lactose		**1.8**	**1.8**	**5.6**
Polysaccharides	**Dextrin**		**1.1**	**1.4**	**6.3**
Sugar alcohols	**D-mannitol**		**1.5**	**1.8**	**5.8**
	Glycerol		**1.3**	**2.0**	**5.9**
Sugar phosphates	**D,L-α-glycerol-phosphate**		**1.5**	**2.0**	**7.3**
	Fructose-6-phosphate	6	**2.1**	**2.3**	**8.8**
	Glucose-1-phosphate		**2.3**	**1.9**	**5.8**
	Glucose-6-phosphate		**1.4**	**1.9**	**6.9**
Acetic acids	**Acetic acid**		**3.4**	**2.1**	**6.8**
Dicarboxylic acids	**Bromo succinic acid**		**3.0**	**4.0**	**7.1**
	D,L-malic acid		**2.9**	**3.1**	**6.6**
	Dihydroxy fumaric acid		**1.6**	**2.0**	**>24**
	D-malic acid		**3.3**	**3.3**	**7.3**
	Fumaric acid		3.6	3.3	6.8
	L-malic acid		3.0	3.0	6.5

Chemical sub-class	Substrates	*SS	λ (hr)		
			[1]EP	[2]SP	Starved
	Mono methyl succinate		**>24**	**2.1**	**6.3**
	Succinic acid		2.3	2.0	5.5
Hydroxy acids	**L-lactic acid**		**1.8**	**2.1**	**6.0**
Keto acids	Methyl pyruvate		1.8	2.1	5.3
	Pyruvic acid		**2.3**	**2.3**	**6.5**
Propionates	Propionic acid		>24	15.8	>24
Sugar acids	**D-glucuronic acid**		**1.8**	**2.0**	**6.4**
	L-galactonic acid-γ-lactone		2.6	2.9	6.0
	Mucic acid		5.8	3.8	7.3
Nucleosides	**2-deoxy adenosine**		**1.9**	**2.0**	**6.4**
	Adenosine		**1.6**	**2.1**	**5.8**
	Inosine		**1.6**	**2.0**	**6.0**
	Thymidine	7	**1.5**	**2.1**	**7.9**
	Uridine	8	**4.1**	**3.3**	**10.1**
Amino acids	**D-alanine**		**2.5**	**2.3**	**6.5**
	L-alanine		**3.5**	**3.1**	**8.0**
	L-asparagine		**3.0**	**2.6**	**6.8**
	L-aspartic acid		**3.1**	**2.8**	**6.9**
	L-glutamic acid		16.5	18.5	15.4
	L-glutamine	9	**3.5**	**14.1**	**9.5**
	L-proline		**4.9**	**9.5**	**9.6**
	L-serine		**2.1**	**2.1**	**7.4**
	L-threonine		**>24**	**14.6**	**10.4**
Other amino acids	Glycyl-L-aspartic acid		18.8	>24	>24
	Glycyl-L-proline		**9.3**	**3.4**	**7.3**
	L-alanyl-glycine		**3.4**	**3.1**	**7.4**

*SS, significant substrates correspond to the numbered substrates in Figure 4-3.

[1]EP, exponential phase

[2]SP, stationary phase

4.2.1.3 Rate of NCTC12900 substrate utilisation

The rate of substrate use was defined as the rate of exponential substrate metabolism (μ_{exp}) measured in $A_{activity}$ hr^{-1}. Overall, μ_{exp} for substrates used by exponential phase cells was slightly lower than stationary phase and starved cells (Figure 4-4 A and B).

Scatter plot comparisons of μ_{exp} for substrates used by exponential and stationary phase cells showed that data points scattered toward the right of the r = 1 line, eight of which were outside of the $LSD_{95\%}$ boundary (SS 1, 3, 4, 6, 8, 11, 12 and 14, Figure 4-4 A and Table 4-3). Similar trends were observed for the starved to exponential comparison where eight substrates were found to be utilised at a significantly higher rate (p<0.05) for starved cells (SS 2, 5, 7, 8, 11 to 13 and 15, Figure 4-4 B and Table 4-3). Comparisons of μ_{exp} for starved cells to exponential and stationary phase cells showed that μ_{exp} for D-galacturonic acid (SS 2) and glucose-1-phosphate (SS 7) were significantly (p<0.05) higher for starved cells (Figure 4-4 B and C, and Table 4-3). Additionally, for starved to stationary phase comparison, μ_{exp} for D-galactose (SS 1), D-gluconic acid (SS 3), D-ribose (SS 4), glycerol (SS 9) and D,L-α-glycerol-phosphate (SS 10) were significantly lower (p<0.05) for starved cells (Figure 4-4 C, and Table 4-3).

Interestingly, μ_{exp} for all four sugar phosphates tested (SS 10 to 13) varied significantly between cells harvested during different growth stages (Figure 4-4 and Table 4-3). Highest μ_{exp} for D,L-α-glycerol-phosphate (SS10) was observed for stationary phase cells, with the greatest significant difference observed between stationary phase and starved cells (p<0.05; Table 4-3 and Figure 4-4 C). For fructose-6-phosphate (SS 11), glucose-1-phsophate (SS 12) and glucose-6-phosphate (SS 13), highest μ_{exp} was observed for starved cells and the differences were significant (p<0.05) between starved and exponential phase cells (Table 4-3 and Figure 4-4 B). No significant variation was observed in the rate of pyruvic acid (solid green squares Figure 4-4) or acetic acid (hollow green squares Figure 4-4) utilisation between cells harvested during different growth stages.

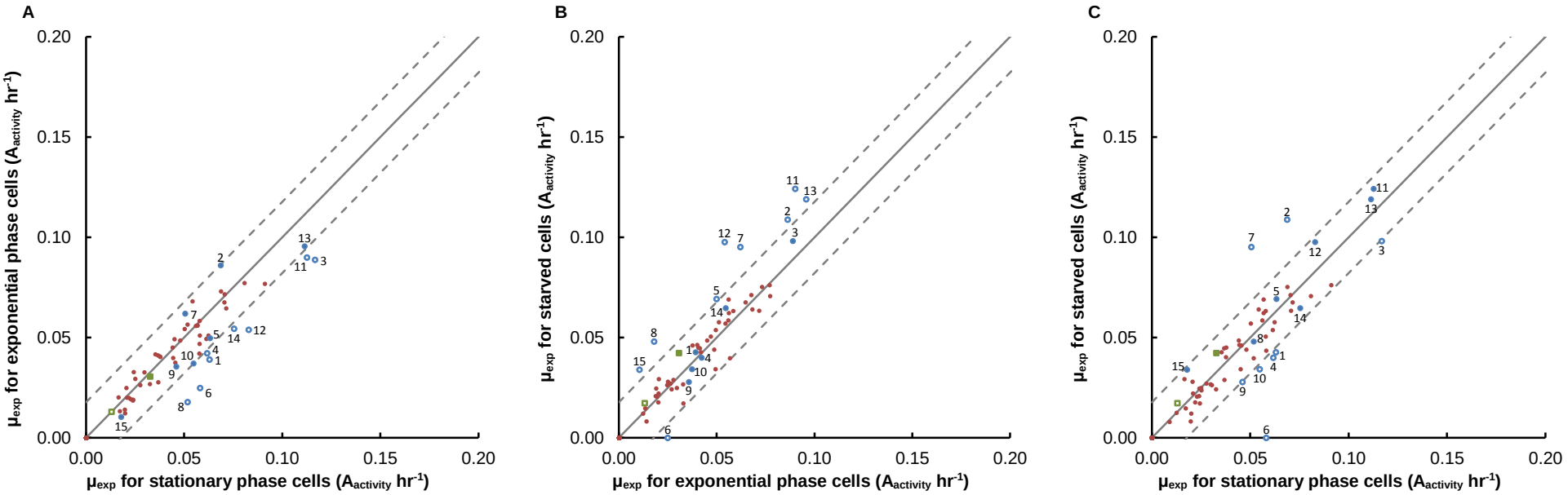

Figure 4-4 Scatter plot comparison of average rate (μ_{exp}) of substrate utilisation by NCTC12900 harvested during exponential phase, stationary phase, and after starvation at 4°C. Pairwise comparisons of μ_{exp} between exponential and stationary phase cells (A), starved and exponential phase cells (B), and starved and stationary phase cells (C) are shown. The 95% LSD boundaries are marked by dash lines and correlation coefficient (r) = 1 is indicated by the solid grey line. Numbered substrates marked by blue dots (solid or hollow) correspond to the numbered substrates in Table 4-3; hollow dots mark data points where statistically significant (p<0.05) difference was observed in the pairwise comparison. Pyruvic acid is marked by solid green squares and acetic acid is marked by hollow green squares. Each data point represents the average of duplicates.

Table 4-3 Rate of substrates used (μ_{exp}) by exponential phase, stationary phase and starved NCTC12900 cells. Dash (–) indicates substrates not utilised. Results are the average of duplicates. Substrates where a significant different (p<0.05) average μ_{exp} was observed between exponential, stationary and starved cells are in bold and are numbered.

Chemical sub-class	Substrates	*SS	μ_{exp} ($A_{activity}$ hr^{-1})		
			[1]EP	[2]SP	Starved
Glycosides	α-methyl-D-glucoside		0.051	0.058	0.044
	β-methyl-D-galactoside		0.041	0.038	0.040
Monosaccharides	D-fructose		0.077	0.081	0.071
	D-galactose	1	**0.039**	**0.063**	**0.043**
	D-galacturonic acid	2	**0.086**	**0.069**	**0.109**
	D-gluconic acid	3	**0.089**	**0.117**	**0.098**
	Dihydroxy acetone		0.004	–	–
	D-mannose		0.073	0.069	0.075
	D-ribose	4	**0.042**	**0.062**	**0.040**
	D-xylose	5	**0.050**	**0.063**	**0.069**
	L-arabinose		0.040	0.044	0.046
	L-fucose		0.047	0.058	0.051
	L-rhamnose		0.037	0.045	0.046
	N-acetyl-D-galactosamine		0.057	0.052	0.040
	N-acetyl-D-glucosamine		0.056	0.057	0.069
	N-acetyl-neuramic acid		0.042	0.035	0.043
	N-acetyl-β-D-mannosamine		–	–	0.015
	α-D-glucose		0.065	0.071	0.068
Oligosaccharides	**3-O-β-D-galactopyranosyl-D-arabinose**	6	**0.025**	**0.058**	**–**
	D-melibiose		0.049	0.061	0.054
	D-raffinose		0.056	0.056	0.059
	D-trehalose	7	**0.062**	**0.051**	**0.095**
	Lactulose	8	**0.018**	**0.052**	**0.048**
	Maltose		0.051	0.062	0.058
	Maltotriose		0.068	0.054	0.064
	Melibionic acid		0.049	0.048	0.044
	α-D-lactose		0.056	0.057	0.062
Polysaccharides	Dextrin		0.049	0.045	0.034
Sugar alcohols	D-mannitol		0.058	0.058	0.063
	Glycerol	9	**0.036**	**0.046**	**0.028**
Sugar phosphates	**D,L-α-glycerol-phosphate**	10	**0.037**	**0.055**	**0.034**
	Fructose-6-phosphate	11	**0.090**	**0.113**	**0.124**
	Glucose-1-phosphate	12	**0.054**	**0.083**	**0.098**
	Glucose-6-phosphate	13	**0.096**	**0.111**	**0.119**
Acetic acids	Acetic acid		0.013	0.013	0.017
Dicarboxylic acids	Bromo succinic acid		0.020	0.017	0.029
	D,L-malic acid		0.019	0.024	0.021
	Dihydroxy fumaric acid		0.042	0.058	–
	D-malic acid		0.020	0.021	0.022
	Fumaric acid		0.025	0.021	0.028
	L-malic acid		0.026	0.028	0.027

Chemical sub-class	Substrates	*SS	μ_{exp} ($A_{activity}$ hr^{-1})		
			[1]EP	[2]SP	Starved
	Mono methyl succinate		–	0.025	0.024
	Succinic acid		0.020	0.022	0.018
Hydroxy acids	L-lactic acid		0.029	0.025	0.025
Keto acids	Methyl pyruvate		0.040	0.038	0.045
	Pyruvic acid		0.031	0.033	0.042
Propionates	Propionic acid		–	0.018	–
Sugar acids	D-glucuronic acid		0.077	0.091	0.076
	L-galactonic acid-γ-lactone		0.041	0.037	0.045
	Mucic acid		0.019	0.024	0.025
Nucleosides	**2-deoxy adenosine**	14	**0.054**	**0.075**	**0.065**
	Adenosine		0.072	0.071	0.063
	Inosine		0.068	0.070	0.071
	Thymidine		0.054	0.050	0.057
	Uridine		0.045	0.044	0.049
Amino acids	D-alanine		0.012	0.020	0.012
	L-alanine		0.013	0.017	0.015
	L-asparagine		0.027	0.033	0.024
	L-aspartic acid		0.025	0.030	0.026
	L-glutamic acid	15	**0.010**	**0.018**	**0.034**
	L-glutamine		0.033	0.024	0.017
	L-proline		0.033	0.030	0.027
	L-serine		0.028	0.037	0.029
	L-threonine		–	0.013	0.013
Other amino acids	Glycyl-L-aspartic acid		0.008	–	–
	Glycyl-L-proline		0.014	0.020	0.008
	L-alanyl-glycine		0.019	0.023	0.021

*SS, significant substrates correspond to the numbered substrates in Figure 4-13

[1]EP, exponential phase

[2]SP, stationary phase

4.2.1.4 NCTC12900 utilisation of substrates involved in glycolysis

Glycolysis is one of the central pathways for cell metabolism (Madigan *et al.*, 2012). Of the 190 sole carbon sources included in the Biolog PM1 and PM2A MicroPlates^{TM}, five were involved in glycolysis: glucose-1-phosphate, D-glucose, glucose-6-phosphate, fructose-6-phosphate and pyruvic acid. Overall, very little difference in glycolic substrate utilisation was observed between exponential and stationary phase NCTC12900, while a significantly longer (p<0.05) duration of lag was observed for starved cells in all cases (Figure 4-5). No significant difference in $A_{endpoint}$ was observed for D-glucose, fructose-6-phosphate and pyruvic acid, however, $A_{endpoint}$ for glucose-1-phosphate was significantly higher (p<0.05) for starved cells compared to exponential phase cells (SS 9, Figure 4-5 and Table 4-1). There was no significant difference in λ between exponential and stationary phase cells (Figure 4-5), however, λ for the starved cells was significantly longer (p<0.05) than for exponential and stationary phase cells in all cases (Figure 4-5). Interestingly, while there was no significant difference in μ_{exp} for the five glycolytic substrates was observed for stationary phase and starved cells, μ_{exp} for glucose-6-phosphate, glucose-1-phosphate and fructose-6-phosphate was significantly lower (p<0.05) for exponential phase cells compared to stationary phase and starved cells (Figure 4-5).

4.2.1.5 NCTC12900 substrate use in anaerobic conditions

The metabolic pathway used by *E. coli* under anaerobic conditions differs from that used during aerobic growth (Ingledew & Poole, 1984). To test the effect of anaerobic growth on substrate use, PM1 plates were inoculated with stationary phase cells or cells starved at 4°C for 90 days and incubated in an anaerobic chamber with an atmosphere of 5% H_2, 10% CO_2 and 85% N_2. The maximum level of utilisation for each substrate after 24 hours of incubation ($A_{endpoint}$) was measured. The reducing atmosphere of the anaerobic environment resulted in greater background colour development in the negative control than observed in aerobic incubation, due to reduction of the tetrazolium violet dye. However, metabolism of carbon in the test wells resulted in a higher intensity of colour development and $A_{endpoint}$ was successfully measured by subtracting the negative control measurement from the carbon source measurement.

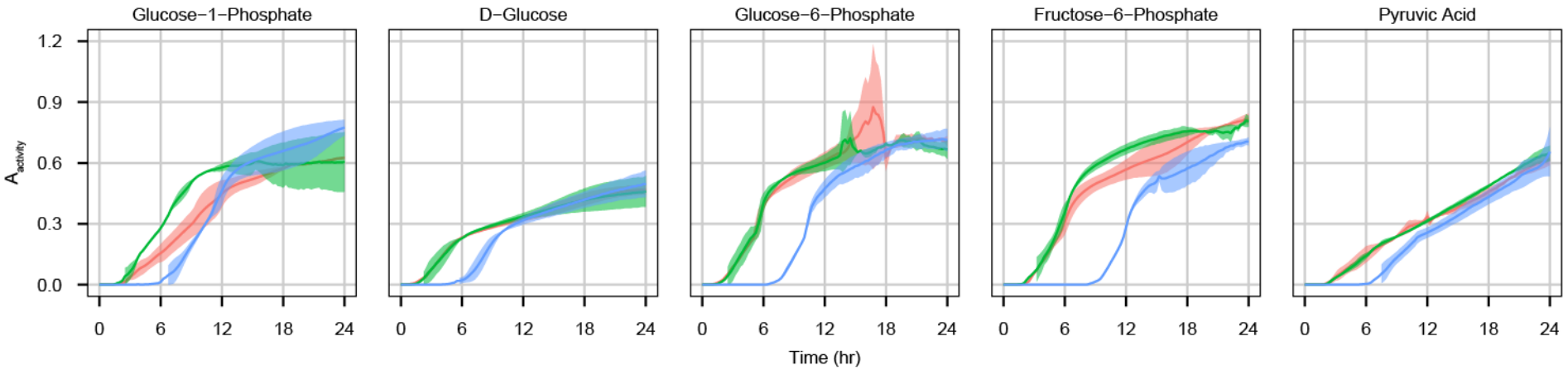

Figure 4-5 Utilisation kinetics of substrates involved in glycolysis by exponential phase, stationary phase and 4°C-starved NCTC12900. Substrate use for exponential phase (red), stationary phase (green) and starved (blue) cells are shown. Lines indicate average of duplicates and the standard deviations are shown by shaded areas.

Comparisons of substrate use by stationary phase and starved cells during anaerobic recovery showed three distinct clusters of substrates. No significant difference was observed in the utilisation of 55 substrates, utilisation of 23 substrates were significantly higher ($p<0.05$) for stationary phase cells, and 22 substrates were significantly higher ($p<0.05$) for starved cells (Figure 4-6 C and Table 4-4). The ethylene glycols tested were only utilised by stationary phase cells under anaerobic conditions. Higher utilisation by stationary phase cells was observed for the majority of monosaccharides, oligosaccharides and amino acids (Table 4-4). Anaerobic metabolism of all sugar phosphates, sugar acids and nucleotides tested were significantly higher ($p<0.05$) for starved cells compared to stationary phase cells. In addition, anaerobic metabolism of methyl pyruvate and pyruvic acid were also significantly higher ($p<0.05$) for starved cells (Table 4-4).

In general, $A_{endpoint}$ for substrates used during anaerobic growth was lower than that observed during aerobic growth (Figure 4-6 A and B). A significant difference ($p<0.05$) in $A_{endpoint}$ was observed between anaerobically and aerobically grown cells for 42 and 41 substrates utilised by stationary phase (Figure 4-6 A) and starved cells (Figure 4-6 B), respectively (Table 4-4). No significant difference in $A_{endpoint}$ for D-alanine and glycyl-L-proline was observed between aerobic and anaerobic growth for either stationary phase or starved cells. $A_{endpoint}$ for pyruvate utilisation was lower for both stationary phase and starved cells under anaerobic growth conditions compared to aerobic growth (Figure 4-6 A and B, Table 4-4). Anaerobic metabolism of acetic acid was significantly lower compared to aerobic metabolism for stationary phase cells; no significant difference was observed for starved cells (Figure 4-6 B, Table 4-4).

4.2.2 Substrate utilisation by clinical and bovine isolates of *E. coli* O157:H7

Although NCTC12900 was originally a clinical isolate from an Austrian public health laboratory (Best *et al.*, 2005), it has been used within the laboratory as a naturally toxin-minus *E. coli* O157:H7 reference strain for many studies. To investigate whether recently isolated *E. coli* O157:H7 strains produce a different metabolic profile to NCTC12900, substrate utilisation by three New Zealand clinical strains isolated during 2010 (ERL10621, ERL10630 and ERL10780) was tested during aerobic growth using PM1 plates. Clinical *E. coli* O157:H7 cases

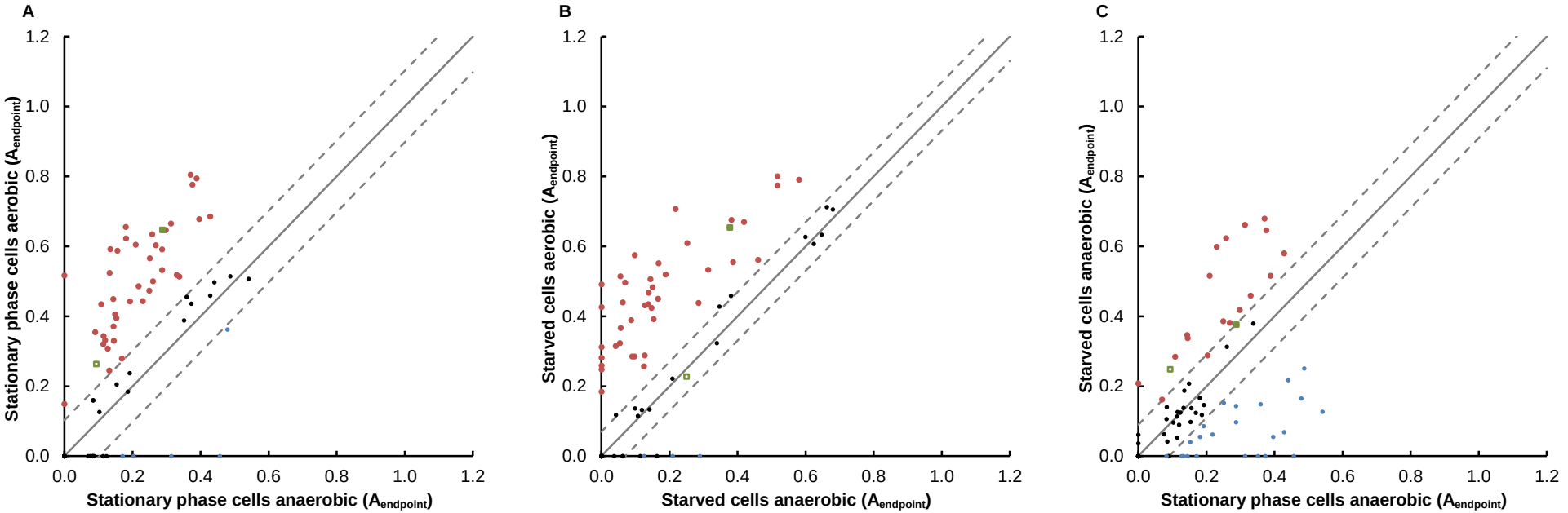

Figure 4-6 Scatter plot comparisons of the average $A_{endpoint}$ of aerobic and anaerobic substrate utilisation by NCTC12900 harvested during stationary phase and after 90 days of starvation at 4°C. Pairwise comparisons of $A_{endpoint}$ during anaerobic and aerobic growth for stationary phase (A) and starved cells (B), and during anaerobic growth for starved and stationary phase cells (C) are shown. The 95% LSD boundaries are marked by dash lines and correlation coefficient (r) = 1 is indicated by the solid line. Pyruvic acid is marked by solid green squares and acetic acid is marked by hollow green squares. Substrates with significantly higher (p<0.05) $A_{endpoint}$ from the y-axis culture than the x-axis culture are marked by red dots; substrates with significantly higher (p<0.05) $A_{endpoint}$ from the x-axis culture than the y-axis culture are marked by blue dots. Black dots mark the substrates where the difference in pairwise comparison was not statistically significant. Each data point represents the average of duplicates.

Table 4-4 $A_{endpoint}$ for the substrate utilisation by anaerobically grown stationary phase and 4°C-starved NCTC12900. Dash (–) indicates substrates not utilised. Results are the average of duplicates. Substrates where significantly higher (p<0.05) $A_{endpoint}$ was observed under anaerobic conditions compared to aerobic incubation are marked by "*"; substrates with significantly lower (p<0.05) $A_{endpoint}$ were marked by "n". Substrates with $A_{endpoint}$ that differed significantly (p<0.05) between the anaerobically grown 24-hour and starved cells are in bold; and the cell type with the higher $A_{endpoint}$ is listed in the "Significantly higher" column.

Chemical sub-class	Substrates	Stationary phase cells		Starved cells		Significantly higher
Ethylene glycols	**Tween 20**	**0.457**	*****	**–**		**stationary**
	Tween 40	0.088		–		
	Tween 80	**0.314**	*****	**–**		**stationary**
Glycosides	α-methyl-D-glucoside	0.180	n	0.167	n	
	β-methyl-D-glucoside	0.123		0.125	*	
Monosaccharides	**D-fructose**	**0.396**	**n**	**0.055**	**n**	**stationary**
	D-galactose	0.135	n	0.188	n	
	D-galacturonic acid	**0.428**	**n**	**0.581**	**n**	**starved**
	D-gluconic acid	**0.388**	**n**	**0.516**	**n**	**starved**
	D-mannose	**0.287**	**n**	**0.097**	**n**	**stationary**
	D-ribose	**0.251**	**n**	**0.153**	**n**	**stationary**
	D-xylose	**0.373**		**–**	**n**	**stationary**
	L-arabinose	**0.351**		**–**	**n**	**stationary**
	L-fucose	0.132	n	0.138	n	
	L-rhamnose	**0.152**	**n**	**0.041**	**n**	**stationary**
	***N*-acetyl-D-glucosamine**	**0.541**		**0.127**	**n**	**stationary**
	N-acetyl-β-D-mannosamine	0.083		0.106		
	α-D-glucose	**0.428**		**0.069**	**n**	**stationary**
Oligosaccharides	**D-melibiose**	**0.287**	**n**	**0.143**	**n**	**stationary**
	D-trehalose	**0.440**		**0.217**	**n**	**stationary**
	Lactulose	**0.192**		**0.086**	**n**	**stationary**
	Maltose	0.338	n	0.380		
	Maltotriose	**0.488**		**0.251**	**n**	**stationary**
	Sucrose	**0.171**	*****	**–**		**stationary**
	α-D-lactose	**0.479**	*****	**0.166**	**n**	**stationary**
Sugar alcohols	**D-mannitol**	**0.359**		**0.149**	**n**	**stationary**
	D-sorbitol	–		0.061		
	Dulcitol	**–**		**0.209**	*****	**starved**
	Glycerol	0.148	n	0.208		
Sugar phosphates	**D,L-α-glycerol-phosphate**	**0.145**	**n**	**0.338**		**starved**
	Fructose-6-phosphate	**0.370**	**n**	**0.680**		**starved**
	Glucose-1-phosphate	**0.210**	**n**	**0.516**	**n**	**starved**
	Glucose-6-phosphate	**0.313**	**n**	**0.662**		**starved**
Acetic acids	**Acetic acid**	**0.094**	**n**	**0.249**		**starved**
Dicarboxylic acids	**Bromo succinic acid**	**0.132**	**n**	**–**	**n**	**stationary**
	Citramalic acid	–		–		
	D,L-malic acid	0.090	n	–	n	
	D-malic acid	0.115	n	0.126	n	
	Fumaric acid	0.114	n	0.053	n	

Chemical sub-class	Substrates	Stationary phase cells		Starved cells		Significantly higher
	L-malic acid	–	n	–	n	
	Mono methyl succinate	0.085		0.042		
	Succinic acid	0.120	n	0.090	n	
	α-keto-glutaric acid	–		0.037		
Hydroxy acids	**L-lactic acid**	**0.108**	**n**	**0.285**	**n**	**starved**
Keto acids	**Acetoacetic acid**	**0.082**		**0.000**		**stationary**
	Methyl pyruvate	**0.298**	**n**	**0.418**	**n**	**starved**
	Pyruvic acid	**0.288**	**n**	**0.377**	**n**	**starved**
Propionates	Propionic acid	–	n	–		
Sugar acids	**D-glucuronic acid**	**0.376**	**n**	**0.646**		**starved**
	Glucuronamide	**0.203**	*****	**0.288**	*****	**starved**
	L-galactonic acid-γ-lactone	**0.250**	**n**	**0.386**	**n**	**starved**
	Mucic acid	**0.143**	**n**	**0.346**		**starved**
Fatty acids	Formic acid	0.076		0.063		
Nucleosides	**2-deoxy adenosine**	**0.230**	**n**	**0.599**		**starved**
	Adenosine	**0.258**	**n**	**0.624**		**starved**
	Inosine	**0.269**	**n**	**0.382**	**n**	**starved**
	Thymidine	**0.330**	**n**	**0.459**	**n**	**starved**
	Uridine	0.260	n	0.313	n	
Amino acids	D-alanine	0.154		0.098		
	Glycyl-L-aspartic acid	0.114		0.114		
	Glycyl-L-glutamic acid	**0.070**		**0.162**		**starved**
	Glycyl-L-proline	0.186		0.118		
	L-alanine	**0.128**	**n**	**–**	**n**	**stationary**
	L-alanyl-glycine	**0.144**	**n**	**–**	**n**	**stationary**
	L-asparagine	**0.181**	**n**	**0.056**	**n**	**stationary**
	L-aspartic acid	**0.218**	**n**	**0.062**	**n**	**stationary**
	L-glutamic acid	0.103		0.097	n	
	L-glutamine	0.169	n	0.125	n	
Amino acids	L-proline	0.193	n	0.147	n	
	L-serine	0.156	n	0.137	n	
	L-threonine	0.084		0.140		

in New Zealand are predominantly associated with rural environment rather than foodborne transmission. To investigate the metabolic similarities and differences between isolates of clinical and rural origin, two O157-positive bovine isolates were also tested using PM1 plates under both aerobic and anaerobic conditions. One of the bovine isolates, H11-, was confirmed to be *E. coli* O157:H7, however, H11+ was later identified to be an *E. fergusonii* strain that cross-reacted with the anti-O157 immunomagnetic beads used for *E. coli* O157 isolation.

Cells were harvested during exponential phase, stationary phase, and after 37 to 57 days of starvation at 4°C. $A_{endpoint}$, λ and μ_{exp} were compared between the clinical strains and the bovine strains. Heat map profiles were used to compare substrate utilisation between strains. Strain variations were determined based on pair-wise analyses using the 95% least significant difference test ($LSD_{95\%}$). Where more than two strains were compared, utilisation of a given substrate was deemed significantly different if a statistically significant difference ($p<0.05$) was observed in at least one pair-wise comparisons. The relationship of cell status prior to recovery (e.g. exponential growth, stationary phase and starvation at 4°C) and carbon utilisation during subsequent growth was also examined.

4.2.2.1 $A_{endpoint}$ for substrates utilised by clinical and bovine cells under aerobic conditions

Overall, similar numbers of carbon sources were utilised by the clinical isolates, ERL10621, ERL10630 and ERL10780 (Table 4-5). $A_{endpoint}$ of all substrates utilised by ERL10621, ERL10630 and ERL10780 are shown in Appendix 2, Appendix 3 and Appendix 4, respectively. For the bovine isolates, more substrates were utilised by H11+ than H11- (Table 4-5). $A_{endpoint}$ of all substrates utilised by H11+ and H11- are shown in Appendix 5 and Appendix 6, respectively. Comparison between clinical cells harvested during exponential, stationary phase and starved stages showed that, overall, the highest number of substrates was utilised by stationary phase cells (Table 4-5). Equal numbers of substrates were used by exponential and stationary phase H11- and H11+ (Table 4-5). Interestingly, the number of substrates utilised by starved H11- was higher than exponential and stationary phase cells; while fewer substrates were utilised by starved H11+ compared to exponential and stationary phase cells.

Table 4-5 Number of substrates tested using PM1 MicroPlate™ incubated under aerobic conditions that were utilised by clinical and bovine strains harvested during exponential phase, stationary phase and after starvation at 4°C.

Cell state	ERL10621	ERL10630	ERL10780	H11-	H11+
Exponential	50	54	54	45	62
Stationary	55	57	61	45	62
Starved	50	50	55	51	51

The $A_{endpoint}$ profiles were similar for the clinical strains regardless of the growth stage at which the cells were harvested (Figure 4-7 A, B and C). However, $A_{endpoint}$ for majority of the substrates used by ERL10780 was significantly higher ($p<0.05$) than ERL10621 and ERL10630. A significant difference ($p<0.05$) in $A_{endpoint}$ was observed for 11, 30 and 30 substrates between the three clinical isolates harvested during exponential, stationary phase and starved state, respectively (red arrows, Figure 4-7). When comparing cells harvested during different growth stages, highest $A_{endpoint}$ was observed for cells harvested during stationary phase and lowest for starved cells (Table 4-6).

For bovine strains, a significant difference ($p<0.05$) in $A_{endpoint}$ was observed between H11- and H11+ for the majority of substrates (Figure 4-8 A, B and C). Significant difference ($p<0.05$) in $A_{endpoint}$ was observed between the bovine strains for 38, 42 and 34 substrates harvested at exponential, stationary phase and starved cells, respectively (red arrows, Figure 4-8). For cells harvested during exponential and stationary phase, overall, significantly higher ($p<0.05$) $A_{endpoint}$ for carboxylic acids and peptides was observed for H11+ compared to H11- (red arrows, Figure 4-8 A and B). When cells harvested during different growth stages were compared, the trend was similar to that observed for the clinical strains, where highest $A_{endpoint}$ was observed for cells harvested during stationary phase and lowest for starved cells (Table 4-7).

4.2.2.2 Lag in the substrate utilisation by clinical and bovine cells under aerobic conditions

Little variation in λ was observed among the clinical strains harvested during exponential, stationary phase and starved state (red arrows, Figure 4-9). The majority of the differences observed were due to substrates not being utilised by at least one of the three clinical strains tested (substrates 20, 27, 35, 44, 62, 67, 68, 83 to 85, 88, 90, 92 and 94, Figure 4-9). When compared between cells harvested during different growth stages, no significant difference in lag was observed between exponential and stationary phase cells for the majority of substrates tested (Figure 4-10). Significantly longer ($p<0.05$) λ was observed for starved cells compared to ribose, D-xylose, *N*-acetyl-β-D-mannosamine, thymidine, uridine and L-alanine compared to the non-starved cells. λ for all substrates

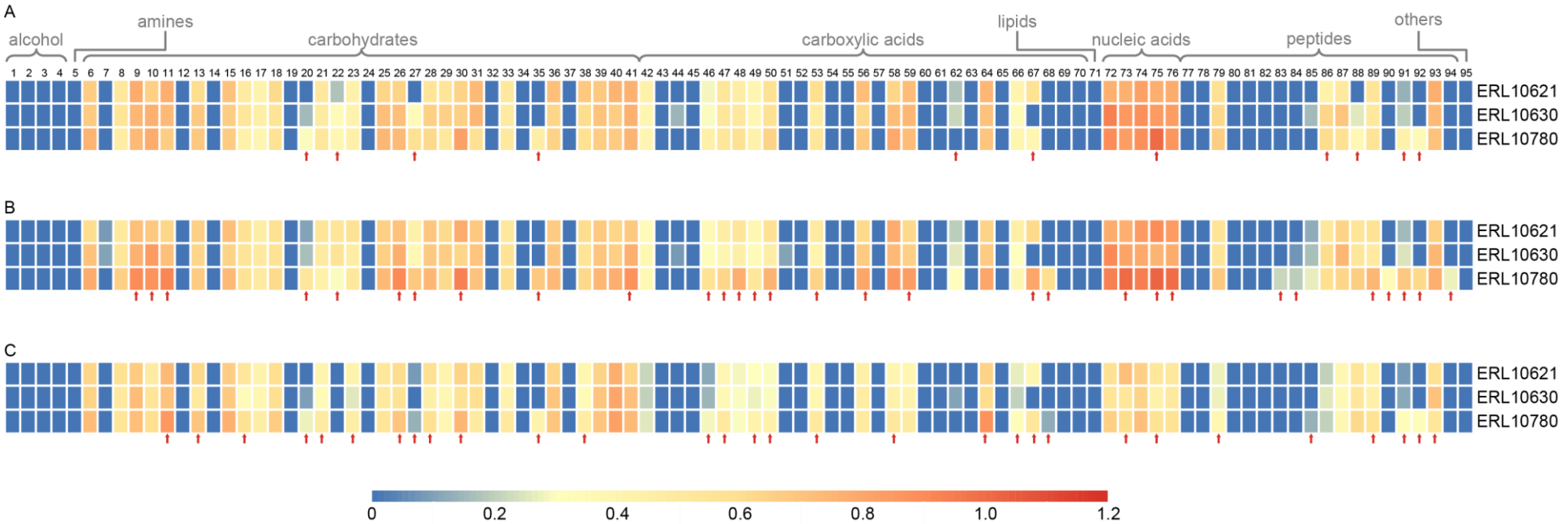

Figure 4-7 $A_{endpoint}$ profiles of clinical strains determined using PM1 MicroPlate™. Substrates are clustered according to the first-level chemical class outlined in Appendix 1 and comparisons made between strains harvested during exponential phase (A), stationary phase (B) and after starvation at 4°C (C). Substrates not utilised were considered to have an $A_{endpoint}$ of 0. The colour-coding of $A_{endpoint}$ levels is indicated by the key. Red arrows and numbers indicate substrates where statistically significant ($p<0.05$) differences were observed between the $A_{endpoint}$ levels of the strains tested. Arbitrary numbers were assigned to each substrate tested and refer to the substrates listed in Table 4-6. Data used for ERL10621, ERL10630 and ERL10780 are listed in Appendices 2 to 4, respectively.

Table 4-6 List of substrates where a statistically significant difference (p<0.05) in $A_{endpoint}$ observed between clinical cells harvested during exponential phase, stationary phase and after starvation at 4°C. Relationships of inequality between $A_{endpoint}$ observed for exponential phase (EP), stationary phase (SP) and 4°C-starved cells (starved) are shown.

Chemical sub-class	Substrates	Number*	ERL10621	ERL10630	ERL10780
Monosaccharides	D-galacturonic acid	10	EP & SP > starved	EP & SP > starved	SP > starved
	D-gluconic acid	11	EP> SP		SP > EP
	D-mannose	13		EP & SP > starved	
	D-xylose	16		EP & SP > starved	
	L-arabinose	17		SP > starved	
	L-rhamnose	20			SP > EP & starved
	N-acetyl-D-glucosamine	21	SP > starved	EP & SP > starved	
	N-acetyl-β-D-mannosamine	22	(EP > SP) > starved	(EP > SP) > starved	EP & SP > starved
	α-D-glucose	23	SP > EP & starved	EP & SP > starved	
Oligosaccharides	D-melibiose	25	SP > starved	EP & SP > starved	
	Lactulose	27	SP > EP & starved	EP & SP > starved	EP & SP > starved
	Maltose	28	SP > EP	EP & SP > starved	
	Maltotriose	29	EP & SP > starved	EP & SP > starved	SP > starved
	Sucrose	30	SP > EP & starved		
	α-D-lactose	31	EP> starved	EP> starved	
Sugar alcohols	D-mannitol	33		SP > starved	
	Dulcitol	35			SP > starved
Sugar phosphates	D,L-α-glycerol-phosphate	38	EP & SP > starved	EP & SP > starved	
	Glucose-1-phosphate	40	starved > SP	starved > EP & SP	
	Glucose-6-phosphate	41	EP> starved		
Acetic acids	Acetic acid	42	EP & SP > starved	EP & SP > starved	
Butyric acids	α-hydroxy Butyric acid	44		EP> starved	
Dicarboxylic acids	Bromo succinic acid	46	EP & SP > starved	EP & SP > starved	SP > starved
	D,L-malic acid	47	EP> starved	EP > SP & starved	
	D-malic acid	48	EP & SP > starved	EP & SP > starved	EP & SP > starved
	L-malic acid	50	EP & SP > starved	EP & SP > starved	SP > starved
	Succinic acid	53	EP> starved		
Hydroxy acids	L-lactic acid	56	EP & SP > starved	EP & SP > starved	SP > starved
Keto acids	Methyl pyruvate	58	(EP > SP) > starved	EP & SP > starved	EP & SP > starved
	Pyruvic acid	59	EP & SP > starved	EP & SP > starved	EP & SP > starved
Propionates	Propionic acid	62	EP & SP > starved	EP & SP > starved	SP > EP & starved
Sugar acids	Glucuronamide	66	EP & SP > starved	EP> starved	
	L-galactonic acid-γ-lactone	67	EP & SP > starved		SP > EP & starved
	Mucic acid	68			SP > EP & starved
Nucleosides	2-deoxy adenosine	72	EP & SP > starved	EP & SP > starved	EP & SP > starved
	Adenosine	73		EP & SP > starved	EP & SP > starved
	Inosine	74	EP & SP > starved	EP & SP > starved	
	Thymidine	75	EP & SP > starved	EP & SP > starved	EP & SP > starved
	Uridine	76	EP & SP > starved	EP & SP > starved	EP & SP > starved
	D-alanine	79	EP & SP > starved	EP & SP > starved	EP & SP > starved
Amino acids	Glycyl-L-proline	85		EP & SP > starved	SP > EP
	L-alanine	86	EP & SP > starved	EP & SP > starved	EP & SP > starved
	L-alanyl-glycine	87	(EP > SP) > starved	EP & SP > starved	SP > starved
	L-asparagine	88	SP & starved > EP	SP & starved > EP	SP & starved > EP
	L-glutamic acid	90			SP > EP & starved
	L-glutamine	91		SP > starved	SP > EP & starved
	L-proline	92			SP > EP & starved
	L-serine	93	EP> starved		SP > starved
	L-threonine	94			SP > EP & starved

*Arbitrary number assigned to each substrate tested refers to the numbered substrates in Figure 4-7.

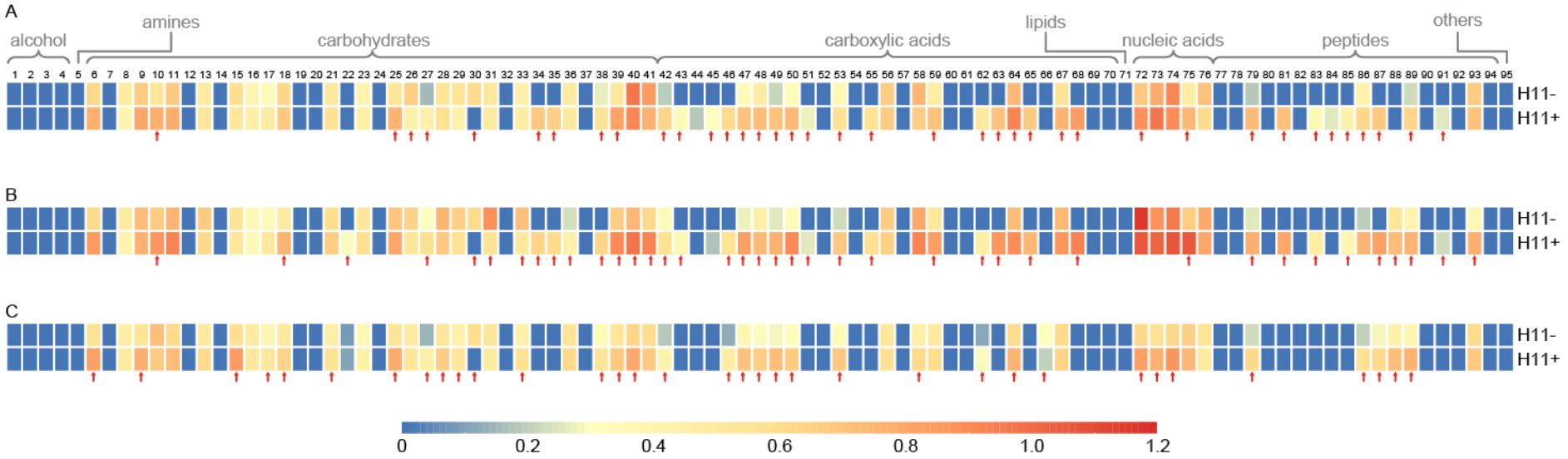

Figure 4-8 $A_{endpoint}$ profiles of bovine strains determined using PM1 MicroPlate^{TM}. Substrates are clustered according to the first-level chemical class outlined in Appendix 1 and comparisons made between strains harvested during exponential phase (A), stationary phase (B) and after starvation at 4°C (C). Substrates not utilised were considered to have an $A_{endpoint}$ of 0. The colour-coding of $A_{endpoint}$ levels is indicated by the key. Red arrows and numbers indicate substrates where statistically significant ($p<0.05$) differences were observed between the $A_{endpoint}$ levels of the strains tested. Arbitrary numbers were assigned to each substrates tested and refer to the substrate listed in Table 4-6. Data used for H11+ and H11- are listed in Appendices 5 to 6, respectively.

Table 4-7 List of substrates where a statistically significant difference ($p<0.05$) in $A_{endpoint}$ observed between bovine cells harvested during exponential phase, stationary phase and after starvation at 4°C. Relationships of inequality between $A_{endpoint}$ observed for exponential phase (EP), stationary phase (SP) and 4°C-starved cells (starved) are shown.

Chemical sub-class	Substrates	Number*	H11-	H11+
Monosaccharides	D-galacturonic acid	10		SP > starved
	D-gluconic acid	11		SP > starved
	D-ribose	15		starved > EP & SP
	N-acetyl-β-D-mannosamine	22		SP > EP & starved
Oligosaccharides	Maltose	28	SP > EP & starved	
	Maltotriose	29	SP > starved	
	α-D-lactose	31	SP > EP & starved	
Sugar alcohols	D-mannitol	33	SP > EP & starved	
	D-sorbitol	34		EP & SP > starved
	Dulcitol	35		EP & SP > starved
	Glycerol	36	EP & starved > SP	starved > SP
Sugar phosphates	D,L-α-glycerol-phosphate	38	EP & starved > SP	
	Fructose-6-phosphate	39		SP > starved
	Glucose-1-phosphate	40	EP > SP & starved	SP > starved
	Glucose-6-phosphate	41	EP > SP & starved	SP > starved
Acetic acids	Acetic acid	42		EP> starved
Aldehydic acids	Glyoxylic acid	43		EP & SP > starved
Butyric acids	α-hydroxy Butyric acid	44		EP > SP & starved
	α-keto-butyric acid	45		EP> starved
Dicarboxylic acids	L-malic acid	50		SP > starved
	Mono methyl succinate	51		EP & SP > starved
Glycolates	Glycolic acid	55		EP & SP > starved
Keto acids	Methyl pyruvate	58	EP & SP > starved	SP > EP & starved
	Pyruvic acid	59		SP > starved
Propionates	Propionic acid	62		EP> starved
Sugar acids	D-galactonic acid-γ-lactone	63		EP & SP > starved
	D-saccharic acid	65		EP & SP > starved
Sugar acids	Glucuronamide	66	starved > EP & SP	starved > EP & SP
	L-galactonic acid-γ-lactone	67		SP > starved
	Mucic acid	68		EP & SP > starved
Nucleosides	2-deoxy adenosine	72	SP > EP & starved	SP > EP & starved
	Adenosine	73	EP & SP > starved	EP & SP > starved
	Inosine	74	EP & SP > starved	SP > EP & starved
	Thymidine	75		SP > EP & starved
	Uridine	76	SP > starved	SP > EP & starved
Amino acids	D-serine	81		EP & SP > starved
	Glycyl-L-aspartic acid	83		EP & SP > starved
	Glycyl-L-glutamic acid	84		EP > SP & starved
	Glycyl-L-proline	85		EP & SP > starved
	L-alanine	86	EP > SP & starved	SP > starved
	L-alanyl-glycine	87	starved > EP & SP	SP > starved
	L-asparagine	88	SP & starved > EP	SP & starved > EP
	L-glutamine	91		EP & SP > starved
	L-serine	93	EP & starved > SP	

*Arbitrary number assigned to each substrate tested refers to the numbered substrates in Figure 4-8.

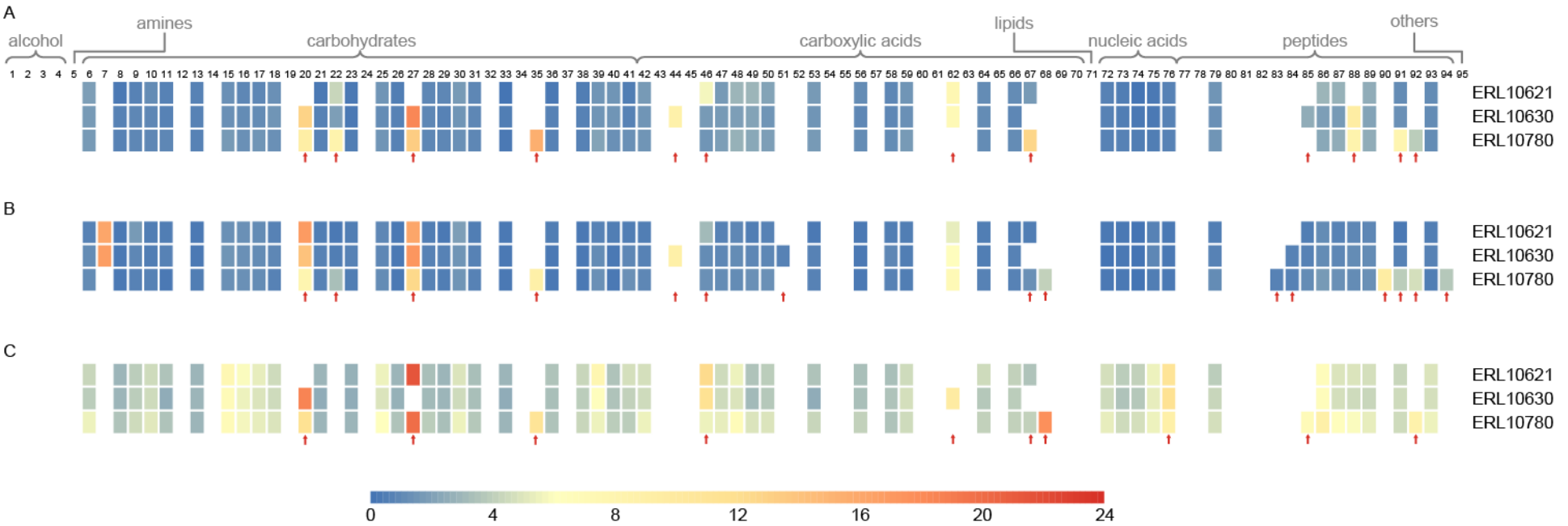

Figure 4-9 Lag time (λ) profiles of clinical strains in hours determined using PM1 MicroPlate™. Substrates are clustered according to the first-level chemical class outlined in Appendix 1 and comparisons made between strains harvested during exponential phase (A), stationary phase (B) and after starvation at 4°C (C). The colour-coding of lag time is indicated by the key. Red arrows indicate substrates where statistically significant (p<0.05) differences were observed between the lag times of the strains tested. Arbitrary numbers were assigned to each substrate tested. Substrates not utilised within the 24-hour assay period were considered to have no lag and are shown in white. Data used for ERL10621, ERL10630 and ERL10780 are listed in Appendices 7 to 9, respectively.

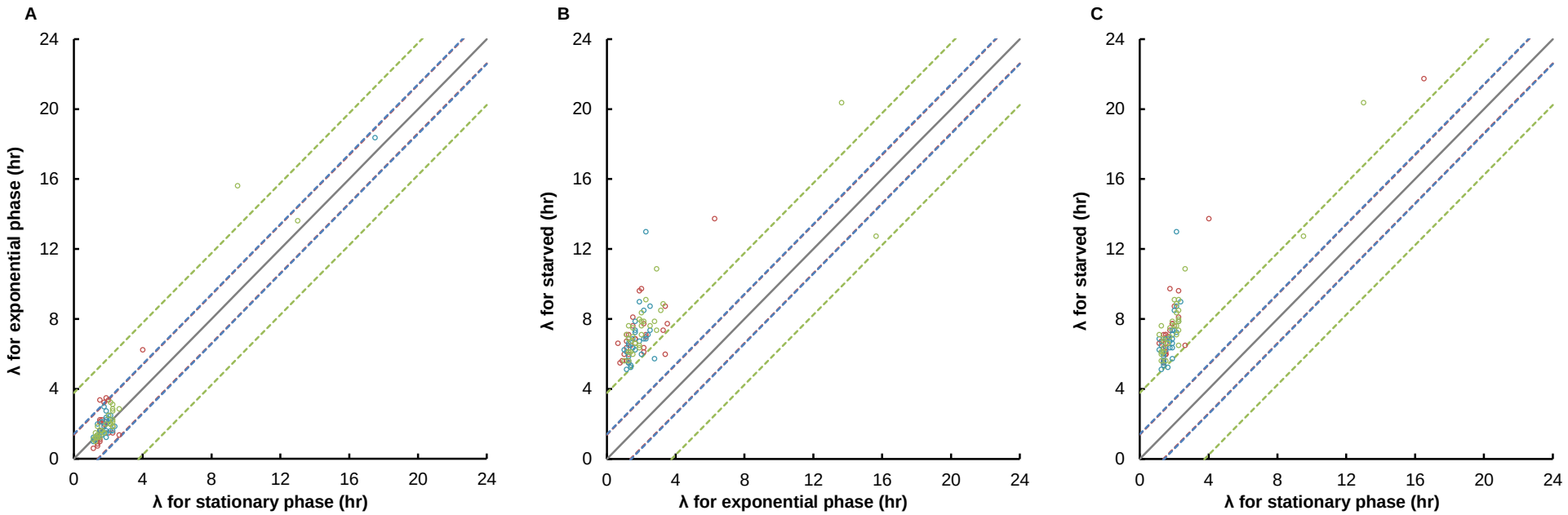

Figure 4-10 Scatter plot comparison of average lag (λ) in substrates used by clinical strains harvested during exponential phase, stationary phase, and after starvation at 4°C. Pairwise comparisons of λ between exponential and stationary phase cells (A), starved and exponential phase cells (B), and starved and stationary phase cells (C) are shown. The 95% LSD boundaries are marked by dash lines and correlation coefficient (r) = 1 is indicated by the solid line. ERL10780 data points and 95% LSD boundaries are shown in green, ERL10630 in blue, and ERL10621 in red. Each data point represents the average of duplicates.

utilised by ERL10621, ERL10630 and ERL10780 are shown in Appendix 7, Appendix 8 and Appendix 9, respectively.

Greater variation in λ was observed between H11- and H11+ for cells harvested during exponential and stationary phase, particularly carboxylic acids and peptides (42 to 70 and 77 to 94, Figure 4-11). When compared between cells harvested during different growth stages, no significant difference in λ was observed between exponential and stationary phase cells for most substrates (Figure 4-12). λ was significantly longer (p<0.05) for starved cells compared to exponential and stationary phase cells for the majority of substrates tested (Figure 4-12). However, λ for D-alanine was consistently shorter (p<0.05) for starved cells compared to exponential and stationary phase cells. λ for all substrates utilised by H11+ and H11- are shown in Appendix 10 and Appendix 11, respectively

4.2.2.3 Rate of substrate utilisation by clinical and bovine cells under aerobic conditions

Significant difference (p<0.05) in the rate of substrate utilisation (μ_{exp}) among the clinical strains was observed for 9, 18 and 13 substrates from exponential, stationary phase and starved cells, respectively (red arrows, Figure 4-13). The number of substrates where significant difference (p<0.05) in μ_{exp} was observed between strains was comparatively higher for the bovine isolates than the clinical, where μ_{exp} for 41, 43 and 26 substrates were significantly different between H11- and H11+ harvested during exponential, stationary and starved state, respectively (Figure 4-14). In general, higher μ_{exp} was observed for the H11+ cells compared to H11-. In most cases, μ_{exp} for starved cells was lower than exponential and/or stationary phase cells and highest μ_{exp} was observed for stationary phase cells (Table 4-8 and Table 4-9). However, for the clinical isolates, μ_{exp} for glucose-1-phosphate was higher for starved cells compared to exponential and stationary phase cells (40, Table 4-8). μ_{exp} of all substrates utilised by ERL10621, ERL10630, ERL10780, H11+ and H11- are shown in Appendix 12, Appendix 13, Appendix 14, Appendix 15 and Appendix 16, respectively.

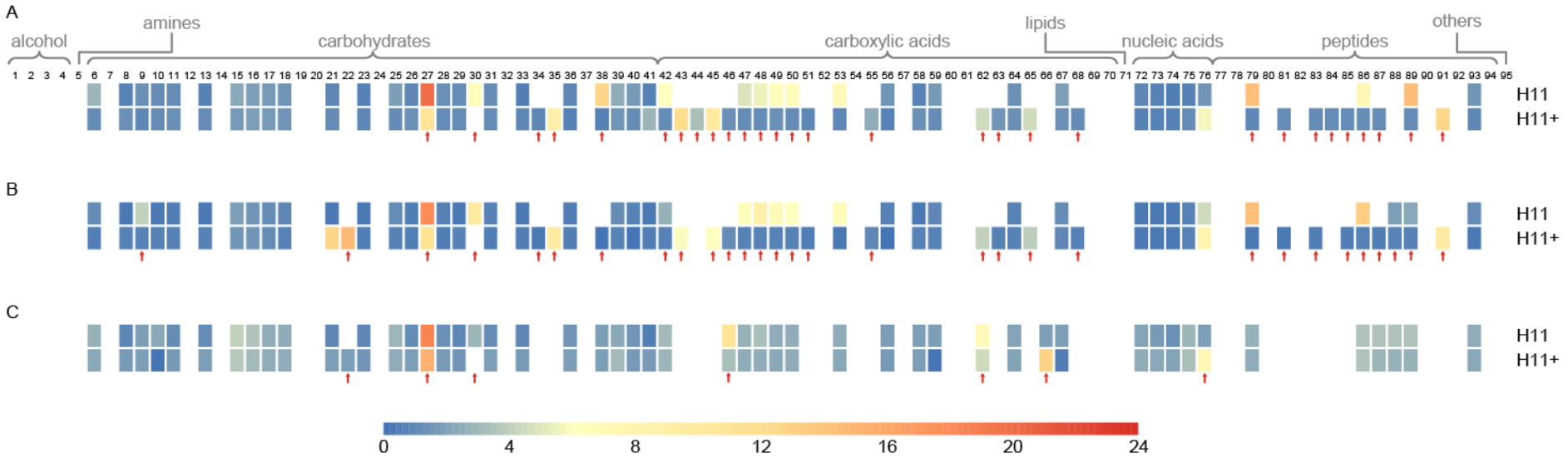

Figure 4-11 Lag time (λ) profiles of bovine strains in hours determined using PM1 MicroPlate™. Substrates are clustered according to the first-level chemical class outlined in Appendix 1 and comparisons made between strains harvested during exponential phase (A), stationary phase (B) and after starvation at 4°C (C). The colour-coding of lag time is indicated by the key. Red arrows indicate substrates where statistically significant (p<0.05) differences were observed between the lag times of the strains tested. Arbitrary numbers were assigned to each substrate tested. Substrates not utilised within the 24-hour assay period were considered to have no lag and are shown in white. Data used for H11+ and H11- are listed in Appendices 10 to 11, respectively.

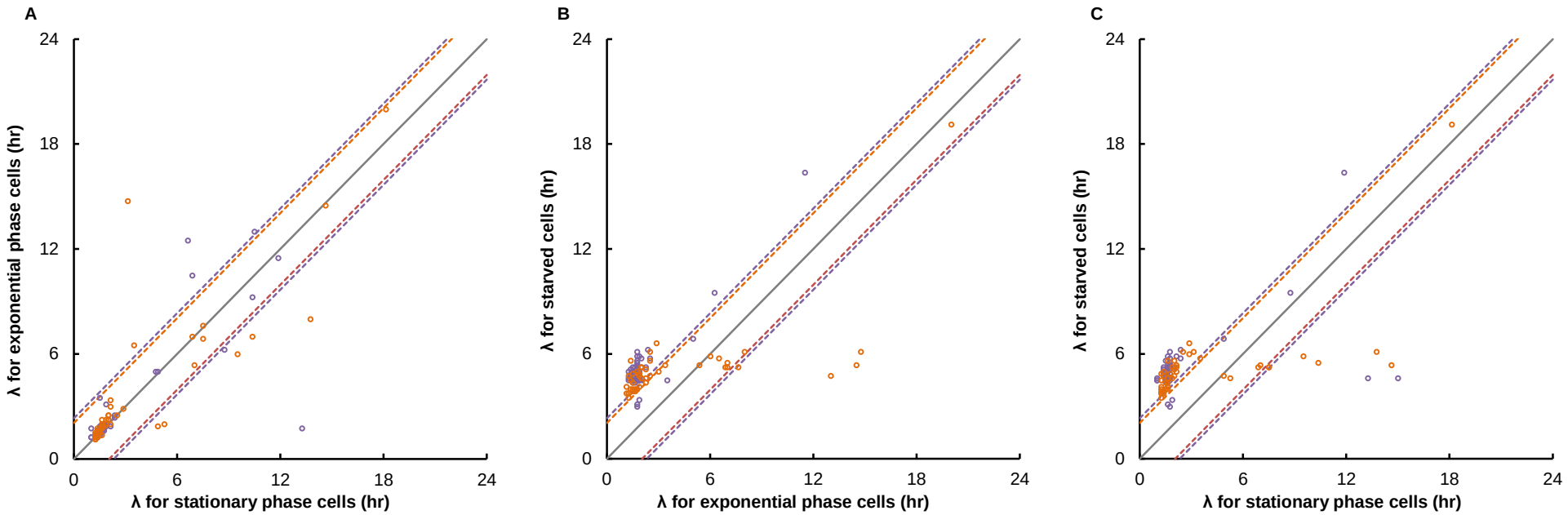

Figure 4-12 Scatter plot comparison of average lag (λ) in substrates used by bovine strains harvested during exponential phase, stationary phase, and after starvation at 4°C. Pairwise comparisons of λ between exponential and stationary phase cells (A), starved and exponential phase cells (B), and starved and stationary phase cells (C) are shown. The 95% LSD boundaries are marked by dash lines and correlation coefficient (r) = 1 is indicated by the solid line. H11- data points and 95% LSD boundaries are shown in orange and H11+ in purple. Each data point represents the average of duplicates.

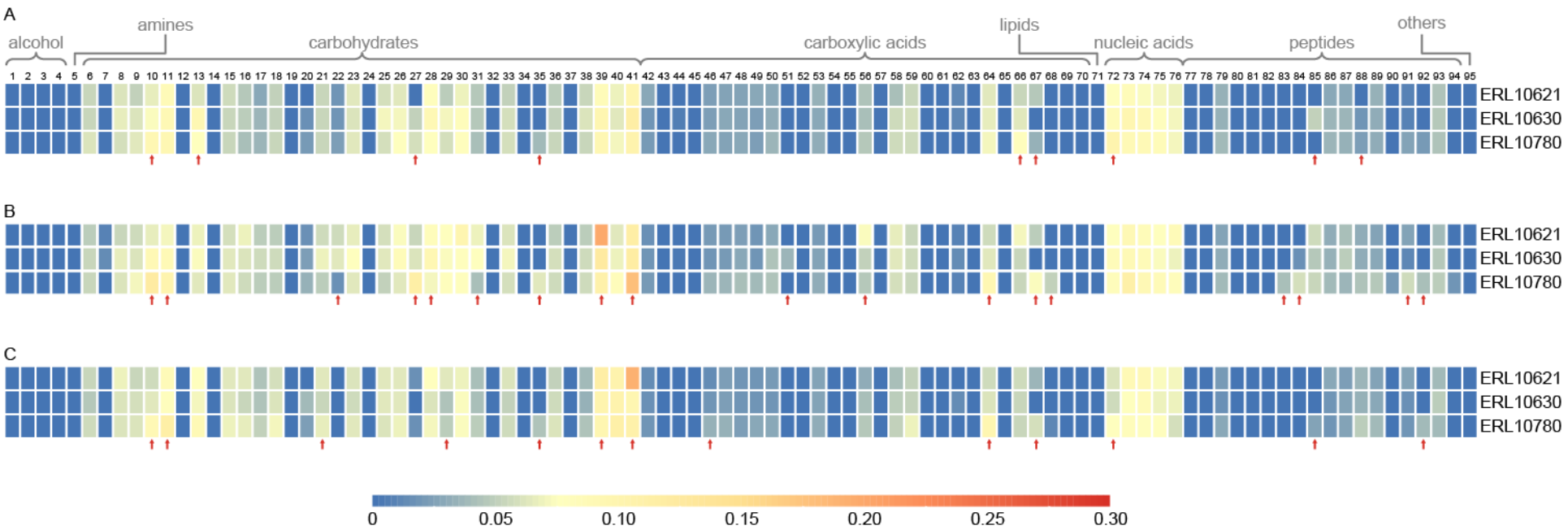

Figure 4-13 Rate of substrate utilisation (μ_{exp}) profiles of clinical strains determined using PM1 MicroPlate™. Substrates are clustered according to the first-level chemical class outlined in Appendix 1 and comparisons made between strains harvested during exponential phase (A), stationary phase (B) and after starvation at 4°C (C). Substrates not utilised were considered to have μ_{exp} 0f 0. The colour-coding of the rate of utilisation is indicated by the key. Red arrows indicate substrates where statistically significant (p<0.05) differences were observed between the strains tested. Arbitrary numbers were assigned to each substrate tested and refer to the substrates listed in Table 4-8. Data used for ERL10621, ERL10630 and ERL10780 are listed in Appendices 12 to 14, respectively.

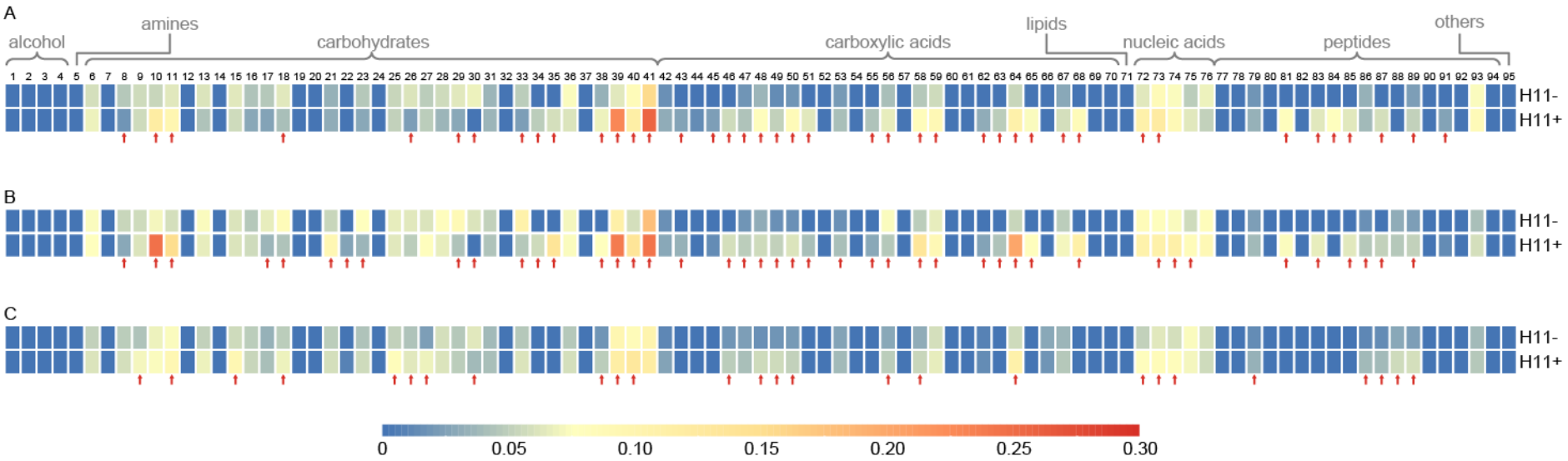

Figure 4-14 Rate of substrate utilisation (μ_{exp}) profiles of bovine strains determined using PM1 MicroPlate™. Substrates are clustered according to the first-level chemical class outlined in Appendix 1 and comparisons made between strains harvested during exponential phase (A), stationary phase (B) and after starvation at 4°C (C). Substrates not utilised were considered to have μ_{exp} of 0. The colour-coding of the rate of utilisation is indicated by the key. Red arrows indicate substrates where statistically significant (p<0.05) differences were observed between the strains tested. Arbitrary numbers were assigned to each substrates tested and refer to the substrate listed in Table 4-8. Data used for H11+ and H11- are listed in Appendices 15 to 16, respectively.

Table 4-8 List of substrates where a statistically significant difference (p<0.05) in μ_{exp} observed between clinical cells harvested during exponential phase, stationary phase and after starvation at 4°C. Relationships of inequality between μ_{exp} observed for exponential phase (EP), stationary phase (SP) and 4°C-starved cells (starved) are shown.

Chemical sub-class	Substrates	Number*	ERL10621	ERL10630	ERL10780
Monosaccharides	D-galacturonic acid	10		SP > starved	SP > EP & starved
	D-mannose	13		EP > SP & starved	starved > SP
	D-xylose	16	SP & starved > EP		starved > EP
	L-arabinose	17	SP > EP	SP > EP	
	L-fucose	18			starved > SP
	L-rhamnose	20		starved > EP	
	N-acetyl-β-D-mannosamine	22	(EP > SP) > starved	(EP > SP) > starved	EP > starved
	α-D-glucose	23		SP > starved	
Oligosaccharides	D-trehalose	26		SP > starved	
	Lactulose	27	SP > EP & starved	EP & SP > starved	(EP > SP) > starved
	Maltose	28		EP & SP > starved	
	Maltotriose	29	SP > EP	EP & SP > starved	SP > starved
	Sucrose	30	SP > EP & starved		
	α-D-lactose	31	SP > EP & starved	SP > EP & starved	
Sugar alcohols	D-mannitol	33		SP > starved	
	Dulcitol	35			SP > EP
	Fructose-6-phosphate	39	(SP > starved) > EP	SP > EP & starved	
	Glucose-1-phosphate	40	starved > EP & SP	starved > EP & SP	starved > EP & SP
	Glucose-6-phosphate	41	starved > EP & SP	EP & SP > starved	SP > EP & starved
Dicarboxylic acids	L-malic acid	50		SP > starved	
	Mono methyl succinate	51		SP > EP & starved	
Hydroxy acids	L-lactic acid	56	SP > EP & starved		
Keto acids	Methyl pyruvate	58	SP > EP & starved		
Sugar acids	D-glucuronic acid	64			starved > EP
	Glucuronamide	66			EP > SP & starved
	L-galactonic acid-γ-lactone	67			SP & starved > EP
	Mucic acid	68			SP > EP & starved
Nucleosides	2-deoxy adenosine	72		EP & SP > starved	EP > starved
	Adenosine	73		EP > starved	SP > starved
Amino acids	D-alanine	79		EP > starved	
	Glycyl-L-aspartic acid	83			SP > EP & starved
	Glycyl-L-glutamic acid	84			SP > EP & starved
	Glycyl-L-proline	85	SP > EP & starved	EP & SP > starved	(SP > starved) > EP
	L-alanine	86		EP > starved	
	L-alanyl-glycine	87	SP > starved	SP > starved	
	L-asparagine	88	SP & starved > EP		starved > EP
	L-glutamine	91	SP & starved > EP		SP > EP & starved

*Arbitrary number assigned to each substrate tested refers to the numbered substrates in Figure 4-13.

Table 4-9 List of substrates where a statistically significant difference ($p<0.05$) in μ_{exp} observed between bovine cells harvested during exponential phase, stationary phase and after starvation at 4°C. Relationships of inequality between μ_{exp} observed for exponential phase (EP), stationary phase (SP) and 4°C-starved cells (starved) are shown.

Chemical sub-class	Substrates	Number	H11-	H11+
Glycosides	α-methyl-D-glucoside	6	SP > starved	
Monosaccharides	D-fructose	8		starved > EP & SP
	D-galacturonic acid	10		(EP > SP) > starved
	D-gluconic acid	11		SP > EP & starved
	D-mannose	13	SP > starved	
	D-ribose	15		starved > EP & SP
	L-arabinose	17	SP > EP & starved	
	L-fucose	18	SP > EP & starved	
	N-acetyl-D-glucosamine	21	SP > EP	SP > EP & starved
	α-D-glucose	23	SP > EP & starved	
Oligosaccharides	D-trehalose	26	EP & SP > starved	starved > EP
	Lactulose	27	EP & SP > starved	SP > EP
	Maltose	28	SP > EP	
	Maltotriose	29	SP > EP & starved	
	Sucrose	30		starved > EP & SP
Sugar alcohols	D-mannitol	33	SP > EP & starved	starved > EP
	D-sorbitol	34		EP & SP > starved
	Dulcitol	35		(EP > SP) > starved
	Glycerol	36	EP & SP > starved	
Sugar phosphates	D,L-α-glycerol-phosphate	38	EP & starved > SP	
	Fructose-6-phosphate	39	SP & starved > EP	EP & SP > starved
	Glucose-1-phosphate	40	EP & starved > SP	
	Glucose-6-phosphate	41	(EP > SP) > starved	EP & SP > starved
Aldehydic acids	Glyoxylic acid	43		SP > starved
Dicarboxylic acids	Bromo succinic acid	46	starved > EP & SP	
	D-malic acid	48	EP > starved	
	L-malic acid	50		EP > starved
	Mono methyl succinate	51		EP & SP > starved
Glycolates	Glycolic acid	55		EP > starved
Hydroxy acids	L-lactic acid	56	SP > EP & starved	
Keto acids	Methyl pyruvate	58		SP > EP & starved
Sugar acids	D-galactonic acid-γ-lactone	63		EP & SP > starved
	D-glucuronic acid	64		SP > EP & starved
	D-saccharic acid	65		EP & SP > starved
	Glucuronamide	66	starved > EP & SP	
	L-galactonic acid-γ-lactone	67	SP > EP	
	Mucic acid	68		EP & SP > starved
Nucleosides	2-deoxy adenosine	72	SP > EP & starved	
	Adenosine	73	EP > starved	EP > starved
	Thymidine	75	starved > EP	
	Uridine	76	SP > starved	SP > EP & starved
Amino acids	D-serine	81		EP & SP > starved
	Glycyl-L-aspartic acid	83		EP & SP > starved
	Glycyl-L-glutamic acid	84		EP > SP & starved
	Glycyl-L-proline	85		EP & SP > starved
	L-alanine	86	EP > SP & starved	
	L-alanyl-glycine	87		
	L-asparagine	88	SP & starved > EP	SP & starved > EP
	L-serine	93	EP > SP & starved	EP > starved

*Arbitrary number assigned to each substrate tested refers to the numbered substrates in Figure 4-14.

4.2.2.4 Utilisation of carbon sources involved in glycolysis by the clinical and bovine strains

Glycolysis is the central pathway by which *E. coli* converts carbon sources into energy (Madigan *et al.*, 2012). Five carbon sources involved in glycolysis (glucose-1-phosphate, D-glucose, glucose-6-phosphate, fructose-6-phosophate and pyruvic acid) are included in the PM1 MicroPlate™. The overall trend $A_{endpoint}$, λ and μ_{exp} of the glycolytic substrates were similar between the clinical strains, ERL10621, ERL0630 and ERL10780. In all cases, $A_{endpoint}$ for pyruvate for starved cells was significantly lower ($p<0.05$) than exponential and stationary phase cells and significantly longer ($p<0.05$) λ was observed for starved cells compared to exponential and stationary phase cells (Figure 4-15).

For the bovine isolates, although the trend in utilisation kinetics for the five glycolytic substrates was similar, higher $A_{endpoint}$ was observed for H11+ overall, particularly for fructose-6-phosphate and pyruvic acid utilisation (Figure 4-16). A significantly longer ($p<0.05$) λ was observed for starved cells compared to exponential and stationary phase cells for most of the five carbon sources used by H11- and H11+ (Figure 4-16). However, no significant increase in λ was observed for utilisation of pyruvic acid by starved H11+ compared to exponential and stationary phase cells (Figure 4-16).

4.2.2.5 Substrate utilisation by bovine strains under anaerobic conditions

Substrate utilisation by stationary and starved H11- and H11+ cells under anaerobic growth conditions was tested, and the $A_{endpoint}$ compared. For stationary phase cells, $A_{endpoint}$ for 38 substrates differed significantly ($p<0.05$) between H11+ and H11- and 66 differed significantly ($p<0.05$) for 81-day starved cells (red arrows, Figure 4-17). $A_{endpoint}$ of 43 substrates were significantly higher ($p<0.05$) for the stationary phase H11- compared to starved cells (Table 4-10). For H11+, $A_{endpoint}$ of 12 substrates was significantly higher ($p<0.05$) for the stationary phase cells compared to the starved, while $A_{endpoint}$ for 9 substrates was higher for starved cells compared to stationary phase cells (Table 4-10). Overall, 21 of the 95 substrates tested differed significantly ($p<0.05$) between stationary and starved H11+ cells (Table 4-10).

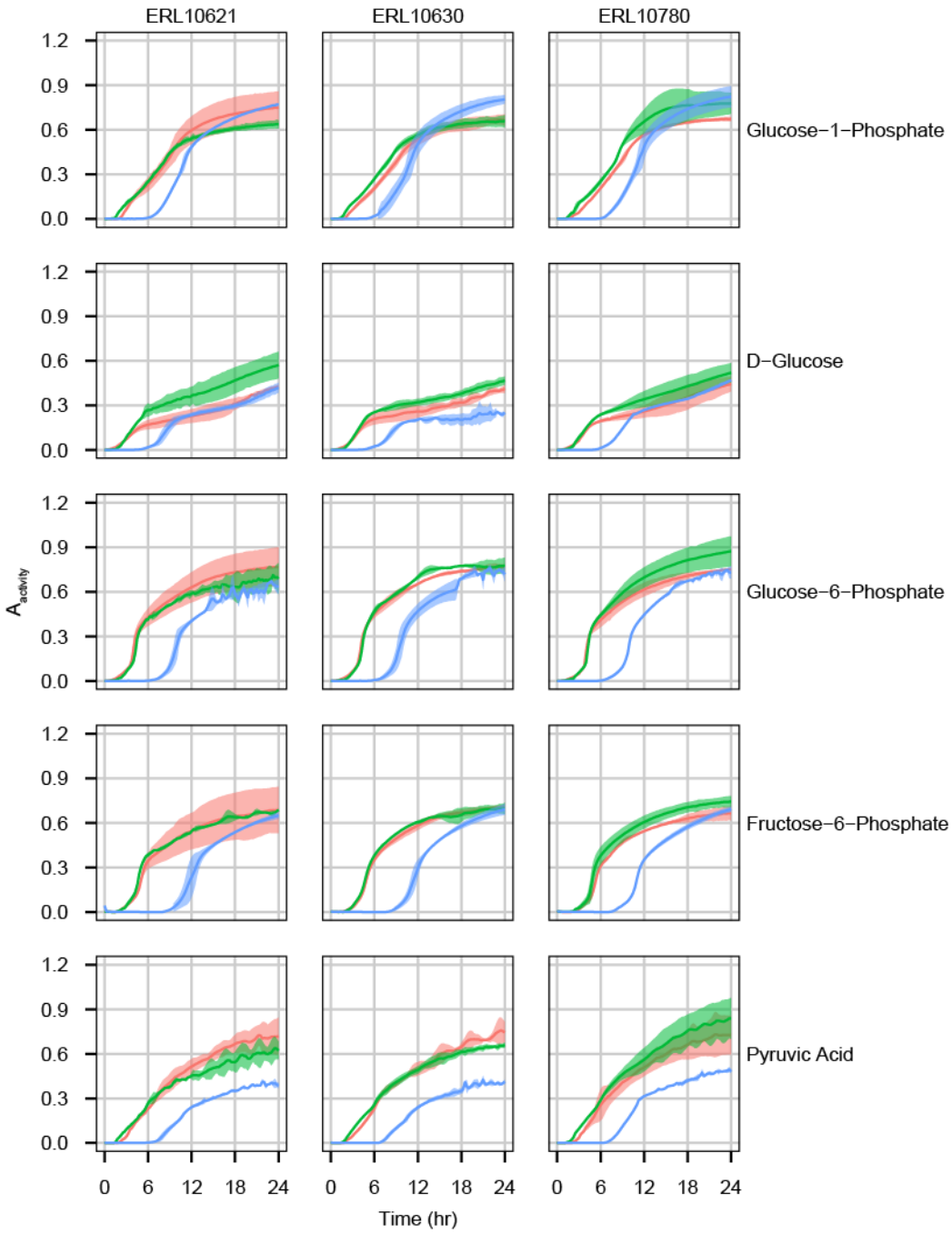

Figure 4-15 Utilisation kinetics of substrates involved in glycolysis by clinical strains. Substrate use for exponential phase (red), stationary phase (green) and starved (blue) cells are shown. Cultures were incubated at 37°C for 24 hours and measurements taken every 15 minutes. Lines indicate average of duplicates and the standard deviations are shown by shaded areas.

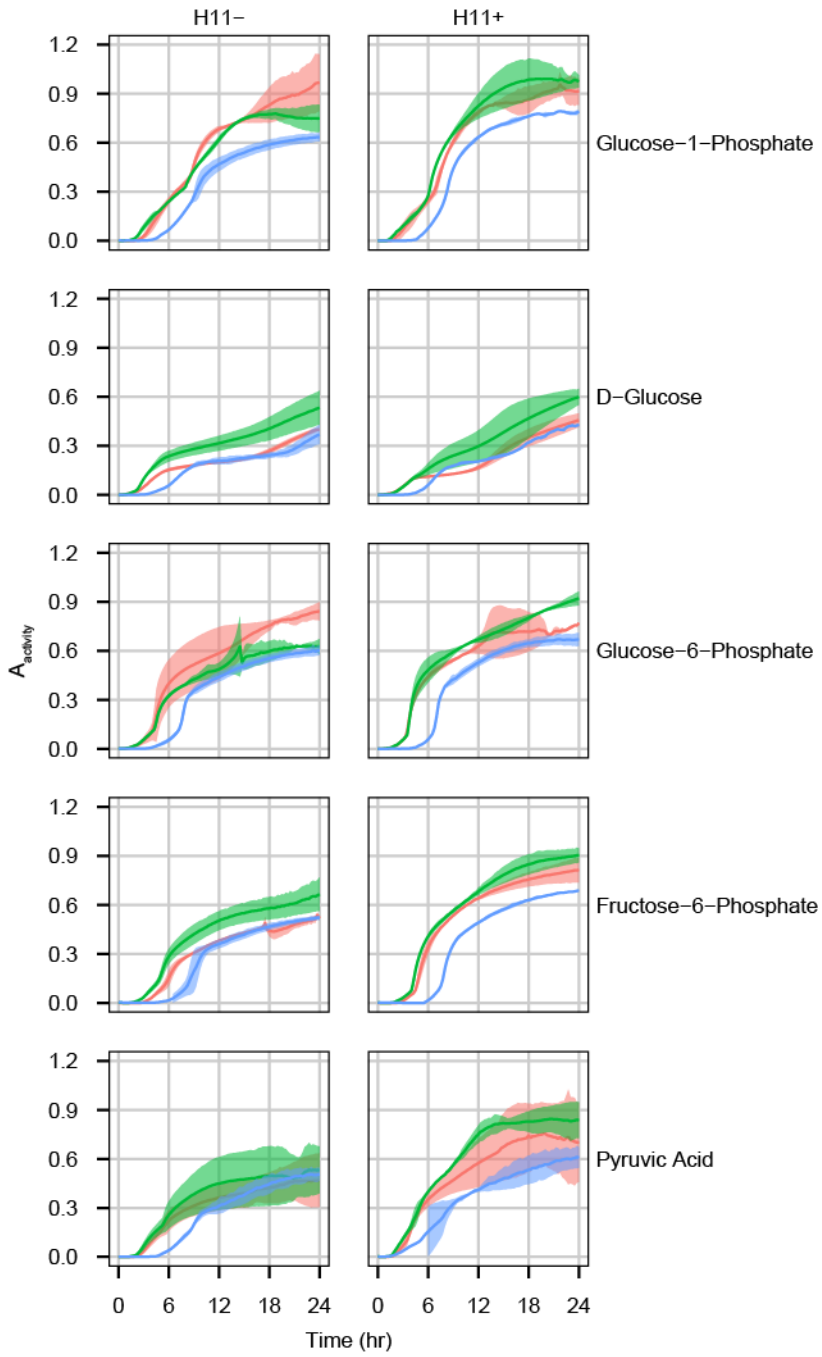

Figure 4-16 Utilisation kinetics of substrates involved in glycolysis by bovine strains. Substrate use for exponential phase (red), stationary phase (green) and starved (blue) cells are shown. Cultures were incubated at 37°C for 24 hours and measurements taken every 15 minutes. Lines indicate average of duplicates and the standard deviations are shown by shaded areas.

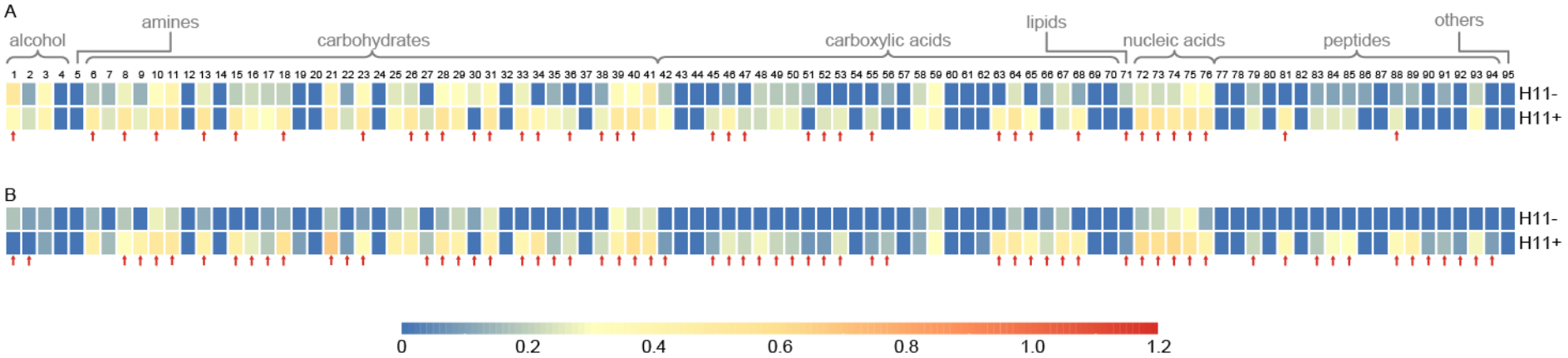

Figure 4-17 $A_{endpoint}$ profiles of bovine strains determined using PM1 MicroPlate^{TM} under anaerobic conditions. Substrates are clustered according to the first-level chemical class outlined in Appendix 1 and comparisons made between strains harvested during stationary phase (A) and after starvation at 4°C (B). Substrates not utilised were considered to have an $A_{endpoint}$ of 0. The colour-coding of $A_{endpoint}$ levels is indicated by the key. Red arrows and numbers indicate substrates where statistically significant (p<0.05) differences were observed between the $A_{endpoint}$ levels of the strains tested. Arbitrary numbers were assigned to each substrate tested and refer to the substrates listed in Table 4-10.

Table 4-10 Comparison of $A_{endpoint}$ observed between bovine O157 strains harvested during stationary phase (SP) and after starvation at 4°C. Numbers are in bold where a significant difference (p<0.05) was observed. Dash (–) indicates substrates tested but not utilised. Results are the average of duplicates.

Chemical class	Chemical sub-class	Substrates	Number*	H11-			H11+		
				SP		Starved	SP		Starved
Alcohols	Ethylene glycols	Tween 20	1	**0.510**	>	**0.176**	**0.346**	>	**–**
		Tween 40	2	0.113		0.093	**0.231**	>	**–**
		Tween 80	3	**0.352**	>	**0.130**	**0.400**	>	**0.107**
Carbohydrates	Glycosides	α-methyl-D-glucoside	6	0.187		0.157	0.471		0.457
		β-methyl-D-glucoside	7	**0.141**	>	**–**	0.248		0.151
	Monosaccharides	D-fructose	8	**0.278**	>	**0.188**	**0.517**	>	**0.315**
		D-galactose	9	**0.134**	>	**–**	**0.265**	<	**0.428**
		D-galacturonic acid	10	0.312		0.274	0.506		0.517
		D-gluconic acid	11	**0.402**	>	**0.212**	0.522		0.513
		D-mannose	13	**0.264**	>	**0.122**	0.525		0.439
		D-ribose	15	**0.191**	>	**–**	0.482		0.455
		D-xylose	16	**0.230**	>	**–**	0.360		0.262
		L-arabinose	17	**0.204**	>	**0.096**	0.309		0.186
		L-fucose	18	0.205		0.134	0.458		0.569
		L-lyxose	19	–		–	–		0.097
		N-acetyl-D-glucosamine	21	**0.411**	>	**0.172**	**0.495**	<	**0.680**
		N-acetyl-β-D-mannosamine	22	**0.091**	>	**–**	**0.233**	>	**0.081**
		α-D-glucose	23	**0.339**	>	**0.091**	**0.502**	>	**0.347**
	Oligosaccharides	D-melibiose	25	**0.260**	>	**0.144**	0.380		0.431
		D-trehalose	26	0.234		0.215	0.501		0.456
		Lactulose	27	–		–	0.236		0.173
		Maltose	28	**0.306**	>	**0.142**	0.556		0.490
		Maltotriose	29	**0.318**	>	**0.220**	0.451		0.424
		Sucrose	30	**0.270**	>	**0.109**	–		–
		α-D-lactose	31	**0.363**	>	**0.263**	0.516		0.448
	Sugar alcohols	D-mannitol	33	**0.271**	>	**–**	0.446		0.385
		D-sorbitol	34	–		–	**0.386**	<	**0.518**
		Dulcitol	35	**0.138**	>	**–**	0.284		0.164
		Glycerol	36	–		–	0.270		0.249
	Sugar phosphates	D,L-α-glycerol-phosphate	38	**0.112**	>	**–**	0.272		0.230
		Fructose-6-phosphate	39	0.335		0.293	0.500		0.423
		Glucose-1-phosphate	40	0.303		0.233	0.532		0.596
		Glucose-6-phosphate	41	**0.472**	>	**0.256**	0.484		0.518
Carboxylic acids	Acetic acids	Acetic acid	42	**0.178**	>	**–**	**0.307**	>	**0.087**
	Butyric acids	α-keto-butyric acid	45	–		–	**0.250**	>	**0.117**
	Dicarboxylic acids	Bromo succinic acid	46	**0.104**	>	**–**	**0.412**	>	**0.262**
		D,L-malic acid	47	–		–	0.224		0.220
		D-malic acid	48	**0.201**	>	**–**	0.229		0.289
		Fumaric acid	49	**0.186**	>	**–**	0.275		0.215
		L-malic acid	50	**0.184**	>	**–**	0.278		0.197
		Mono methyl succinate	51	**0.165**	>	**–**	–		0.079
		meso-tartaric acid	52	–		–	**0.241**	>	**0.083**
		Succinic acid	53	–		–	0.262		0.252
	Glycolates	Glycolic acid	55	–		–	**0.234**	>	**0.104**
	Hydroxy acids	L-lactic acid	56	**0.132**	>	**–**	**–**	<	**0.164**
	Keto acids	Methyl pyruvate	58	**0.228**	>	**0.093**	**0.310**	>	**0.125**
		Pyruvic acid	59	0.313		0.253	0.357		0.306
	Propionates	Propionic acid	62	–		–	–		0.066
	Sugar acids	D-galactonic acid-γ-lactone	63	–		–	0.392		0.466
		D-glucuronic acid	64	0.249		0.175	0.529		0.483
		D-saccharic acid	65	–		–	0.310		0.371
		Glucuronamide	66	0.135		0.083	**–**	<	**0.227**
		L-galactonic acid-γ-lactone	67	0.242		0.185	**0.253**	<	**0.464**
		Mucic acid	68	**0.117**	>	**–**	0.382		0.416
Lipids	Fatty acids	Formic acid	71	**0.195**	>	**–**	–		0.078
Nucleic acids	Nucleosides	2-deoxy adenosine	72	**0.256**	>	**0.164**	0.567		0.603
		Adenosine	73	0.227		0.216	0.548		0.585
		Inosine	74	0.238		0.279	**0.491**	<	**0.622**
		Thymidine	75	0.340		0.321	0.528		0.554
		Uridine	76	**0.327**	>	**0.127**	0.490		0.419
Peptides	Amino acids	D-alanine	79	**0.168**	>	**–**	0.276		0.217
		D-serine	81	–		–	0.437		0.361
		Glycyl-L-aspartic acid	83	**0.111**	>	**–**	0.245		0.185
		Glycyl-L-glutamic acid	84	**0.107**	>	**–**	0.255		0.291
		Glycyl-L-proline	85	**0.117**	>	**–**	0.251		0.310
		L-alanine	86	**0.107**	>	**–**	–		–
		L-asparagine	88	**0.110**	>	**–**	0.266		0.357
		L-aspartic acid	89	**0.141**	>	**–**	**–**	<	**0.446**
		L-glutamic acid	90	–		–	–		0.120
		L-glutamine	91	**0.126**	>	**–**	**–**	<	**0.155**
		L-proline	92	–		–	–		0.088
		L-serine	93	**0.203**	>	**–**	0.342		0.289
		L-threonine	94	–		–	–		0.099

*Arbitrary number assigned to each substrate tested refers to the numbered substrates in Figure 4-17.

4.3 Discussion

During its lifecycle as a zoonotic pathogen, *E. coli* is likely to encounter changes in temperature and nutrient availability, particularly during the transitions from an animal host to non-host environments and vice versa. Results from starvation studies showed that all *E. coli* O157:H7 strains tested can enter the VBNC state where the number of colonies recovered on solid media decreased gradually during 84 days of starvation in PBS, reflecting the increased proportion of non-culturable cells within the starved population, particularly for those held at 4°C (see Chapter 3). Moreover, the number and diameter of colonies recovered from starved cultures were dependent on nutrient levels of the media and presence of key metabolic substrates such as sodium pyruvate and sodium acetate (see Chapter 3). Although pyruvate has been identified as a "resuscitation factor" for VBNC cells (Oliver, 2010), little is known about the metabolic impact of pyruvate. It has been suggested that pyruvate and catalase may act as antioxidants for oxidative-stress-induced VBNC cells (Oliver, 2010). We hypothesised that the metabolic state of starved cells differed from that of non-starved cells, and the effect of pyruvate and acetate on colony growth observed was due to their impact on cell metabolism as metabolic regulators.

Using PM1 and PM2A MicroPlates^{TM}, the overall carbon source utilisation profile for starved cells was compared to non-starve cells harvested during exponential or stationary phase. Three measurable components of utilisation ($A_{endpoint}$, λ and μ_{exp}) were used to profile the metabolic activity of cells for each carbon source (Figure 2-1). The level of substrate utilisation after 24 hours of growth at 37°C ($A_{endpoint}$) was considered an arbitrarily measure of maximal metabolic activity to allow standardised comparison between cultures. The length of the lag period (λ), during which time substrate utilisation was below the limit of detection, may be dependent on the energy level within the cell or the availability of transport systems and/or enzymes required for carbon metabolism at the time of harvesting. Once substrate utilisation became detectable, the maximal rate of exponential substrate utilisation (μ_{exp}) was equated to the rate of carbon catabolism. We hypothesised that as cells aged during starvation, cellular energy level would decline and that the metabolic components required for the metabolism of certain substrates would be gradually degraded and not replaced. Since glycolysis is an

important metabolic pathway for energy conversion from carbon sources (Figure 1-5) (Madigan *et al.*, 2012), particular focus was given to the utilisation of glycolytic substrates.

A 24-hour limit on incubation was used to standardise the MicroPlate^{TM} assay for the determination of endpoint $A_{activity}$ ($A_{endpoint}$). This also limited the potential for other issues that might occur during prolonged incubation at 37°C, such as evaporation of media, potential saturation of the tetrazolium violet dye, and cryptic growth. In most cases, substrate use peaked within the first 12 hours of incubation, after which metabolic activity ceased. However, it is important to note that where λ was greater than 10 hours, the remaining incubation time might not had been sufficient for maximal substrate utilisation to be achieved within the 24-hour incubation period.

Lowered metabolic rates are generally believed to be the cause for the loss of culturability for VBNC cells (Oliver, 2010). Comparisons of the kinetics of sole substrate use in this study showed that in most cases, regardless of the strains tested, $A_{endpoint}$ and μ_{exp} were similar between starved, exponential and stationary phase cells. The greatest difference in substrate use between cells harvested during different growth stages was observed in the lag phase. The longer lag observed in initial substrate utilisation by starved cells during recovery could be due to the lack of available transport systems and/or enzymes required for carbon metabolism, which are unlikely to be synthesised rapidly due to the likely depletion of cellular energy during starvation. The absence of substrate transport components and/or metabolic enzymes may be the cause of lowered metabolic activities observed for VBNC cells.

The overall utilisation kinetics for the five glycolytic substrates tested were similar for exponential and stationary phase cells for all strains, with the exception of NCTC12900 utilisation of glucose-1-phosphate, where the μ_{exp} was significantly lower for exponential phase cells compared to stationary phase cells. This suggested that the metabolic components required for conversion of carbon into energy via glycolysis were functional in both exponential and stationary phase cells. For non-glycolytic substrates, little difference in utilisation was observed between exponential and stationary phase cells for all strains tested.

Interestingly, $A_{endpoint}$ for phosphate sugars were significantly higher than D-glucose in all cases. Entrance of D-glucose into the glycolytic pathway requires ATP for its conversion to glucose-6-phosphate, whereas phosphate sugars enter into the glycolytic pathway without costing any additional ATP. Since more energy is required for D-glucose catabolism, it is not surprising that the metabolic activities were higher for cells grown on sugar phosphates as the sole carbon source compared to growth on D-glucose.

The lag in utilisation for the majority of substrates, including the glycolic substrates, was consistently longer for starved cells compared to exponential and stationary phase cells. Significant differences in $A_{endpoint}$ and μ_{exp} was also observed between starved and non-starved cells for some substrates. Changes in metabolic profiles after starvation differed for clinical and bovine *E. coli* O157:H7 isolates. $A_{endpoint}$ for at least 29 substrates differed significantly between starved and non-starved clinical cells, while only 18 substrates differed for H11-. This suggested that starved bovine *E. coli* O157:H7 cells can metabolise a wider range of substrates compared to the clinical strains and may reflect the difference in selective pressure in the ruminant and human gut, as well as the range of substrates available within each system. The lag in substrate utilisation after starvation also differed between the clinical and bovine strains tested, for example, the extended λ for D-ribose, D-xylose and uridine utilisation observed for starved clinical cells (Figure 4-9).

The lag times observed for the utilisation of the pentose sugars, D-ribose and D-xylose, were consistently more than six hours longer for starved cells compared to exponential phase cells (Appendix 7, Appendix 8 and Appendix 9). The same trend in λ was not observed for the other pentose sugars, L-arabinose and L-lyxose. D-ribose and D-xylose are transported by specific ABC transporters (Shilton *et al.*, 1996; Song & Park, 1998). D-ribose uptake can also be facilitated by D-xylose transport systems (Song & Park, 1998). As pentoses follow similar catabolic pathways once inside the cell, the difference in λ observed for the pentoses tested was likely due to a lack of specific D-ribose and D-xylose transport systems in starved cells in addition to low cell energy levels rather than the lack of catabolic enzymes per se.

λ for uridine was also consistently longer for starved clinical cells compared to exponential phase cells by at least ten hours. Uridine is transported by the proton symporter, NupC, which is also the transporter for all other nucleosides except guanosine (Park *et al.*, 1999). If the transport system is absent or at levels too low to sustain cell metabolic activity in the starved cells, similar differences in λ should be observed for the other nucleotides tested. However, λ observed for starved-cell utilisation of thymidine, inosine and adenosine were shorter than that observed for uridine. Therefore, the extended lag observed for starved clinical-cell utilisation of uridine was likely due to a lack of metabolic enzyme(s) necessary for uridine catabolism rather than a lack of transport system.

Supplementation of PCA with sodium pyruvate resulted in significantly higher recovery from 4°C starved cultures compared to PCA alone (see Chapter 3). The improved recovery may be due to either pyruvate as a carbon source or as part of the regulation of PTS (Figure 1-6). If the observed increased in colony count was due to pyruvate being an additional carbon source, the utilisation kinetics of pyruvate by the starved cells would be expected to have either a higher $A_{endpoint}$ or μ_{exp}, or a shorter λ compared to other substrates tested. However, this was not the case. $A_{endpoint}$ for pyruvate was significantly lower for the starved cells compared to exponential and stationary phase cells for the three clinical strains. No significant difference in μ_{exp} was observed for exponential, stationary phase and starved cells. In addition, the λ for pyruvate was significantly longer for starved cells compared to exponential and stationary phase cells in all cases. These results suggested that the improvement in recovery on PCA observed with pyruvate supplementation was unlikely to be the result of pyruvate solely acting as an addition carbon source, but rather the alteration of the PEP to pyruvate ratio leading to changes in nutrient transport via PTS.

During passage through the bovine gut, initiation of growth after starvation may occur in anaerobic conditions. Anaerobic metabolism follows different pathways to aerobic catabolism, therefore, we hypothesised metabolism during recovery after starvation at 4°C under anaerobic conditions would be different to that observed during aerobic growth. Similar numbers of substrates were fermented by stationary phase NCTC12900, H11- and H11+ cells. For NCTC12900, significantly higher utilisation was observed for sugar phosphates, sugar acids,

keto acids and nucleosides under anaerobic growth compared to aerobic growth. The same trend was not observed for either H11- or H11+. In addition, starved H11- cells were unable to metabolise the dicarboxylic acids and amino acids during anaerobic growth (Table 4-10), while H11+ and NCTC12900 retained the ability to do so after starvation (Table 4-10 and Table 4-4). This suggested that starved H11- may have a limited metabolic capability for growth under anaerobic conditions within the ruminant gut.

In summary, carbon catabolism by starved cells differed significantly to that of non-starved cells, particularly in the length of lag period before substrate use was detected. Furthermore, results presented here showed differences between anaerobic and aerobic metabolism during recovery after starvation. While little strain variation was observed in glycolic substrate utilisation, analysis of the metabolic profiles identified trends specific to the clinical strains tested. Although comparison of the metabolic profiles suggested the difference in the selective pressures encountered by the clinical and bovine isolates, selecting for persistence of specific metabolic phenotypes such as the available carbon sources in ruminant gut compared to the mono-gastric human system, no conclusive results can be drawn with only a few strains tested. A larger survey of New Zealand clinical and bovine isolates for metabolic changes, before and after starvation, is required to confirm the hypothesis that such selective pressure exists on metabolic versatility of *E. coli* O157:H7.

Chapter 5 Involvement of LuxS during starvation and recovery

5.1 Introduction

Starvation of *E. coli* O157:H7 in PBS at 15 and 4°C resulted in a decrease in culturability and the formation of sub-populations with different nutritional requirements for growth (see Chapter 3). Sole substrate use studies of exponential phase, stationary phase and 4°C-starved NCTC12900 showed that whilst the rate and level of substrate utilisation during 24-hour recovery at 37°C did not vary significantly between cells harvested during different stages of growth, a significantly longer lag was observed for starved cells (see Chapter 4). Sodium pyruvate is a resuscitation factor that increased recovery of 4°C-starved cells on PCA (see Chapter 3). Interestingly, as sole carbon source, the level of pyruvate utilisation by starved cells was not higher than that of other glycolytic substrates, nor was it utilised at a higher rate (see Chapter 4). This suggested that carbon source utilisation may not be the only determinant of resuscitation and that other metabolic regulation may be involved.

The activated methyl cycle (AMC) is an important pathway for methylation and amino acid synthesis. LuxS is one of the enzymes of AMC (Figure 1-2b) (Winzer *et al.*, 2003). *E. coli* O157:H7 strains lacking *luxS* have increased growth rate, decreased motility and decreased type III secretion (Sperandio *et al.*, 2002a; Sperandio *et al.*, 1999; Sperandio *et al.*, 2001; Sperandio *et al.*, 2002b). In addition, over-expression of LuxS in *E. coli* K-12 resulted in altered expression of genes involved in key cellular processes such as cell division, cell morphology and biofilm formation (DeLisa *et al.*, 2001c). The by-product of LuxS conversion of *S*-ribosyl-homocysteine (SRH) to homocysteine is 4,5-dihydroxy-2,3-pentanedione (DPD), the precursor of autoinducer-2 (AI-2) (Figure 1-2). The AI-2 quorum sensing system is used by both Gram-negative and Gram-positive bacteria and AI-2 has been proposed to be the universal "language" for bacterial communication (Schauder & Bassler, 2001). Since late-exponential cultures used in starvation studies are of high cell density, density-dependent phenotype and/or metabolic regulation may have occurred during starvation.

5.2 Results

The potential role of the AI-2 synthase, LuxS, in *E. coli* O157:H7 starvation was investigated using NCTC12900 *luxS*$^{-}$. Complementation of the mutation was achieved using the plasmid pSS03. pCR2.1 was transformed into NCTC12900 *luxS*$^{-}$ and used as the vector only control. NCTC12900 (NWt), NCTC12900 *luxS*$^{-}$ (NLux), NCTC12900 *luxS*$^{-}$ pSS03 (NCom) and NCTC12900 *luxS*$^{-}$ pCR2.1 (NVec) cultures were harvested cells during late-exponential growth phase (Figure 3-5; OD_{600} between 1.2 and 1.4), washed in PBS, and resuspended in PBS to a final OD_{600} of 1.0. Cultures were starved at 15 and 4°C for 84 days and the phenotypic characteristics of viability and colony recovery measured. Viability was defined by membrane integrity, and colony recovery was defined by colony formation on agar. The metabolic profiles of NCTC12900 and the *luxS* mutant harvested during exponential phase, stationary phase, and after 51 and 53 days of starvation at 4°C were determined using PM1 and PM2A MicroPlates^{TM}.

5.2.1 Viability and colony recovery of starved NCTC12900 *luxS*$^{-}$ compared with the parental NCTC12900

Overall, the change in viable count and the number of colonies recovered differed between cells starved at 15 and 4°C. Differences in viability and colony recovery were observed between the *luxS*-containing NWt and NCom, and the *luxS*$^{-}$ deficient NLux and NVec.

5.2.1.1 Viability and growth potential prior to starvation

Viable cell counts, colony recovery on PCA, PCA with 0.2% sodium pyruvate (PCApyr), PCA with 0.2% sodium acetate (PCAace) and TSA on day 0 of starvation were compared to identify any disparities in growth potential, prior to prolonged starvation at 15 and 4°C. Similar viable counts and colony recovery was observed for NWt and NCom; both strains had higher viable and colony counts than NLux and NVec overall.

Viable counts for NWt and NCom were significantly higher (p<0.05) than NLux and NVec (Table 5-1). Similar observations were made for colony count on PCA

Table 5-1 Viable count and colony counts on PCA, PCApyr, PCAace and TSA for late-exponential cells on day 0 of starvation. Viable counts are the average of duplicates and colony counts are the average of four technical replicates. The standard deviations are indicated in brackets.

Strains	Viable count (log_{10} cells/mL)	Colony count (log_{10} cfu/mL)			
		PCA	PCApyr	PCAace	TSA
NCTC12900 (NWt)	8.63 (0.04)	8.49 (0.04)	8.59 (0.08)	8.51 (0.07)	8.59 (0.07)
NCTC12900 *luxS*$^-$ (NLux)	8.23 (0.06)	8.36 (0.04)	8.42 (0.08)	8.38 (0.05)	8.41 (0.09)
NCTC12900 *luxS*$^-$ pSS03 (NCom)	8.57 (0.07)	8.53 (0.08)	8.63 (0.05)	8.38 (0.05)	8.56 (0.08)
NCTC12900 *luxS*$^-$ pCR2.1 (NVec)	8.28 (0.20)	8.41 (0.05)	8.44 (0.05)	8.40 (0.06)	8.54 (0.13)

Table 5-2 Average diameter of colonies recovered on PCA, PCApyr, PCAace and TSA on day 0 of starvation in PBS. The number of colonies measured is shown in brackets.

	Average diameter (pixels)			
Strains	**PCA**	**PCApyr**	**PCAace**	**TSA**
NCTC12900 (NWt)	47.4 (*n*=98)	47.8 (*n*=106)	25.8 (*n*=205)	45.3 (*n*=115)
NCTC12900 *luxS*$^{-}$ (NLux)	35.8 (*n*=85)	38.1 (*n*=87)	22.9 (*n*=73)	45.5 (*n*=99)
NCTC12900 *luxS*$^{-}$ pSS03 (NCom)	44.0 (*n*=97)	46.0 (*n*=125)	22.9 (*n*=91)	42.7 (*n*=103)
NCTC12900 *luxS*$^{-}$ pCR2.1 (NVec)	31.5 (*n*=95)	36.9 (*n*=94)	20.0 (*n*=89)	39.6 (*n*=112)

and PCApyr, where colony counts for NWt and NCom were significantly higher (p<0.05) than NLux and NVec (Table 5-1). Colony count on TSA was significantly lower (p<0.05) for NLux than NWt and NCom (Table 5-1). No significant difference in colony count on PCAace was observed between strains (Table 5-1). No significant difference in average colony diameter on PCApyr, PCAace and TSA was observed between strains (Table 5-2). However, the averaged diameter of NVec colonies on PCA was significantly smaller (p<0.05) than that of NWt (Table 5-2).

5.2.1.2 Viability during starvation at 15 and 4°C

For starved cultures held at 15°C, a gradual decrease in viable counts was observed for all strains. A significant decrease (p<0.05) in viable count was observed within the first 28 days of starvation for all strains (Figure 5-1). The final viable count on day 84 was 0.8, 0.4, 0.7 and 0.5 logs lower than day 0 for NWt, NLux, NCom and NVec, respectively. For cells harvested on day 84, no significant difference in viable count was observed between strains.

The viable count for cultures held at 4°C remained largely unchanged during 84 days of starvation (Figure 5-1). However, viable count for NWt on day 84 was 0.3 logs lower (p<0.05) than the starting viable count of 8.6 logs day 0 (Figure 5-1). No significant difference in viable count was observed between day 0 and day 84 NLux, NCom and NVec cultures.

5.2.1.3 Colony recovery of cells starved at 15 and 4°C

Generally, the number of colonies recovered from cultures starved at 15°C was higher than 4°C-starved cultures, regardless of the strain or media used. In addition, less strain variation in colony recovery was observed for 15°C-starved cultures compared to 4°C-starved cultures.

An approximately one log decrease in recovery was observed for all strains held at 15°C within 28 days with little difference observed between strains (Figure 5-2). After 84 days of starvation at 15°C, colony count on PCA and

PCAace was significantly higher (p<0.05) for NWt and NCom compared to NLux and NVec

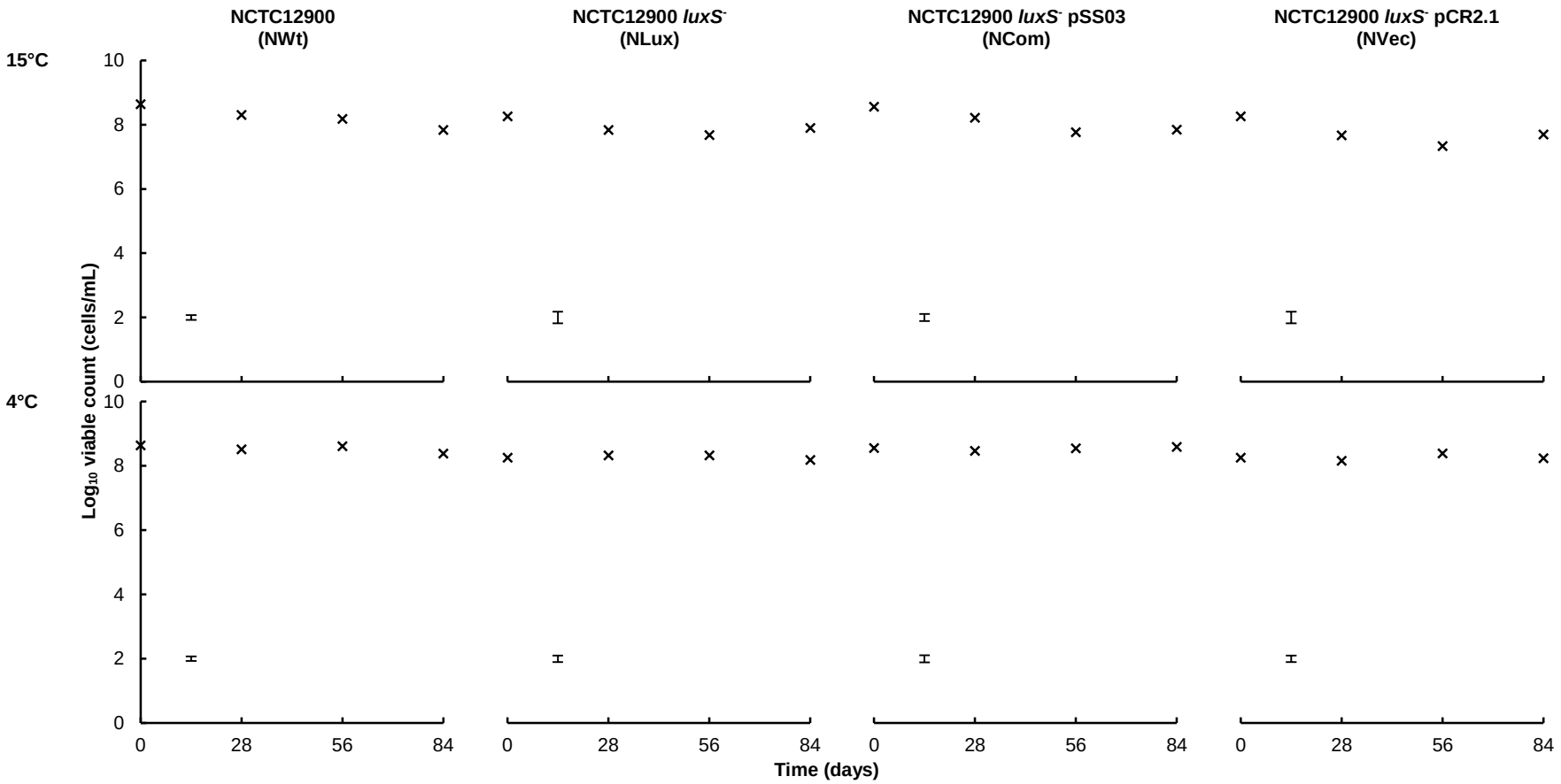

Figure 5-1 Viable counts of late exponential NCTC12900, NCTC12900 *luxS*-, NCTC12900 *luxS*- pSS03, NCTC12900 *luxS*- pCR2.1 cells starved in PBS at 15 and 4°C for 84 days. Each viable count data point shows the average of two technical repeats. The maximum standard deviation (SD_{max}) is indicated by the error bar on each graph. Data shown are representative of two biological repeats.

by less than one log. In addition, colony count on PCApyr for NCom was significantly higher (p<0.05) than NLux and NVec by 0.49 and 0.54 logs, respectively. Significantly higher (p<0.05) colony count on TSA was observed for NWt and NCom on day 84 compared to NLux and NVec.

For cultures starved at 4°C, a continual decline in colony count over 84 days was observed for all strains on all media tested (Figure 5-2). Overall, highest recovery was observed for NLux and NVec, and the lowest recovery was observed for NCom. For NWt and NCom, the decline in recovery on PCA, PCAace and PCApyr during the first 28 days of starvation was greater than for NLux and NVec. The decline in recovery plateaued for NWt from day 28 to day 84 while a continual decline in recovery was observed for NLux, NCom and NVec. Recovery of NWt, NLux and NVec on TSA decreased gradually at similar rates over time, while a rapid decline was observed for NCom. By day 84, recovery of NCom on PCA, PCAace, PCApyr and TSA was significantly lower (p<0.05) than NWt, NLux and NVec (Figure 5-2).

5.2.1.4 Change in the diameter of colonies recovered after starvation

By standardizing the duration of incubation as well as the method of photography, comparisons of the diameter of colonies formed on PCA, PCApyr, PCAace and TSA on day 0 and day 84 of starvation at 4 and 15°C were made. No significant difference in mean colony diameter was observed for colonies grown from day 0 and day 84 cells starved at 15°C. Furthermore, the variance in colony diameter distribution was similar for day 0 and day 84 cells.

For 4°C-starved cultures, greater variation was observed for colonies recovered on day 84 compared to those recovered from day 0 cells, with the exception of colonies grown on PCAace (Figure 5-3). No significant difference in mean diameter was observed between day 0 and day 84 colonies for NLux and NVec on all media tested. For NWt, the mean diameter for day 84 colonies on PCA was significantly lower (p<0.05) than day 0; no significant difference was observed for PCAace, PCApyr or TSA. The mean diameter for day 84 NCom colonies on all media tested was significantly lower than for day 0.

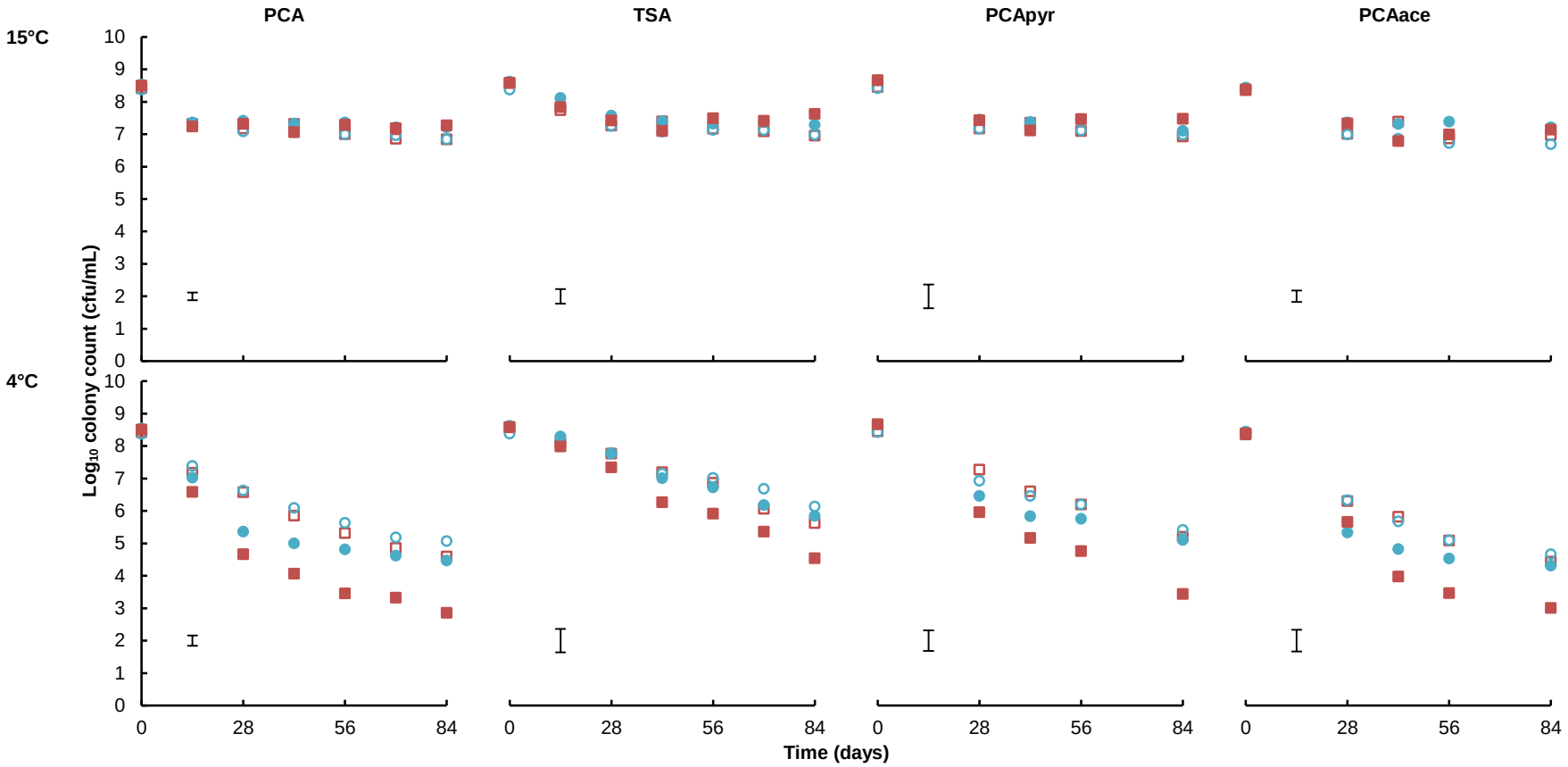

Figure 5-2 Comparison of colony recovery on PCA, TSA, PCApyr and PCAace for late exponential cells starved in PBS at 15 and 4°C for 84 days. Recovery of NCTC12900 (●), NCTC12900 *luxS*$^{-}$ (○), NCTC12900 *luxS*$^{-}$ pSS03 (■), NCTC12900 *luxS*$^{-}$ pCR2.1 (□) are shown. Each colony count data point is the average of four technical replicates. The maximum standard deviation (SD_{max}) is indicated by the error bar on each graph. Data shown are representative of two biological repeats.

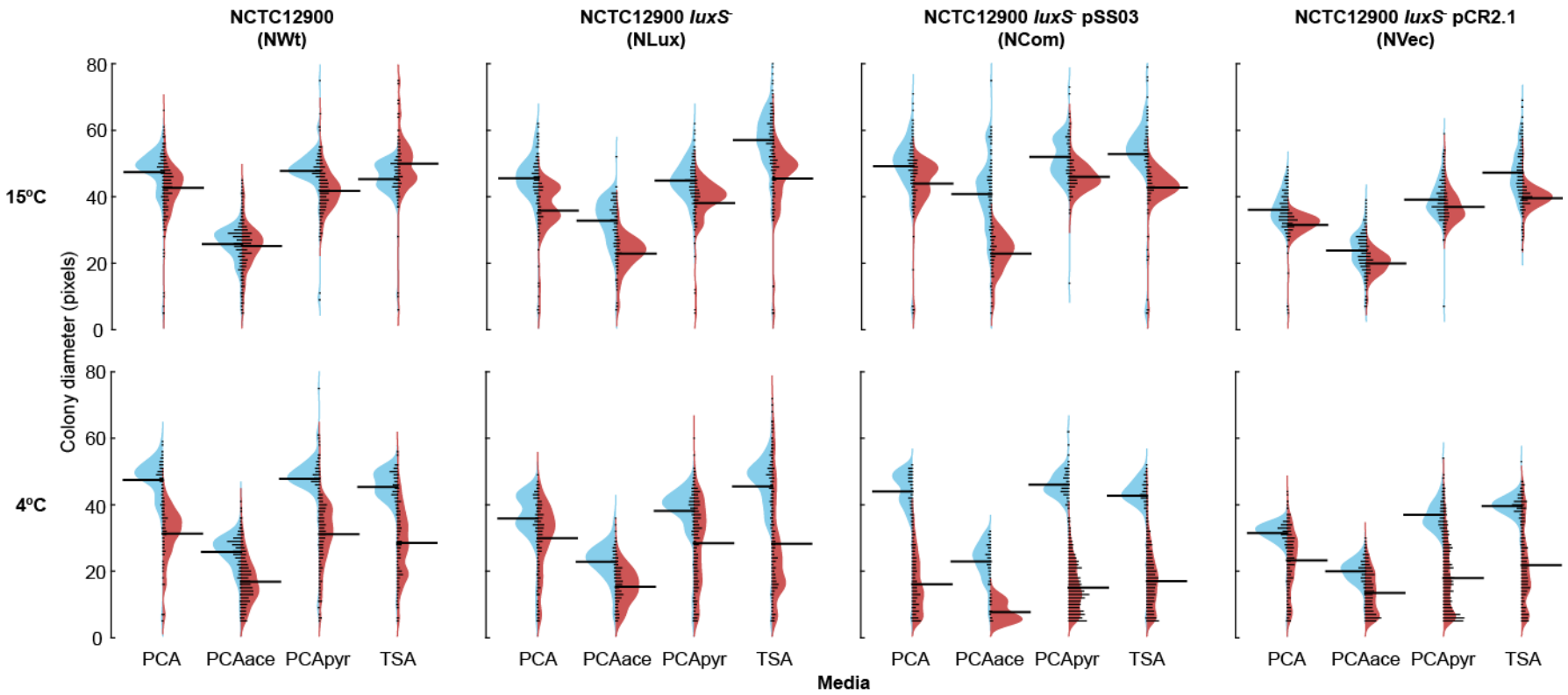

Figure 5-3 Distribution and mean colony diameter of cells recovered on day 0 and day 84 of starvation at 4°C. Plates were incubated at 37°C for 24 hours under aerobic or anaerobic conditions. Diameters of colonies recovered on PCA, PCAace, PCApyr, and TSA, from day 0 (blue) and day 84 (red) cells were measured. The beanlines for each half of a bean are vertical histograms of the data distribution; the thicker long bean lines indicate the mean of each distribution. The shape of each half of the asymmetric bean represents the Gaussian density estimation of the distribution.

5.2.1.5 Role of AI-2 in recovery

To investigate whether the lowered recovery observed for starved NWt compared NLux, particularly on PCA, was due to the presence of AI-2, NLux cells starved at 4°C for 42 days were grown on conditioned media agar (CMA). CMA was made using CM from NWt (CM-wt) or NLux (CM-lux) culture supernatants. NWt contains *luxS*, the gene encoding the protein required for AI-2 production while NLux lacks *luxS* and its supernatant has no AI-2. If AI-2 was important for lowering recovery after starvation at 4°C, colony count for day 42-starved NLux cells on CM-wt agar should be lower than on CM-lux agar. Following incubation at 37°C for 24 hours, colony counts on CM-wt agar and CM-lux agar were higher than PCA and lower than TSA, but no significant difference in recovery was observed between CM-wt agar and CM-lux agar (Figure 5-4).

To determine whether AI-2 was produced during starvation at 15 and 4°C, CM were harvested from day 42 cultures of NWt, NLux, NCom and NVec, and the presence of AI-2 detected using VHBA. CM-wt was used as the positive control and CM-lux as the negative control. The CM-wt positive control induced production of luminescence from *V. harveyi* MM32 to an average of 7895704 light units after 10 hours of incubation. Background luminescence averaging 198270 light units was measured for the CM-lux negative control. Luminescence induced by CM harvested from NWt, NLux, NCom and NVec was lower than both negative and positive controls, averaging 65819, 72622, 72855 and 65443 light units, respectively. No AI-2 was present in the supernatant of NWt, NLux, NCom and NVec cultures starved at 4°C for 42 days.

5.2.2 Growth comparison between NCTC12900 and NCTC12900 *luxS*$^{-}$ during broth recovery

To investigate whether recovery in broth differed between NWt and NLux, late exponential phase and starved cells were used to inoculate PCB, PCB with 0.2% sodium acetate (PCBace), PCB with 0.2% sodium pyruvate (PCBpyr) and TSB. All cultures were incubated at 37°C for 12 hours. Late-exponential cells grown to an OD_{600} of 1.0 were used as a pre-starvation control to compare with cells starved at 4 and 15°C for 34 days.

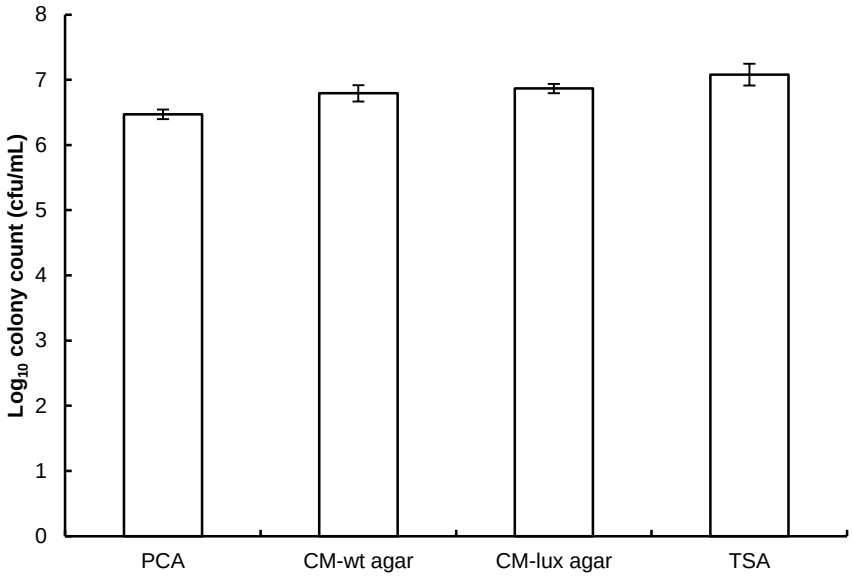

Figure 5-4 Number of colonies on PCA, CM-wt agar, CM-lux agar and TSA recovered from NLux after 42 days of starvation at 4°C. Colony counts shown are the average of four technical replicates. The standard deviation is indicated by the error bars. Data shown are representative of two biological repeats.

Overall, similar trends in growth kinetics were observed for both NWt and NLux, particularly during lag and exponential growth phases (Figure 5-5). Variation between NWt and NLux was observed at the transition into stationary phase and during stationary phase. In general, NLux entered stationary phase at a lower OD_{600} than NWt. In addition, greater variation between technical repeats was observed for NLux than for NWt. Despite regular shaking during incubation, visible aggregates were observed in wells containing NLux cultures, particularly those grown in TSB. Aggregates were not observed for NWt cultures. The duration of lag and rate of exponential growth were similar for NWt and NLux in most cases, except for 4°C-starved cells grown in TSB, where the duration of lag for NLux was significantly shorter ($p<0.05$) than for NWt (Figure 5-5).

Growth in PCBace showed the least variation between strains. For cells grown in PCB, PCBpyr and TSB, a greater decline in OD_{600} during stationary phase was observed for NLux than NWt (Figure 5-5). For cells grown in TSB, the difference in growth between NWt and NLux was particularly pronounced. While slowed growth after entry into stationary phase was observed for NWt, declines in OD_{600} was observed for NLux for approximately 4 hours after cells had entered stationary phase (Figure 5-5).

5.2.3 Comparison of metabolic activities between NCTC12900 and NCTC12900 *luxS*$^{-}$ mutant during recovery after starvation

Differences in growth kinetics in broth observed for NWt and NLux were more prominent in nutrient-rich TSB compared to PCB-based media (Figure 5-5). In addition, after starvation at 4°C for at least 28 days, the number of NLux colonies recovered was significantly higher than NWt, particularly on low-nutrient PCA (Figure 5-2). These results suggested that the carbon requirement for growth was likely to be different between NWt and NLux, particularly after 4°C starvation. Using PM1 and PM2A MicroPlates^{TM}, sole carbon utilisations of 190 substrates by exponential phase, stationary phase and 4°C-starved NWt and NLux cells were measured over 24 hours of incubation at 37°C. Exponential cells were harvested after 2 hours of growth in LB at 37°C to an OD_{600} of 0.2 and stationary phase cells were harvested after 24 hours of growth in LB. Starved cells were harvested between 51 and 59 days of starvation at 4°C. Optical densities were measured

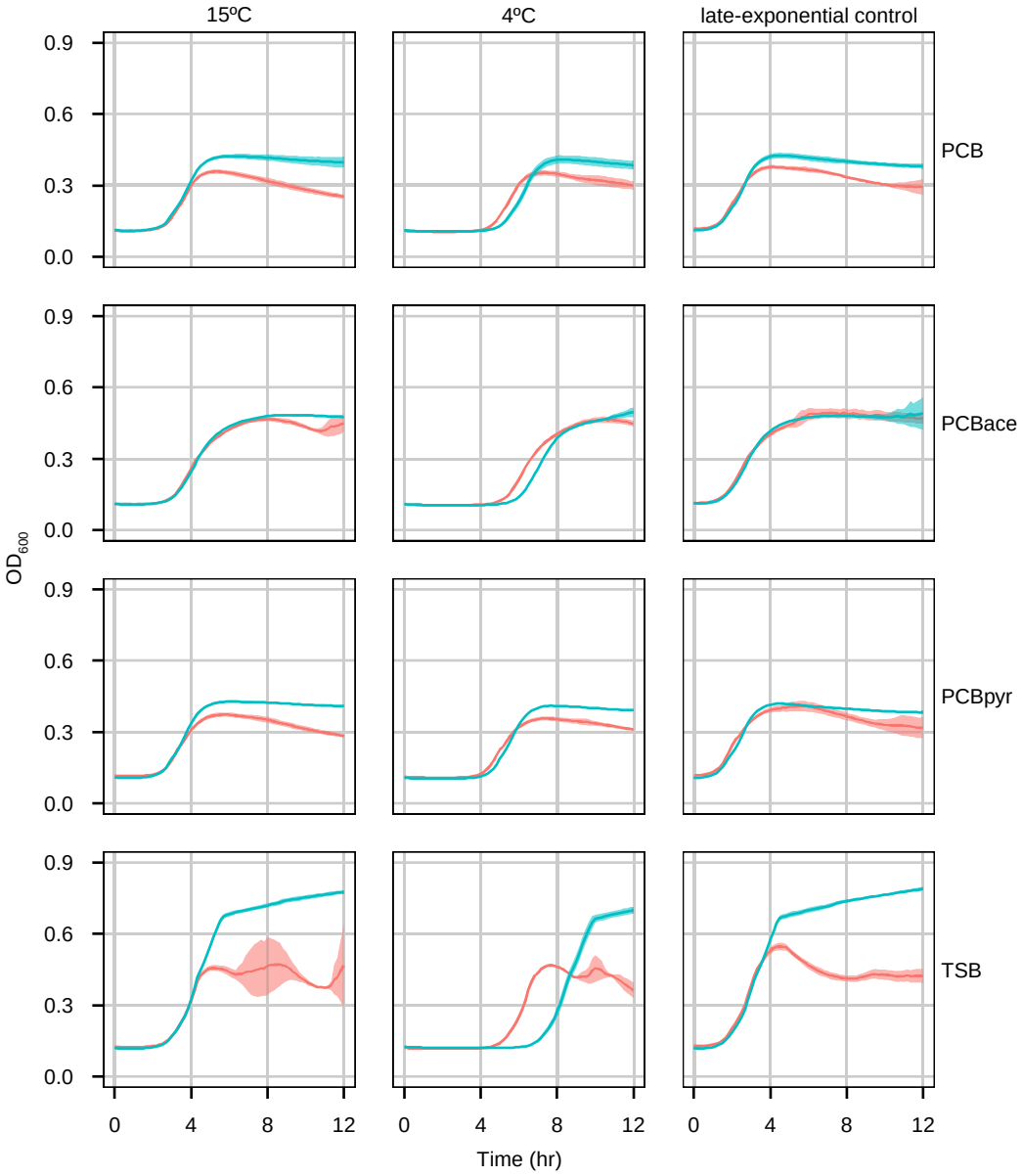

Figure 5-5 Comparison of growth kinetics of late-exponential pre-starvation control and starved NWt (blue) and NLux (red). Pre-starvation control, and cells starved at 4 and 15°C for 34 days were harvested and used to inoculate 200 µL broths in a 96-well microtitre plate. Cultures were incubated at 37°C for 24 hours. Plates were shaken and OD_{600} were recorded every 10 minutes. Lines indicate average of duplicate readings and the standard deviation is shown by shaded areas. Data shown are the average of three technical repeats for the first 12 hours of incubation.

every 15 minutes. The kinetics of substrate use, the duration of lag (λ), the rate of exponential utilisation (μ_{exp}) and the endpoint level of substrate use ($A_{endpoint}$), were determined (Figure 2-1). Substrates numbered in figures correspond to the number shown in the PM1 and PM2A column of Appendix 1.

5.2.3.1 $A_{endpoint}$ comparison between NWt and NLux

Comparison between NWt and NLux utilisation of 190 substrates identified 31, 36 and 42 substrates whose utilisation differed significantly between strains when cells were harvested during exponential phase, stationary phase and after 4°C starvation, respectively (Figure 5-6). In most cases, the observed difference was due to NLux having a higher $A_{endpoint}$ than NWt (Table 5-3). For 16 substrates, a significant difference in $A_{endpoint}$ was observed between NWt and NLux regardless of the stage of growth at which the cells were harvested (Figure 5-6 and Table 5-3). The $A_{endpoint}$ for D-gluconic acid, melibionic acid, fructose-6-phosphate, D-malic acid, L-galactonic acid-γ-lactone and L-proline were consistently higher for NWt; whereas $A_{endpoint}$ for sucrose, D-arabitol, acetic acid, D,L-malic acid, D-lactic acid methyl ester, D-saccharic acid, D-alanine, L-alanine, mucic acid and L-alanyl-glycine were higher for NLux (Table 5-3). $A_{endpoint}$ for all substrates utilised by NWt and NLux are shown in Table 4-1and Appendix 17, respectively.

The general trend for pairwise comparisons of exponential to stationary phase, starved to exponential, and starved to stationary phase were similar for NWt and NLux with most pairwise comparisons of $A_{endpoint}$ data points within the 95% LSD boundaries (Figure 5-7). However, more substrates appeared outside of the 95% LSD boundaries of each pairwise comparison for NLux compared to NWt. For NLux, significant difference in $A_{endpoint}$ was observed for the utilisation of 30 substrates by exponential phase, stationary phase and 4°C-starved cells, 14 more than that observed for NWt (Table 4-1).

For the exponential to stationary phase comparison, $A_{endpoint}$ for the utilisation of 17 substrates differed significantly ($p<0.05$) for NLux compared to five substrates for NWt (Figure 5-7 A). While the majority of data points appeared inside the 95% LSD boundaries, comparison of $A_{endpoint}$ profiles for carbon utilisation by

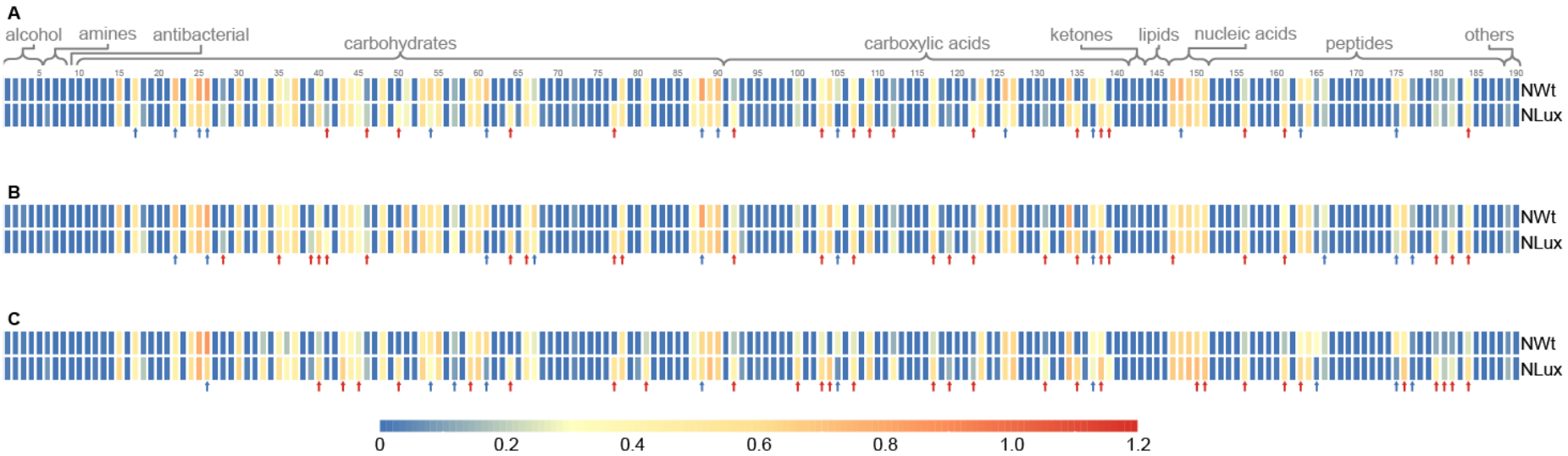

Figure 5-6 $A_{endpoint}$ profiles for substrate utilisation by NWt and NLux were determined using PM1 and PM2A MicroPlates™. Substrates are clustered and ordered according to the first-level chemical class outlined in Appendix 1. Cells were harvested during exponential phase (A), stationary phase (B) and after starvation at 4°C (C). The colour-coding of the rate of utilisation is indicated by the key. Utilisations of substrates that differed significantly (p<0.05) between NWt and NLux are indicated by arrows. Substrates for which $A_{endpoint}$ was higher for NWt are indicated by blue arrows, and those higher for NLux are indicated by red arrows.

Table 5-3 List of substrates where a statistically significant difference (p<0.05) in $A_{endpoint}$ observed between NWt and NLux harvested during exponential phase (EP), stationary phase (SP) and after starvation at 4°C. Relationships of inequality between $A_{endpoint}$ observed for NWt and NLux cells are shown.

Class	Number	Substrates	EP	SP	starved
Glycosides	17	β-methyl-D-galactoside	NWt > NLux		
Monosaccharides	22	D-fructose	NWt > NLux	NWt > NLux	
	25	D-galacturonic acid	NWt > NLux		
	26	D-gluconic acid	NWt > NLux	NWt > NLux	NWt > NLux
	28	Dihydroxy acetone		NWt < NLux	
	35	D-xylose		NWt < NLux	
	39	L-lyxose		NWt < NLux	
	40	L-rhamnose		NWt < NLux	NWt < NLux
	41	L-sorbose	NWt < NLux	NWt < NLux	
	43	*N*-acetyl-D-galactosamine			NWt < NLux
	45	*N*-acetyl-neuramic acid			NWt < NLux
	46	*N*-acetyl-β-D-mannosamine	NWt < NLux	NWt < NLux	
	50	β-D-allose	NWt < NLux		NWt < NLux
Oligosaccharides	54	D-raffinose	NWt > NLux		NWt > NLux
	57	Lactulose			NWt > NLux
	59	Maltose			NWt < NLux
	61	Melibionic acid	NWt > NLux	NWt > NLux	NWt > NLux
	64	Sucrose	NWt < NLux	NWt < NLux	NWt < NLux
	66	α-D-lactose		NWt < NLux	
Polysaccharides	67	Dextrin		NWt > NLux	
Sugar alcohols	77	D-arabitol	NWt < NLux	NWt < NLux	NWt < NLux
	78	D-mannitol		NWt < NLux	
	81	Glycerol			NWt < NLux
Sugar phosphates	87	D,L-α-glycerol-phosphate		NWt < NLux	NWt < NLux
	88	Fructose-6-phosphate	NWt > NLux	NWt > NLux	NWt > NLux
	90	Glucose-6-phosphate	NWt > NLux		
Acetic acids	92	Acetic acid	NWt < NLux	NWt < NLux	NWt < NLux
Dicarboxylic acids	100	Bromo succinic acid			NWt < NLux
	103	D,L-malic acid	NWt < NLux	NWt < NLux	NWt < NLux
	104	Dihydroxy fumaric acid			NWt < NLux
	105	D-malic acid	NWt > NLux	NWt > NLux	NWt > NLux
	107	Fumaric acid	NWt < NLux	NWt < NLux	
	109	L-malic acid	NWt < NLux		NWt < NLux
	112	Mono methyl succinate	NWt < NLux		NWt < NLux
	117	Succinic acid		NWt < NLux	NWt < NLux
Glycolates	119	Glycolic acid		NWt < NLux	NWt < NLux
Hydroxy acids	122	D-lactic acid methyl ester	NWt < NLux	NWt < NLux	NWt < NLux
	123	L-lactic acid			NWt < NLux
Keto acids	126	Methyl pyruvate	NWt > NLux		
Propionates	131	Propionic acid		NWt < NLux	NWt < NLux
Sugar acids	135	D-saccharic acid	NWt < NLux	NWt < NLux	NWt < NLux
	137	L-galactonic acid-γ-lactone	NWt > NLux	NWt > NLux	NWt > NLux
	138	Mucic acid	NWt < NLux	NWt < NLux	NWt < NLux
	139	β-methyl-D-glucuronic acid	NWt < NLux		
Nucleosides	147	2-deoxy adenosine		NWt < NLux	
	148	Adenosine	NWt > NLux		
	150	Thymidine			NWt < NLux
	151	Uridine			NWt < NLux
Amino acids	156	D-alanine	NWt < NLux	NWt < NLux	NWt < NLux
	161	Glycine	NWt < NLux	NWt < NLux	NWt < NLux
	163	Glycyl-L-glutamic acid	NWt > NLux		NWt < NLux
	165	Hydroxy-L-proline			NWt > NLux
	166	L-alanine		NWt > NLux	
	175	L-isoleucine	NWt > NLux	NWt > NLux	NWt > NLux
	176	L-leucine			NWt < NLux
	177	L-lysine		NWt > NLux	NWt > NLux
	180	L-phenylalanine		NWt < NLux	NWt < NLux
	181	L-proline			NWt < NLux
	182	L-pyroglutamic acid		NWt < NLux	NWt < NLux
	184	L-threonine	NWt < NLux	NWt < NLux	NWt < NLux

*Arbitrary number assigned to each substrate tested referring to the numbered substrates in Figure 5-6.

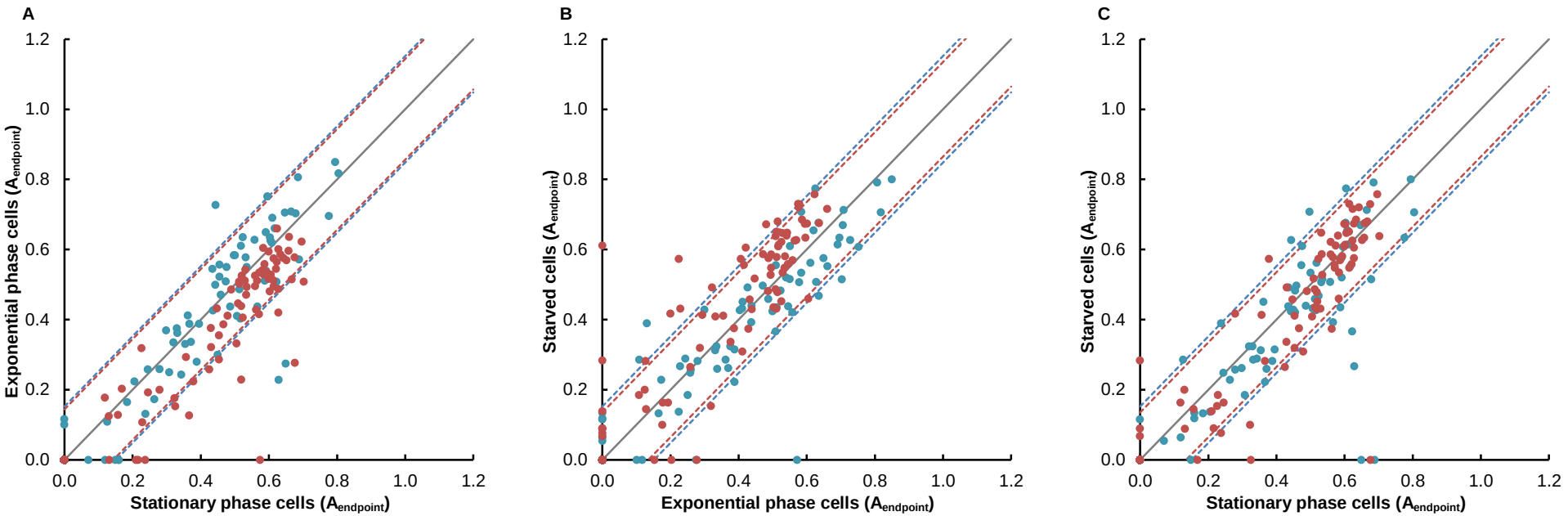

Figure 5-7 Scatter plot comparisons of average $A_{endpoint}$ for substrates used by cells harvested during exponential phase, stationary phase, and after starvation at 4°C. Pairwise comparisons of substrate use between exponential and stationary phase cells (A), starved and exponential phase cells (B), and starved and stationary phase cells (C) are shown. Comparisons for NWt cells are shown in blue and comparisons for NLux are shown in red. The 95% LSD boundaries are marked by dash lines and correlation coefficient (r) = 1 is indicated by the solid line. Each data point represents the average of duplicates.

NLux exponential and stationary phase cells clustered toward the right of the $r = 1$ line, showing a general trend of lower $A_{endpoint}$ for substrate utilisation by exponential phase cells compared to stationary phase cells (Figure 5-7 A). For the starved to exponential phase comparison, $A_{endpoint}$ for the utilisation of 19 substrates differed significantly for NLux compared to seven substrates for NWt (Figure 5-7 B). Scatter graph comparison of $A_{endpoint}$ profiles for carbon utilisation by starved and exponential phase NLux cells showed a cluster of data points toward the left of the $r = 1$ line, showing a general trend of lower $A_{endpoint}$ for substrate utilisation by exponential phase cells compared to starved cells (Figure 5-7 B). For the starved to stationary phase comparison, however, the number of substrates with significantly different $A_{endpoint}$ was similar between NLux and NWt with 11 and 12 substrates found to differ significantly ($p<0.05$), respectively (Figure 5-7 C).

5.2.3.2 Differences in lag of substrate utilisation by NWt and NLux

Overall, a longer lag period was observed for NWt than NLux (blue arrows, Figure 5-8; Table 5-4). In addition, greater variation in λ between NWt and NLux was observed for starved cells (Table 5-4). λ for all substrates utilised by NWt and NLux are shown in Table 4-2 and Appendix 18, respectively. The duration of lag for the utilisation of 24, 23 and 25 substrates differed significantly ($p<0.05$) between NWt and NLux harvested during exponential phase, stationary phase and after 4°C starvation, respectively (Figure 5-8). For 57 substrates, where a significant difference in λ was observed between NWt and NLux, a significant difference in $A_{endpoint}$ was also observed. λ for L-galactonic acid-γ-lactone, D-malic acid, melibionic acid, D-raffinose and L-glutamic acid were shorter for NWt compared to NLux in all cases (Table 5-4 and Table 4-2). Longer λ periods were observed for NWt compared to NLux for L-rhamnose, *N*-acetyl-β-D-monosamine, L-alaninamide, glycyl-L-aspartic acid, propionic acid, sucrose, glycyl-L-glutamic acid, D-saccharic acid, D-lactic acid methyl ester and D-arabitol (Table 5-4 and Table 4-2).

Differences in λ for NWt and NLux cells harvested during exponential phase, stationary phase or after 4°C starvation were compared (Figure 5-9). In general,

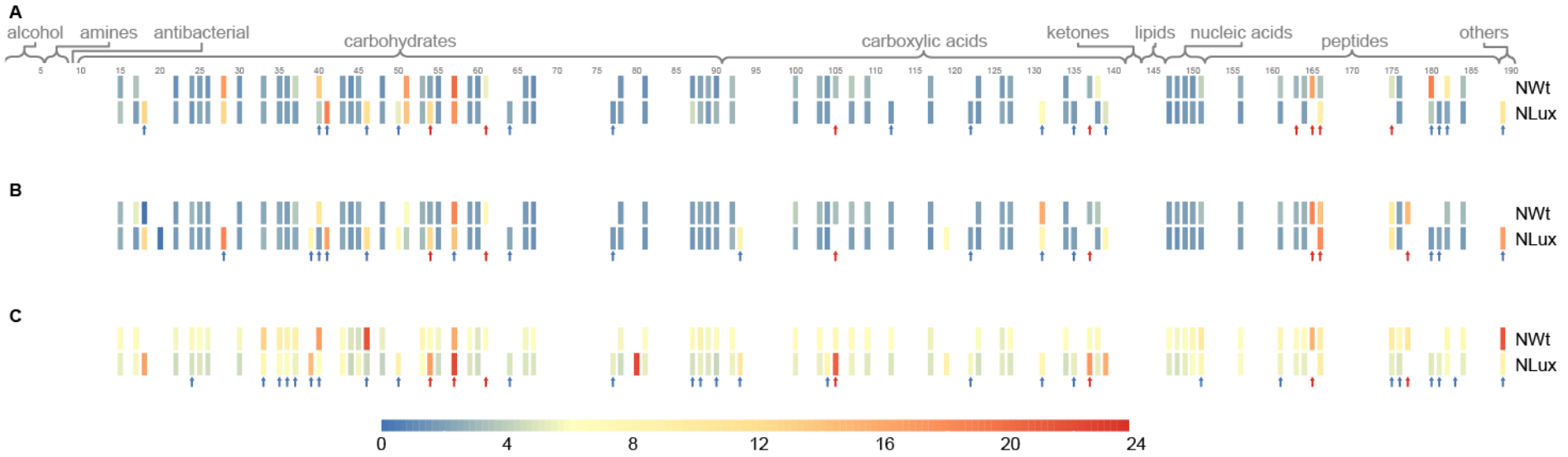

Figure 5-8 Lag time (λ) profiles for substrate utilisation by NWt and NLux were determined using PM1 and PM2A MicroPlates™. Substrates are clustered and ordered according to the first-level chemical class outlined in Appendix 1. Cells were harvested during exponential phase (A), stationary phase (B) and after starvation at 4°C (C). The colour-coding of lag time is indicated by the key. White colour indicates where no detectable utilisation was observed within 24 hours for a substrate. Utilisations of substrates that differed significantly (p<0.05) between NWt and NLux are indicated by arrows. Substrates for which the duration of lag was longer for NWt are indicated by blue arrows, and those higher for NLux are indicated by red arrows.

Table 5-4 List of substrates where a statistically significant difference (p<0.05) in λ observed between NWt and NLux harvested during exponential phase (EP), stationary phase (SP) and after starvation at 4°C. Relationships of inequality between λ observed for NWt and NLux cells are shown.

Class	Number	Substrates	EP	SP	starved
Glycosides	18	β-methyl-D-glucoside	NWt > NLux		
Monosaccharides	24	D-galactose			NWt > NLux
	28	Dihydroxy acetone		NWt > NLux	
	33	D-ribose			NWt > NLux
	35	D-xylose			NWt > NLux
	36	L-arabinose			NWt > NLux
	37	L-fucose			NWt > NLux
	39	L-lyxose		NWt > NLux	NWt > NLux
	40	L-rhamnose	NWt > NLux	NWt > NLux	NWt > NLux
	41	L-sorbose	NWt > NLux	NWt > NLux	
	46	*N*-acetyl-β-D-mannosamine	NWt > NLux	NWt > NLux	NWt > NLux
	50	β-D-allose	NWt > NLux		NWt > NLux
Oligosaccharides	54	D-raffinose	NWt < NLux	NWt < NLux	NWt < NLux
	57	Lactulose		NWt > NLux	NWt < NLux
	61	Melibionic acid	NWt < NLux	NWt < NLux	NWt < NLux
	64	Sucrose	NWt > NLux	NWt > NLux	NWt > NLux
Sugar alcohols	77	D-arabitol	NWt > NLux	NWt > NLux	NWt > NLux
Sugar phosphates	87	D,L-α-glycerol-phosphate			NWt > NLux
	88	Fructose-6-phosphate			NWt > NLux
	90	Glucose-6-phosphate			NWt > NLux
Aldehydic acids	93	Glyoxylic acid		NWt > NLux	NWt > NLux
Dicarboxylic acids	104	Dihydroxy fumaric acid			NWt > NLux
	105	D-malic acid	NWt < NLux	NWt < NLux	NWt < NLux
	112	Mono methyl succinate	NWt > NLux		
Glycolates	119	Glycolic acid		NWt > NLux	NWt > NLux
Hydroxy acids	122	D-lactic acid methyl ester	NWt > NLux	NWt > NLux	NWt > NLux
Propionates	131	Propionic acid	NWt > NLux	NWt > NLux	NWt > NLux
Sugar acids	135	D-saccharic acid	NWt > NLux	NWt > NLux	NWt > NLux
	137	L-galactonic acid-γ-lactone	NWt < NLux	NWt < NLux	NWt < NLux
	139	β-methyl-D-glucuronic acid	NWt > NLux		
Nucleosides	151	Uridine			NWt > NLux
Amino acids	161	Glycine			NWt > NLux
	163	Glycyl-L-glutamic acid	NWt < NLux		
	165	Hydroxy-L-proline	NWt < NLux	NWt < NLux	NWt < NLux
	166	L-alanine	NWt < NLux	NWt < NLux	
	175	L-isoleucine	NWt < NLux		NWt > NLux
	176	L-leucine			NWt > NLux
	177	L-lysine		NWt < NLux	NWt < NLux
	180	L-phenylalanine	NWt > NLux	NWt > NLux	NWt > NLux
	181	L-proline	NWt > NLux	NWt > NLux	NWt > NLux
	182	L-pyroglutamic acid	NWt > NLux		
	184	L-threonine			NWt > NLux
Scleroproteins	189	L-alaninamide	NWt > NLux	NWt > NLux	NWt > NLux

*Arbitrary number assigned to each substrate tested referring to the numbered substrates in Figure 5-8.

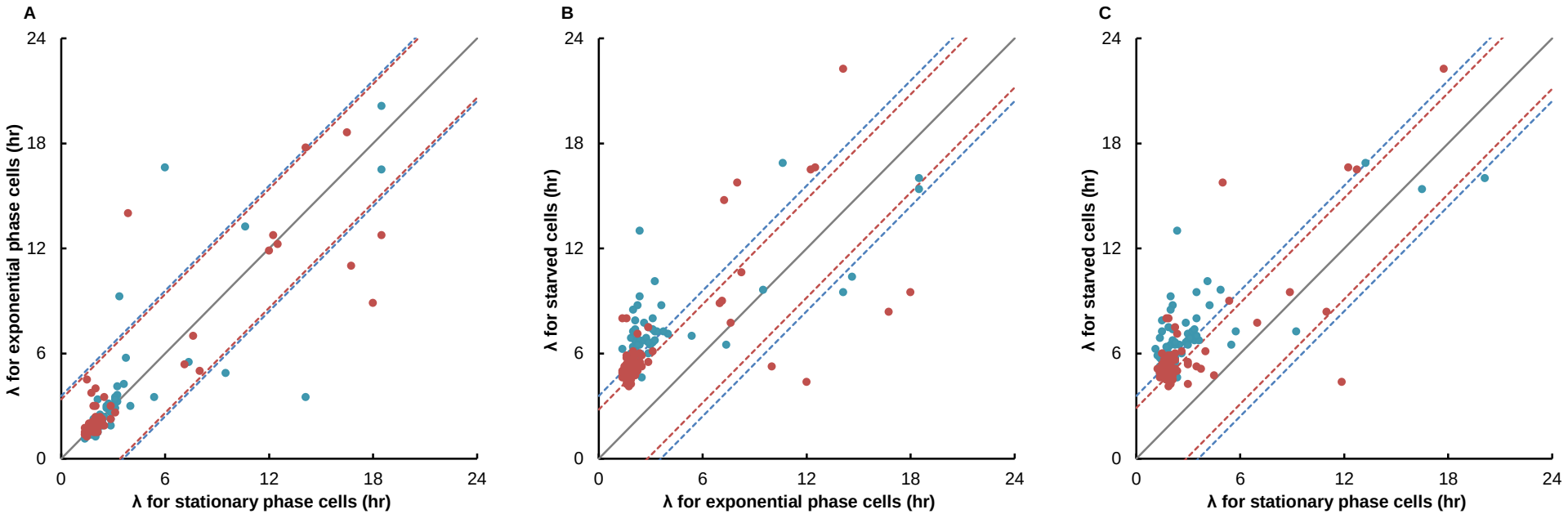

Figure 5-9 Scatter plot comparison of average lag (λ) in substrate use by cells harvested during exponential phase, stationary phase, and after starvation at 4°C. Pairwise comparisons of substrate use between exponential and stationary phase cells (A), starved and exponential phase cells (B), and starved and stationary phase cells (C) are shown. Comparisons for NWt cells are shown in blue and comparisons for NLux are shown in red. The 95% LSD boundaries are marked by dash lines and correlation coefficient (r) = 1 is indicated by the solid line. Each data point represents the average of duplicates.

similar trends in pairwise comparisons of exponential and stationary phase cells were observed for NWt and NLux (Figure 5-9 A). However, when starved cells were compared with exponential phase cells, λ for substrates used by starved cells appeared shorter in general for NLux compared to NWt (Figure 5-9 B). In addition, data points appeared to be more closely clustered for NLux than NWt. Similar trends were observed for the starved to stationary phase comparison (Figure 5-9 C).

5.2.3.3 Differences in rate of substrate use between NWt and NLux

Significant variation in μ_{exp} of carbon utilisation was observed between NWt and NLux (Figure 5-10). μ_{exp} for all substrates utilised by NWt and NLux are shown in Table 4-3 and Appendix 19, respectively. μ_{exp} for the utilisation of 30, 31 and 35 substrates varied significantly (p<0.05) between the NWt and NLux harvested during exponential phase, stationary phase and after 4°C starvation, respectively. 56 of the substrates found to differ significantly in μ_{exp} also differed significantly (p<0.05) in $A_{endpoint}$ between the two strains. μ_{exp} for D-fructose, D-mannose, *N*-acetyl-D-glucosamine, D-glucose and melibionic acid was consistently higher for NWt compared to NLux, regardless of the growth state at which cells were harvested (Table 5-5 and Table 4-3). Conversely, a consistently higher (p<0.05) μ_{exp} was observed for NLux for β-D-allose, sucrose, D-arabitol, mono methyl succinate, D-lactic acid methyl ester, pyruvic acid, D-saccharic acid, mucic acid, glycyl-L-proline and glycyl-L-glutamic acid (Table 5-5 and Table 4-3). Pairwise μ_{exp} comparisons between exponential phase and stationary phase, starved and exponential phase, and starved and stationary phase cells were similar between NWt and NLux, where similar data point spreads and cluster were observed (Figure 5-11).

5.2.3.4 Utilisation of substrates involved in glycolysis

Glycolysis is a central pathway for cell metabolism. Five substrates from the glycolysis pathway are included as carbon sources in the MicroPlates™ (glucose-1-phosphate, glucose-6-phospate, D-glucose, fructose-6-phosphate and pyruvic acid). Overall, little difference was observed between exponential and stationary

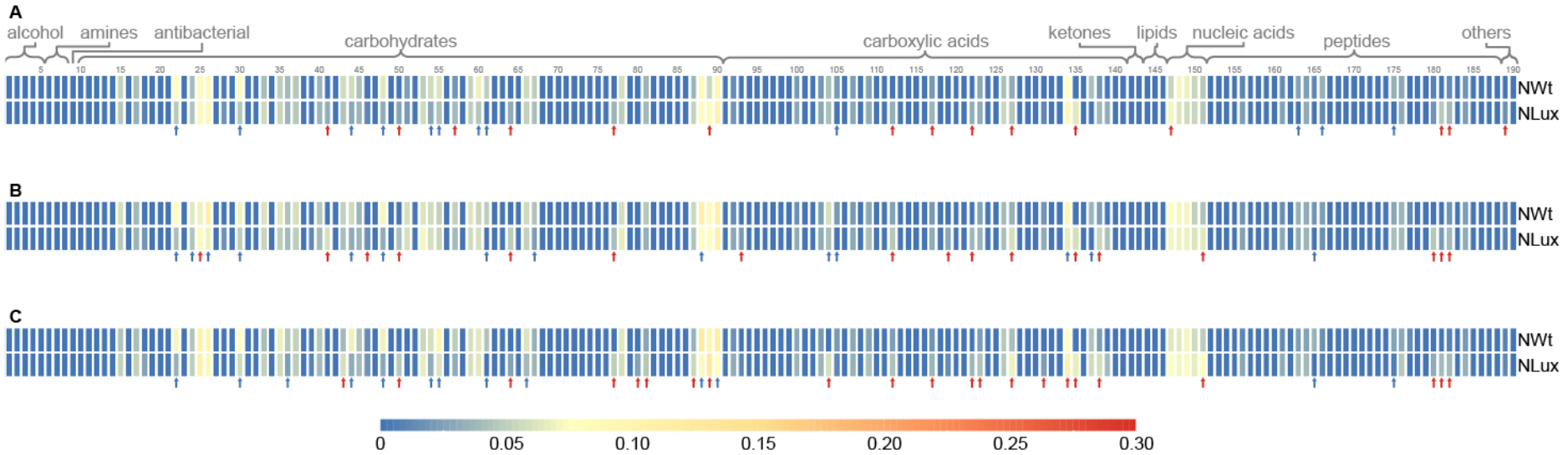

Figure 5-10 Rate of substrate sole carbon substrate use (μ_{exp}) profiles for NWt and NLux determined using PM1 and PM2A MicroPlates™. Substrates are clustered and ordered according to the first-level chemical class outlined in Appendix 1. Cells were harvested during exponential phase (A), stationary phase (B) and after starvation at 4°C (C). Substrates not utilised were considered to have a rate of 0. The colour-coding of the rate of utilisation is indicated by the key. Utilisations of substrates that differed significantly (p<0.05) between NWt and NLux are indicated by arrows. Substrates for which the rate of utilisation was higher for NWt are indicated by blue arrows, and those higher for NLux are indicated by red arrows.

Table 5-5 List of substrates where a statistically significant difference ($p<0.05$) in μ_{exp} observed between NWt and NLux harvested during exponential phase (EP), stationary phase (SP) and after starvation at 4°C. Relationships of inequality between μ_{exp} observed for NWt and NLux cells are shown.

Class	Number	Substrates	EP	SP	starved
Monosaccharides	22	D-fructose	NWt > NLux	NWt > NLux	NWt > NLux
	24	D-galactose		NWt > NLux	
	25	D-galacturonic acid		NWt < NLux	
	26	D-gluconic acid		NWt > NLux	
	30	D-mannose	NWt > NLux	NWt > NLux	NWt > NLux
	36	L-arabinose			NWt > NLux
	41	L-sorbose	NWt < NLux	NWt < NLux	
	43	*N*-acetyl-D-galactosamine			NWt < NLux
	44	*N*-acetyl-D-glucosamine	NWt > NLux	NWt > NLux	NWt > NLux
	46	*N*-acetyl-β-D-mannosamine		NWt < NLux	
	48	α-D-glucose	NWt > NLux	NWt > NLux	NWt > NLux
	50	β-D-allose	NWt < NLux	NWt < NLux	NWt < NLux
Oligosaccharides	54	D-raffinose	NWt > NLux		NWt > NLux
	55	D-trehalose	NWt > NLux		NWt > NLux
	57	Lactulose	NWt < NLux		
	60	Maltotriose	NWt > NLux		
	61	Melibionic acid	NWt > NLux	NWt > NLux	NWt > NLux
	64	Sucrose	NWt < NLux	NWt < NLux	NWt < NLux
	66	α-D-lactose			NWt > NLux
Polysaccharides	67	Dextrin		NWt > NLux	
Sugar alcohols	77	D-arabitol	NWt < NLux	NWt < NLux	NWt < NLux
	80	Dulcitol			NWt < NLux
	81	Glycerol			NWt < NLux
Sugar phosphates	87	D,L-α-glycerol-phosphate			NWt < NLux
	88	Fructose-6-phosphate		NWt > NLux	NWt > NLux
	89	Glucose-1-phosphate	NWt < NLux		NWt < NLux
	90	Glucose-6-phosphate			NWt > NLux
Aldehydic acids	93	Glyoxylic acid		NWt < NLux	
Dicarboxylic acids	104	Dihydroxy fumaric acid		NWt > NLux	NWt < NLux
	105	D-malic acid	NWt > NLux	NWt > NLux	
	112	Mono methyl succinate	NWt < NLux	NWt < NLux	NWt < NLux
	117	Succinic acid	NWt < NLux		NWt < NLux
Glycolates	119	Glycolic acid		NWt < NLux	
Hydroxy acids	122	D-lactic acid methyl ester	NWt < NLux	NWt < NLux	NWt < NLux
	123	L-lactic acid			NWt < NLux
Keto acids	127	Pyruvic acid	NWt < NLux	NWt < NLux	NWt < NLux
Propionates	131	Propionic acid			NWt < NLux
Sugar acids	134	D-glucuronic acid		NWt > NLux	NWt < NLux
	135	D-saccharic acid	NWt < NLux	NWt < NLux	NWt < NLux
	137	L-galactonic acid-γ-lactone	NWt > NLux	NWt > NLux	
	138	Mucic acid	NWt < NLux	NWt < NLux	NWt < NLux
	139	β-methyl-D-glucuronic acid	NWt < NLux		
Nucleosides	147	2-deoxy adenosine	NWt < NLux		
	151	Uridine		NWt < NLux	NWt < NLux
Amino acids	163	Glycyl-L-glutamic acid	NWt > NLux		
	165	Hydroxy-L-proline		NWt > NLux	NWt > NLux
	166	L-alanine	NWt > NLux		
	175	L-isoleucine	NWt > NLux		NWt > NLux
	180	L-phenylalanine		NWt < NLux	NWt < NLux
	181	L-proline	NWt < NLux	NWt < NLux	NWt < NLux
	182	L-pyroglutamic acid	NWt < NLux	NWt < NLux	NWt < NLux
Scleroproteins	189	L-alaninamide	NWt < NLux		

*Arbitrary number assigned to each substrate tested referring to the numbered substrates in Figure 5-10.

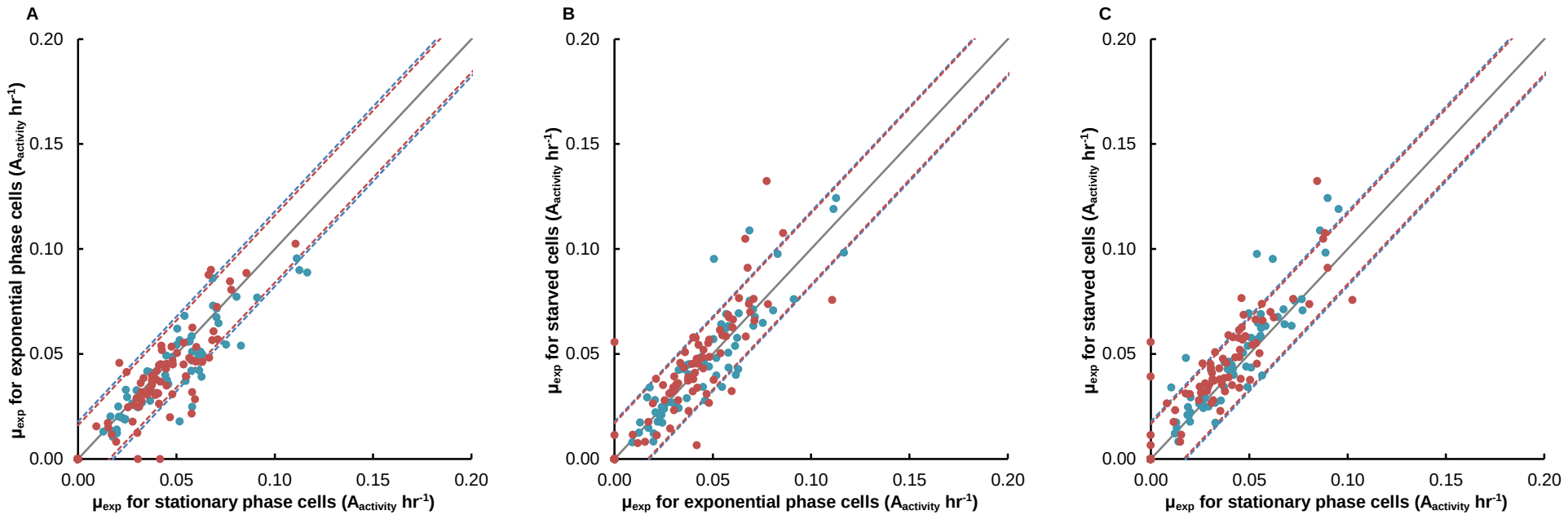

Figure 5-11 Scatter plot comparison of average rate (μ_{exp}) in substrate use by cells harvested during exponential phase, stationary phase, and after starvation at 4°C. Pairwise comparisons of substrate use between exponential and stationary phase cells (A), starved and exponential phase cells (B), and starved and stationary phase cells (C) are shown. Comparisons for NWt cells are shown in blue and comparisons for NLux are shown in red. The 95% LSD boundaries are marked by dash lines and correlation coefficient (r) = 1 is indicated by the solid line. Each data point represents the average of duplicates.

phase cells for the same strain, while a longer lag time was observed for starved cells (Figure 5-12).

For cells harvested at exponential phase and after 4°C-starvation, μ_{exp} for glucose-1-phosphate utilisation was significantly higher (p<0.05) for NLux compared to NWt (Figure 5-12 and Table 5-5). The rate of glucose-1-phosphate utilisation by exponential phase and starved NLux was 0.085 and 0.132 $A_{activity}$ hr^{-1} (Appendix 19), respectively, compared to 0.054 and 0.098 $A_{activity}$ hr^{-1} for exponential phase and starved NWt, respectively (Table 4-3). No significantly difference in μ_{exp} for glucose-1-phosphate utilisation was observed between stationary phase NLux and NWt. No significant difference in $A_{endpoint}$ or λ for glucose-1-phosphate utilisation was observed between NLux and NWt.

Utilisation of D-glucose by NLux occurred at a significantly lower rate than NWt in all cases (Figure 5-12 and Table 5-5). μ_{exp} for D-glucose utilisation by NLux was 0.032, 032 and 0.028 $A_{activity}$ hr^{-1} for exponential phase, stationary phase and starved cells, respectively (Appendix 19), which were significantly lower (p<0.05) than the 0.065, 0.071 and 0.068 $A_{activity}$ hr^{-1} rates observed for NWt, respectively (Table 4-3). No significant difference in $A_{endpoint}$ or λ was observed between NLux and NWt utilisation of D-glucose.

$A_{endpoint}$ for glucose-6-phosphate utilisation by exponential phase NLux was 0.502 (Appendix 17), significantly lower (p<0.05) than the $A_{endpoint}$ of 0.625 observed for NWt (Table 4-1). λ and μ_{exp} for glucose-6-phosphate utilisation by starved NLux were shorter and lower (p<0.05) than that observed for NWt (Figure 5-12, Table 5-4 and Table 5-5). The lag time for glucose-6-phosphate utilisation by starved NLux was 5.0 hours (Appendix 18), significantly shorter (p<0.05) than the 6.9-hour lag observed for NWt (Table 4-2). The rate of glucose-6-phosphate utilisation by starved NLux was 0.076 $A_{activity}$ hr^{-1} (Appendix 19), compared to the rate of 0.119 $A_{activity}$ hr^{-1} observed for NWt (Table 4-3).

Of the glycolic substrates tested, utilisation of fructose-6-phosphate differed the most between NLux and NWt, where a significant difference in utilisation was observed in $A_{endpoint}$, λ and μ_{exp} in most cases (Figure 5-12). $A_{endpoint}$ utilisation of

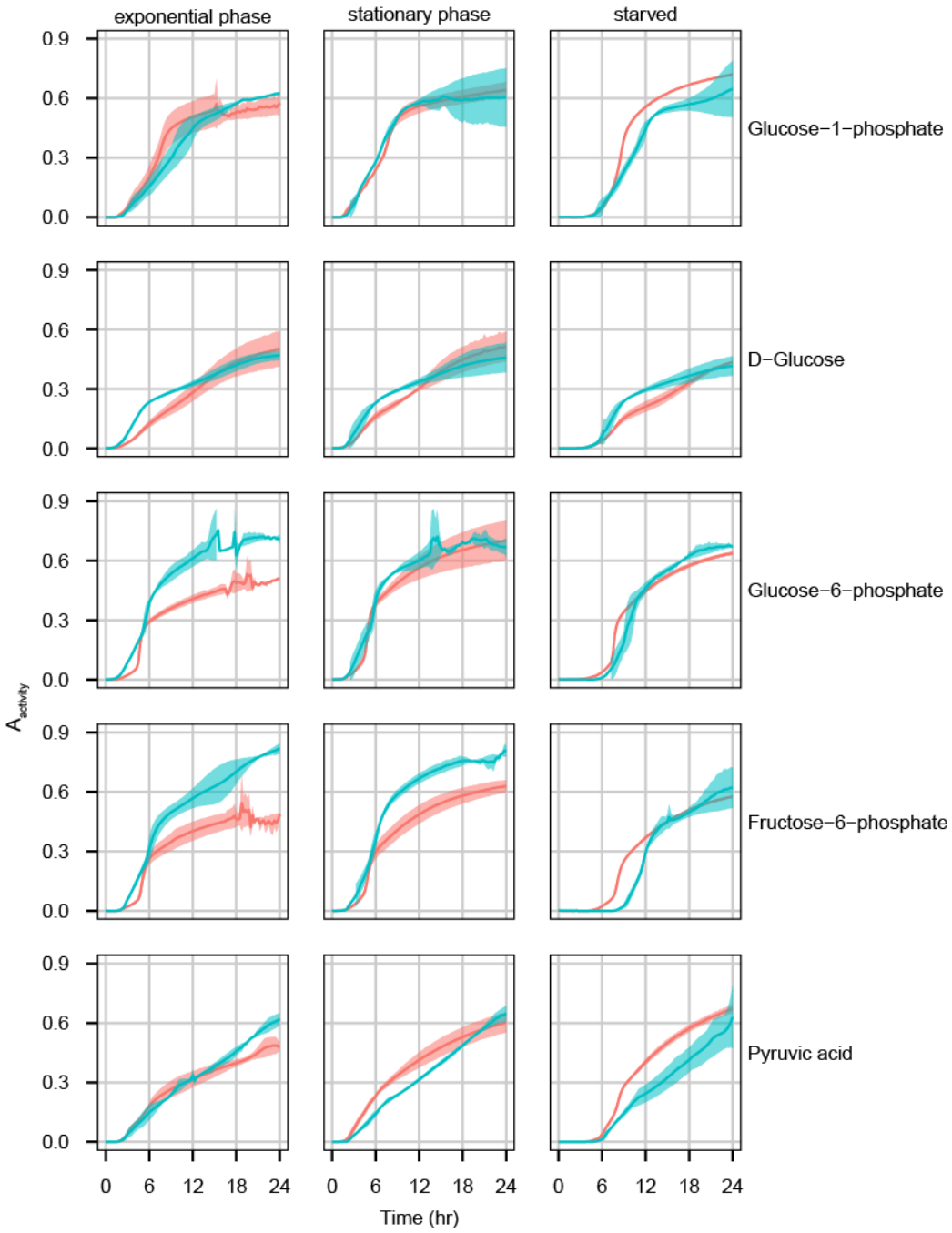

Figure 5-12 Utilisation kinetics of substrates involved in glycolysis by exponential phase, stationary phase and 4°C-starved NWt and NLux. Substrate use for NWt (blue) and NLux (red) are shown. Cultures were incubated at 37°C for 24 hours and measurements taken every 15 minutes. Lines indicate average of duplicates and the standard deviations are shown by shaded areas.

fructose-6-phosphate by NLux was significantly lower (p<0.05) than that observed for NWt in all cases (Table 5-3). $A_{endpoint}$ observed for exponential phase, stationary phase and starved NLux were 0.488, 0.629 and 0.576, respectively (Appendix 17), compared to 0.817, 0.805 and 0.706 observed for NWt, respectively (Table 4-1). The lag time observed for fructose-6-phosphate utilisation by starved NLux was 5.4 hours (Appendix 18); significantly shorter than the 8.8-hour lag observed for starved NWt (Table 4-2). The rate of fructose-6-phosphate utilisation by stationary phase and starved NLux were 0.078 and 0.084 $A_{activity}$ hr^{-}, respectively (Appendix 19), significantly lower than the rates observed for NWt, which were 0.113 and 0.124 $A_{activity}$ hr^{-}, respectively (Table 4-3).

Significant differences in μ_{exp} were observed for pyruvic acid utilisation by NLux and NWt in all cases (Figure 5-12 and Table 5-5), while no significant difference in $A_{endpoint}$ or λ was observed. μ_{exp} for pyruvic acid utilisation by NLux was 0.047, 0.058 and 0.069 $A_{activity}$ hr^{-1} for exponential phase, stationary phase and starved cells, respectively (Appendix 19), which were significantly higher (p<0.05) than the 0.031, 0.033 and 0.042 $A_{activity}$ hr^{-1} rates observed for NWt, respectively (Table 4-3).

5.3 Discussion

The activated methyl cycle (AMC) is an important metabolic pathway for amino synthesis and methylation in *E. coli* (Winzer *et al.*, 2003). Conversion of *S*-ribosyl-homocysteine (SRH) to homocysteine by LuxS, as part of AMC, also produces the precursor (4,5-dihydroxy-2,3-pentanedione (DPD)) of autoinducer-2 (AI-2), a quorum sensing (QS) molecule (Pereira *et al.*, 2013). In *E. coli*, the production of AI-2 is dependent on LuxS and the availability of SRH (Pereira *et al.*, 2013). The loss of LuxS function is associated with increased growth rate, decreased motility and decreased type III secretion system (TTSS) activity in *E. coli* O157:H7 (Sperandio *et al.*, 2002a; Sperandio *et al.*, 1999; Sperandio *et al.*, 2001; Sperandio *et al.*, 2002b). As a zoonotic pathogen, *E. coli* O157:H7 can survive starvation at sub-optimal temperatures. Recovery after starvation was dependent on the level of available nutrient and the presence of specific metabolic substrates (Chapter 3). Since LuxS function is associated with virulence

phenotypes, such as motility and TTSS function, and is also involved in core cell metabolism, we hypothesised that LuxS function affected *E. coli* O157:H7 recovery after starvation.

Using NCTC12900 (NWt), NCTC12900 *luxS*$^{-}$ (NLux) and the complemented strain NCTC12900 *luxS*$^{-}$ pSS03 (NCom), the role of LuxS in *E. coli* O157:H7 maintenance of viability and colony recovery during and after starvation at 4 and 15°C was investigated. NCTC12900 *luxS*$^{-}$ pCR2.1 (NVec) was used as a control for the growth cost of plasmid carriage on the cells. Viability during starvation, as determined by maintenance of membrane integrity, was not affected by the absence of LuxS (Figure 5-1). Although no significant difference in colony recovery was observed between NWt and NLux when starved at 15°C, colony recovery during 84 days of starvation at 4°C was affected by the absence of LuxS. However, recovery of NWt cultures harvested between 28 to 56 days of 4°C starvation on PCA, PCAace and PCApyr was significantly lower than NLux (Figure 5-2).

Complementation of *luxS* (NCom) reversed the phenotype observed for NLux, resulting in a significantly lower colony count on all media compared to NLux, NWt and NVec (Figure 5-2). Since no significant difference in colony count was observed between NLux and NCTC12900 *luxS*$^{-}$ with plasmid control, NVec, the phenotype observed for NCom was likely due to the presence of LuxS and/or the production of AI-2. The effect of LuxS on colony recovery was also evident in the diameter of colonies generated by for NCom and NVec. A significantly lower mean colony diameter was observed for NCom starved at 4°C for 84 days compared to day 0 cells, while the same trend was not observed for NVec. The role of LuxS in *E. coli* O157:H7 recovery after starvation may be due to its metabolic function, AI-2 production, or the combination of both. An attempt to use exogenous AI-2, as a QS signal, to reverse the higher colony recovery phenotype associated with the absence of LuxS using AI-2-containing conditioned-media (CM) from NWt (CM-wt) was not successful in complementing the LuxS deficiency (Figure 5-4). While CM has been widely-used to test the role of AI-2 as a signalling molecule, purified AI-2 has recently become commercially available and may be included in future investigation into

the role of AI-2 QS in culturability of starved *E. coli* O157:H7 (Pereira *et al.*, 2013).

The difference in culturability observed between starved NWt and NLux was dependent on the media used. The same trend was observed for NWt and NLux growth in broth where the nutrient level of the media used influenced growth. The final OD_{600} achieved by NLux was lower than NWt in PCB, PCBpyr and TSB, both before and after starvation (Figure 5-5). When starved at 4°C, there was a shorter lag period for NLux, particularly in TSB. It is unclear whether growth kinetics in broth are related to culturability on solid media, however, results presented here suggested that NLux has a lower growth potential in broth and a higher growth potential on agar compared to NWt.

The difference in colony recovery and growth in broth observed for starved NWt and NLux was dependent on the nutrient level of the media used. This is likely to be due to the nutrient dependency of LuxS-mediated gene expression or the substrate availability for AMC to cycle (Wang *et al.*, 2005). The intertwining relationship between AI-2 and LuxS metabolism function was also demonstrated by the involvement of the phosphoenolpyruvate phosphotransferase system (PEP:PTS) in the detection and internalisation of extracellular AI-2 (Pereira *et al.*, 2012). The absence of Enzyme I (EI), a key component of PTS, resulted in depleted Lsr, an ATP-binding cassette transporter responsible for AI-2 internalisation, expression and the failure to remove AI-2 from the culture fluid (Pereira *et al.*, 2012).Therefore, the difference in growth phenotype observed between NWt and NLux is likely to be caused by multiple factors, which were likely to be more metabolic than AI-2-induced since AI-2 was not actively produced by starved cells.

Metabolic profiling of single substrate use for NWt and NLux showed that, in general, NLux substrate utilisation had shorter λ and higher μ_{exp} than NWt. In the majority of these cases, the shorter λ and higher μ_{exp} observed were reflected in the higher $A_{endpoint}$ observed. Greater variation in $A_{endpoint}$, λ and μ_{exp} were observed for substrates use by starved NWt and NLux compared to cells harvested from exponential and stationary phase. This is likely to reflect the difference in metabolic status between NWt and NLux, which may affect the change energy

level within the cell during the course of starvation and thereby carbon utilisation during recovery. An example of this is the difference in μ_{exp} observed for D-glucose and pyruvic acid utilisation between NLux and NWt. The growth rate for *E. coli* on D-glucose is typically higher than on pyruvate (Holms, 1996). Interestingly, μ_{exp} for D-glucose was lower for NLux than NWt while μ_{exp} for pyruvic acid was consistently higher for NLux (Table 5-3). This suggested that the absence of LuxS altered the efficiency at which D-glucose and pyruvic acid were catabolised.

The observed difference in recovery on solid media and metabolic profiles between NWt and NLux, and the inability to complement LuxS with CM-wt agar suggested that LuxS was involved in starved *E. coli* O157:H7 recovery; not as a QS synthase, but as a metabolic enzyme. *luxS* is highly conserved in both Gram-positive and Gram-negative bacteria (Cluzel *et al.*, 2010; Xavier & Bassler, 2005a). VBNC as a dormancy state may be evolutionarily advantageous for persistence of microbial population in changing environments, a global phenomenon affecting a wide range of bacteria (Buerger *et al.*, 2012; Lennon & Jones, 2011). It is possible the carriage of *luxS* reflects the conservation of LuxS metabolic function rather than AI-2 QS, and the lowered culturability observed for NWt was evolutionarily driven as a survival mechanism in nutrient limiting environments at sub-optimal temperatures, which enables *E. coli* O157:H7 to live a dual lifestyle in both host and non-host environments.

Chapter 6 Discussion

Incidence of *E. coli* O157:H7 infections in New Zealand is sporadic, and generally associated with rural contacts, either animal or environment, rather than contaminated food (The Institute of Environmental Science and Research Ltd., 2013). As a zoonotic pathogen, *E. coli* O157:H7 is likely to have evolved alongside its mammalian hosts, developing a dual lifestyle of growth in the hindgut of its ruminant reservoirs, and survival in non-host environments once shed (Boutte & Crosson, 2013; Money *et al.*, 2010). Conditions in non-host environments may limit bacterial growth, with adverse conditions such as nutrient starvation likely to occur (Hengge-Aronis, 1993; Ropers *et al.*, 2006). Continued bacterial existence within a given environment therefore depends on their ability to adapt during the transition from feast to famine and vice versa (Koch, 1971). Intrinsic to the dual lifestyle of *E. coli* O157:H7 is its ability to survive during these transitions, which depends on the detection of changes and, more importantly, the elicitation of appropriate responses (Battesti *et al.*, 2011; Ferenci, 2001).

We hypothesised that entrance into the viable but nonculturable (VBNC) state, where the growth phenotype of viable cells is lost after exposure to stress factors, is the result of adaptive survival response used by *E. coli* O157:H7 in non-host environments. This study aimed to characterise the impact of carbon starvation at refrigeration and environmental temperatures on the recovery of *E. coli* O157:H7, including New Zealand clinical and bovine isolates, and the impact of changes in metabolic potential during starvation on recovery. In addition, the potential role of *luxS*-mediated quorum sensing in starved-cell recovery was also investigated.

The current consensus for the definition of the VBNC state relies on the demonstration that cells can be (i) induced into the VBNC state by the introduction of stress(es), which results in (ii) a decline in colony recovery of culture samples on routine culturing media over the duration of stress exposure, while (iii) viability, as determined by culture-independent methods, is maintained and are (iv) able to be rescued, regaining the ability to grow on routine culturing media. Results from this study showed that *E. coli* O157:H7, including clinical and bovine isolates, can form metabolic sub-populations as the cells entered the

VBNC state when starved in PBS. The proportion of VBNC cells within the staved population was greater for cells held at 4°C compared to those held at 15 or 25°C. Colony count for cultures starved at 25 or 15°C decreased by a maximum of two logs, while starvation at 4°C resulted in a decline in colony count by at least five logs on PCA by day 84. The effect of starvation temperature on colony recovery observed in this study was consistent with Zhao & Matthews' (2000) observation on *E. coli* O157:H7 starved in PBS. However, Wang and Doyle (1998) reported entire populations of *E. coli* O157:H7 becoming unculturable within 70 days of incubation in reservoir or lake water at 25°C. It is likely that the effect of starvation temperature on colony recovery was dependent on the starvation media used.

Colony recovery of starved cells was also dependent on nutrient composition of the media used. By using TSA, a nutrient-rich media, and PCA, a nutrient-poor media, the effect of nutrient availability on recovery of starved cultures was assessed. Little difference in recovery on PCA and TSA was observed for cultures starved at 15 and 25°C. However, for cultures starved at 4°C, the level of recovery on TSA was consistently higher than on PCA. The difference in colony count observed on TSA and PCA suggested the existence of bacterial sub-populations within the starved culture with different nutrient requirements for recovery. In addition, variation in the size of the colonies recovered on both TSA and PCA was significantly greater than non-starved cells. This is likely to be reflective of the difference in energy and/or metabolic state of individual cells within the starved cell population. Results from this study support the hypothesis that bacterial populations are heterogenic, at different growth stages with different metabolic requirements, and this heterogeneity contributes to the persistence of the population in fluctuating environments (Buerger *et al.*, 2012; Lennon & Jones, 2011).

Cell populations harvested for starvation studies are likely to be heterogeneous prior to starvation, which would account for the heterogeneity in colony development phenotypes observed during recovery following starvation. Three distinct sub-populations were identified from the 4°C-starved culture based on their colony recovery phenotype: (i) the population not recoverable on neither

TSA or PCA and therefore VBNC, (ii) the population recovered only on TSA but not PCA and thus requiring more nutrients for recovery, and (iii) the population recovered on PCA requiring lower nutrient levels for colony formation (Figure 3-6). In addition to the variability in colony count on different media observed during starvation, variations in colony size also increased over time, particularly for the clinical and bovine cultures (Figure 3-17 and Figure 3-18).

In a heterogeneous population, individual cells with different energy and/or metabolic status are likely to exist. The energy level and metabolic status differ between cells in different growth phases, which may affect cell population dynamics during starvation. For example, heterogeneity in respiratory activity and membrane potential during starvation varied between *E. coli* cultures harvested during exponential and stationary growth phases (Rezaeinejad & Ivanov, 2011). Similarly, the ratio of the three sub-populations observed during starvation at 4°C differed between cells harvested at different growth stages (Figure 3-6). Heterogeneous phenotypes of *E. coli* populations after exposure to a variety of stresses, such as UV irradiation and super-optimal temperature stress, have also been demonstrated (McCool *et al.,* 2004; Van Derlinden *et al.,* 2011). McCool *et al.* (2004) hypothesised that heterogeneity in *E. coli* SOS response to DNA damage was the result of pre-existing heterogeneity in SOS expression prior to exposure to stress. Van Derlinden et al. (2011) showed that heterogeneity in temperature resistance was due to the presence of at least two sub-populations with different sensitivity to elevated temperature.

Based on current knowledge, a model was proposed to describe the changes in VBNC sub-populations of *E. coli* O157:H7 in a host, non-host environments and upon re-entry into a host (Figure 6-1). Within a given heterogeneous cell population, a sub-population of unculturable cells is likely to exist (Lewis, 2007) (Figure 6-1 A). Upon transition from the host to non-host environments, such as exposure to nutrient limitation and low temperatures, the intrinsic heterogeneity in energy and/or metabolic state of cells within the population leads to a gradual decrease in the culturability of the population. This is likely to be the result of an increasing number of cells over time becoming VBNC, rather than a population-coordinated entry into VBNC (Figure 6-1 B). In addition, the change in population dynamics is likely to be driven, in part, by the lack of nutrient in non-

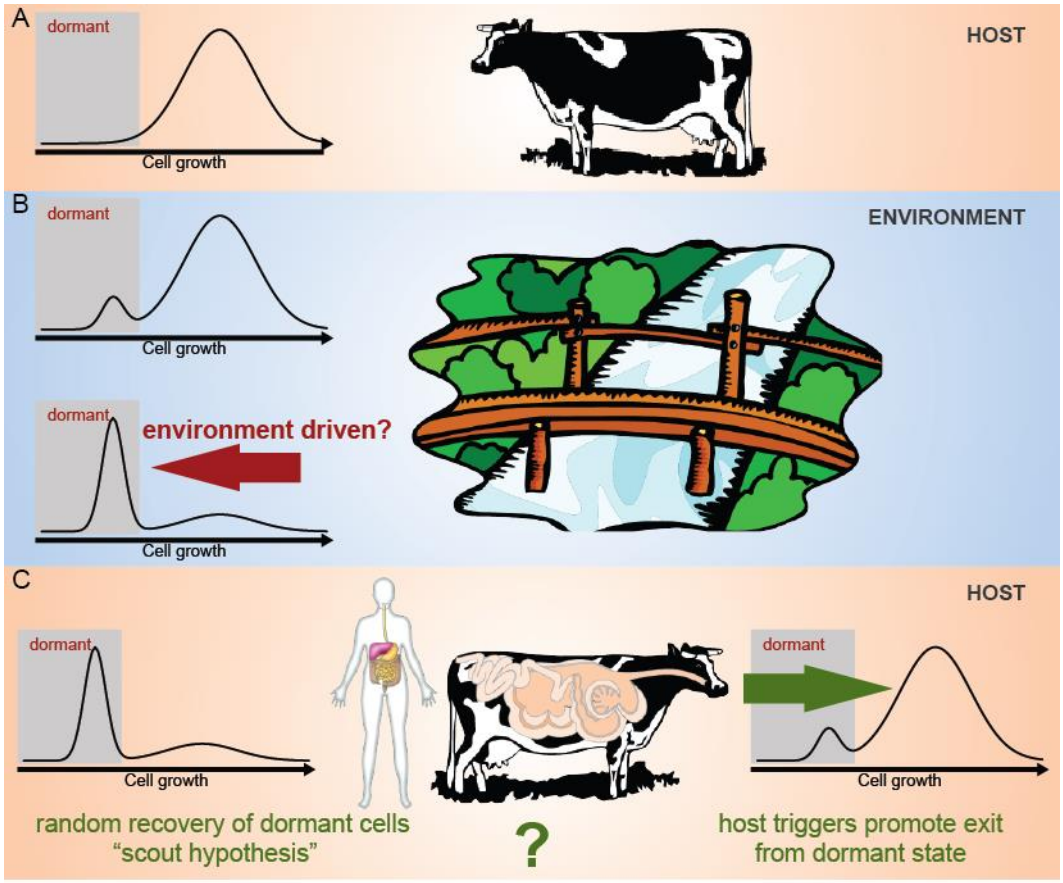

Figure 6-1 Proposed model of the changes in *E. coli* O157:H7 VBNC cell populations in a host, in non-host environments and upon re-entry into a host. (A) Within an actively growing cell population in favourable growth conditions, such as the conditions within a host, a proportion of the cell population is VBNC. (B) In non-host environments, where cells are likely to be exposed to nutrient limitation and low temperature, more cells enter to the VBNC state over time resulting in an increase in the number of non-culturable cells, a phenomenon likely to be driven by the unfavourable conditions outside of a host. (C) Once the starved cells enter into a host, recovery could be random, as the "scout hypothesis" proposed by Buerger *et al.* (2012), and/or triggered by biological and physical factors in the host.

host environments where conservation or recycle of cellular energy may be key to survival (Figure 6-1 B). Exit from the VBNC state may be stochastic, triggered by specific stimuli, or a combination of random recovery and growth stimuli (Figure 6-1 C).

The variation in the number of colonies recovered on PCA and TSA not only suggested the existence of sub-populations within the starved culture with different nutrient requirements for growth, it also suggested the possibility of manipulating the nutrient level, or specific nutrients, in recovery media to promote cell exit from the VBNC state. Both physical and biological factors have been shown to resuscitate VBNC cells (Oliver, 2010). For *E. coli*, removal of temperature stress was not sufficient for resuscitation (Oliver, 2010). However, VBNC *E. coli* can be resuscitated by biological factors such as co-culture with eukaryotic cells and supplementation of recovery media with catalase, sodium pyruvate or enterobacterial autoinducers (Mizunoe *et al.*, 1999; Reissbrodt *et al.*, 2002; Senoh *et al.*, 2012).

Catalase and pyruvate supplementation have been used as hydrogen peroxide-degrading compounds for resuscitating cells under salinity or oxidative stress (Mizunoe *et al.*, 1999). Pyruvate is a carbon source, a regulator of substrate transport via PTS (Figure 1-6), and is also part of the PEP-pyruvate oxaloacetate (PPO) node that act as a "metabolic switch" to regulate carbohydrate flux (Figure 1-7) (Sauer & Eikmanns, 2005). Therefore, the increase in pyruvate concentration may act as a carbon source or a metabolic stimulant for the VBNC cells by regulating nutrient transport and/or the direction of nutrient flux. Resuscitation by co-culture with eukaryotic cells or addition of enterobacterial autoinducers to recovery media suggested the involvement cell-to-cell communication in the recovery of VBNC cells (Reissbrodt *et al.*, 2002; Senoh *et al.*, 2012). In addition, release of other host factors, such as nutrients, may also be involved in VBNC cell resuscitation by co-culture with eukaryotic cells. Metabolic resuscitation and the potential role of AI-2 signalling on resuscitation of VBNC *E. coli* O157:H7 were both explored in this study.

Since the nutrient level of recovery media was found to affect the number of colonies recovered from starved cultures in this study, we hypothesised that

substrates involved in central metabolism, particularly pathways involved in energy production, were likely to be key in resuscitating VBNC *E. coli* O157:H7. Supplementation of PCA with 0.2% sodium pyruvate resulted in a significant increase in colony count compared to PCA and for glucose supplementation (Table 3-2). In addition, pyruvate, as a sole carbon source, was not utilised at a higher rate or to a higher level compared to other glycolytic substrates (Holms, 2001)(see Chapter 4). If the increase in recovery from starved cultures was due to pyruvate as a carbon source, the "stimulation" should had been due to pyruvate being a "preferential" carbon source, and thereby resuscitating cells that were otherwise unculturable on PCA. Further, utilisation of pyruvate as sole carbon source would be likely to have different kinetics, such as shorter λ or higher $A_{endpoint}$ or μ_{exp}, compared to utilisation of other nutrients. However, $A_{endpoint}$ for pyruvate was not higher than for utilisation of other glycolic substrates, neither was μ_{exp} higher or λ shorter. Therefore, pyruvate-resuscitation of VBNC cells is unlikely to be due to the provision of an additional carbon source, but rather the involvement of pyruvate in other metabolic activities such as nutrient transport via the phosphoenolpyruvate: phosphotransferase system (PEP:PTS).

Based on the assumption that the increased colony count on PCA with pyruvate supplementation was not due to provision of an additional carbon source, we propose a model that depicts the role of PEP, PTS and pyruvate on starved cell recovery on TSA, PCA and pyruvate-supplemented PCA (Figure 6-2). It should be noted that the model proposed applies to pyruvate resuscitation of individual cells, not the entire heterogeneous population. The variation in colony size which occurred for starved cultures is likely to reflect the heterogeneity of the population where individual cells within the populations were at different growth stages with different levels of PTS function. Furthermore, the decreasing colony count on PCA over 84 days for 4°C starved cultures may be due to the deterioration of PTS function over time.

During growth on TSA, nutrients in the media are transported into the cell via the PTS system which requires the conversion of PEP to pyruvate (Figure 6-2A). Pyruvate may either feed into TCA, or be converted to PEP and further increase substrate importation (Figure 6-2A). When grown on PCA however, the nutrient level is too low to enable PTS function, therefore PEP accumulates resulting in an

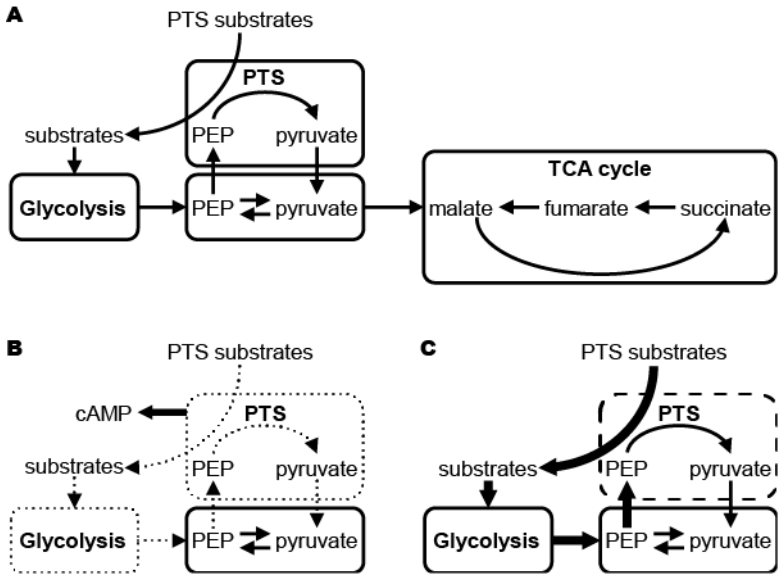

Figure 6-2 Proposed model for phosphotransferase system (PTS) substrates and metabolism during post-starvation growth on TSA (A), PCA (B) and pyruvate-supplemented PCA (C). Bold arrows represent increased conversion, dotted arrows indicate low conversion, dotted boxes represent processes with low activity, dashed boxes represent processes with increasing activity, and solid boxes represent processes with optimal activity.

increase in cAMP level (Figure 6-2B). Low substrate transport may result in slow or no colony growth. Pyruvate is transported through the proton symport and accumulates in cells grown on pyruvate-supplemented PCA (Figure 6-2C). Increased pyruvate level changes the PEP-to-pyruvate ratio and drives pyruvate conversion to PEP, which increases nutrient import and partially restores PTS function. This then creates a positive feedback loop through glycolysis, leading to further production of PEP.

For successful survival of *E. coli* O157:H7 with its dual lifestyle, we hypothesise that being able to respond to both high- and low-nutrient environments may also be advantageous for re-entry into a host. Upon ingestion by a mammalian host, the temperature will be optimal for *E. coli* growth. If high levels of nutrient are present as well, the cells exit the VBNC state and initiate growth. Where less transportable nutrients are readily available, then other signals may be required to prompt the cell to exit from the VBNC state. Since pyruvate is a component of mammalian saliva (Silwood *et al.*, 2002), it may be detected by *E. coli* O157:H7 as a signal of entry into a host and stimulate growth in the presence of lower levels of available nutrient.

Bacterial cell-to-cell signalling molecules such as AHLs are present in rumen fluid (B. S. Govan, personal communication, June 30, 2013). *E. coli* can detect some AHLs but cannot produce the signal molecule but since *E. coli* O157:H7 is likely to encounter AHLs during passage through the rumen, we hypothesised that these signalling molecules may be involved in starved cell resuscitation, growth or host colonisation. The presence of C12-HSL and 3-oxo-C6-HSL can alter cell motility of EPEC and *E. coli* O157:H7 (B. S. Govan, personal communication, June 30, 2013). Supplementation of PCA with C12-HSL and 3-oxo-C6-HSL, however, did not increase the number of colonies recovered from 4°C-starved NCTC12900, nor did it have any effect on colony size. Alternative quorum sensing systems exist, including Lux/AI-2, which may co-ordinate population response to starvation and recovery through quorum sensing or through the metabolic function of the proteins involved.

In *E. coli*, AI-2 precursor is synthesised by LuxS, an enzyme that plays an important role in *E. coli* central metabolism, the activated methyl cycle.

Interestingly, recovery of a mutant NCTC12900 strain lacking *luxS* on PCA after starvation at 4°C was significantly higher than that observed for the parent strain (Figure 5-2). This phenotype can be complemented by *luxS* expressed from a plasmid but not by supplementation of PCA with conditioned media containing AI-2. The inability to complement the phenotype observed for the *luxS* mutant with conditioned media suggested that the phenotype associated with the lack of *luxS* was the result of metabolic disruption rather than quorum sensing per se. In addition, density-dependent quorum sensing, such as LuxS/AI-2, requires the accumulation of quorum sensing signals, which is unlikely to occur in aqueous environments with limited carbon. LuxS is found in both Gram-negative and Gram-positive bacteria and AI-2 has been suggested to be the "universal language" for bacterial communication. Based on findings in this study, we proposed that conservation of *luxS* in bacteria may also be driven by the evolutionary pressure of conserving the non-growth phenotype associated with VBNC, a survival mechanism by which bacterial populations persist in adverse environments.

Once inside a host, bacteria are likely to encounter a wide range of nutrients depending on the host diet. The ability to metabolise a wide range of carbon sources would be advantageous for *E. coli* O157:H7 in preparation for colonisation of the colon. However, it is unclear whether growth during passage through the rumen is required for colonisation at the anal-rectal junction of bovine hosts. For the bovine *E. coli* O157:H7 strain used in this study, starvation had the least impact on the level of substrate use and the number of substrates metabolised compared to the clinical *E. coli* O157:H7 strains. This may be indicative of the existence of different selective pressures in bovine rumen and mono-gastric human gut. Findings from this study suggested that the difference in metabolic profiles may reflect the different adaptation required for *E. coli* O157:H7 to establish infections in bovine and human hosts.

Carbon source analysis can be used to profile differences in metabolic phenotype and similarities in substrate utilisation between *E. coli* O157:H7 strains. Analysis of utilisation kinetics in addition to endpoint level of substrate use allowed us to postulate the underlying mechanism for the metabolic profiles observed. For example, of the pentose sugars tested, λ for D-ribose and D-xylose were found to

be consistently longer for starved cells compared to exponential or stationary phase cells. Assuming μ_{exp} reflects the rate of metabolism and λ indicates the time required for the synthesis of substrate importers and/or catabolic enzymes, we hypothesised that the proton symporter for D-ribose and D-xylose, NupC, was likely to be absent in starved cells. Using the same principle and assumptions, we postulated that the higher λ observed for thymidine and uridine utilisation for starved cells was likely to be the result of the absence of catabolic enzymes.

The carbon source profiling analysis developed in this study contributed to the identification of substrates that can be used to differentiate *E. coli* O157:H7 from a close relative, *E. fergusonii*, by culture. A number of *E. fergusonii* isolates were initially identified as *E. coli* O157:H7 in a recent calf study, due to surface antigen cross-reacting with the IMS beads used for *E. coli* O157:H7 isolation from environmental samples (H. L. Withers, personal communication, June 12, 2012). One of the strains, H11+, was included in this study and was subsequently identified as being *E. fergusonii*. Comparison of carbon utilisation profiles for H11- and H11+ identified that sucrose was one of the substrates utilised by H11- but not H11+. Metabolic profiling of additional bovine *E. coli* O157:H7 and *E. fergusonii* strains showed that sucrose was used by all *E. coli* O157:H7 tested but not *E. fergusonii* (T. Gupta, personal communication, May 30, 2013). Using this knowledge, a new culturing media, MacConkey agar supplemented with 1% sucrose, was developed for culture-based differentiation of *E. coli* O157:H7 and *E. fergusonii* in environmental samples.

Using current knowledge, we propose a model to describe adaptive differences between starved clinical and bovine *E. coli* O157:H7 based on the likely difference in conditions encountered prior to and after ingestion by ruminant and human hosts (Figure 6-3). *E. coli* O157:H7 can survive starvation and sub-optimal growth temperatures, and enter into the VBNC state. Once ingested by a bovine or human host, starved cells encounter pyruvate present in saliva which causes the cell to exit from the VBNC state. In the bovine rumen, cells will encounter a wide range of carbon sources as well as volatile fatty acids, products of fermentation, which can cause acid shock and cell death (Callaway *et al.*, 2009). While AHLs are likely to be present in the ruminant gut, it is not clear whether they have any direct contribution to *E. coli* O157:H7 resuscitation during passage through the

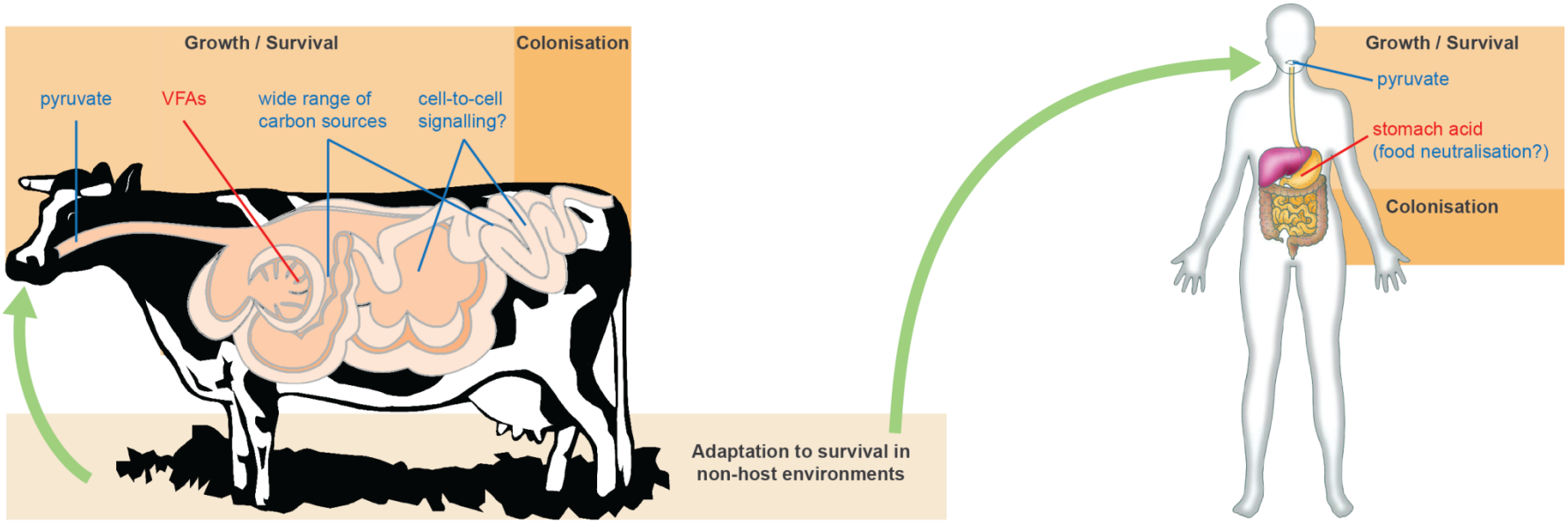

Figure 6-3 Proposed model representing the possible factors encountered by *E. coli* O157:H7 prior to host ingestion, and during passage through bovine and human gastrointestinal tracts. Factors likely to enhance bacterial colonisation are in blue and factors likely to prevent colonisation are in red. Green arrows indicate ingestion of bacteria. VFAs, volatile fatty acids.

ruminant gut or colonisation. In human stomach, *E. coli* O157:H7 is likely to encounter low pH which may result in acid shock and cell death. However, stomach acid may be neutralised by food in the stomach (Russell & Jarvis, 2001). Cells, potentially resuscitated by pyruvate in saliva, that have survived passage through the stomach may then go onto colonise the human colon.

Controversies surrounding VBNC largely rest upon the difficulty in deciphering the physiological state of individual cells within a population (Oliver, 2010). Future work aimed at dissecting the sub-populations using flow cytometry may address the current "missing link" between population dynamics and individual cell physiology. Nevertheless, bacteria populations in their natural niche are likely to be heterogeneous, and it is this heterogeneity that is key to the survival and success of the species in response to fluctuating environmental conditions. While it is important to understand the physiology of individual cells, the implication of the existence of VBNC cells within a heterogeneous population that can persist should not be underestimated. VBNC *E. coli* O157:H7 has particularly important implications for food safety (Dinu *et al.*, 2009).

Persistence of *E. coli* O157:H7 in agricultural environments not only acts as a source for food contamination, it also increases the risk of human exposure in the rural setting and may account for the sporadic clinical cases in New Zealand. Another concern is the presence of or the increased transition of cells into VBNC during food processing, and the likelihood of these non-growing cells being less susceptible to antimicrobial treatments that require cell growth to be effective. Lowered susceptibility to mitigation treatments increases the risk of food processing environments becoming reservoir for food contamination. Using information gathered in this study, it may be possible to promote the exit of stressed cells from the VBNC state using pyruvate or other stimuli prior to application of mitigation strategies during food processing or as part of the mitigation strategy in an agricultural setting. Stimulation of metabolic activity of otherwise unculturable cells may improve the efficacy of exiting mitigation strategies for the control of persistent *E. coli* O157:H7 by increasing their susceptibility to antimicrobial compounds. Expansion of this study to include more bovine and clinical isolates will further enhance our understanding of

starved cell metabolism with the possibility of identifying substrates with similar function as pyruvate or other stimuli that can be used in pathogen control.

Chapter 7 Conclusion

A key finding of this study was the observation of the importance of metabolic heterogeneity within the cell population prior to starvation, on the proportion of sub-populations able to recover during starvation. The phenotypic determinants used in this study identified the appearance of three sub-populations following starvation: (i) viable cells incapable of initiating growth on either tryptic soy agar (TSA) or plate count agar (PCA), (ii) cells requiring rich media, in this case TSA, for growth, (iii) and cells capable of growth on the relatively nutrient limited PCA. In addition, the change in colony size and size distribution observed during the course of starvation showed that even within a sub-population there was variation in cell physiology

In the late-exponential starting culture used in this study, it is likely that the population was heterogeneous with a spectrum of cells with different physiological and metabolic competency. Heterogeneity was not phenotypically manifested prior to starvation, as there was not a significant difference between viability and culturability on TSA or PCA, however as the cells aged during starvation, particularly at 4°C, the discrepancy between the number of viable cells and cells recovered on TSA or PCA became apparent. While the use of different media and the measurement of colony size confirmed population heterogeneity and the existence of sub-populations within a starved culture, these methods could not identify the continuum of cell populations and the subsequent population shifts that occurred within the continuum during starvation. A combination of stains and/or other fluorescent markers and flow cytometry may be useful for the detection of population change during starved cell recovery.

The detection of sub-populations within a starved culture with varying abilities to respond to environment signals, such as nutrient availability, highlighted the limitation of culture-based detection methods for *E. coli* O157:H7 in food and natural environments. This study examined the potential discrepancy between the number of viable cells detected based on culture-independent methods compared to culture on nutrient-rich and nutrient-poor media based on the hypothesis that prolonged starvation induces the “viable but non-culturable” (VBNC) state in *E. coli* O157:H7. Regardless of the starvation temperature, culture-based

enumeration underestimated the number of viable cells compared to culture-independent detection based on membrane integrity. This implies that current culture-based methods underestimate the number of viable *E. coli* O157:H7 cells in food, particularly minimally processed foods such as ready-to-eat salads that are usually stored at refrigeration temperature. In addition, water in puddles and water troughs, which are part of the agricultural environment, may act as reservoirs for VBNC *E. coli* O157:H7 for contamination onto animal hides that would not be detectable by routine culture-based monitoring programmes. Therefore, improved resuscitation of VBNC cells should be part of a culture-based detection method.

Within a heterogeneous starved cell population, the VBNC sub-population consists of cells that are metabolically incapable of responding to the nutrients present in conventional culture media. The literature documented resuscitation of VBNC cells by supplementing conventional culture media with sodium pyruvate, however, pyruvate supplementation was only found to increase recovery on the nutrient-poor PCA and not on the nutrient-rich TSA. This suggested pyruvate, as well as being a potential energy and carbon source, might act as a metabolic regulator that increased nutrient metabolism in cells that would otherwise not respond to available nutrients in PCA. Therefore, supplementation of PCA, a media routinely used as a non-selective medium for the enumeration of microorganisms in water and food, with sodium pyruvate could be used to improve recovery of VBNC cells.

This study combined experimental findings with information in the literature to propose a model depicting pyruvate's role as a regulator of the phosphotransferase system and the phosphoenolpyruvate-pyruvate-oxaloacetate node. To our knowledge, this is the first model proposed to explain the role of pyruvate in resuscitation of VBNC cells. In order to test the hypotheses posed in the model, the VBNC sub-population of cells within the starved culture will need to be isolated and analysed independently. To date, the successful isolation of VBNC subpopulations, however, has not been documented. Cell sorting by flow cytometry or differential centrifugation may be used to isolate sub-populations when specific VBNC markers are identified. Once the VBNC sub-population is

isolated, utilisation of ^{13}C-labeled pyruvate in flux analyses can be used to define the role of pyruvate in VBNC cell metabolism.

Understanding the underlying physiology of the phenotypic behaviour of single cells, sub-populations and complex heterogeneous populations is important for the development of food safety monitoring regimes and can contribute to the development of targeted mitigation strategies. This study showed that New Zealand *E. coli* O157:H7 strains, both bovine and clinical, can enter the VBNC state during starvation at temperatures found in the New Zealand environment. Identification of specific genetic markers for VBNC will be required before the existence of these cells can be confirmed in environmental samples. Findings from this study confirmed at least partial resuscitation of VBNC cell by supplementing growth media with sodium pyruvate. Additional work is required to fully understand the mechanism by which such resuscitation occurs and to develop methods that can resuscitate the entire VBNC sub-population and eliminate the potential for underestimation of viable *E. coli* O157:H7 in the environment and more importantly in the food that we eat.

Chapter 8 References

Albertini, M. C., Accorsi, A., Teodori, L., et al. (2006). Use of multiparameter analysis for *Vibrio alginolyticus* viable but nonculturable state determination. *Cytometry Part A, 69*(4), 260-265.

Amit-Romach, E., Sklan, D., & Uni, Z. (2004). Microflora ecology of the chicken intestine using 16S ribosomal DNA primers. *Poultry Science, 83*(7), 1093-1098.

Angerer, A., Enz, S., Ochs, M., et al. (1995). Transcriptional regulation of ferric citrate transport in *Escherichia coli* K-12. Fecl belongs to a new subfamily of σ70-type factors that respond to extracytoplasmic stimuli. *Molecular Microbiology, 18*(1), 163-174.

Antonova, E. S., & Hammer, B. K. (2011). Quorum-sensing autoinducer molecules produced by members of a multispecies biofilm promote horizontal gene transfer to *Vibrio cholerae*. *FEMS Microbiology Letters, 322*(1), 68-76.

Armbruster, C. E., Hong, W., Pang, B., et al. (2009). LuxS promotes biofilm maturation and persistence of nontypeable *Haemophilus influenzae* in vivo via modulation of lipooligosaccharides on the bacterial surface. *Infection and Immunity, 77*(9), 4081-4091.

Armbruster, C. E., Pang, B., Murrah, K., et al. (2011). RbsB (NTHI-0632) mediates quorum signal uptake in nontypeable *Haemophilus influenzae* strain 86-028NP. *Molecular Microbiology, 82*(4), 836-850.

Arthur, T. M., Nou, X., Kalchayanand, N., et al. (2011). Survival of *Escherichia coli* O157:H7 on cattle hides. *Applied and Environmental Microbiology, 77*(9), 3002-3008.

Arumugam, M., Raes, J., Pelletier, E., et al. (2011). Enterotypes of the human gut microbiome. *Nature, 473*(7346), 174-180.

Asakura, H., Igimi, S., Kawamoto, K., et al. (2005). Role of in vivo passage on the environmental adaptation of enterohemorrhagic *Escherichia coli* O157:H7: Cross-induction of the viable but nonculturable state by osmotic and oxidative stresses. *FEMS Microbiology Letters, 253*(2), 243-249.

Atkinson, S., & Williams, P. (2009). Quorum sensing and social networking in the microbial world. *Journal of the Royal Society Interface, 6*(40), 959-978.

Atlas, R. M. (1995). *Handbook of microbiological media for the examination of food*. Roca Raton: CRC Press.

Aurass, P., Prager, R., & Flieger, A. (2011). EHEC/EAEC O104:H4 strain linked with the 2011 German outbreak of haemolytic uremic syndrome enters into the viable but non-culturable state in response to various stresses and resuscitates upon stress relief. *Environmental Microbiology*.

Avery, L. M., Killham, K., & Jones, D. L. (2005). Survival of *E. coli* O157:H7 in organic wastes destined for land application. *Journal of Applied Microbiology, 98*(4), 814-822.

Avery, S. V. (2006). Microbial cell individuality and the underlying sources of heterogeneity. *Nature Reviews Microbiology, 4*(8), 577-587.

Baffone, W., Casaroli, A., Citterio, B., et al. (2006). *Campylobacter jejuni* loss of culturability in aqueous microcosms and ability to resuscitate in a mouse model. *International Journal of Food Microbiology, 107*(1), 83-91.

Baffone, W., Citterio, B., Vittoria, E., et al. (2003). Retention of virulence in viable but non-culturable halophilic *Vibrio* spp. *International Journal of Food Microbiology, 89*(1), 31-39.

Balaban, N. Q., Merrin, J., Chait, R., et al. (2004). Bacterial persistence as a phenotypic switch. *Science, 305*(5690), 1622-1625.

Bansal, T., Jesudhasan, P., Pillai, S., et al. (2008). Temporal regulation of enterohemorrhagic *Escherichia coli* virulence mediated by autoinducer-2. *Applied Microbiology and Biotechnology, 78*(5), 811-819.

Barcina, I., & Arana, I. (2009). The viable but nonculturable phenotype: A crossroads in the life-cycle of non-differentiating bacteria? *Reviews in Environmental Science and Biotechnology, 8*(3), 245-255.

Barer, M. R. (1997). Viable but non-culturable and dormant bacteria: time to resolve an oxymoron and a misnomer? *Journal of Medical Microbiology, 46*(8), 629-631.

Bassler, B. L. (1999). How bacteria talk to each other: Regulation of gene expression by quorum sensing. *Current Opinion in Microbiology, 2*(6), 582-587.

Bassler, B. L., Greenberg, E. P., & Stevens, A. M. (1997). Cross-species induction of luminescence in the quorum-sensing bacterium *Vibrio harveyi*. *Journal of Bacteriology, 179*(12), 4043-4045.

Bassler, B. L., & Losick, R. (2006). Bacterially Speaking. *Cell, 125*(2), 237-246.

Bassler, B. L., Wright, M., & Silverman, M. R. (1994). Multiple signalling systems controlling expression of luminescence in *Vibrio harveyi*: sequence and function of genes encoding a second sensory pathway. *Molecular Microbiology, 13*(2), 273-286.

Bates, T. C., & Oliver, J. D. (2004). The viable but nonculturable state of Kanagawa positive and negative strains of *Vibrio parahaemolyticus*. *Journal of Microbiology, 42*(2), 74-79.

Battesti, A., & Bouveret, E. (2006). Acyl carrier protein/SpoT interaction, the switch linking SpoT-dependent stress response to fatty acid metabolism. *Molecular Microbiology, 62*(4), 1048-1063.

Battesti, A., Majdalani, N., & Gottesman, S. (2011). The RpoS-mediated general stress response in *Escherichia coli*. *Annual Review of Microbiology, 65*, 189-213.

Benjamin, M. M., & Datta, A. R. (1995). Acid tolerance of enterohemorrhagic *Escherichia coli*. *Applied and Environmental Microbiology, 61*(4), 1669-1672.

Berlin, D. L., Herson, D. S., Hicks, D. T., et al. (1999). Response of pathogenic *Vibrio* species to high hydrostatic pressure. *Applied and Environmental Microbiology, 65*(6), 2776-2780.

Best, A., La Ragione, R. M., Sayers, A. R., et al. (2005). Role for flagella but not intimin in the persistent infection of the gastrointestinal tissues of specific-pathogen-free chicks by Shiga toxin-negative *Escherichia coli* O157:H7. *Infection and Immunity, 73*(3), 1836-1846.

Beumer, R. R., De Vries, J., & Rombouts, F. M. (1992). *Campylobacter jejuni* non-culturable coccoid cells. *International Journal of Food Microbiology, 15*(1-2), 153-163.

Bezuidt, O., Pierneef, R., Mncube, K., et al. (2011). Mainstreams of horizontal gene exchange in enterobacteria: Consideration of the outbreak of enterohemorrhagic *E. coli* O104:H4 in Germany in 2011. *PLoS ONE, 6*(10).

Bjergbæk, L. A., & Roslev, P. (2005). Formation of nonculturable *Escherichia coli* in drinking water. *Journal of Applied Microbiology, 99*(5), 1090-1098.

Boaretti, M., Lleò, M. D. M., Bonato, B., et al. (2003). Involvement of rpoS in the survival of *Escherichia coli* in the viable but non-culturable state. *Environmental Microbiology, 5*(10), 986-996.

Boerlin, P., McEwen, S. A., Boerlin-Petzold, F., et al. (1999). Associations between virulence factors of Shiga toxin-producing *Escherichia coli* and disease in humans. *Journal of Clinical Microbiology, 37*(3), 497-503.

Bogosian, G., & Bourneuf, E. V. (2001). A matter of bacterial life and death. *EMBO Reports, 2*(9), 770-774.

Bougdour, A., Cunning, C., Baptiste, P. J., et al. (2008). Multiple pathways for regulation of σ^S (RpoS) stability in *Escherichia coli* via the action of multiple anti-adaptors. *Molecular Microbiology, 68*(2), 298-313.

Bougdour, A., & Gottesman, S. (2007). ppGpp regulation of RpoS degradation via anti-adaptor protein IraP. *Proceedings of the National Academy of Sciences of the United States of America, 104*(31), 12896-12901.

Boutte, C. C., & Crosson, S. (2013). Bacterial lifestyle shapes stringent response activation. *Trends in Microbiology, 21*(4), 174-180.

Boyer, M., & Wisniewski-Dyé, F. (2009). Cell-cell signalling in bacteria: Not simply a matter of quorum. *FEMS Microbiology Ecology, 70*(1), 1-19.

Breed, R. S., & Dotterrer, W. D. (1916). The number of colonies allowable on satisfactory agar plates. *Journal of Bacteriology, 1*, 321-331.

Breeuwer, P., & Abee, T. (2000). Assessment of viability of microorganisms employing fluorescence techniques. *International Journal of Food Microbiology, 55*(1-3), 193-200.

Brzuszkiewicz, E., Thürmer, A., Schuldes, J., et al. (2011). Genome sequence analyses of two isolates from the recent *Escherichia coli* outbreak in Germany reveal the emergence of a new pathotype: Entero-Aggregative-Haemorrhagic *Escherichia coli* (EAHEC). *Archives of Microbiology, 193*(12), 883-891.

Buerger, S., Spoering, A., Gavrish, E., et al. (2012). Microbial scout hypothesis, stochastic exit from dormancy, and the nature of slow growers. *Applied and Environmental Microbiology, 78*(9), 3221-3228.

Callaway, T. R., Carr, M. A., Edrington, T. S., et al. (2009). Diet, *Escherichia coli* O157:H7, and cattle: A review after 10 years. *Current Issues in Molecular Biology, 11*(2), 67-80.

Campellone, K. G. (2010). Cytoskeleton-modulating effectors of enteropathogenic and enterohaemorrhagic *Escherichia coli*: Tir, EspFU and actin pedestal assembly. *FEBS Journal, 277*(11), 2390-2402.

Cappelier, J. M., Besnard, V., Roche, S., et al. (2005). Avirulence of viable but non-cultureable *Listeria monocytogenes* cells demonstrated by in vitro and in vivo models. *Veterinary Research, 36*(4), 589-599.

Cappelier, J. M., Besnard, V., Roche, S. M., et al. (2007). Avirulent viable but non culturable cells of *Listeria monocytogenes* need the presence of an embryo to be recovered in egg yolk and regain virulence after recovery. *Veterinary Research, 38*(4), 573-583.

Cappelier, J. M., Minet, J., Magras, C., et al. (1999). Recovery in embryonated eggs of viable but nonculturable *Campylobacter jejuni* cells and maintenance of ability to adhere to HeLa cells after resuscitation. *Applied and Environmental Microbiology, 65*(11), 5154-5157.

Caspi, R., Altman, T., Billington, R., et al. (2014). The MetaCyc database of metabolic pathways and enzymes and the BioCyc collection of Pathway/Genome Databases. *Nucleic Acids Research, 42*(D1), D459-D471.

Castanie-Cornet, M. P., Penfound, T. A., Smith, D., et al. (1999). Control of acid resistance in *Escherichia coli*. *Journal of Bacteriology, 181*(11), 3525-3535.

Castaño-Cerezo, S., Bernal, V., Blanco-Catalá, J., et al. (2011). cAMP-CRP co-ordinates the expression of the protein acetylation pathway with central metabolism in *Escherichia coli*. *Molecular Microbiology, 82*(5), 1110-1128.

Cellini, L., Di Campli, E., Grande, R., et al. (2005). Detection of *Helicobacter pylori* associated with zooplankton. *Aquatic Microbial Ecology, 40*(2), 115-120.

Centers for Disease Control. (1982). Isolation of *E. coli* O157:H7 from sporadic cases of hemorrhagic colitis - United States. *MMWR. Morbidity and mortality weekly report, 31*(43).

Chaisowwong, W., Kusumoto, A., Hashimoto, M., et al. (2012). Physiological characterization of *Campylobacter jejuni* under cold stresses conditions: Its potential for public threat. *Journal of Veterinary Medical Science, 74*(1), 43-50.

Chaiyanan, S., Huq, A., Maugel, T., et al. (2001). Viability of the nonculturable *Vibrio cholerae* O1 and O139. *Systematic and Applied Microbiology, 24*(3), 331-341.

Chang, D. E., Smalley, D. J., & Conway, T. (2002). Gene expression profiling of *Escherichia coli* growth transitions: An expanded stringent response model. *Molecular Microbiology, 45*(2), 289-306.

Chase-Topping, M., Gally, D., Low, C., et al. (2008). Super-shedding and the link between human infection and livestock carriage of *Escherichia coli* O157. *Nature Reviews Microbiology, 6*(12), 904-912.

Chaveerach, P., Ter Huurne, A. A. H. M., Lipman, L. J. A., et al. (2003). Survival and resuscitation of ten strains of Campylobacter jejuni and Campylobacter coli under acid conditions. *Applied and Environmental Microbiology, 69*(1), 711-714.

Chen, S. Y., Jane, W. N., Chen, Y. S., et al. (2009). Morphological changes of *Vibrio parahaemolyticus* under cold and starvation stresses. *International Journal of Food Microbiology, 129*(2), 157-165.

Chen, X., Schauder, S., Potier, N., et al. (2002). Structural identification of a bacterial quorum-sensing signal containing boron. *Nature, 415*(6871), 545-549.

Cheville, A. M., Arnold, K. W., Buchrieser, C., et al. (1996). rpoS regulation of acid, heat, and salt tolerance in *Escherichia coli* O157:H7. *Applied and Environmental Microbiology, 62*(5), 1822-1824.

Chiang, P. K., Gordon, R. K., Tal, J., et al. (1996). *S*-Adenosylmethionine and methylation. *FASEB Journal, 10*(4), 471-480.

Choi, J., Shin, D., Kim, M., et al. (2012). LsrR-mediated quorum sensing controls invasiveness of *Salmonella typhimurium* by regulating SPI-1 and flagella genes. *PLoS ONE, 7*(5).

Choi, J., Shin, D., & Ryu, S. (2007). Implication of quorum sensing in *Salmonella enterica* serovar typhimurium virulence: The *luxS* gene is necessary for expression of genes in pathogenicity island 1. *Infection and Immunity, 75*(10), 4885-4890.

Cluzel, M. E., Zanella-Cléon, I., Cozzone, A. J., et al. (2010). The *Staphylococcus aureus* autoinducer-2 synthase LuxS is regulated by Ser/Thr phosphorylation. *Journal of Bacteriology, 192*(23), 6295-6301.

Colwell, R. R., Brayton, P. R., Grimes, D. J., et al. (1985). Viable but non-culturable *Vibrio cholerae* and related pathogens in the environment: implications for release of genetically engineered microorganisms. *Nature Biotechnology, 3*(9), 817-820.

Control, C. f. D. (2009). Outbreak of Shiga toxin-producing *Escherichia coli* O157 infection associated with a day camp petting zoo - Pinellas County, Florida, May-June 2007. *Morbidity and Mortality Weekly Report, 58*(16), 426-428.

Coulthurst, S. J., Kurz, C. L., & Salmond, G. P. C. (2004). *luxS* mutants of *Serratia* defective in autoinducer-2-dependent 'quorum sensing' show strain-dependent impacts on virulence and production of carbapenem and prodigiosin. *Microbiology, 150*(6), 1901-1910.

Crosa, J. H. (1995). Transcription of the region encoding the ferric dicitrate-transport system in *Escherichia coli*: Similarity between promoters for *fecA* and for extracytoplasmic function sigma factors. *Gene, 163*(1), 13-18.

Day, A. P., & Oliver, J. D. (2004). Changes in membrane fatty acid composition during entry of *Vibrio vulnificus* into the viable but nonculturable state. *Journal of Microbiology, 42*(2), 69-73.

DeLisa, M. P., Valdes, J. J., & Bentley, W. E. (2001a). Mapping stress-induced changes in autoinducer AI-2 production in chemostat-cultivated *Escherichia coli* K-12. *Journal of Bacteriology, 183*(9), 2918-2928.

DeLisa, M. P., Valdes, J. J., & Bentley, W. E. (2001b). Quorum signaling via Al-2 communicates the "metabolic burden" associated with heterologous protein production in *Escherichia coli*. *Biotechnology and Bioengineering, 75*(4), 439-450.

DeLisa, M. P., Wu, C. F., Wang, L., et al. (2001c). DNA microarray-based identification of genes controlled by autoinducer 2-stimulated quorum sensing in *Escherichia coli*. *Journal of Bacteriology, 183*(18), 5239-5247.

Deutscher, J., Francke, C., & Postma, P. W. (2006). How phosphotransferase system-related protein phosphorylation regulates carbohydrate metabolism in bacteria. *Microbiology and Molecular Biology Reviews, 70*(4), 939-1031.

Dills, S. S., Apperson, A., Schmidt, M. R., et al. (1980). Carbohydrate transport in bacteria. *Microbiological Reviews, 44*(3), 385-418.

Dinu, L. D., Delaquis, P., & Bach, S. (2009). Nonculturable response of animal enteropathogens in the agricultural environment and implications for food safety. *Journal of Food Protection, 72*(6), 1342-1354.

Doherty, N., Holden, M. T. G., Qazi, S. N., et al. (2006). Functional analysis of *luxS* in *Staphylococcus aureus* reveals a role in metabolism but not quorum sensing. *Journal of Bacteriology, 188*(8), 2885-2897.

Dong, T., & Schellhorn, H. E. (2009a). Control of RpoS in global gene expression of *Escherichia coli* in minimal media. *Molecular Genetics and Genomics, 281*(1), 19-33.

Dong, T., & Schellhorn, H. E. (2009b). Global effect of RpoS on gene expression in pathogenic *Escherichia coli* O157:H7 strain EDL933. *BMC Genomics, 10*.

Du, M., Chen, J., Zhang, X., et al. (2007a). Characterization and resuscitation of viable but nonculturable *Vibrio alginolyticus* VIB283. *Archives of Microbiology, 188*(3), 283-288.

Du, M., Chen, J., Zhang, X., et al. (2007b). Retention of virulence in a viable but nonculturable *Edwardsiella tarda* isolate. *Applied and Environmental Microbiology, 73*(4), 1349-1354.

Dusserre, E., Ginevra, C., Hallier-Soulier, S., et al. (2008). A PCR-based method for monitoring *Legionella pneumophila* in water samples detects viable but noncultivable legionellae that can recover their cultivability. *Applied and Environmental Microbiology, 74*(15), 4817-4824.

Dwidjosiswojo, Z., Richard, J., Moritz, M. M., et al. (2011). Influence of copper ions on the viability and cytotoxicity of *Pseudomonas aeruginosa* under conditions relevant to drinking water environments. *International Journal of Hygiene and Environmental Health, 214*(6), 485-492.

Dyszel, J. L., Soares, J. A., Swearingen, M. C., et al. (2010). *E. coli* K-12 and EHEC genes regulated by SdiA. *PLoS ONE, 5*(1), 1-15.

Eberl, L. (1999). N-acyl homoserinelactone-mediated gene regulation in Gram-negative bacteria. *Systematic and Applied Microbiology, 22*(4), 493-506.

Egland, K. A., & Greenberg, E. P. (2000). Conversion of the *Vibrio fischeri* transcriptional activator, LuxR, to a repressor. *Journal of Bacteriology, 182*(3), 805-811.

Engebrecht, J. A., & Silverman, M. (1984). Identification of genes and gene products necessary for bacterial bioluminescence. *Proceedings of the National Academy of Sciences of the United States of America, 81*(13 I), 4154-4158.

Ensign, J. C. (1970). Long-term starvation survival of rod and spherical cells of *Arthrobacter crystallopoietes*. *Journal of Bacteriology, 103*(3), 569-577.

Erickson, M. C., & Doyle, M. P. (2007). Food as a vehicle for transmission of Shiga toxin-producing *Escherichia coli*. *Journal of Food Protection, 70*(10), 2426-2449.

Escalante, A., Salinas Cervantes, A., Gosset, G., et al. (2012). Current knowledge of the *Escherichia coli* phosphoenolpyruvate-carbohydrate phosphotransferase system: peculiarities of regulation and impact on growth and product formation. *Applied microbiology and biotechnology, 94*(6), 1483-1494.

Etcheverría, A. I., & Padola, N. L. (2013). Shiga toxin-producing *Escherichia coli*: Factors involved in virulence and cattle colonization. *Virulence, 4*(5), 12-11.

Ethelberg, S., Olsen, K. E. P., Scheutz, F., et al. (2004). Virulence factors for hemolytic uremic syndrome, Denmark. *Emerging Infectious Diseases, 10*(5), 842-847.

Farfan, M. J., & Torres, A. G. (2012). Molecular mechanisms that mediate colonization of shiga toxin-producing *Escherichia coli* strains. *Infection and Immunity, 80*(3), 903-913.

Ferenci, T. (2001). Hungry bacteria - Definition and properties of a nutritional state. *Environmental Microbiology, 3*(10), 605-611.

Ferguson, D. D., Scheftel, J., Cronquist, A., et al. (2005). Temporally distinct *Escherichia coli* O157 outbreaks associated with alfalfa sprouts linked to a common seed source - Colorado and Minnesota, 2003. *Epidemiology and Infection, 133*(3), 439-447.

Fong, K. P., Chung, W. O., Lamont, R. J., et al. (2001). Intra- and interspecies regulation of gene expression by *Actinobacillus actinomycetemcomitans* LuxS. *Infection and Immunity, 69*(12), 7625-7634.

Fong, K. P., Gao, L., & Demuth, D. R. (2003). *luxS* and *arcB* control aerobic growth of *Actinobacillus actinomycetemcomitans* under iron limitation. *Infection and Immunity, 71*(1), 298-308.

Fontecave, M., Atta, M., & Mulliez, E. (2004). *S*-adenosylmethionine: Nothing goes to waste. *Trends in Biochemical Sciences, 29*(5), 243-249.

Foster, J. W. (2004). *Escherichia coli* acid resistance: Tales of an amateur acidophile. *Nature Reviews Microbiology, 2*(11), 898-907.

Frank, C., Werber, D., Cramer, J. P., et al. (2011). Epidemic profile of Shiga-toxin-producing *Escherichia coli* O104:H4 outbreak in Germany. *New England Journal of Medicine, 365*(19), 1771-1780.

Fuller, C. A., Pellino, C. A., Flagler, M. J., et al. (2011). Shiga toxin subtypes display dramatic differences in potency. *Infection and Immunity, 79*(3), 1329-1337.

Fuqua, W. C., Winans, S. C., & Greenberg, E. P. (1994). Quorum sensing in bacteria: The LuxR-LuxI family of cell density- responsive transcriptional regulators. *Journal of Bacteriology, 176*(2), 269-275.

Gabor, E., Göhler, A. K., Kosfeld, A., et al. (2011). The phospho*enol*pyruvate-dependent glucose-phosphotransferase system from *Escherichia coli* K-12 as the center of a network regulating carbohydrate flux in the cell. *European Journal of Cell Biology, 90*(9), 711-720.

Gangaiah, D., Kassem, I. I., Liu, Z., et al. (2009). Importance of polyphosphate kinase 1 for *Campylobacter jejuni* viable-but-nonculturable cell formation, natural transformation, and antimicrobial resistance. *Applied and Environmental Microbiology, 75*(24), 7838-7849.

Gordon, D. M., & Cowling, A. (2003). The distribution and genetic structure of *Escherichia coli* in Australian vertebrates: Host and geographic effects. *Microbiology, 149*(12), 3575-3586.

Görke, B., & Stülke, J. (2008). Carbon catabolite repression in bacteria: Many ways to make the most out of nutrients. *Nature Reviews Microbiology, 6*(8), 613-624.

Gormley, F. J., Little, C. L., Rawal, N., et al. (2011). A 17-year review of foodborne outbreaks: describing the continuing decline in England and Wales (1992-2008). *Epidemiology and Infection, 139*(5), 688-699.

Greenberg, E. P., Hastings, J. W., & Ulitzur, S. (1979). Induction of luciferase synthesis in *Beneckea harvey* by other marine bacteria. *Archives of Microbiology, 120*(2), 87-91.

Griffin, P. M., & Tauxe, R. V. (1991). The epidemiology of infections caused by *Escherichia coli* O157:H7, other enterohemorrhagic *E. coli*, and the associated hemolytic uremic syndrome. *Epidemiologic Reviews, 13*, 60-98.

Grimes, D. J., & Colwell, R. R. (1986). Viability and virulence of *Escherichia coli* suspended by membrane chamber in semitropical ocean water. *FEMS Microbiology Letters, 34*(2), 161-165.

Gruzdev, N., Pinto, R., & Sela Saldinger, S. (2012). Persistence of *Salmonella enterica* during dehydration and subsequent cold storage. *Food Microbiology, 32*(2), 415-422.

Guarner, F., & Malagelada, J. R. (2003). Gut flora in health and disease. *Lancet, 361*(9356), 512-519.

Gummesson, B., Magnusson, L. U., Lovmar, M., et al. (2009). Increased RNA polymerase availability directs resources towards growth at the expense of maintenance. *EMBO Journal, 28*(15), 2209-2219.

Gupte, A. R., De Rezende, C. L. E., & Joseph, S. W. (2003). Induction and resuscitation of viable but nonculturable *Salmonella enterica* serovar Typhimurium DT104. *Applied and Environmental Microbiology, 69*(11), 6669-6675.

Hanzelka, B. L., & Greenberg, E. P. (1996). Quorum sensing in *Vibrio fischeri*: Evidence that S-adenosylmethionine is the amino acid substrate for autoinducer synthesis. *Journal of Bacteriology, 178*(17), 5291-5294.

Hanzelka, B. L., Stevens, A. M., Parsek, M. R., et al. (1997). Mutational analysis of the *Vibrio fischeri* LuxI polypeptide: Critical regions of an autoinducer synthase. *Journal of Bacteriology, 179*(15), 4882-4887.

Hegde, M., Englert, D. L., Schrock, S., et al. (2011). Chemotaxis to the quorum-sensing signal AI-2 requires the Tsr chemoreceptor and the periplasmic LsrB AI-2-binding protein. *Journal of Bacteriology*, *193*(3), 768-773.

Heim, S., Lleo, M. D. M., Bonato, B., et al. (2002). The viable but nonculturable state and starvation are different stress responses of *Enterococcus faecalis*, as determined by proteome analysis. *Journal of Bacteriology*, *184*(23), 6739-6745.

Helmann, J. D. (1991). Alternative sigma factors and the regulation of flagellar gene expression. *Molecular Microbiology*, *5*(12), 2875-2882.

Helmann, J. D., & Chamberlin, M. J. (1988). Structure and function of bacterial sigma factors. *Annual Review of Biochemistry, 57*, 839-872.

Hengge-Aronis, R. (1993). Survival of hunger and stress: The role of rpoS in early stationary phase gene regulation in *E. coli*. *Cell, 72*(2), 165-168.

Hengge-Aronis, R., Lange, R., Henneberg, N., et al. (1993). Osmotic regulation of *rpoS*-dependent genes in *Escherichia coli*. *Journal of Bacteriology, 175*(1), 259-265.

Hengge, R. (2009). Proteolysis of σ^S (RpoS) and the general stress response in *Escherichia coli*. *Research in Microbiology, 160*(9), 667-676.

Heurlier, K., Vendeville, A., Halliday, N., et al. (2009). Growth deficiencies of *Neisseria meningitidis pfs* and *luxS* mutants are not due to inactivation of quorum sensing. *Journal of Bacteriology, 191*(4), 1293-1302.

Höller, C., Witthuhn, D., & Janzen-Blunck, B. (1998). Effect of low temperatures on growth, structure, and metabolism of *Campylobacter coli* SP10. *Applied and Environmental Microbiology, 64*(2), 581-587.

Holms, H. (1996). Flux analysis and control of the central metabolic pathways in *Escherichia coli*. *FEMS Microbiology Reviews, 19*(2), 85-116.

Holms, H. (2001). Flux analysis: A basic tool of microbial physiology. *Advances in Microbial Physiology, 45*, 271-340.

Hughes, D. T., Terekhova, D. A., Liou, L., et al. (2010). Chemical sensing in mammalian host-bacterial commensal associations. *Proceedings of the National Academy of Sciences of the United States of America, 107*(21), 9831-9836.

Ibekwe, A. M., Watt, P. M., Shouse, P. J., et al. (2004). Fate of *Escherichia coli* O157:H7 in irrigation water on soils and plants as validated by culture method and real-time PCR. *Canadian Journal of Microbiology, 50*(12), 1007-1014.

Ingledew, W. J., & Poole, R. K. (1984). The respiratory chains of *Escherichia coli*. *Microbiological Reviews, 48*(3), 222-271.

Institute of Environmental Science and Research Limited. (2004). Editorial: *E. coli* O157 and otherVTECin New Zealand. *New Zealand Public Health Surveillance Report, 2*(2).

James, C. E., Hasegawa, Y., Park, Y., et al. (2006a). LuxS involvement in the regulation of genes coding for hemin and iron acquisition systems in *Porphyromonas gingivalis*. *Infection and Immunity, 74*(7), 3834-3844.

James, D., Shao, H., Lamont, R. J., et al. (2006b). The *Actinobacillus actinomycetemcomitans* ribose binding protein RbsB interacts with cognate and heterologous autoinducer 2 signals. *Infection and Immunity, 74*(7), 4021-4029.

Jenkins, D. E., Chaisson, S. A., & Matin, A. (1990). Starvation-induced cross protection against osmotic challenge in *Escherichia coli*. *Journal of Bacteriology, 172*(5), 2779-2781.

Jensen, K. F. (1993). The *Escherichia coli* K-12 'wild types' W3110 and MG1655 have an *rph* frameshift mutation that leads to pyrimidine starvation due to low *pyrE* expression levels. *Journal of Bacteriology, 175*(11), 3401-3407.

Jolivet-Gougeon, A., Sauvager, F., Bonnaure-Mallet, M., et al. (2006). Virulence of viable but nonculturable *S.* Typhimurium LT2 after peracetic acid treatment. *International Journal of Food Microbiology, 112*(2), 147-152.

Jones, M. B., & Blaser, M. J. (2003). Detection of a *luxS*-signaling molecule in *Bacillus anthracis*. *Infection and Immunity, 71*(7), 3914-3919.

Jones, M. B., Peterson, S. N., Benn, R., et al. (2010). Role of *luxS* in *Bacillus anthracis* growth and virulence factor expression. *Virulence, 1*(2), 72-83.

Jones, S. A., Gibson, T., Maltby, R. C., et al. (2011). Anaerobic respiration of *Escherichia coli* in the mouse intestine. *Infection and Immunity, 79*(10), 4218-4226.

Kadirvel, M., Stimpson, W. T., Moumene-Afifi, S., et al. (2010). Synthesis and bioluminescence-inducing properties of autoinducer (S)-4,5-dihydroxypentane-2,3-dione and its enantiomer. *Bioorganic and Medicinal Chemistry Letters, 20*(8), 2625-2628.

Kahm, M., Hasenbrink, G., Lichtenberg-Fraté, H., et al. (2010). Grofit: Fitting biological growth curves with R. *Journal of Statistical Software, 33*(7), 1-21.

Kamaraju, K., Smith, J., Wang, J., et al. (2011). Effects on membrane lateral pressure suggest permeation mechanisms for bacterial quorum signaling molecules. *Biochemistry, 50*(32), 6983-6993.

Kanamaru, K., Kanamaru, K., Tatsuno, I., et al. (2000). SdiA, an *Escherichia coil* homologue of quorum-sensing regulators, controls the expression of virulence factors in enterohaemorrhagic Escherichia coli O157:H7. *Molecular Microbiology, 38*(4), 805-816.

Kandror, O., DeLeon, A., & Goldberg, A. L. (2002). Trehalose synthesis is induced upon exposure of *Escherichia coli* to cold and is essential for viability at low temperatures. *Proceedings of the National Academy of Sciences of the United States of America, 99*(15), 9727-9732.

Kanjee, U., Ogata, K., & Houry, W. A. (2012). Direct binding targets of the stringent response alarmone (p)ppGpp. *Molecular Microbiology, 85*(6), 1029-1043.

Kaper, J. B., Nataro, J. P., & Mobley, H. L. T. (2004). Pathogenic *Escherichia coli*. *Nature Reviews Microbiology, 2*(2), 123-140.

Karmali, M. A. (1989). Infection by verocytotoxin-producing *Escherichia coli*. *Clinical Microbiology Reviews, 2*(1), 15-38.

Karmali, M. A., Gannon, V., & Sargeant, J. M. (2010). Verocytotoxin-producing *Escherichia coli* (VTEC). *Veterinary Microbiology, 140*(3-4), 360-370.

Karmali, M. A., Steele, B. T., Petric, M., et al. (1983). Sporadic cases of haemolytic-uraemic syndrome associated with faecal cytotoxin and cytotoxin-producing *Escherichia coli* in stools. *Lancet, 1*(8325), 619-620.

Kawano, K., Okada, M., Haga, T., et al. (2008). Relationship between pathogenicity for humans and stx genotype in Shiga toxin-producing *Escherichia coli* serotype O157. *European Journal of Clinical Microbiology and Infectious Diseases, 27*(3), 227-232.

Kelly, D., King, T., & Aminov, R. (2007). Importance of microbial colonization of the gut in early life to the development of immunity. *Mutation Research*

- *Fundamental and Molecular Mechanisms of Mutagenesis, 622*(1-2), 58-69.

Kenny, B., DeVinney, R., Stein, M., et al. (1997). Enteropathogenic *E. coli* (EPEC) transfers its receptor for intimate adherence into mammalian cells. *Cell, 91*(4), 511-520.

Kim, S. Y., Lee, S. E., Kim, Y. R., et al. (2003). Regulation of *Vibrio vulnificus* virulence by the LuxS quorum-sensing system. *Molecular Microbiology, 48*(6), 1647-1664.

Klančnik, A., Guzej, B., Jamnik, P., et al. (2009). Stress response and pathogenic potential of *Campylobacter jejuni* cells exposed to starvation. *Research in Microbiology, 160*(5), 345-352.

Koch, A. L. (1971) The adaptive responses of *Escherichia coli* to a feast and famine existence. *Vol. 6* (pp. 147-217).

Kolter, R., Siegele, D. A., & Tormo, A. (1993). The stationary phase of the bacterial life cycle. *Annual Review of Microbiology, 47*, 855-874.

Kotrba, P., Inui, M., & Yukawa, H. (2001). Bacterial phosphotransferase system (PTS) in carbohydrate uptake and control of carbon metabolism. *Journal of Bioscience and Bioengineering, 92*(6), 502-517.

Kurath, G., & Morita, R. Y. (1983). Starvation-survival physiological studies of a marine *Pseudomonas* sp. *Applied and Environmental Microbiology, 45*(4), 1206-1211.

Kusumoto, A., Asakura, H., & Kawamoto, K. (2012). General stress sigma factor RpoS influences time required to enter the viable but non-culturable state in *Salmonella enterica*. *Microbiology and Immunology, 56*(4), 228-237.

Lai, C. J., Chen, S. Y., Lin, I. H., et al. (2009). Change of protein profiles in the induction of the viable but nonculturable state of *Vibrio parahaemolyticus*. *International Journal of Food Microbiology, 135*(2), 118-124.

Lai, E. M., Nair, U., Phadke, N. D., et al. (2004). Proteomic screening and identification of differentially distributed membrane proteins in *Escherichia coli*. *Molecular Microbiology, 52*(4), 1029-1044.

Lange, R., & Hengge-Aronis, R. (1991). Identification of a central regulator of stationary-phase gene expression in *Escherichia coli*. *Molecular Microbiology, 5*(1), 49-59.

LeJeune, J. T., Besser, T. E., & Hancock, D. D. (2001). Cattle water troughs as reservoirs of *Escherichia coli* O157. *Applied and Environmental Microbiology, 67*(7), 3053-3057.

LeJeune, J. T., Besser, T. E., Rice, D. H., et al. (2004). Longitudinal study of fecal shedding of *Escherichia coli* O157:H7 in feedlot cattle: predominance and persistence of specific clonal types despite massive cattle population Turnover. *Applied and Environmental Microbiology, 70*(1), 377-384.

Lennon, J. T., & Jones, S. E. (2011). Microbial seed banks: The ecological and evolutionary implications of dormancy. *Nature Reviews Microbiology, 9*(2), 119-130.

Lewis, K. (2007). Persister cells, dormancy and infectious disease. *Nature Reviews Microbiology, 5*(1), 48-56.

Leyer, G. J., Wang, L. L., & Johnson, E. A. (1995). Acid adaptation of *Escherichia coli* O157:H7 increases survival in acidic foods. *Applied and Environmental Microbiology, 61*(10), 3752-3755.

Li, M., Villaruz, A. E., Vadyvaloo, V., et al. (2008). AI-2-dependent gene regulation in *Staphylococcus epidermidis*. *BMC Microbiology, 8*.

Liao, J. C., Chao, Y. P., & Patnaik, R. (1994) Alteration of the biochemical valves in the central metabolism of *Escherichia coli*. *Vol. 745* (pp. 21-34).

Licence, K., Oates, K. R., Synge, B. A., et al. (2001). An outbreak of *E. coli* O157 infection with evidence of spread from animals to man through contamination of a private water supply. *Epidemiology and Infection, 126*(1), 135-138.

Lin, J., Smith, M. P., Chapin, K. C., et al. (1996). Mechanisms of acid resistance in enterohemorrhagic *Escherichia coli*. *Applied and Environmental Microbiology, 62*(9), 3094-3100.

Liu, Y., Wang, C., Tyrrell, G., et al. (2010). Production of Shiga-like toxins in viable but nonculturable *Escherichia coli* O157:H7. *Water Research, 44*(3), 711-718.

Lleò, M. M., Bonato, B., Tafi, M. C., et al. (2001). Resuscitation rate in different enterococcal species in the viable but non-culturable state. *Journal of Applied Microbiology, 91*(6), 1095-1102.

Lleò, M. M., Pierobon, S., Tafi, M. C., et al. (2000). mRNA detection by reverse transcription-PCR for monitoring viability over time in an *Enterococcus faecalis* viable but nonculturable population maintained in a laboratory microcosm. *Applied and Environmental Microbiology, 66*(10), 4564-4567.

Lleò, M. M., Tafi, M. C., & Canepari, P. (1998). Nonculturable *Enterococcus faecalis* cells are metabolically active and capable of resuming active growth. *Systematic and Applied Microbiology, 21*(3), 333-339.

Loewen, P. C., Hu, B., Strutinsky, J., et al. (1998). Regulation in the *rpoS* regulon of *Escherichia coli*. *Canadian Journal of Microbiology, 44*(8), 707-717.

Loewen, P. C., & Triggs, B. L. (1984). Genetic mapping of *katF*, a locus that with *katE* affects the synthesis of a second catalase species in *Escherichia coli*. *Journal of Bacteriology, 160*(2), 668-675.

Loh, J. T., Forsyth, M. H., & Cover, T. L. (2004). Growth phase regulation of *flaA* expression in *Helicobacter pylori* is *luxS* dependent. *Infection and Immunity, 72*(9), 5506-5510.

Lombardía, E., Rovetto, A. J., Arabolaza, A. L., et al. (2006). A LuxS-dependent cell-to-cell language regulates social behavior and development in *Bacillus subtilis*. *Journal of Bacteriology, 188*(12), 4442-4452.

Lothigius, Å., Sjöling, Å., Svennerholm, A. M., et al. (2010). Survival and gene expression of enterotoxigenic *Escherichia coli* during long-term incubation in sea water and freshwater. *Journal of Applied Microbiology, 108*(4), 1441-1449.

Lyon, W. R., Madden, J. C., Levin, J. C., et al. (2001). Mutation of *luxS* affects growth and virulence factor expression in *Streptococcus pyogenes*. *Molecular Microbiology, 42*(1), 145-157.

Maalej, S., Denis, M., & Dukan, S. (2004). Temperature and growth-phase effects on *Aeromonas hydrophila* survival in natural seawater microcosms: Role of protein synthesis and nucleic acid content on viable but temporarily nonculturable response. *Microbiology, 150*(1), 181-187.

Maciag, M., Nowicki, D., Szalewska-Pałasz, A., et al. (2012). Central carbon metabolism influences fidelity of DNA replication in *Escherichia coli*. *Mutation Research - Fundamental and Molecular Mechanisms of Mutagenesis, 731*(1-2), 99-106.

Mackie, R. I., Sghir, A., & Gaskins, H. R. (1999). Developmental microbial ecology of the neonatal gastrointestinal tract. *American Journal of Clinical Nutrition, 69*(5), 1035S-1045S.

Madigan, M. T., Martinko, J. M., Stahl, D. A., et al. (2012). *Brock Biology of Microorganisms*. Harlow: Pearson Education.

Majdalani, N., Chen, S., Murrow, J., et al. (2001). Regulation of RpoS by a novel small RNA: The characterization of RprA. *Molecular Microbiology, 39*(5), 1382-1394.

Makino, S. I., Kii, T., Asakura, H., et al. (2000). Does enterohemorrhagic *Escherichia coli* O157:H7 enter the viable but nonculturable state in salted salmon roe? *Applied and Environmental Microbiology, 66*(12), 5536-5539.

Mandel, M. J., & Silhavy, T. J. (2005). Starvation for different nutrients in *Escherichia coli* results in differential modulation of RpoS levels and stability. *Journal of Bacteriology, 187*(2), 434-442.

Marouni, M. J., & Sela, S. (2003). The *luxS* gene of *Streptococcus pyogenes* regulates expression of genes that affect internalization by epithelial cells. *Infection and Immunity, 71*(10), 5633-5639.

Marques, J. C., Lamosa, P., Russell, C., et al. (2011). Processing the interspecies quorum-sensing signal autoinducer-2 (AI-2): Characterization of phospho-(*S*)-4,5-dihydroxy-2,3-pentanedione isomerization by LsrG protein. *Journal of Biological Chemistry, 286*(20), 18331-18343.

Masmoudi, S., Denis, M., & Maalej, S. (2010). Inactivation of the gene *katA* or *sodA* affects the transient entry into the viable but non-culturable response of *Staphylococcus aureus* in natural seawater at low temperature. *Marine Pollution Bulletin, 60*(12), 2209-2214.

McCool, J. D., Long, E., Petrosino, J. F., et al. (2004). Measurement of SOS expression in individual *Escherichia coli* K-12 cells using fluorescence microscopy. *Molecular Microbiology, 53*(5), 1343-1357.

Meng, J., Doyle, M., Zhao, T., et al. (2007). *Enterohemorrhagic Escherichia coli*. Washington, DC, USA: ASM Press.

Merrick, M. J. (1993). In a class of its own - The RNA polymerase sigma factor σ^{54} (σ^{N}). *Molecular Microbiology, 10*(5), 903-909.

Michael, B., Smith, J. N., Swift, S., et al. (2001). SdiA of *Salmonella enterica* is a LuxR homolog that detects mixed microbial communities. *Journal of Bacteriology, 183*(19), 5733-5742.

Mika, F., & Hengge, R. (2005). A two-component phosphotransfer network involving ArcB, ArcA, and RssB coordinates synthesis and proteolysis of σ^{S} (RpoS) in *E. coli*. *Genes and Development, 19*(22), 2770-2781.

Miller, M. B., Skorupski, K., Lenz, D. H., et al. (2002). Parallel quorum sensing systems converge to regulate virulence in *Vibrio cholerae*. *Cell, 110*(3), 303-314.

Miller, S. T., Xavier, K. B., Campagna, S. R., et al. (2004). *Salmonella typhimurium* recognizes a chemically distinct form of the bacterial quorum-sensing signal AI-2. *Molecular Cell, 15*(5), 677-687.

Mizunoe, Y., Wai, S. N., Ishikawa, T., et al. (2000). Resuscitation of viable but nonculturable cells of *Vibrio parahaemolyticus* induced at low temperature under starvation. *FEMS Microbiology Letters, 186*(1), 115-120.

Mizunoe, Y., Wai, S. N., Takade, A., et al. (1999). Restoration of culturability of starvation-stressed and low-temperature-stressed *Escherichia coli* O157 cells by using H_2O_2-degrading compounds. *Archives of Microbiology, 172*(1), 63-67.

Money, P., Kelly, A. F., Gould, S. W. J., et al. (2010). Cattle, weather and water: Mapping *Escherichia coli* O157:H7 infections in humans in England and Scotland. *Environmental Microbiology, 12*(10), 2633-2644.

Moré, M. I., Finger, L. D., Stryker, J. L., et al. (1996). Enzymatic synthesis of a quorum-sensing autoinducer through use of defined substrates. *Science, 272*(5268), 1655-1658.

Morgan, D., Newman, C. P., Hutchinson, D. N., et al. (1993). Verotoxin producing *Escherichia coli* O157 infections associated with the consumption of yoghurt. *Epidemiology and Infection, 111*(2), 181-187.

Muela, A., Seco, C., Camafeita, E., et al. (2008). Changes in *Escherichia coli* outer membrane subproteome under environmental conditions inducing the viable but nonculturable state. *FEMS Microbiology Ecology, 64*(1), 28-36.

Myoung, G. H., Katayama, H., & Ohgaki, S. (2006). Effect of intracellular resuscitation of *Legionella pneumophila* in *Acanthamoeba polyphage* cells on the antimicrobial properties of silver and copper. *Environmental Science and Technology, 40*(23), 7434-7439.

Na, S. H., Miyanaga, K., Unno, H., et al. (2006). The survival response of *Escherichia coli* K12 in a natural environment. *Applied Microbiology and Biotechnology, 72*(2), 386-392.

Nataro, J. P., & Kaper, J. B. (1998). Diarrheagenic *Escherichia coli*. *Clinical Microbiology Reviews, 11*(1), 142-201.

National Institute of Water and Atmospheric Research. (2011). *Water quality maps and information, July to September 2011*.

Navarro Llorens, J. M., Tormo, A., & Martínez-García, E. (2010). Stationary phase in gram-negative bacteria. *FEMS Microbiology Reviews, 34*(4), 476-495.

Naylor, S. W., Low, J. C., Besser, T. E., et al. (2003). Lymphoid follicle-dense mucosa at the terminal rectum is the principal site of colonization of enterohemorrhagic *Escherichia coli* O157:H7 in the bovine host. *Infection and Immunity, 71*(3), 1505-1512.

Nealson, K. H., Platt, T., & Hastings, J. W. (1970). Cellular control of the synthesis and activity of the bacterial luminescent system. *Journal of Bacteriology, 104*(1), 313-322.

Nedvidek, W., Ledl, F., & Fischer, P. (1992). Detection of 5-hydroxymethyl-2-methyl-3(2H)-furanone and of α-dicarbonyl compounds in reaction mixtures of hexoses and pentoses with different amines. *Zeitschrift für Lebensmittel-Untersuchung und Forschung, 194*(3), 222-228.

Nelson, L. M., & Parkinson, D. (1978). Effect of starvation on survival of three bacterial isolates from an arctic soil. *Canadian Journal of Microbiology, 24*(12), 1460-1467.

Newlands, J. T., Gaal, T., Mecsas, J., et al. (1993). Transcription of the *Escherichia coli rrnB* P1 promoter by the heat shock RNA polymerase ($E\sigma^{32}$) in vitro. *Journal of Bacteriology, 175*(3), 661-668.

Newman, E. B., & Lin, R. (1995). Leucine-responsive regulatory protein: A global regulator of gene expression in *E. coli*. *Annual Review of Microbiology, 49*, 747-775.

Nilsson, L., Oliver, J. D., & Kjelleberg, S. (1991). Resuscitation of *Vibrio vulnificus* from the viable but nonculturable state. *Journal of Bacteriology, 173*(16), 5054-5059.

Notley, L., & Ferenci, T. (1995). Differential expression of mal genes under cAMP and endogenous inducer control in nutrient-stressed *Escherichia coli*. *Molecular Microbiology, 16*(1), 121-129.

Novitsky, J. A., & Morita, R. Y. (1978). Possible strategy for the survival of marine bacteria under starvation conditions. *Marine Biology, 48*(3), 289-295.

Nyström, T. (2001). Not quite dead enough: On bacterial life, culturability, senescence, and death. *Archives of Microbiology, 176*(3), 159-164.

Nyström, T. (2003). Nonculturable bacteria: Programmed survival forms or cells at death's door? *BioEssays, 25*(3), 204-211.

Nyström, T. (2004). Growth versus maintenance: A trade-off dictated by RNA polymerase availability and sigma factor competition? *Molecular Microbiology, 54*(4), 855-862.

O'Brien, A. D., & Holmes, R. K. (1987). Shiga and Shiga-like toxins. *Microbiological Reviews, 51*(2), 206-220.

O'Brien, A. D., Lively, T. A., & Chen, M. E. (1983). *Escherichia coli* O157:H7 strains associated with haemorrhagic colitis in the United States produce a *Shigella dysenteriae* 1 (Shiga) like cytotoxin. *Lancet, 1*(8326), 702.

O'Brien, A. D., Tesh, V. L., Donohue-Rolfe, A., et al. (1992). Shiga toxin: Biochemistry, genetics, mode of action, and role in pathogenesis. *Current Topics in Microbiology and Immunology, 180*, 65-94.

Ogden, I. D., Hepburn, N. F., MacRae, M., et al. (2002). Long-term survival of *Escherichia coli* O157 on pasture following an outbreak associated with sheep at a scout camp. *Letters in Applied Microbiology, 34*(2), 100-104.

Ohtani, K., Hayashi, H., & Shimizu, T. (2002). The *luxS* gene is involved in cell-cell signalling for toxin production in *Clostridium perfringens*. *Molecular Microbiology, 44*(1), 171-179.

Ohtomo, R., & Saito, M. (2001). Increase in the culturable cell number of *Escherichia coli* during recovery from saline stress: Possible implication for resuscitation from the VBNC state. *Microbial Ecology, 42*(2), 208-214.

Oliver, J. D. (2010). Recent findings on the viable but nonculturable state in pathogenic bacteria. *FEMS Microbiology Reviews, 34*(4), 415-425.

Oliver, J. D., & Bockian, R. (1995). *In vivo* resuscitation, and virulence towards mice, of viable but nonculturable cells of *Vibrio vulnificus*. *Applied and Environmental Microbiology, 61*(7), 2620-2623.

Oliver, J. D., Nilsson, L., & Kjelleberg, S. (1991). Formation of nonculturable *Vibrio vulnificus* cells and its relationship to the starvation state. *Applied and Environmental Microbiology, 57*(9), 2640-2644.

Orskov, I., Orskov, F., Jann, B., et al. (1977). Serology, chemistry, and genetics of O and K antigens of *Escherichia coli*. *Bacteriological Reviews, 41*(3), 667-710.

Orth, D., Grif, K., Khan, A. B., et al. (2007). The Shiga toxin genotype rather than the amount of Shiga toxin or the cytotoxicity of Shiga toxin in vitro correlates with the appearance of the hemolytic uremic syndrome. *Diagnostic Microbiology and Infectious Disease, 59*(3), 235-242.

Park, Y., Cho, Y. J., Ahn, T., et al. (1999). Molecular interactions in ribose transport: The binding protein module symmetrically associates with the homodimeric membrane transporter. *EMBO Journal, 18*(15), 4149-4156.

Park, Y. H., Lee, B. R., Seok, Y. J., et al. (2006). *In vitro* reconstitution of catabolite repression in *Escherichia coli*. *Journal of Biological Chemistry, 281*(10), 6448-6454.

Parsek, M. R., Val, D. L., Hanzelka, B. L., et al. (1999). Acyl homoserine-lactone quorum-sensing signal generation. *Proceedings of the National Academy of Sciences of the United States of America, 96*(8), 4360-4365.

Parveen, N., & Cornell, K. A. (2011). Methylthioadenosine/*S*-adenosylhomocysteine nucleosidase, a critical enzyme for bacterial metabolism. *Molecular Microbiology, 79*(1), 7-20.

Patel, J., Millner, P., Nou, X., et al. (2010). Persistence of enterohaemorrhagic and nonpathogenic *E. coli* on spinach leaves and in rhizosphere soil. *Journal of Applied Microbiology, 108*(5), 1789-1796.

Paunio, M., Pebody, R., Keskimäki, M., et al. (1999). Swimming-associated outbreak of *Escherichia coli* O157:H7. *Epidemiology and Infection, 122*(1), 1-5.

Pearson, J. P., Van Delden, C., & Iglewski, B. H. (1999). Active efflux and diffusion are involved in transport of *Pseudomonas aeruginosa* cell-to-cell signals. *Journal of Bacteriology, 181*(4), 1203-1210.

Pei, D., & Zhu, J. (2004). Mechanism of action of *S*-ribosylhomocysteinase (LuxS). *Current Opinion in Chemical Biology, 8*(5), 492-497.

Penders, J., Thijs, C., Vink, C., et al. (2006). Factors influencing the composition of the intestinal microbiota in early infancy. *Pediatrics, 118*(2), 511-521.

Pennington, H. (2010). *Escherichia coli* O157. *The Lancet, 376*(9750), 1428-1435.

Pereira, C. S., De Regt, A. K., Brito, P. H., et al. (2009). Identification of functional LsrB-like autoinducer-2 receptors. *Journal of Bacteriology, 191*(22), 6975-6987.

Pereira, C. S., Santos, A. J. M., Bejerano-Sagie, M., et al. (2012). Phosphoenolpyruvate phosphotransferase system regulates detection and processing of the quorum sensing signal autoinducer-2. *Molecular Microbiology, 84*(1), 93-104.

Pereira, C. S., Thompson, J. A., & Xavier, K. B. (2013). AI-2-mediated signalling in bacteria. *FEMS Microbiology Reviews, 37*(2), 156-181.

Plummer, P., Sahin, O., Burrough, E., et al. (2012). Critical role of *luxs* in the virulence of *Campylobacter jejuni* in a guinea pig model of abortion. *Infection and Immunity, 80*(2), 585-593.

Pommepuy, M., Butin, M., Derrien, A., et al. (1996). Retention of enteropathogenicity by viable but nonculturable *Escherichia coli* exposed to seawater and sunlight. *Applied and Environmental Microbiology, 62*(12), 4621-4626.

Postgate, J. R. (1969). Chapter XVIII Viable counts and Viability. *Methods in Microbiology, 1,* 611-628.

Rader, B. A., Campagna, S. R., Semmelhack, M. F., et al. (2007). The quorum-sensing molecule autoinducer 2 regulates motility and flagellar morphogenesis in *Helicobacter pylori*. *Journal of Bacteriology, 189*(17), 6109-6117.

Rader, B. A., Wreden, C., Hicks, K. G., et al. (2011). *Helicobacter pylori* perceives the quorum-sensing molecule AI-2 as a chemorepellent via the chemoreceptor TlpB. *Microbiology, 157*(9), 2445-2455.

Rahman, I., Shahamat, M., Chowdhury, M. A. R., et al. (1996). Potential virulence of viable but nonculturable *Shigella dysenteriae* type 1. *Applied and Environmental Microbiology, 62*(1), 115-120.

Rahman, I., Shahamat, M., Kirchman, P. A., et al. (1994). Methionine uptake and cytopathogenicity of viable but nonculturable *Shigella dysenteriae* type 1. *Applied and Environmental Microbiology, 60*(10), 3573-3578.

Rahman, M., Hasan, M. R., Oba, T., et al. (2006). Effect of rpoS gene knockout on the metabolism of *Escherichia coli* during exponential growth phase and early stationary phase based on gene expressions, enzyme activities

and intracellular metabolite concentrations. *Biotechnology and Bioengineering, 94*(3), 585-595.

Rahmati, S., Yang, S., Davidson, A. L., et al. (2002). Control of the AcrAB multidrug efflux pump by quorum-sensing regulator SdiA. *Molecular Microbiology, 43*(3), 677-685.

Rangel, J. M., Sparling, P. H., Crowe, C., et al. (2005). Epidemiology of *Escherichia coli* O157:H7 outbreaks, United States, 1982-2002. *Emerging Infectious Diseases, 11*(4), 603-609.

Ravel, J., Knight, I. T., Monahan, C. E., et al. (1995). Temperature-induced recovery of *Vibrio cholerae* from the viable but nonculturable state: Growth or resuscitation? *Microbiology, 141*(2), 377-383.

Reeser, R. J., Medler, R. T., Billington, S. J., et al. (2007). Characterization of *Campylobacter jejuni* biofilms under defined growth conditions. *Applied and Environmental Microbiology, 73*(6), 1908-1913.

Reissbrodt, R., Rienaecker, I., Romanova, J. M., et al. (2002). Resuscitation of *Salmonella enterica* serovar Typhimurium and enterohemorrhagic *Escherichia coli* from the viable but nonculturable state by heat-stable enterobacterial autoinducer. *Applied and Environmental Microbiology, 68*(10), 4788-4794.

Rettner, R. E., & Saier Jr, M. H. (2010). The autoinducer-2 exporter superfamily. *Journal of Molecular Microbiology and Biotechnology, 18*(4), 195-205.

Rey, J., Sánchez, S., Blanco, J. E., et al. (2006). Prevalence, serotypes and virulence genes of Shiga toxin-producing *Escherichia coli* isolated from ovine and caprine milk and other dairy products in Spain. *International Journal of Food Microbiology, 107*(2), 212-217.

Rezaeinejad, S., & Ivanov, V. (2011). Heterogeneity of *Escherichia coli* population by respiratory activity and membrane potential of cells during growth and long-term starvation. *Microbiological Research, 166*(2), 129-135.

Rigsbee, W., Simpson, L. M., & Oliver, J. D. (1996). Detection of the viable but nonculturable state in *Escherichia coli* O157:H7. *Journal of Food Safety, 16*(4), 255-262.

Riley, L. W., Remis, R. S., & Helgerson, S. D. (1983a). Hemmorhagic colitis associated with a rare *Escherichia coli* serotype. *New England Journal of Medicine, 308*(12), 681-685.

Riley, L. W., Remis, R. S., & Helgerson, S. D. (1983b). Hemorrhagic colitis associated with a rare *Escherichia coli* serotype. *New England Journal of Medicine, 308*(12), 681-685.

Rollins, D. M., & Colwell, R. R. (1986). Viable but nonculturable stage of *Campylobacter jejuni* and its role in survival in the natural aquatic environment. *Applied and Environmental Microbiology, 52*(3), 531-538.

Ropers, D., de Jong, H., Page, M., et al. (2006). Qualitative simulation of the carbon starvation response in *Escherichia coli*. *BioSystems, 84*(2), 124-152.

Roszak, D. B., & Colwell, R. R. (1987a). Metabolic activity of bacterial cells enumerated by direct viable count. *Applied and Environmental Microbiology, 53*(12), 2889-2893.

Roszak, D. B., & Colwell, R. R. (1987b). Survival strategies of bacteria in the natural environment. *Microbiological Reviews, 51*(3), 365-379.

Roszak, D. B., Grimes, D. J., & Colwell, R. R. (1984). Viable but nonrecoverable stage of *Salmonella enteritidis* in aquatic systems. *Canadian Journal of Microbiology, 30*(3), 334-338.

Rouvière, P. E., De Las Peñas, A., Mecsas, J., et al. (1995). *rpoE*, the gene encoding the second heat-shock sigma factor, σ^E, in *Escherichia coli*. *EMBO Journal, 14*(5), 1032-1042.

Russell, J. B., & Jarvis, G. N. (2001). Practical mechanisms for interrupting the oral-fecal lifecycle of *Escherichia coli*. *Journal of Molecular Microbiology and Biotechnology, 3*(2), 265-272.

Russo, T. A., & Johnson, J. R. (2003). Medical and economic impact of extraintestinal infections due to *Escherichia coli*: Focus on an increasingly important endemic problem. *Microbes and Infection, 5*(5), 449-456.

Sak, B. D., Eisenstark, A., & Touati, D. (1989). Exonuclease III and the catalase hydroperoxidase II in *Escherichia coli* are both regulated by the *katF* gene product. *Proceedings of the National Academy of Sciences of the United States of America, 86*(9), 3271-3275.

Sammartano, L. J., Tuveson, R. W., & Davenport, R. (1986). Control of sensititivity to inactivation by H_2O_2 and broad-spectrum near-UV radiation by the *Escherichia coli katF* locus. *Journal of Bacteriology, 168*(1), 13-21.

Sauer, U., & Eikmanns, B. J. (2005). The PEP-pyruvate-oxaloacetate node as the switch point for carbon flux distribution in bacteria. *FEMS Microbiology Reviews, 29*(4), 765-794.

Schaefer, A. L., Val, D. L., Hanzelka, B. L., et al. (1996). Generation of cell-to-cell signals in quorum sensing: Acyl homoserine lactone synthase activity of a purified *Vibrio fischeri* LuxI protein. *Proceedings of the National Academy of Sciences of the United States of America, 93*(18), 9505-9509.

Schauder, S., & Bassler, B. L. (2001). The languages of bacteria. *Genes and Development, 15*(12), 1468-1480.

Scheiring, J., Andreoli, S. P., & Zimmerhackl, L. B. (2008). Treatment and outcome of Shiga-toxin-associated hemolytic uremic syndrome (HUS). *Pediatric Nephrology, 23*(10), 1749-1760.

Schmidt, M. A. (2010). LEEways: Tales of EPEC, ATEC and EHEC. *Cellular Microbiology, 12*(11), 1544-1552.

Sears, C. L. (2005). A dynamic partnership: Celebrating our gut flora. *Anaerobe, 11*(5), 247-251.

Senoh, M., Ghosh-Banerjee, J., Ramamurthy, T., et al. (2012). Conversion of viable but nonculturable enteric bacteria to culturable by co-culture with eukaryotic cells. *Microbiology and Immunology, 56*(5), 342-345.

Shao, H., James, D., Lamont, R. J., et al. (2007a). Differential interaction of *Aggregatibacter (Actinobacillus) actinomycetemcomitans* LsrB and RbsB proteins with autoinducer 2. *Journal of Bacteriology, 189*(15), 5559-5565.

Shao, H., Lamont, R. J., & Demuth, D. R. (2007b). Autoinducer 2 is required for biofilm growth of *Aggregatibacter* (*Actinobacillus*) *actinomycetemcomitans*. *Infection and Immunity, 75*(9), 4211-4218.

Sharma, U. K., & Chatterji, D. (2010). Transcriptional switching in *Escherichia coli* during stress and starvation by modulation of σ^{70} activity. *FEMS Microbiology Reviews, 34*(5), 646-657.

Shilton, B. H., Flocco, M. M., Nilsson, M., et al. (1996). Conformational changes of three periplasmic receptors for bacterial chemotaxis and transport: The maltose-, glucose/galactose- and ribose-binding proteins. *Journal of Molecular Biology, 264*(2), 350-363.

Shimada, T., Fujita, N., Yamamoto, K., et al. (2011). Novel roles of cAMP receptor protein (CRP) in regulation of transport and metabolism of carbon sources. *PLoS ONE, 6*(6).

Shleeva, M. O., Bagramyan, K., Telkov, M. V., et al. (2002). Formation and resuscitation of 'non-culturable' cells of *Rhodococcus rhodochrous* and *Mycobacterium tuberculosis* in prolonged stationary phase. *Microbiology, 148*(5), 1581-1591.

Signoretto, C., Lleò, M. D. M., & Canepari, P. (2002). Modification of the peptidoglycan of *Escherichia coli* in the viable but nonculturable state. *Current Microbiology, 44*(2), 125-131.

Siller, M., Janapatla, R. P., Pirzada, Z. A., et al. (2008). Functional analysis of the group A streptococcal *luxS*/AI-2 system in metabolism, adaptation to stress and interaction with host cells. *BMC Microbiology, 8*.

Silwood, C. J. L., Lynch, E., Claxson, A. W. D., et al. (2002). ^{1}H and ^{13}C NMR spectroscopic analysis of human saliva. *Journal of Dental Research, 81*(6), 422-427.

Sircili, M. P., Walters, M., Trabulsi, L. R., et al. (2004). Modulation of enteropathogenic *Escherichia coli* virulence by quorum sensing. *Infection and Immunity, 72*(4), 2329-2337.

Sledjeski, D. D., Gupta, A., & Gottesman, S. (1996). The small RNA, DsrA, is essential for the low temperature expression of RpoS during exponential growth in *Escherichia coli*. *EMBO Journal, 15*(15), 3993-4000.

Small, P., Blankenhorn, D., Welty, D., et al. (1994). Acid and base resistance in *Escherichia coli* and *Shigella flexneri*: Role of rpoS and growth pH. *Journal of Bacteriology, 176*(6), 1729-1737.

Song, S., & Park, C. (1998). Utilization of D-ribose through D-xylose transporter. *FEMS Microbiology Letters, 163*(2), 255-261.

Soni, K. A., Lu, L., Jesudhasan, P. R., et al. (2008). Influence of autoinducer-2 (AI-2) and beef sample extracts on *E. coli* O157:H7 survival and gene expression of virulence genes yadK and hhA. *Journal of Food Science, 73*(3), M135-M139.

Sperandio, V., Li, C. C., & Kaper, J. B. (2002a). Quorum-sensing *Escherichia coli* regulator A: A regulator of the LysR family involved in the regulation of the locus of enterocyte effacement pathogenicity island in enterohemorrhagic *E. coli*. *Infection and Immunity, 70*(6), 3085-3093.

Sperandio, V., Mellies, J. L., Nguyen, W., et al. (1999). Quorum sensing controls expression of the type III secretion gene transcription and protein secretion in enterohemorrhagic and enteropathogenic *Escherichia coli*. *Proceedings of the National Academy of Sciences of the United States of America, 96*(26), 15196-15201.

Sperandio, V., Torres, A. G., Girón, J. A., et al. (2001). Quorum sensing is a global regulatory mechanism in enterohemorrhagic *Escherichia coli* O157:H7. *Journal of Bacteriology, 183*(17), 5187-5197.

Sperandio, V., Torres, A. G., & Kaper, J. B. (2002b). Quorum sensing *Escherichia coli* regulators B and C (QseBC): A novel two-component regulatory system involved in the regulation of flagella and motility by quorum sensing in *E. coli*. *Molecular Microbiology, 43*(3), 809-821.

Stenberg, F., Chovanec, P., Maslen, S. L., et al. (2005). Protein complexes of the *Escherichia coli* cell envelope. *Journal of Biological Chemistry, 280*(41), 34409-34419.

Stevens, A. M., Fujita, N., Ishihama, A., et al. (1999). Involvement of the RNA polymerase α-subunit C-terminal domain in LuxR- dependent activation of the *Vibrio fischeri* luminescence genes. *Journal of Bacteriology, 181*(15), 4704-4707.

Strachan, N. J. C., Dunn, G. M., Locking, M. E., et al. (2006). *Escherichia coli* O157: Burger bug or environmental pathogen? *International Journal of Food Microbiology, 112*(2), 129-137.

Strachan, N. J. C., Fenlon, D. R., & Ogden, I. D. (2001). Modelling the vector pathway and infection of humans in an environmental outbreak of *Escherichia coli* O157. *FEMS Microbiology Letters, 203*(1), 69-73.

Su, C.-P., Jane, W.-N., & Wong, H.-c. (2013). Changes of ultrastructure and stress tolerance of *Vibrio parahaemolyticus* upon entering viable but nonculturable state. *International Journal of Food Microbiology, 160*(3), 360-366.

Sun, F., Chen, J., Zhong, L., et al. (2008). Characterization and virulence retention of viable but nonculturable *Vibrio harveyi*. *FEMS Microbiology Ecology, 64*(1), 37-44.

Surette, M. G., & Bassler, B. L. (1998). Quorum sensing in *Escherichia coli* and *Salmonella typhimurium*. *Proceedings of the National Academy of Sciences of the United States of America, 95*(12), 7046-7050.

Surette, M. G., Miller, M. B., & Bassler, B. L. (1999). Quorum sensing in *Escherichia coli*, *Salmonella typhimurium*, and *Vibrio harveyi*: A new family of genes responsible for autoinducer production. *Proceedings of the National Academy of Sciences of the United States of America, 96*(4), 1639-1644.

Taga, M. E., Miller, S. T., & Bassler, B. L. (2003). Lsr-mediated transport and processing of Al-2 in *Salmonella typhimurium*. *Molecular Microbiology, 50*(4), 1411-1427.

Taga, M. E., Semmelhack, J. L., & Bassler, B. L. (2001). The LuxS-dependent autoinducer Al-2 controls the expression of an ABC transporter that functions in Al-2 uptake in *Salmonella typhimurium*. *Molecular Microbiology, 42*(3), 777-793.

Takumi, K., De Jonge, R., & Havelaar, A. (2000). Modelling inactivation of *Escherichia coli* by low pH: Application to passage through the stomach of young and elderly people. *Journal of Applied Microbiology, 89*(6), 935-943.

Tanaka, K., Takayanagi, Y., Fujita, N., et al. (1993). Heterogeneity of the principal σ factor in *Escherichia coli*: The *rpoS* gene product, σ^{38}, is a second principal σ factor of RNA polymerase in stationary-phase *Escherichia coli*. *Proceedings of the National Academy of Sciences of the United States of America, 90*(8), 3511-3515.

Tarighi, S., & Taheri, P. (2011). Different aspects of bacterial communication signals. *World Journal of Microbiology and Biotechnology, 27*(6), 1267-1280.

Tarr, P. I., Gordon, C. A., & Chandler, W. L. (2005). Shiga-toxin-producing *Escherichia coli* and haemolytic uraemic syndrome. *Lancet, 365*(9464), 1073-1086.

Tesh, V. L., Burris, J. A., Owens, J. W., et al. (1993). Comparison of the relative toxicities of Shiga-like toxins type I and type II for mice. *Infection and Immunity, 61*(8), 3392-3402.

The Institute of Environmental Science and Research Ltd. (2013). *Notifiable and Other Diseases in New Zealand: Annual Report 2012*. Porirua, New Zealand.

Tomasz, A. (1965). Control of the competent state in *Pneumococcus* by a hormone-like cell product: An example for a new type of regulatory mechanism in bacteria. *Nature, 208*(5006), 155-159.

Touati, E., Dassa, E., & Boquet, P. L. (1986). Pleiotropic mutations in *appR* reduce pH 2.5 acid phosphatase expression and restore succinate utilisation in CRP-deficient strains of *Escherichia coli*. *Molecular and General Genetics, 202*(2), 257-264.

Trappetti, C., Potter, A. J., Paton, A. W., et al. (2011). LuxS mediates iron-dependent biofilm formation, competence, and fratricide in *Streptococcus pneumoniae*. *Infection and Immunity, 79*(11), 4550-4558.

Traxler, M. F., Zacharia, V. M., Marquardt, S., et al. (2011). Discretely calibrated regulatory loops controlled by ppGpp partition gene induction across the 'feast to famine' gradient in *Escherichia coli*. *Molecular Microbiology, 79*(4), 830-845.

Tree, J. J., Wolfson, E. B., Wang, D., et al. (2009). Controlling injection: regulation of type III secretion in enterohaemorrhagic *Escherichia coli*. *Trends in Microbiology, 17*(8), 361-370.

Turovskiy, Y., Kashtanov, D., Paskhover, B., et al. (2007). Quorum Sensing: Fact, Fiction, and Everything in Between. In A. I. Laskin, S. Sariaslani & G. M. Gadd (Eds.), *Advances in Applied Microbiology* (Vol. 62, pp. 191-234).

Tuveson, R. W., & Jonas, R. B. (1979). Genetic control of near-UV (300-400 NM) sensitivity independent of the *recA* gene in strains of *Escherichia coli* K12. *Photochemistry and Photobiology, 30*(6), 667-676.

Ueguchi, C., Misonou, N., & Mizuno, T. (2001). Negative control of *rpoS* expression by phosphoenolpyruvate: Carbohydrate phosphotransferase system in *Escherichia coli*. *Journal of Bacteriology, 183*(2), 520-527.

Val, D. L., & Cronan Jr, J. E. (1998). In vivo evidence that *S*-adenosylmethionine and fatty acid synthesis intermediates are the substrates for the LuxI family of autoinducer synthases. *Journal of Bacteriology, 180*(10), 2644-2651.

Van Derlinden, E., Boons, K., & Van Impe, J. F. (2011). *Escherichia coli* population heterogeneity: Subpopulation dynamics at super-optimal temperatures. *Food Microbiology, 28*(4), 667-677.

Vendeville, A., Winzer, K., Heurlier, K., et al. (2005). Making 'sense' of metabolism: Autoinducer-2, LuxS and pathogenic bacteria. *Nature Reviews Microbiology, 3*(5), 383-396.

Vidal, J. E., Ludewick, H. P., Kunkel, R. M., et al. (2011). The *luxs*-dependent quorum-sensing system regulates early biofilm formation by *Streptococcus pneumoniae* strain D39. *Infection and Immunity, 79*(10), 4050-4060.

Vinella, D., Albrecht, C., Cashel, M., et al. (2005). Iron limitation induces SpoT-dependent accumulation of ppGpp in *Escherichia coli*. *Molecular Microbiology, 56*(4), 958-970.

Voet, D., & Voet, J. (2011). *Biochemistry* (4th ed.). Hoboken, NJ: John Wiley & Sons, Inc.

Wai, S. N., Mizunoe, Y., Takade, A., et al. (2000). A comparison of solid and liquid media for resuscitation of starvation- and low-temperature-induced nonculturable cells of *Aeromonas hydrophila*. *Archives of Microbiology, 173*(4), 307-310.

Wang, G., & Doyle, M. P. (1998). Survival of Enterohemorrhagic *Escherichia coli* O157:H7 in Water. *Journal of Food Protection, 61*(6), 662-667.

Wang, L., Li, J., March, J. C., et al. (2005). *luxS*-dependent gene regulation in *Escherichia coli* K-12 revealed by genomic expression profiling. *Journal of Bacteriology, 187*(24), 8350-8360.

Wang, X., De Boer, P. A. J., & Rothfield, L. I. (1991). A factor that positively regulates cell division by activating transcription of the major cluster of essential cell division genes of *Escherichia coli*. *EMBO Journal, 10*(11), 3363-3372.

Weber, H., Polen, T., Heuveling, J., et al. (2005). Genome-wide analysis of the general stress response network in *Escherichia coli*: σ^S-dependent genes, promoters, and sigma factor selectivity. *Journal of Bacteriology, 187*(5), 1591-1603.

Wei, Y., Lee, J. M., Smulski, D. R., et al. (2001a). Global impact of *sdiA* amplification revealed by comprehensive gene expression profiling of *Escherichia coli*. *Journal of Bacteriology, 183*(7), 2265-2272.

Wei, Y., Vollmer, A. C., & LaRossa, R. A. (2001b). *In vivo* titration of mitomycin C action by four *Escherichia coli* genomic regions on multicopy plasmids. *Journal of Bacteriology, 183*(7), 2259-2264.

Wendrich, T. M., Blaha, G., Wilson, D. N., et al. (2002). Dissection of the mechanism for the stringent factor RelA. *Molecular Cell, 10*(4), 779-788.

Wesche, A. M., Gurtler, J. B., Marks, B. P., et al. (2009). Stress, sublethal injury, resuscitation, and virulence of bacterial foodborne pathogens. *Journal of Food Protection, 72*(5), 1121-1138.

West, S. A., Winzer, K., Gardner, A., et al. (2012). Quorum sensing and the confusion about diffusion. *Trends in Microbiology, 20*(12), 586-594.

Wheeler, W. E., & Noller, C. H. (1977). Gastrointestinal tract pH and starch in feces of ruminants. *Journal of Animal Science, 44*(1), 131-135.

White-Ziegler, C. A., Um, S., Pérez, N. M., et al. (2008). Low temperature (23°C) increases expression of biofilm-, cold-shock- and RpoS-dependent genes in *Escherichia coli* K-12. *Microbiology, 154*(1), 148-166.

Whitehead, N. A., Barnard, A. M. L., Slater, H., et al. (2001). Quorum-sensing in Gram-negative bacteria. *FEMS Microbiology Reviews, 25*(4), 365-404.

Williams, A. P., Avery, L. M., Killham, K., et al. (2005). Persistence of *Escherichia coli* O157 on farm surfaces under different environmental conditions. *Journal of Applied Microbiology, 98*(5), 1075-1083.

Williams, K. P., Gillespie, J. J., Sobral, B. W. S., et al. (2010). Phylogeny of gammaproteobacteria. *Journal of Bacteriology, 192*(9), 2305-2314.

Williams, P., Winzer, K., Chan, W. C., et al. (2007). Look who's talking: Communication and quorum sensing in the bacterial world. *Philosophical Transactions of the Royal Society B: Biological Sciences, 362*(1483), 1119-1134.

Winzer, K., Hardie, K. R., Burgess, N., et al. (2002a). LuxS: Its role in central metabolism and the *in vitro* synthesis of 4-hydroxy-5-methyl-3(*2H*)-furanone. *Microbiology, 148*(4), 909-922.

Winzer, K., Hardie, K. R., & Williams, P. (2003). LuxS and autoinducer-2: their contribution to quorum sensing and metabolism in bacteria. *Advances in Applied Microbiology, 53*, 291-396.

Winzer, K., Sun, Y. H., Green, A., et al. (2002b). Role of *Neisseria meningitidis luxS* in cell-to-cell signaling and bacteremic infection. *Infection and Immunity, 70*(4), 2245-2248.

Wolfe, A. J. (2005). The acetate switch. *Microbiology and Molecular Biology Reviews, 69*(1), 12-50.

Wong, H. C., Shen, C. T., Chang, C. N., et al. (2004). Biochemical and virulence characterization of viable but nonculturable cells of *Vibrio parahaemolyticus*. *Journal of Food Protection, 67*(11), 2430-2435.

Wong, T. L., MacDiarmid, S., & Cook, R. (2009). *Salmonella*, *Escherichia coli* O157:H7 and *E. coli* biotype 1 in a pilot survey of imported and New Zealand pig meats. *Food Microbiology, 26*(2), 177-182.

Wu, V. C. H. (2008). A review of microbial injury and recovery methods in food. *Food Microbiology, 25*(6), 735-744.

Xavier, K. B., & Bassler, B. L. (2005a). Interference with AI-2-mediated bacterial cell-cell communication. *Nature, 437*(7059), 750-753.

Xavier, K. B., & Bassler, B. L. (2005b). Regulation of uptake and processing of the quorum-sensing autoinducer AI-2 in *Escherichia coli*. *Journal of Bacteriology, 187*(1), 238-248.

Xiao, H., Kalman, M., Ikehara, K., et al. (1991). Residual guanosine 3',5'-bispyrophosphate synthetic activity of *relA* null mutants can be eliminated by spoT null mutations. *Journal of Biological Chemistry, 266*(9), 5980-5990.

Xu, H. S., Roberts, N., Singleton, F. L., et al. (1982). Survival and viability of nonculturable *Escherichia coli* and *Vibrio cholerae* in the estuarine and marine environment. *Microbial Ecology, 8*(4), 313-323.

Xu, L., Li, H., Vuong, C., et al. (2006). Role of the *luxS* quorum-sensing system in biofilm formation and virulence of *Staphylococcus epidermidis*. *Infection and Immunity, 74*(1), 488-496.

Zhao, L., & Matthews, K. R. (2000). Influence of starvation, temperature, and pH on culturability of *Escherichia coli* O157:H7. *Journal of Food Safety, 20*(3), 193-208.

Zhao, L., Xue, T., Shang, F., et al. (2010). *Staphylococcus aureus* AI-2 quorum sensing associates with the KdpDE two-component system to regulate capsular polysaccharide synthesis and virulence. *Infection and Immunity, 78*(8), 3506-3515.

Appendices

Appendix 1 Chemical classes and sub-classes of the substrates in the PM1 and PM2A MicroPlates™. Classification information compiled from PubChem Compound (http://www.ncbi.nlm.nih.gov/pccompound) and Kyoto Encyclopedia of Genes and Genomes (KEGG) Compound (http://www.genome.jp/kegg/compound/) databases.

Class	Sub-class	PM1	PM1 & PM2A	Substrates
Alcohols	Ethylene glycols	1	1	Tween 20
		2	2	Tween 40
		3	3	Tween 80
	Glycols	4	4	1,2-propanediol
			5	2,3-butanediol
Amines	Aniline compounds		6	Succinamic acid
	Ethylamines	5	7	Phenylethylamine
	Quaternary ammonium compounds		8	D,L-carnitine
Antibacterial			9	Sec-butylamine
Carbohydrates	Glycosaminoglycans		10	Chondroitin sulfate C
	Glycosides		11	3-methyl glucose
			12	Amygdalin
			13	Arbutin
			14	Salicin
		6	15	α-methyl-D-glucoside
			16	α-methyl-D-mannoside
			17	β-methyl-D-galactoside
		7	18	β-methyl-D-glucoside
			19	β-methyl-D-xyloside
	Monosaccharides		20	2-deoxy-D-ribose
			21	D-arabinose
		8	22	D-fructose
			23	D-fucose
		9	24	D-galactose
		10	25	D-galacturonic acid
		11	26	D-gluconic acid
		12	27	D-glucosaminic acid
			28	Dihydroxy acetone
			29	D-lyxose
		13	30	D-mannose
		14	31	D-psicose
			32	D-ribono-1,4-lactone
		15	33	D-ribose
			34	D-tagatose
		16	35	D-xylose
		17	36	L-arabinose
		18	37	L-fucose
			38	L-glucose
		19	39	L-lyxose
		20	40	L-rhamnose

Class	Sub-class	PM1	PM1 & PM2A	Substrates
			41	L-sorbose
			42	L-xylose
Carbohydrates (continued)	Monosaccharides (continued)		43	*N*-acetyl-D-galactosamine
		21	44	*N*-acetyl-D-glucosamine
			45	*N*-acetyl-neuramic acid
		22	46	*N*-acetyl-β-D-mannosamine
			47	Sedoheptulosan
		23	48	α-D-glucose
			49	α-methyl-D-galactoside
			50	β-D-allose
	Oligosaccharides		51	3-O-β-D-galactopyranosyl-D-arabinose
		24	52	D-cellobiose
		25	53	D-melibiose
			54	D-raffinose
		26	55	D-trehalose
			56	Gentiobiose
		27	57	Lactulose
			58	Maltitol
		28	59	Maltose
		29	60	Maltotriose
			61	Melibionic acid
			62	Palatinose
			63	Stachyose
		30	64	Sucrose
			65	Turanose
		31	66	α-D-lactose
	Polysaccharides		67	Dextrin
			68	Glycogen
			69	Inulin
			70	Laminarin
			71	Mannan
			72	Pectin
			73	α-cyclodextrin
			74	β-cyclodextrin
			75	γ-cyclodextrin
	Sugar alcohols	32	76	Adonitol
			77	D-arabitol
		33	78	D-mannitol
		34	79	D-sorbitol
		35	80	Dulcitol
		36	81	Glycerol
			82	Erythritol
			83	Lactitol
			84	L-arabitol
		37	85	meso-inositol
			86	Xylitol
	Sugar phosphates	38	87	D,L-α-glycerol-phosphate

Class	Sub-class	PM1	PM1 & PM2A	Substrates
Carbohydrates (continued)	Sugar phosphates (continued)	39	88	Fructose-6-phosphate
		40	89	Glucose-1-phosphate
		41	90	Glucose-6-phosphate
Carboxylic acids	Acetic acids		91	Acetamide
		42	92	Acetic acid
	Aldehydic acids	43	93	Glyoxylic acid
	Butyric acids		94	Butyric acid
		44	95	α-hydroxy butyric acid
		45	96	α-keto-butyric acid
			97	β-hydroxy butyric acid
			98	γ-hydroxy butyric acid
	Caproates		99	Caproic acid
	Dicarboxylic acids	46	100	Bromo succinic acid
			101	Citraconic acid
			102	Citramalic acid
		47	103	D,L-malic acid
			104	Dihydroxy fumaric acid
		48	105	D-malic acid
			106	D-tartaric acid
		49	107	Fumaric acid
			108	Itaconic acid
		50	109	L-malic acid
			110	L-tartaric acid
			111	Malonic acid
		51	112	Mono methyl succinate
		52	113	meso-tartaric acid
			114	Oxalic acid
			115	Oxalomalic acid
			116	Sebacic acid
		53	117	Succinic acid
		54	118	α-keto-glutaric acid
	Glycolates	55	119	Glycolic acid
	Hydroxy acids		120	2-hydroxy benzoic acid
			121	4-hydroxy benzoic acid
			122	D-lactic acid methyl ester
		56	123	L-lactic acid
			124	Quinic acid
	Keto acids	57	125	Acetoacetic acid
		58	126	Methyl pyruvate
		59	127	Pyruvic acid
			128	β-hydroxy pyruvic acid
	Phenylacetates	60	129	3-hydroxyphenylacetate
		61	130	4-hydroxyphenylacetate
	Propionates	62	131	Propionic acid
	Sugar acids		132	5-keto-D-gluconic acid
		63	133	D-galactonic acid-γ-lactone
		64	134	D-glucuronic acid

Class	Sub-class	PM1	PM1 & PM2A	Substrates
Carboxylic acids (continued)	Sugar acids (continued)	65	135	D-saccharic acid
		66	136	Glucuronamide
		67	137	L-galactonic acid-γ-lactone
		68	138	Mucic acid
			139	β-methyl-D-glucuronic acid
	Tricarboxylic acids	69	140	Citric acid
		70	141	Tricarballylic acid
Ketones	Butanones		142	2,3-butanone
			143	3-hydroxy 2-butanone
Lipids	Fatty acids		144	Capric acid
		71	145	Formic acid
			146	Sorbic acid
Nucleic acids	Nucleosides	72	147	2-deoxy adenosine
		73	148	Adenosine
		74	149	Inosine
		75	150	Thymidine
		76	151	Uridine
Peptides	Amines	77	152	2-aminoethanol
			153	D,L-octopamine
			154	Putrescine
		78	155	Tyramine
	Amino acids	79	156	D-alanine
			157	D-amino valeric acid
		80	158	D-aspartic acid
		81	159	D-serine
		82	160	D-threonine
			161	Glycine
		83	162	Glycyl-L-aspartic acid
		84	163	Glycyl-L-glutamic acid
		85	164	Glycyl-L-proline
			165	Hydroxy-L-proline
		86	166	L-alanine
		87	167	L-alanyl-glycine
			168	L-arginine
		88	169	L-asparagine
		89	170	L-aspartic acid
		90	171	L-glutamic acid
		91	172	L-glutamine
			173	L-histidine
			174	L-homoserine
			175	L-isoleucine
			176	L-leucine
			177	L-lysine
			178	L-methionine
			179	L-ornithine
			180	L-phenylalanine
Peptides	Amino acids	92	181	L-proline

Class	Sub-class	PM1	PM1 & PM2A	Substrates
(continued)	(continued)		182	L-pyroglutamic acid
		93	183	L-serine
		94	184	L-threonine
			185	L-valine
			186	*N*-acetyl-L-glutamic acid
			187	γ-amino Butyric acid
Proteins	Scleroproteins		188	Gelatin
Others			189	L-alaninamide
		95	190	α-hydroxy glutaric acid-γ-lactone

Appendix 2 $A_{endpoint}$ for substrate use by ERL10621 harvested during exponential phase (EP), stationary phase (SP) and starved state. Dash (–) indicates substrates tested but not utilised. Results are the average of duplicates.

Sub-class	Substrates	PM1	Endpoint ($A_{endpoint}$)		
			EP	SP	Starved
Glycosides	α-methyl-D-glucoside	6	0.669	0.602	0.636
	β-methyl-D-glucoside	7	–	0.089	–
Monosaccharides	D-fructose	8	0.514	0.508	0.576
	D-galactose	9	0.785	0.712	0.678
	D-galacturonic acid	10	0.657	0.686	0.487
	D-gluconic acid	11	0.775	0.640	0.731
	D-mannose	13	0.608	0.655	0.629
	D-ribose	15	0.701	0.711	0.669
	D-xylose	16	0.485	0.575	0.538
	L-arabinose	17	0.419	0.468	0.410
	L-fucose	18	0.614	0.575	0.592
	L-rhamnose	20	–	0.105	–
	N-acetyl-D-glucosamine	21	0.512	0.546	0.409
	N-acetyl-β-D-mannosamine	22	0.175	0.540	–
	α-D-glucose	23	0.425	0.571	0.420
Oligosaccharides	D-melibiose	25	0.637	0.655	0.530
	D-trehalose	26	0.646	0.702	0.603
	Lactulose	27	–	0.429	0.080
	Maltose	28	0.549	0.694	0.584
	Maltotriose	29	0.542	0.613	0.400
	Sucrose	30	0.650	0.789	0.649
	α-D-lactose	31	0.740	0.686	0.605
Sugar alcohols	D-mannitol	33	0.512	0.516	0.407
	Glycerol	36	0.720	0.671	0.634
Sugar phosphates	D,L-α-glycerol-phosphate	38	0.686	0.608	0.382
	Fructose-6-phosphate	39	0.687	0.686	0.650
	Glucose-1-phosphate	40	0.751	0.636	0.771
	Glucose-6-phosphate	41	0.768	0.690	0.635
Acetic acids	Acetic acid	42	0.427	0.341	0.214
Dicarboxylic acids	Bromo succinic acid	46	0.288	0.355	0.112
	D,L-malic acid	47	0.534	0.479	0.380
	D-malic acid	48	0.465	0.540	0.285
	Fumaric acid	49	0.390	0.375	0.305
	L-malic acid	50	0.570	0.576	0.299
	Succinic acid	53	0.590	0.493	0.371
Hydroxy acids	L-lactic acid	56	0.712	0.618	0.447
Keto acids	Methyl pyruvate	58	0.640	0.787	0.396
	Pyruvic acid	59	0.720	0.623	0.387
Propionates	Propionic acid	62	0.172	0.196	–
Sugar acids	D-glucuronic acid	64	0.747	0.640	0.642
	Glucuronamide	66	0.404	0.452	0.266
	L-galactonic acid-γ-lactone	67	0.567	0.612	0.400

Sub-class	Substrates	PM1	Endpoint ($A_{endpoint}$)		
			EP	SP	Starved
Nucleosides	2-deoxy adenosine	72	0.768	0.787	0.572
	Adenosine	73	0.769	0.778	0.719
	Inosine	74	0.823	0.842	0.651
	Thymidine	75	0.777	0.891	0.521
	Uridine	76	0.789	0.842	0.517
Amino acids	D-alanine	79	0.581	0.555	0.274
	Glycyl-L-proline	85	–	0.123	–
	L-alanine	86	0.435	0.512	0.209
	L-alanyl-glycine	87	0.504	0.649	0.375
	L-asparagine	88	–	0.546	0.548
	L-aspartic acid	89	0.548	0.561	0.439
	L-glutamine	91	0.135	0.153	0.083
	L-serine	93	0.775	0.658	0.579

Appendix 3 $A_{endpoint}$ for substrate use by ERL10630 harvested during exponential phase (EP), stationary phase (SP) and starved state. Dash (–) indicates substrates tested but not utilised. Results are the average of duplicates.

Sub-class	Substrates	PM1	Endpoint ($A_{endpoint}$)		
			EP	SP	Starved
Glycosides	α-methyl-D-glucoside	6	0.673	0.708	0.647
	β-methyl-D-glucoside	7	–	0.108	–
Monosaccharides	D-fructose	8	0.542	0.538	0.506
	D-galactose	9	0.746	0.767	0.726
	D-galacturonic acid	10	0.766	0.846	0.550
	D-gluconic acid	11	0.738	0.716	0.704
	D-mannose	13	0.682	0.632	0.506
	D-ribose	15	0.668	0.645	0.688
	D-xylose	16	0.534	0.553	0.347
	L-arabinose	17	0.456	0.501	0.381
	L-fucose	18	0.555	0.569	0.598
	L-rhamnose	20	0.158	0.165	0.092
	N-acetyl-D-glucosamine	21	0.481	0.482	0.345
	N-acetyl-β-D-mannosamine	22	0.330	0.551	–
	α-D-glucose	23	0.412	0.467	0.250
Oligosaccharides	D-melibiose	25	0.711	0.658	0.501
	D-trehalose	26	0.720	0.777	0.562
	Lactulose	27	0.347	0.369	–
	Maltose	28	0.654	0.689	0.455
	Maltotriose	29	0.651	0.666	0.387
	Sucrose	30	0.660	0.630	0.567
	α-D-lactose	31	0.745	0.695	0.596
Sugar alcohols	D-mannitol	33	0.495	0.562	0.416
	Glycerol	36	0.630	0.695	0.694
Sugar phosphates	D,L-α-glycerol-phosphate	38	0.606	0.556	0.334
	Fructose-6-phosphate	39	0.703	0.697	0.690
	Glucose-1-phosphate	40	0.667	0.658	0.806
	Glucose-6-phosphate	41	0.768	0.776	0.719
Acetic acids	Acetic acid	42	0.391	0.377	0.206
Butyric acids	α-hydroxy Butyric acid	44	0.150	0.087	–
Dicarboxylic acids	Bromo succinic acid	46	0.292	0.330	0.142
	D,L-malic acid	47	0.535	0.395	0.365
	D-malic acid	48	0.517	0.456	0.293
	Fumaric acid	49	0.375	0.344	0.271
	L-malic acid	50	0.575	0.461	0.297
	Mono methyl succinate	51	–	0.108	–
	Succinic acid	53	0.475	0.409	0.371
Hydroxy acids	L-lactic acid	56	0.625	0.671	0.476
Keto acids	Methyl pyruvate	58	0.722	0.735	0.431
	Pyruvic acid	59	0.745	0.659	0.412
Propionates	Propionic acid	62	0.217	0.251	0.101
Sugar acids	D-glucuronic acid	64	0.709	0.676	0.601

Sub-class	Substrates	PM1	Endpoint ($A_{endpoint}$)		
			EP	SP	Starved
	Glucuronamide	66	0.345	0.307	0.201
Nucleosides	2-deoxy adenosine	72	0.933	0.908	0.549
	Adenosine	73	0.855	0.815	0.536
	Inosine	74	0.881	0.794	0.642
	Thymidine	75	0.842	0.756	0.433
	Uridine	76	0.837	0.782	0.506
Amino acids	D-alanine	79	0.625	0.549	0.274
	Glycyl-L-glutamic acid	84	–	0.079	–
	Glycyl-L-proline	85	0.150	0.164	–
	L-alanine	86	0.634	0.607	0.253
	L-alanyl-glycine	87	0.695	0.749	0.367
	L-asparagine	88	0.256	0.527	0.523
	L-aspartic acid	89	0.517	0.497	0.440
	L-glutamine	91	0.197	0.245	0.116
	L-serine	93	0.734	0.745	0.709

Appendix 4 $A_{endpoint}$ for substrate use by ERL10780 harvested during exponential phase (EP), stationary phase (SP) and starved state. Dash (–) indicates substrates tested but not utilised. Results are the average of duplicates.

Sub-class	Substrates	PM1	Endpoint ($A_{endpoint}$)		
			EP	SP	Starved
Glycosides	α-methyl-D-glucoside	6	0.752	0.790	0.730
Monosaccharides	D-fructose	8	0.480	0.655	0.547
	D-galactose	9	0.738	0.898	0.711
	D-galacturonic acid	10	0.781	0.877	0.594
	D-gluconic acid	11	0.664	0.910	0.856
	D-mannose	13	0.687	0.671	0.696
	D-ribose	15	0.672	0.738	0.761
	D-xylose	16	0.426	0.568	0.578
	L-arabinose	17	0.397	0.495	0.460
	L-fucose	18	0.565	0.613	0.661
	L-rhamnose	20	0.290	0.533	0.272
	N-acetyl-D-glucosamine	21	0.524	0.437	0.498
	N-acetyl-β-D-mannosamine	22	0.373	0.293	–
	α-D-glucose	23	0.443	0.520	0.469
Oligosaccharides	D-melibiose	25	0.743	0.740	0.543
	D-trehalose	26	0.737	0.902	0.694
	Lactulose	27	0.577	0.685	0.132
	Maltose	28	0.621	0.748	0.589
	Maltotriose	29	0.520	0.618	0.380
	Sucrose	30	0.824	0.935	0.747
	α-D-lactose	31	0.589	0.703	0.496
Sugar alcohols	D-mannitol	33	0.506	0.606	0.506
	Dulcitol	35	0.461	0.689	0.417
	Glycerol	36	0.642	0.734	0.698
Sugar phosphates	D,L-α-glycerol-phosphate	38	0.581	0.623	0.474
	Fructose-6-phosphate	39	0.664	0.742	0.692
	Glucose-1-phosphate	40	0.672	0.779	0.822
	Glucose-6-phosphate	41	0.751	0.872	0.730
Acetic acids	Acetic acid	42	0.399	0.361	0.253
Dicarboxylic acids	Bromo succinic acid	46	0.447	0.562	0.283
	D,L-malic acid	47	0.535	0.639	0.504
	D-malic acid	48	0.575	0.774	0.293
	Fumaric acid	49	0.431	0.523	0.416
	L-malic acid	50	0.642	0.757	0.420
	Succinic acid	53	0.540	0.649	0.502
Hydroxy acids	L-lactic acid	56	0.687	0.807	0.493
Keto acids	Methyl pyruvate	58	0.793	0.869	0.519
	Pyruvic acid	59	0.725	0.839	0.482
Propionates	Propionic acid	62	–	0.319	–
Sugar acids	D-glucuronic acid	64	0.699	0.810	0.878
	Glucuronamide	66	0.395	0.378	0.321
	L-galactonic acid-γ-lactone	67	0.387	0.807	0.524

Sub-class	Substrates	PM1	Endpoint ($A_{endpoint}$)		
			EP	SP	Starved
	Mucic acid	68	–	0.596	0.124
Nucleosides	2-deoxy adenosine	72	0.890	0.938	0.653
	Adenosine	73	0.838	1.007	0.604
	Inosine	74	0.887	0.945	0.717
	Thymidine	75	1.002	1.024	0.567
	Uridine	76	0.864	0.992	0.567
Amino acids	D-alanine	79	0.662	0.687	0.390
	Glycyl-L-aspartic acid	83	–	0.214	–
	Glycyl-L-glutamic acid	84	–	0.200	–
	Glycyl-L-proline	85	–	0.264	0.132
	L-alanine	86	0.603	0.600	0.207
	L-alanyl-glycine	87	0.585	0.635	0.377
	L-asparagine	88	0.366	0.665	0.623
	L-aspartic acid	89	0.553	0.749	0.570
	L-glutamic acid	90	–	0.335	–
	L-glutamine	91	0.421	0.689	0.322
	L-proline	92	0.354	0.628	0.322
	L-serine	93	0.704	0.777	0.540
	L-threonine	94	–	0.276	–

Appendix 5 $A_{endpoint}$ for substrate use by H11+ harvested during exponential phase (EP), stationary phase (SP) and starved state. Dash (–) indicates substrates tested but not utilised. Results are the average of duplicates.

Sub-class	Substrates	PM1	Endpoint ($A_{endpoint}$)		
			EP	SP	Starved
Glycosides	α-methyl-D-glucoside	6	0.780	0.846	0.826
	β-methyl-D-glucoside	7			
Monosaccharides	D-fructose	8	0.402	0.407	0.481
	D-galactose	9	0.803	0.764	0.774
	D-galacturonic acid	10	0.775	0.869	0.671
	D-gluconic acid	11	0.781	0.921	0.724
	D-mannose	13	0.534	0.627	0.611
	D-ribose	15	0.534	0.540	0.847
	D-xylose	16	0.455	0.352	0.516
	L-arabinose	17	0.482	0.502	0.520
	L-fucose	18	0.683	0.754	0.647
	L-lyxose	19			
	L-rhamnose	20			
	N-acetyl-D-glucosamine	21	0.563	0.668	0.571
	N-acetyl-β-D-mannosamine	22	–	0.298	0.108
	α-D-glucose	23	0.457	0.600	0.427
Oligosaccharides	D-melibiose	25	0.755	0.809	0.788
	D-trehalose	26	0.434	0.529	0.530
	Lactulose	27	0.444	0.570	0.459
	Maltose	28	0.574	0.683	0.662
	Maltotriose	29	0.424	0.579	0.538
	α-D-lactose	31	0.485	0.561	0.480
Sugar alcohols	D-mannitol	33	0.476	0.504	0.566
	D-sorbitol	34	0.684	0.647	–
	Dulcitol	35	0.651	0.618	–
	Glycerol	36	0.503	0.434	0.626
Sugar phosphates	D,L-α-glycerol-phosphate	38	0.565	0.638	0.541
	Fructose-6-phosphate	39	0.813	0.903	0.687
	Glucose-1-phosphate	40	0.914	0.976	0.790
	Glucose-6-phosphate	41	0.768	0.921	0.670
Acetic acids	Acetic acid	42	0.636	0.579	0.414
Aldehydic acids	Glyoxylic acid	43	0.359	0.376	–
Butyric acids	α-hydroxy Butyric acid	44	0.184	–	–
	α-keto-butyric acid	45	0.316	0.175	–
Dicarboxylic acids	Bromo succinic acid	46	0.611	0.579	0.478
	D,L-malic acid	47	0.702	0.825	0.701
	D-malic acid	48	0.729	0.735	0.668
	Fumaric acid	49	0.701	0.761	0.726
	L-malic acid	50	0.735	0.909	0.672
	Mono methyl succinate	51	0.273	0.256	–
	Succinic acid	53	0.575	0.682	0.680
Glycolates	Glycolic acid	55	0.569	0.583	–

Sub-class	Substrates	PM1	Endpoint ($A_{endpoint}$)		
			EP	SP	Starved
Hydroxy acids	L-lactic acid	56	0.678	0.657	0.581
Keto acids	Methyl pyruvate	58	0.662	0.922	0.612
	Pyruvic acid	59	0.702	0.837	0.609
Propionates	Propionic acid	62	0.503	0.452	0.293
Sugar acids	D-galactonic acid-γ-lactone	63	0.709	0.864	–
	D-glucuronic acid	64	0.928	0.895	0.758
	D-saccharic acid	65	0.678	0.746	–
	Glucuronamide	66	–	–	0.210
	L-galactonic acid-γ-lactone	67	0.752	0.862	0.642
	Mucic acid	68	0.844	0.929	–
Nucleosides	2-deoxy adenosine	72	0.884	1.066	0.825
	Adenosine	73	0.968	1.024	0.767
	Inosine	74	0.891	1.079	0.861
	Thymidine	75	0.742	1.061	0.741
	Uridine	76	0.614	0.807	0.497
Amino acids	D-alanine	79	0.727	0.778	0.616
	D-serine	81	0.715	0.810	–
	Glycyl-L-aspartic acid	83	0.367	0.474	–
	Glycyl-L-glutamic acid	84	0.257	–	–
	Glycyl-L-proline	85	0.430	0.381	–
	L-alanine	86	0.636	0.755	0.570
	L-alanyl-glycine	87	0.687	0.822	0.617
	L-asparagine	88	–	0.724	0.723
	L-aspartic acid	89	0.639	0.757	0.759
	L-glutamine	91	0.250	0.221	–
	L-serine	93	0.708	0.771	0.688

Appendix 6 $A_{endpoint}$ for substrate use by H11- harvested during exponential phase (EP), stationary phase (SP) and starved state. Dash (–) indicates substrates tested but not utilised. Results are the average of duplicates.

Sub-class	Substrates	PM1	Endpoint ($A_{endpoint}$)		
			EP	SP	Starved
Glycosides	α-methyl-D-glucoside	6	0.624	0.620	0.563
Monosaccharides	D-fructose	8	0.486	0.484	0.460
	D-galactose	9	0.677	0.721	0.554
	D-galacturonic acid	10	0.528	0.674	0.716
	D-gluconic acid	11	0.683	0.754	0.619
	D-mannose	13	0.493	0.673	0.504
	D-ribose	15	0.593	0.555	0.597
	D-xylose	16	0.391	0.357	0.484
	L-arabinose	17	0.331	0.335	0.375
	L-fucose	18	0.636	0.486	0.508
	N-acetyl-D-glucosamine	21	0.520	0.598	0.452
	N-acetyl-β-D-mannosamine	22	–	–	0.082
	α-D-glucose	23	0.400	0.532	0.368
Oligosaccharides	D-melibiose	25	0.528	0.699	0.552
	D-trehalose	26	0.650	0.645	0.496
	Lactulose	27	0.151	0.312	0.142
	Maltose	28	0.543	0.758	0.525
	Maltotriose	29	0.548	0.651	0.422
	Sucrose	30	0.614	0.619	0.594
	α-D-lactose	31	0.517	0.888	0.533
Sugar alcohols	D-mannitol	33	0.450	0.718	0.440
	Glycerol	36	0.499	0.233	0.555
Sugar phosphates	D,L-α-glycerol-phosphate	38	0.270	–	0.340
	Fructose-6-phosphate	39	0.519	0.665	0.520
	Glucose-1-phosphate	40	0.968	0.750	0.634
	Glucose-6-phosphate	41	0.843	0.626	0.603
Acetic acids	Acetic acid	42	0.195	0.344	0.188
Dicarboxylic acids	Bromo succinic acid	46	–	–	0.124
	D,L-malic acid	47	0.347	0.279	0.374
	D-malic acid	48	0.482	0.451	0.299
	Fumaric acid	49	0.212	0.253	0.286
	L-malic acid	50	0.334	0.338	0.324
	Succinic acid	53	0.368	0.229	0.333
Hydroxy acids	L-lactic acid	56	0.666	0.665	0.515
Keto acids	Methyl pyruvate	58	0.741	0.799	0.456
	Pyruvic acid	59	0.470	0.533	0.506
Propionates	Propionic acid	62	–	–	0.111
Sugar acids	D-glucuronic acid	64	0.732	0.727	0.609
	Glucuronamide	66	–	–	0.324
	L-galactonic acid-γ-lactone	67	0.551	0.733	0.612
Nucleosides	2-deoxy adenosine	72	0.682	1.160	0.623
	Adenosine	73	0.785	0.879	0.561

Sub-class	Substrates	PM1	Endpoint ($A_{endpoint}$)		
			EP	SP	Starved
	Inosine	74	0.918	0.958	0.629
	Thymidine	75	0.476	0.669	0.659
	Uridine	76	0.707	0.794	0.557
Amino acids	D-alanine	79	0.182	0.253	0.225
	L-alanine	86	0.426	0.197	0.210
	L-alanyl-glycine	87	–	–	0.289
	L-asparagine	88	–	0.536	0.428
	L-aspartic acid	89	0.221	0.407	0.382
	L-serine	93	0.678	0.375	0.610

Appendix 7 λ for substrate use by ERL10621 harvested during exponential phase (EP), stationary phase (SP) and starved state. Dash (–) indicates substrates tested but not utilised. Results are the average of duplicates.

Sub-class	Substrates	PM1	λ (hr)		
			EP	SP	Starved
Glycosides	α-methyl-D-glucoside	6	2.5	1.6	6.8
Monosaccharides	D-fructose	8	0.9	1.4	5.6
	D-galactose	9	1.4	2.6	6.5
	D-galacturonic acid	10	1.6	1.5	6.9
	D-gluconic acid	11	1.3	1.5	6.0
	D-mannose	13	1.3	1.4	5.5
	D-ribose	15	1.9	2.3	9.6
	D-xylose	16	1.5	2.3	8.1
	L-arabinose	17	1.5	2.0	7.6
	L-fucose	18	1.9	1.8	6.9
	L-rhamnose	20	–	17.1	–
	N-acetyl-D-glucosamine	21	1.0	1.5	5.6
	N-acetyl-β-D-mannosamine	22	4.8	1.4	–
	α-D-glucose	23	0.9	1.5	5.4
Oligosaccharides	D-melibiose	25	2.1	1.9	7.8
	D-trehalose	26	1.1	1.4	5.6
	Lactulose	27	–	16.5	21.8
	Maltose	28	1.5	1.5	5.9
	Maltotriose	29	1.5	1.4	5.6
	Sucrose	30	2.3	2.9	7.3
	α-D-lactose	31	1.5	1.5	5.9
Sugar alcohols	D-mannitol	33	0.8	1.4	5.5
	Glycerol	36	1.0	1.5	6.0
Sugar phosphates	D,L-α-glycerol-phosphate	38	1.1	1.3	6.8
	Fructose-6-phosphate	39	2.0	1.8	9.8
	Glucose-1-phosphate	40	2.1	1.5	6.1
	Glucose-6-phosphate	41	1.1	1.5	7.1
Acetic acids	Acetic acid	42	2.3	1.5	7.1
Dicarboxylic acids	Bromo succinic acid	46	6.3	4.0	13.8
	D,L-malic acid	47	2.3	1.6	7.0
	D-malic acid	48	3.5	1.9	7.8
	Fumaric acid	49	3.4	1.5	6.0
	L-malic acid	50	2.6	1.8	6.4
	Succinic acid	53	2.4	1.4	6.1
Hydroxy acids	L-lactic acid	56	1.6	1.4	5.9
Keto acids	Methyl pyruvate	58	1.5	1.5	5.9
	Pyruvic acid	59	2.0	1.5	7.0
Propionates	Propionic acid	62	7.9	6.0	–
Sugar acids	D-glucuronic acid	64	1.6	1.5	6.9
	Glucuronamide	66	1.6	1.5	6.6
	L-galactonic acid-γ-lactone	67	2.3	1.5	6.1
Nucleosides	2-deoxy adenosine	72	1.3	1.4	7.1

Sub-class	Substrates	PM1	λ (hr)		
			EP	SP	Starved
	Adenosine	73	1.1	1.4	6.4
	Inosine	74	0.6	1.1	6.6
	Thymidine	75	1.0	1.8	7.8
	Uridine	76	1.4	1.4	12.8
Amino acids	D-alanine	79	2.1	1.5	6.4
	Glycyl-L-proline	85	–	1.5	–
	L-alanine	86	3.4	2.0	8.8
	L-alanyl-glycine	87	3.3	1.8	7.4
	L-asparagine	88	–	1.9	7.4
	L-aspartic acid	89	3.0	1.9	7.1
	L-glutamine	91	1.8	1.4	6.8
	L-serine	93	1.8	1.5	7.3

Appendix 8 λ for substrate use by ERL10630 harvested during exponential phase (EP), stationary phase (SP) and starved state. Dash (–) indicates substrates tested but not utilised. Results are the average of duplicates.

Sub-class	Substrates	PM1	λ (hr)		
			EP	SP	Starved
Glycosides	α-methyl-D-glucoside	6	2.3	2.1	6.5
	β-methyl-D-glucoside	7	–	17.0	–
Monosaccharides	D-fructose	8	1.3	1.4	5.6
	D-galactose	9	1.5	1.9	6.4
	D-galacturonic acid	10	1.5	1.5	6.9
	D-gluconic acid	11	1.4	1.6	5.3
	D-mannose	13	1.3	1.4	5.5
	D-ribose	15	1.9	2.4	9.0
	D-xylose	16	1.6	2.3	7.9
	L-arabinose	17	1.6	2.1	7.3
	L-fucose	18	2.0	1.9	6.9
	L-rhamnose	20	13.3	14.5	19.1
	N-acetyl-D-glucosamine	21	1.3	1.8	5.3
	N-acetyl-β-D-mannosamine	22	2.5	1.5	–
	α-D-glucose	23	1.0	1.6	5.3
Oligosaccharides	D-melibiose	25	1.6	1.9	7.4
	D-trehalose	26	1.4	1.4	5.4
	Lactulose	27	18.4	17.5	–
	Maltose	28	1.5	1.6	5.8
	Maltotriose	29	1.4	1.8	5.6
	Sucrose	30	2.0	2.5	7.0
	α-D-lactose	31	1.5	1.8	5.9
Sugar alcohols	D-mannitol	33	1.1	1.3	5.1
	Glycerol	36	1.3	1.4	5.9
Sugar phosphates	D,L-α-glycerol-phosphate	38	1.3	1.3	6.5
	Fructose-6-phosphate	39	2.1	2.0	8.5
	Glucose-1-phosphate	40	2.0	1.4	6.0
	Glucose-6-phosphate	41	1.3	1.9	6.6
Acetic acids	Acetic acid	42	2.1	1.6	6.9
Butyric acids	α-hydroxy Butyric acid	44	9.1	9.6	–
Dicarboxylic acids	Bromo succinic acid	46	2.3	2.1	13.0
	D,L-malic acid	47	2.3	1.9	6.9
	D-malic acid	48	2.5	2.0	7.4
	Fumaric acid	49	2.8	1.9	5.8
	L-malic acid	50	2.1	1.9	6.3
	Mono methyl succinate	51	–	1.8	–
	Succinic acid	53	2.1	1.6	5.3
Hydroxy acids	L-lactic acid	56	1.5	1.3	5.9
Keto acids	Methyl pyruvate	58	1.5	1.9	6.0
	Pyruvic acid	59	1.9	1.5	7.1
Propionates	Propionic acid	62	7.5	7.0	11.5
	D-glucuronic acid	64	1.6	1.5	6.3

Sub-class	Substrates	PM1	λ (hr)		
			EP	SP	Starved
Sugar acids	Glucuronamide	66	1.5	1.8	6.4
Nucleosides	2-deoxy adenosine	72	1.3	1.1	6.9
	Adenosine	73	1.1	1.3	6.1
	Inosine	74	1.0	1.1	6.3
	Thymidine	75	1.0	1.9	7.6
	Uridine	76	1.3	1.4	13.1
Amino acids	D-alanine	79	1.9	1.8	6.8
	Glycyl-L-glutamic acid	84	–	1.8	–
	Glycyl-L-proline	85	3.0	1.8	–
	L-alanine	86	2.5	2.1	8.8
	L-alanyl-glycine	87	2.4	1.9	7.1
	L-asparagine	88	9.9	2.1	6.9
	L-aspartic acid	89	2.8	2.1	6.8
	L-glutamine	91	1.9	1.8	6.9
	L-serine	93	1.6	1.6	7.1

Appendix 9 λ for substrate use by ERL10780 harvested during exponential phase (EP), stationary phase (SP) and starved state. Dash (–) indicates substrates tested but not utilised. Results are the average of duplicates.

Sub-class	Substrates	PM1	λ (hr)		
			EP	SP	Starved
Glycosides	α-methyl-D-glucoside	6	2.4	2.1	7.8
Monosaccharides	D-fructose	8	1.3	1.4	6.1
	D-galactose	9	1.5	1.8	7.0
	D-galacturonic acid	10	1.5	1.8	7.5
	D-gluconic acid	11	1.5	1.3	6.0
	D-mannose	13	1.3	1.5	5.6
	D-ribose	15	2.3	2.3	9.1
	D-xylose	16	1.9	2.3	8.0
	L-arabinose	17	2.0	2.1	7.6
	L-fucose	18	1.9	1.8	7.4
	L-rhamnose	20	9.8	8.6	13.0
	N-acetyl-D-glucosamine	21	1.3	1.8	5.5
	N-acetyl-β-D-mannosamine	22	8.8	4.3	–
	α-D-glucose	23	1.1	1.5	5.6
Oligosaccharides	D-melibiose	25	2.0	2.1	8.4
	D-trehalose	26	1.4	1.4	6.1
	Lactulose	27	13.6	13.0	20.4
	Maltose	28	1.5	1.8	6.4
	Maltotriose	29	1.5	1.5	5.9
	Sucrose	30	1.9	2.4	7.8
	α-D-lactose	31	1.5	1.6	6.3
Sugar alcohols	D-mannitol	33	1.0	1.3	5.6
	Dulcitol	35	15.6	9.5	12.8
	Glycerol	36	1.3	1.3	6.1
Sugar phosphates	D,L-α-glycerol-phosphate	38	1.4	1.4	6.8
	Fructose-6-phosphate	39	2.8	2.3	7.9
Sugar phosphates	Glucose-1-phosphate	40	1.9	1.4	6.4
	Glucose-6-phosphate	41	1.9	2.3	6.5
Acetic acids	Acetic acid	42	2.0	1.9	7.9
Dicarboxylic acids	Bromo succinic acid	46	2.1	2.3	7.9
	D,L-malic acid	47	2.5	2.0	7.6
	D-malic acid	48	3.3	2.1	8.9
	Fumaric acid	49	2.9	2.3	7.4
	L-malic acid	50	2.5	2.3	7.3
	Succinic acid	53	2.3	1.6	6.8
Hydroxy acids	L-lactic acid	56	1.6	1.4	6.6
Keto acids	Methyl pyruvate	58	1.8	1.8	6.0
	Pyruvic acid	59	2.3	1.5	7.0
Propionates	Propionic acid	62	–	7.8	–
Sugar acids	D-glucuronic acid	64	1.6	1.6	6.6
	Glucuronamide	66	1.6	1.6	6.6
	L-galactonic acid-γ-lactone	67	13.0	2.3	6.6

Sub-class	Substrates	PM1	λ (hr)		
			EP	SP	Starved
	Mucic acid	68	–	5.0	18.5
Nucleosides	2-deoxy adenosine	72	1.3	1.3	7.6
	Adenosine	73	1.3	1.4	6.9
	Inosine	74	1.1	1.1	7.1
	Thymidine	75	1.1	1.5	7.8
	Uridine	76	1.3	1.3	10.9
Amino acids	D-alanine	79	2.0	2.1	7.1
	Glycyl-L-aspartic acid	83	–	1.8	–
	Glycyl-L-glutamic acid	84	–	1.8	–
	Glycyl-L-proline	85	–	2.0	9.1
	L-alanine	86	2.9	2.6	10.9
	L-alanyl-glycine	87	3.1	2.3	8.5
	L-asparagine	88	8.8	2.1	8.1
	L-aspartic acid	89	3.0	2.3	7.6
	L-glutamic acid	90	–	10.1	–
	L-glutamine	91	8.3	4.8	7.0
	L-proline	92	4.5	5.5	10.5
	L-serine	93	1.6	1.5	7.8
	L-threonine	94	–	4.5	–

Appendix 10 λ for substrate use by H11+ harvested during exponential phase (EP), stationary phase (SP) and starved state. Dash (–) indicates substrates tested but not utilised. Results are the average of duplicates.

Sub-class	Substrates	PM1	λ (hr)		
			EP	SP	Starved
Glycosides	α-methyl-D-glucoside	6	1.6	1.5	5.0
Monosaccharides	D-fructose	8	1.9	1.6	4.5
	D-galactose	9	1.5	1.6	4.8
	D-galacturonic acid	10	1.8	1.8	3.0
	D-gluconic acid	11	1.9	1.8	4.5
	D-mannose	13	1.8	1.8	4.6
	D-ribose	15	2.4	2.4	6.3
	D-xylose	16	2.5	2.4	5.8
	L-arabinose	17	2.3	2.0	5.3
	L-fucose	18	2.0	1.6	5.3
	N-acetyl-D-glucosamine	21	1.8	13.3	4.6
	N-acetyl-β-D-mannosamine	22	–	15.0	4.6
	α-D-glucose	23	1.5	1.5	4.4
Oligosaccharides	D-melibiose	25	1.8	1.6	5.3
	D-trehalose	26	1.9	1.5	4.6
	Lactulose	27	11.5	11.9	16.4
	Maltose	28	1.6	1.5	4.5
	Maltotriose	29	1.6	1.6	4.4
	Sucrose	30	–	–	–
	α-D-lactose	31	1.8	1.5	4.8
Sugar alcohols	D-mannitol	33	1.5	1.5	4.5
	D-sorbitol	34	1.5	1.4	–
	Dulcitol	35	9.3	10.4	–
	Glycerol	36	1.4	1.5	4.8
Sugar phosphates	D,L-α-glycerol-phosphate	38	1.3	1.0	4.6
	Fructose-6-phosphate	39	2.0	1.8	5.8
	Glucose-1-phosphate	40	1.8	1.0	4.5
	Glucose-6-phosphate	41	3.5	1.5	4.5
Acetic acids	Acetic acid	42	1.8	1.8	5.5
Aldehydic acids	Glyoxylic acid	43	12.5	6.6	–
Butyric acids	α-hydroxy Butyric acid	44	3.9	–	–
	α-keto-butyric acid	45	10.5	6.9	–
Dicarboxylic acids	Bromo succinic acid	46	1.9	2.1	5.9
	D,L-malic acid	47	1.8	1.6	5.3
	D-malic acid	48	1.6	1.8	5.3
	Fumaric acid	49	1.9	1.6	5.0
	L-malic acid	50	1.8	1.8	5.1
	Mono methyl succinate	51	1.5	1.5	–
	Succinic acid	53	1.5	1.4	5.0
Glycolates	Glycolic acid	55	3.1	1.9	–
Hydroxy acids	L-lactic acid	56	1.3	1.0	4.5
Keto acids	Methyl pyruvate	58	1.9	1.6	4.6

Sub-class	Substrates	PM1	λ (hr)		
			EP	SP	Starved
	Pyruvic acid	59	1.8	1.6	3.1
Propionates	Propionic acid	62	5.0	4.9	6.9
Sugar acids	D-galactonic acid-γ-lactone	63	2.0	1.8	–
	D-glucuronic acid	64	1.9	1.8	4.9
	D-saccharic acid	65	5.0	4.8	–
	Glucuronamide	66	–	–	14.4
	L-galactonic acid-γ-lactone	67	1.9	1.9	3.4
	Mucic acid	68	1.8	1.6	–
Nucleosides	2-deoxy adenosine	72	1.4	1.4	5.1
	Adenosine	73	1.3	1.4	5.0
	Inosine	74	1.4	1.4	4.9
	Thymidine	75	1.8	1.6	5.9
	Uridine	76	6.3	8.8	9.5
Amino acids	D-alanine	79	1.5	1.4	5.3
	D-serine	81	1.6	1.4	–
	Glycyl-L-aspartic acid	83	1.6	1.5	–
	Glycyl-L-glutamic acid	84	1.8	–	–
	Glycyl-L-proline	85	1.8	1.5	–
	L-alanine	86	1.8	1.8	6.1
	L-alanyl-glycine	87	1.8	1.5	5.6
	L-asparagine	88	–	1.6	5.4
	L-aspartic acid	89	1.8	1.8	5.4
	L-glutamine	91	13.0	10.5	–

Appendix 11 λ for substrate use by H11- harvested during exponential phase (EP), stationary phase (SP) and starved state. Dash (–) indicates substrates tested but not utilised. Results are the average of duplicates.

Sub-class	Substrates	PM1	λ (hr)		
			EP	SP	Starved
Glycosides	α-methyl-D-glucoside	6	3.4	2.1	5.4
Monosaccharides	D-fructose	8	1.3	1.4	3.8
	D-galactose	9	1.9	4.9	4.8
	D-galacturonic acid	10	1.8	1.4	5.0
	D-gluconic acid	11	1.6	1.5	4.0
	D-mannose	13	1.4	1.3	4.0
	D-ribose	15	2.9	2.9	6.6
	D-xylose	16	2.5	2.5	6.1
	L-arabinose	17	2.3	2.0	5.1
	L-fucose	18	2.0	1.9	5.3
	N-acetyl-D-glucosamine	21	1.5	1.3	3.9
	α-D-glucose	23	1.3	1.3	3.8
Oligosaccharides	D-melibiose	25	2.5	2.0	5.6
	D-trehalose	26	1.5	1.5	4.0
	Lactulose	27	20.0	18.1	19.1
	Maltose	28	1.9	1.6	4.1
	Maltotriose	29	1.6	1.4	3.9
	Sucrose	30	7.0	10.4	5.5
	α-D-lactose	31	1.8	1.6	4.0
Sugar alcohols	D-mannitol	33	1.1	1.3	3.8
	Glycerol	36	1.5	1.5	4.4
Sugar phosphates	D,L-α-glycerol-phosphate	38	13.0	–	4.8
	Fructose-6-phosphate	39	3.0	2.1	5.0
Sugar phosphates	Glucose-1-phosphate	40	2.3	1.6	4.4
	Glucose-6-phosphate	41	1.3	1.3	3.5
Acetic acids	Acetic acid	42	6.5	3.5	5.8
Dicarboxylic acids	Bromo succinic acid	46	–	–	12.9
	D,L-malic acid	47	5.4	7.0	5.4
	D-malic acid	48	6.0	9.5	5.9
	Fumaric acid	49	6.9	7.5	5.3
	L-malic acid	50	7.0	6.9	5.3
	Succinic acid	53	7.6	7.5	5.3
Hydroxy acids	L-lactic acid	56	2.0	1.6	4.6
Keto acids	Methyl pyruvate	58	1.3	1.4	4.8
	Pyruvic acid	59	2.3	1.9	4.6
Propionates	Propionic acid	62	–	–	9.3
Sugar acids	D-glucuronic acid	64	1.9	1.8	4.9
	Glucuronamide	66	–	–	4.6
	L-galactonic acid-γ-lactone	67	2.5	2.0	4.8
Nucleosides	2-deoxy adenosine	72	1.5	1.3	4.9
	Adenosine	73	1.4	1.3	4.5
	Inosine	74	1.1	1.3	4.1

Sub-class	Substrates	PM1	λ (hr)		
			EP	SP	Starved
	Thymidine	75	1.4	1.6	5.6
	Uridine	76	2.0	5.3	4.6
Amino acids	D-alanine	79	14.5	14.6	5.4
	L-alanine	86	8.0	13.8	6.1
	L-alanyl-glycine	87	–	–	6.0
	L-asparagine	88	–	2.9	6.0
	L-aspartic acid	89	14.8	3.1	6.1
	L-serine	93	2.0	2.1	5.3

Appendix 12 μ_{exp} for substrate use by ERL10621 harvested during exponential phase (EP), stationary phase (SP) and starved state. Dash (–) indicates substrates tested but not utilised. Results are the average of duplicates.

Sub-class	Substrates	PM1	μ_{exp} ($A_{activity}$/hr)		
			EP	SP	Starved
Glycosides	α-methyl-D-glucoside	6	0.054	0.049	0.053
	β-methyl-D-glucoside	7	–	0.009	–
Monosaccharides	D-fructose	8	0.062	0.055	0.068
	D-galactose	9	0.052	0.056	0.053
	D-galacturonic acid	10	0.066	0.067	0.057
	D-gluconic acid	11	0.087	0.071	0.086
	D-mannose	13	0.062	0.068	0.076
	D-ribose	15	0.057	0.059	0.063
	D-xylose	16	0.046	0.070	0.065
	L-arabinose	17	0.029	0.049	0.045
	L-fucose	18	0.051	0.049	0.059
	L-rhamnose	20	–	0.017	–
	N-acetyl-D-glucosamine	21	0.053	0.057	0.064
	N-acetyl-β-D-mannosamine	22	0.018	0.055	–
	α-D-glucose	23	0.063	0.066	0.062
Oligosaccharides	D-melibiose	25	0.059	0.060	0.063
	D-trehalose	26	0.063	0.075	0.064
	Lactulose	27	–	0.055	0.017
	Maltose	28	0.078	0.081	0.076
	Maltotriose	29	0.049	0.076	0.063
	Sucrose	30	0.068	0.100	0.070
	α-D-lactose	31	0.047	0.070	0.042
Sugar alcohols	D-mannitol	33	0.052	0.061	0.060
	Glycerol	36	0.048	0.048	0.052
Sugar phosphates	D,L-α-glycerol-phosphate	38	0.053	0.048	0.039
	Fructose-6-phosphate	39	0.083	0.200	0.115
	Glucose-1-phosphate	40	0.070	0.064	0.103
	Glucose-6-phosphate	41	0.098	0.115	0.191
Acetic acids	Acetic acid	42	0.029	0.016	0.014
Dicarboxylic acids	Bromo succinic acid	46	0.023	0.021	0.015
	D,L-malic acid	47	0.027	0.022	0.025
	D-malic acid	48	0.027	0.024	0.020
	Fumaric acid	49	0.029	0.018	0.018
	L-malic acid	50	0.028	0.028	0.021
	Succinic acid	53	0.034	0.021	0.027
Hydroxy acids	L-lactic acid	56	0.044	0.074	0.031
Keto acids	Methyl pyruvate	58	0.040	0.066	0.042
	Pyruvic acid	59	0.055	0.054	0.051
Propionates	Propionic acid	62	0.011	0.010	–
Sugar acids	D-glucuronic acid	64	0.064	0.056	0.055
	Glucuronamide	66	0.055	0.071	0.056
	L-galactonic acid-γ-lactone	67	0.046	0.048	0.037

Sub-class	Substrates	PM1	μ_{exp} ($A_{activity}$/hr)		
			EP	SP	Starved
Nucleosides	2-deoxy adenosine	72	0.075	0.076	0.063
	Adenosine	73	0.084	0.090	0.089
	Inosine	74	0.074	0.083	0.090
	Thymidine	75	0.072	0.076	0.074
	Uridine	76	0.069	0.086	0.071
Amino acids	D-alanine	79	0.034	0.027	0.020
	Glycyl-L-proline	85	–	0.057	–
	L-alanine	86	0.028	0.032	0.028
	L-alanyl-glycine	87	0.030	0.042	0.023
	L-asparagine	88	–	0.030	0.036
	L-aspartic acid	89	0.034	0.027	0.025
	L-glutamine	91	0.008	0.027	0.027
	L-serine	93	0.043	0.040	0.040

Appendix 13 μ_{exp} for substrate use by ERL10630 harvested during exponential phase (EP), stationary phase (SP) and starved state. Dash (–) indicates substrates tested but not utilised. Results are the average of duplicates.

Sub-class	Substrates	PM1	μ_{exp} ($A_{activity}$/hr)		
			EP	SP	Starved
Glycosides	α-methyl-D-glucoside	6	0.054	0.054	0.047
	β-methyl-D-glucoside	7	–	0.015	–
Monosaccharides	D-fructose	8	0.067	0.067	0.061
	D-galactose	9	0.060	0.060	0.058
	D-galacturonic acid	10	0.074	0.090	0.063
	D-gluconic acid	11	0.091	0.088	0.079
	D-mannose	13	0.095	0.073	0.072
	D-ribose	15	0.053	0.063	0.060
	D-xylose	16	0.049	0.060	0.053
	L-arabinose	17	0.037	0.057	0.044
	L-fucose	18	0.051	0.057	0.062
	L-rhamnose	20	0.016	0.024	0.038
	N-acetyl-D-glucosamine	21	0.054	0.068	0.053
	N-acetyl-β-D-mannosamine	22	0.018	0.063	–
	α-D-glucose	23	0.062	0.076	0.056
Oligosaccharides	D-melibiose	25	0.072	0.063	0.064
	D-trehalose	26	0.072	0.083	0.065
	Lactulose	27	0.052	0.060	–
	Maltose	28	0.090	0.095	0.062
	Maltotriose	29	0.070	0.073	0.043
	Sucrose	30	0.081	0.078	0.074
	α-D-lactose	31	0.046	0.076	0.040
Sugar alcohols	D-mannitol	33	0.058	0.071	0.052
	Glycerol	36	0.052	0.059	0.057
Sugar phosphates	D,L-α-glycerol-phosphate	38	0.062	0.056	0.034
	Fructose-6-phosphate	39	0.096	0.125	0.101
	Glucose-1-phosphate	40	0.065	0.068	0.103
	Glucose-6-phosphate	41	0.116	0.119	0.096
Acetic acids	Acetic acid	42	0.019	0.018	0.015
Butyric acids	α-hydroxy Butyric acid	44	0.005	0.003	–
Dicarboxylic acids	Bromo succinic acid	46	0.023	0.018	0.019
	D,L-malic acid	47	0.029	0.021	0.025
	D-malic acid	48	0.027	0.028	0.018
	Fumaric acid	49	0.023	0.020	0.018
	L-malic acid	50	0.032	0.044	0.019
	Mono methyl succinate	51	–	0.037	–
	Succinic acid	53	0.029	0.026	0.027
Hydroxy acids	L-lactic acid	56	0.041	0.051	0.042
Keto acids	Methyl pyruvate	58	0.057	0.063	0.050
	Pyruvic acid	59	0.060	0.057	0.052
Propionates	Propionic acid	62	0.010	0.013	0.013
	D-galactonic acid-γ-lactone	63			

Sub-class	Substrates	PM1	μ_{exp} ($A_{activity}$/hr)		
			EP	SP	Starved
Sugar acids	D-glucuronic acid	64	0.066	0.064	0.061
	Glucuronamide	66	0.063	0.054	0.053
Nucleosides	2-deoxy adenosine	72	0.083	0.083	0.056
	Adenosine	73	0.095	0.089	0.076
	Inosine	74	0.092	0.085	0.086
	Thymidine	75	0.078	0.075	0.068
	Uridine	76	0.071	0.068	0.069
Amino acids	D-alanine	79	0.035	0.032	0.017
	Glycyl-L-glutamic acid	84	–	0.016	–
	Glycyl-L-proline	85	0.052	0.047	–
	L-alanine	86	0.035	0.034	0.018
	L-alanyl-glycine	87	0.037	0.050	0.026
	L-asparagine	88	0.019	0.030	0.034
	L-aspartic acid	89	0.030	0.028	0.028
	L-glutamine	91	0.009	0.011	0.017
	L-serine	93	0.045	0.046	0.048

Appendix 14 μ_{exp} for substrate use by ERL10780 harvested during exponential phase (EP), stationary phase (SP) and starved state. Dash (–) indicates substrates tested but not utilised. Results are the average of duplicates.

Sub-class	Substrates	PM1	μ_{exp} ($A_{activity}$/hr)		
			EP	SP	Starved
Glycosides	α-methyl-D-glucoside	6	0.061	0.054	0.056
Monosaccharides	D-fructose	8	0.059	0.061	0.061
	D-galactose	9	0.063	0.072	0.062
	D-galacturonic acid	10	0.094	0.121	0.092
	D-gluconic acid	11	0.095	0.102	0.114
	D-mannose	13	0.075	0.063	0.088
	D-ribose	15	0.054	0.064	0.069
	D-xylose	16	0.041	0.057	0.065
	L-arabinose	17	0.036	0.048	0.052
	L-fucose	18	0.054	0.048	0.071
	L-rhamnose	20	0.020	0.034	0.023
	N-acetyl-D-glucosamine	21	0.055	0.048	0.066
	N-acetyl-β-D-mannosamine	22	0.025	0.016	–
	α-D-glucose	23	0.064	0.063	0.063
Oligosaccharides	D-melibiose	25	0.059	0.052	0.061
	D-trehalose	26	0.076	0.063	0.069
	Lactulose	27	0.059	0.113	0.017
	Maltose	28	0.075	0.070	0.072
	Maltotriose	29	0.059	0.078	0.050
	Sucrose	30	0.078	0.079	0.073
	α-D-lactose	31	0.041	0.041	0.048
Sugar alcohols	D-mannitol	33	0.058	0.058	0.057
	Dulcitol	35	0.038	0.063	0.044
	Glycerol	36	0.055	0.057	0.061
Sugar phosphates	D,L-α-glycerol-phosphate	38	0.053	0.055	0.044
	Fructose-6-phosphate	39	0.094	0.109	0.097
	Glucose-1-phosphate	40	0.072	0.082	0.112
	Glucose-6-phosphate	41	0.103	0.180	0.108
Acetic acids	Acetic acid	42	0.022	0.022	0.019
Dicarboxylic acids	Bromo succinic acid	46	0.028	0.037	0.033
	D,L-malic acid	47	0.027	0.036	0.034
	D-malic acid	48	0.030	0.040	0.024
	Fumaric acid	49	0.023	0.038	0.030
	L-malic acid	50	0.035	0.043	0.030
	Succinic acid	53	0.030	0.031	0.032
Hydroxy acids	L-lactic acid	56	0.046	0.045	0.045
Keto acids	Methyl pyruvate	58	0.056	0.060	0.050
	Pyruvic acid	59	0.055	0.054	0.070
Propionates	Propionic acid	62	–	0.010	–
Sugar acids	D-glucuronic acid	64	0.072	0.093	0.097
	Glucuronamide	66	0.079	0.053	0.053
	L-galactonic acid-γ-lactone	67	0.033	0.074	0.058

Sub-class	Substrates	PM1	μ_{exp} ($A_{activity}$/hr)		
			EP	SP	Starved
	Mucic acid	68	–	0.050	0.011
Nucleosides	2-deoxy adenosine	72	0.101	0.080	0.077
	Adenosine	73	0.090	0.110	0.081
	Inosine	74	0.088	0.091	0.078
	Thymidine	75	0.083	0.087	0.080
	Uridine	76	0.072	0.081	0.059
Amino acids	D-alanine	79	0.038	0.038	0.029
	Glycyl-L-aspartic acid	83	–	0.041	–
	Glycyl-L-glutamic acid	84	–	0.058	–
	Glycyl-L-proline	85	–	0.053	0.025
	L-alanine	86	0.035	0.040	0.019
	L-alanyl-glycine	87	0.034	0.036	0.025
	L-asparagine	88	0.023	0.045	0.050
	L-aspartic acid	89	0.031	0.046	0.039
	L-glutamic acid	90	–	0.021	–
	L-glutamine	91	0.027	0.056	0.019
Amino acids	L-proline	92	0.021	0.041	0.039
	L-serine	93	0.044	0.048	0.038
	L-threonine	94	–	0.020	–

Appendix 15 μ_{exp} for substrate use by H11+ harvested during exponential phase (EP), stationary phase (SP) and starved state. Dash (–) indicates substrates tested but not utilised. Results are the average of duplicates.

Sub-class	Substrates	PM1	μ_{exp} ($A_{activity}$/hr)		
			EP	SP	Starved
Glycosides	α-methyl-D-glucoside	6	0.069	0.076	0.061
Monosaccharides	D-fructose	8	0.020	0.028	0.059
	D-galactose	9	0.055	0.062	0.072
	D-galacturonic acid	10	0.119	0.247	0.073
	D-gluconic acid	11	0.096	0.150	0.095
	D-mannose	13	0.045	0.065	0.068
	D-ribose	15	0.056	0.062	0.095
	D-xylose	16	0.028	0.057	0.054
	L-arabinose	17	0.027	0.036	0.041
	L-fucose	18	0.041	0.043	0.068
	N-acetyl-D-glucosamine	21	0.031	0.093	0.058
	N-acetyl-β-D-mannosamine	22	–	0.025	0.008
	α-D-glucose	23	0.028	0.037	0.055
Oligosaccharides	D-melibiose	25	0.051	0.063	0.082
	D-trehalose	26	0.023	0.049	0.063
	Lactulose	27	0.048	0.080	0.070
	Maltose	28	0.037	0.067	0.061
	Maltotriose	29	0.028	0.044	0.048
	Sucrose	30	–	–	0.039
	α-D-lactose	31	0.036	0.043	0.040
Sugar alcohols	D-mannitol	33	0.025	0.046	0.060
	D-sorbitol	34	0.048	0.055	–
	Dulcitol	35	0.060	0.137	–
	Glycerol	36	0.062	0.073	0.058
Sugar phosphates	D,L-α-glycerol-phosphate	38	0.070	0.075	0.049
	Fructose-6-phosphate	39	0.228	0.238	0.117
	Glucose-1-phosphate	40	0.115	0.136	0.130
	Glucose-6-phosphate	41	0.257	0.243	0.118
Acetic acids	Acetic acid	42	0.032	0.029	0.025
Aldehydic acids	Glyoxylic acid	43	0.027	0.035	–
Butyric acids	α-hydroxy Butyric acid	44	0.013	–	–
	α-keto-butyric acid	45	0.024	0.013	–
Dicarboxylic acids	Bromo succinic acid	46	0.056	0.058	0.048
	D,L-malic acid	47	0.045	0.050	0.041
	D-malic acid	48	0.078	0.057	0.055
	Fumaric acid	49	0.052	0.050	0.056
	L-malic acid	50	0.085	0.062	0.051
	Mono methyl succinate	51	0.065	0.042	–
	Succinic acid	53	0.040	0.041	0.039
Glycolates	Glycolic acid	55	0.044	0.028	–
Hydroxy acids	L-lactic acid	56	0.067	0.045	0.048
Keto acids	Methyl pyruvate	58	0.082	0.133	0.054

Sub-class	Substrates	PM1	μ_{exp} ($A_{activity}$/hr)		
			EP	SP	Starved
	Pyruvic acid	59	0.090	0.092	0.067
Propionates	Propionic acid	62	0.031	0.027	0.013
Sugar acids	D-galactonic acid-γ-lactone	63	0.049	0.045	–
	D-glucuronic acid	64	0.110	0.202	0.110
	D-saccharic acid	65	0.073	0.080	–
	Glucuronamide	66	–	–	0.019
	L-galactonic acid-γ-lactone	67	0.059	0.072	0.046
	Mucic acid	68	0.083	0.110	–
Nucleosides	2-deoxy adenosine	72	0.109	0.107	0.079
	Adenosine	73	0.121	0.109	0.084
	Inosine	74	0.088	0.111	0.080
	Thymidine	75	0.063	0.084	0.072
	Uridine	76	0.052	0.091	0.057
Amino acids	D-alanine	79	0.035	0.038	0.033
	D-serine	81	0.079	0.074	–
	Glycyl-L-aspartic acid	83	0.064	0.067	–
	Glycyl-L-glutamic acid	84	0.077	–	–
	Glycyl-L-proline	85	0.064	0.064	–
	L-alanine	86	0.040	0.047	0.038
	L-alanyl-glycine	87	0.059	0.050	0.038
	L-asparagine	88	–	0.046	0.056
	L-aspartic acid	89	0.052	0.050	0.058
	L-glutamine	91	0.027	0.013	–
	L-serine	93	0.086	0.060	0.047

Appendix 16 μ_{exp} for substrate use by H11- harvested during exponential phase (EP), stationary phase (SP) and starved state. Dash (–) indicates substrates tested but not utilised. Results are the average of duplicates.

Sub-class	Substrates	PM1	μ_{exp} ($A_{activity}$/hr)		
			EP	SP	Starved
Glycosides	α-methyl-D-glucoside	6	0.059	0.075	0.050
Monosaccharides	D-fructose	8	0.046	0.054	0.048
	D-galactose	9	0.056	0.056	0.044
	D-galacturonic acid	10	0.054	0.071	0.068
	D-gluconic acid	11	0.063	0.058	0.073
	D-mannose	13	0.062	0.073	0.052
	D-ribose	15	0.064	0.062	0.056
	D-xylose	16	0.043	0.047	0.049
	L-arabinose	17	0.046	0.067	0.035
	L-fucose	18	0.064	0.084	0.049
	N-acetyl-D-glucosamine	21	0.033	0.055	0.048
	α-D-glucose	23	0.045	0.076	0.045
Oligosaccharides	D-melibiose	25	0.053	0.066	0.052
	D-trehalose	26	0.062	0.064	0.043
	Lactulose	27	0.048	0.061	0.024
	Maltose	28	0.056	0.078	0.059
	Maltotriose	29	0.063	0.090	0.045
	Sucrose	30	0.068	0.062	0.065
	α-D-lactose	31	0.035	0.051	0.038
Sugar alcohols	D-mannitol	33	0.050	0.105	0.047
	Glycerol	36	0.074	0.071	0.047
Sugar phosphates	D,L-α-glycerol-phosphate	38	0.034	–	0.019
	Fructose-6-phosphate	39	0.065	0.110	0.097
	Glucose-1-phosphate	40	0.085	0.059	0.084
	Glucose-6-phosphate	41	0.153	0.178	0.101
Acetic acids	Acetic acid	42	0.016	0.016	0.011
Dicarboxylic acids	Bromo succinic acid	46	–	–	0.019
	D,L-malic acid	47	0.018	0.018	0.025
	D-malic acid	48	0.037	0.030	0.017
	Fumaric acid	49	0.013	0.017	0.019
	L-malic acid	50	0.019	0.016	0.021
	Succinic acid	53	0.021	0.017	0.026
Hydroxy acids	L-lactic acid	56	0.041	0.073	0.028
Keto acids	Methyl pyruvate	58	0.045	0.049	0.032
	Pyruvic acid	59	0.057	0.066	0.059
Propionates	Propionic acid	62	–	–	0.009
Sugar acids	D-galactonic acid-γ-lactone	63			
	D-glucuronic acid	64	0.054	0.054	0.056
	Glucuronamide	66	–	–	0.030
	L-galactonic acid-γ-lactone	67	0.030	0.049	0.036
Nucleosides	2-deoxy adenosine	72	0.065	0.085	0.051
	Adenosine	73	0.087	0.079	0.064

Sub-class	Substrates	PM1	μ_{exp} ($A_{activity}$/hr)		
			EP	SP	Starved
	Inosine	74	0.075	0.075	0.059
	Thymidine	75	0.049	0.055	0.074
	Uridine	76	0.069	0.081	0.058
Amino acids	D-alanine	79	0.018	0.023	0.013
	L-alanine	86	0.035	0.016	0.010
	L-alanyl-glycine	87	–	–	0.015
	L-asparagine	88	–	0.030	0.028
	L-aspartic acid	89	0.023	0.024	0.024
	L-serine	93	0.074	0.040	0.040

Appendix 17 $A_{endpoint}$ for substrate use by NCTC12900 *luxS*$^{-}$ harvested during exponential phase (EP), stationary phase (SP) and starved state. Dash (–) indicates substrates tested but not utilised. Results are the average of duplicates.

Sub-class	Substrates	PM1 & PM2A	$A_{endpoint}$		
			EP	SP	Starved
Glycosides	α-methyl-D-glucoside	15	0.525	0.560	0.622
	β-methyl-D-galactoside	17	0.355	0.454	0.411
	β-methyl-D-glucoside	18	0.108	0.229	0.185
Monosaccharides	D-fructose	22	0.439	0.520	0.430
	D-galactose	24	0.536	0.594	0.581
	D-galacturonic acid	25	0.622	0.696	0.758
	D-gluconic acid	26	0.569	0.652	0.627
	Dihydroxy acetone	28	0.203	0.169	–
	D-mannose	30	0.540	0.581	0.639
	D-ribose	33	0.486	0.490	0.481
	D-xylose	35	0.559	0.587	0.570
	L-arabinose	36	0.387	0.467	0.375
	L-fucose	37	0.605	0.584	0.459
	L-lyxose	39	–	0.217	0.090
	L-rhamnose	40	0.529	0.585	0.534
	L-sorbose	41	0.153	0.326	–
	N-acetyl-D-galactosamine	43	0.543	0.532	0.648
	N-acetyl-D-glucosamine	44	0.511	0.530	0.432
	N-acetyl-neuramic acid	45	0.293	0.357	0.414
	N-acetyl-β-D-mannosamine	46	0.192	0.246	0.164
	α-D-glucose	48	0.502	0.514	0.435
	β-D-allose	50	0.322	0.431	0.492
Oligosaccharides	3-O-β-D-galactopyranosyl-D-arabinose	51	0.289	0.677	–
	D-melibiose	53	0.596	0.658	0.634
	D-raffinose	54	0.287	0.454	0.319
	D-trehalose	55	0.496	0.560	0.586
	Lactulose	57	0.176	0.323	0.100
	Maltose	59	0.518	0.602	0.613
	Maltotriose	60	0.528	0.606	0.647
	Sucrose	64	0.429	0.563	0.374
	α-D-lactose	66	0.514	0.519	0.478
Polysaccharides	Dextrin	67	0.376	0.430	0.337
Sugar alcohols	D-arabitol	77	0.493	0.535	0.528
	D-mannitol	78	0.516	0.600	0.609
	Dulcitol	80	–	–	0.090
	Glycerol	81	0.432	0.448	0.457
Sugar phosphates	D,L-α-glycerol-phosphate	87	0.447	0.510	0.517
	Fructose-6-phosphate	88	0.488	0.629	0.576
	Glucose-1-phosphate	89	0.576	0.643	0.721
	Glucose-6-phosphate	90	0.508	0.702	0.638
Acetic acids	Acetic acid	92	0.332	0.505	0.409
Aldehydic acids	Glyoxylic acid	93	–	0.132	0.089

Sub-class	Substrates	PM1 & PM2A	$A_{endpoint}$		
			EP	SP	Starved
Dicarboxylic acids	Bromo succinic acid	100	0.224	0.379	0.573
	D,L-malic acid	103	0.511	0.566	0.578
	Dihydroxy fumaric acid	104	0.601	0.629	0.674
	D-malic acid	105	–	–	0.067
	Fumaric acid	107	0.525	0.521	0.452
	L-malic acid	109	0.565	0.624	0.625
	Mono methyl succinate	112	0.200	0.279	0.417
	Succinic acid	117	0.416	0.571	0.556
Glycolates	Glycolic acid	119	–	0.210	0.139
Hydroxy acids	D-lactic acid methyl ester	122	0.319	0.226	0.153
	L-lactic acid	123	0.471	0.534	0.586
Keto acids	Methyl pyruvate	126	0.406	0.524	0.573
	Pyruvic acid	127	0.480	0.603	0.672
Propionates	Propionic acid	131	0.127	0.367	0.282
Sugar acids	D-glucuronic acid	134	0.578	0.676	0.729
	D-saccharic acid	135	0.420	0.628	0.606
	L-galactonic acid-γ-lactone	137	–	–	0.283
	Mucic acid	138	0.515	0.668	0.680
	β-methyl-D-glucuronic acid	139	0.411	0.480	0.309
Nucleosides	2-deoxy adenosine	147	0.636	0.660	0.675
	Adenosine	148	0.594	0.600	0.673
	Inosine	149	0.660	0.624	0.716
	Thymidine	150	0.575	0.614	0.730
	Uridine	151	0.586	0.635	0.685
Amino acids	D-alanine	156	0.508	0.513	0.486
	Glycyl-L-aspartic acid	162	0.229	0.519	0.431
	Glycyl-L-glutamic acid	163	0.124	0.130	0.200
	Glycyl-L-proline	164	0.258	0.425	0.265
	L-alanine	166	0.534	0.573	0.548
	L-alanyl-glycine	167	0.495	0.614	0.548
	L-asparagine	169	–	0.575	0.612
	L-aspartic acid	170	0.545	0.622	0.558
	L-glutamine	172	0.178	0.119	0.163
	L-proline	181	–	0.238	0.076
	L-serine	183	0.512	0.613	0.651
Scleroproteins	L-alaninamide	189	0.128	0.158	0.144

Appendix 18 λ for substrate use by NCTC12900 *luxS*$^{-}$ harvested during exponential phase (EP), stationary phase (SP) and starved state. Dash (–) indicates substrates tested but not utilised. Results are the average of duplicates.

Sub-class	Substrates	PM1 & PM2A	λ (hr)		
			EP	SP	Starved
Glycosides	α-methyl-D-glucoside	15	3.5	2.5	5.3
	β-methyl-D-galactoside	17	1.9	1.6	5.8
	β-methyl-D-glucoside	18	12.8	12.3	16.5
Monosaccharides	D-fructose	22	1.9	1.6	4.5
	D-galactose	24	1.5	2.1	4.8
	D-galacturonic acid	25	2.4	2.0	5.0
	D-gluconic acid	26	2.1	1.9	4.5
	Dihydroxy acetone	28	12.8	18.5	–
	D-mannose	30	1.8	1.8	4.5
	D-ribose	33	2.3	2.9	7.5
	D-xylose	35	1.9	2.5	5.9
	L-arabinose	36	2.0	2.1	5.9
	L-fucose	37	2.0	2.4	5.5
	L-lyxose	39	–	7.3	14.8
	L-rhamnose	40	4.0	2.0	6.1
	L-sorbose	41	18.6	16.5	–
	N-acetyl-D-galactosamine	43	2.4	2.3	7.1
	N-acetyl-D-glucosamine	44	2.0	1.6	4.3
	N-acetyl-neuramic acid	45	2.3	2.0	5.6
	N-acetyl-β-D-mannosamine	46	11.9	12.0	4.4
	α-D-glucose	48	1.9	1.8	4.1
	β-D-allose	50	5.4	7.1	9.0
Oligosaccharides	3-O-β-D-galactopyranosyl-D-arabinose	51	14.0	3.9	–
	D-melibiose	53	2.6	3.1	6.1
	D-raffinose	54	12.3	12.5	16.6
	D-trehalose	55	1.8	1.6	4.5
	Lactulose	57	17.8	14.1	22.3
	Maltose	59	1.8	1.8	4.9
	Maltotriose	60	1.9	1.8	4.5
	Sucrose	64	2.3	2.3	5.0
	α-D-lactose	66	1.9	1.8	4.9
Polysaccharides	Dextrin	67	1.4	1.4	4.9
Sugar alcohols	D-arabitol	77	1.5	1.6	5.4
	D-mannitol	78	1.8	1.6	4.5
	Dulcitol	80	–	–	22.3
	Glycerol	81	1.5	1.5	5.3
Sugar phosphates	D,L-α-glycerol-phosphate	87	4.5	1.5	4.8
	Fructose-6-phosphate	88	3.0	2.0	5.4
	Glucose-1-phosphate	89	1.6	1.5	5.0
	Glucose-6-phosphate	90	3.0	1.9	4.3
Acetic acids	Acetic acid	92	3.0	2.9	5.5
Aldehydic acids	Glyoxylic acid	93	–	8.3	10.6

Sub-class	Substrates	PM1 & PM2A	λ (hr)		
			EP	SP	Starved
Dicarboxylic acids	Bromo succinic acid	100	2.0	2.3	5.3
	D,L-malic acid	103	2.0	1.9	5.4
	Dihydroxy fumaric acid	104	1.8	1.4	8.0
	D-malic acid	105	–	–	20.8
	Fumaric acid	107	1.9	2.0	5.5
	L-malic acid	109	1.9	2.0	5.1
	Mono methyl succinate	112	1.5	1.9	4.9
	Succinic acid	117	1.5	1.4	5.0
Glycolates	Glycolic acid	119	–	7.0	8.9
Hydroxy acids	D-lactic acid methyl ester	122	1.6	1.9	5.6
	L-lactic acid	123	1.5	1.5	4.8
Keto acids	Methyl pyruvate	126	2.3	2.1	5.1
	Pyruvic acid	127	2.0	1.8	4.9
Propionates	Propionic acid	131	7.0	7.6	7.8
Sugar acids	D-glucuronic acid	134	2.1	1.9	4.8
	D-saccharic acid	135	1.8	2.0	5.3
	L-galactonic acid-γ-lactone	137	–	–	17.4
	Mucic acid	138	1.8	2.1	5.3
	β-methyl-D-glucuronic acid	139	5.0	8.0	15.8
Nucleosides	2-deoxy adenosine	147	1.3	1.5	5.1
	Adenosine	148	1.4	1.4	4.6
	Inosine	149	1.6	1.6	5.4
	Thymidine	150	1.9	1.6	5.9
	Uridine	151	1.9	1.6	8.0
Amino acids	D-alanine	156	1.5	2.0	6.0
	Glycyl-L-aspartic acid	162	3.8	1.8	5.1
	Glycyl-L-glutamic acid	163	1.8	2.1	5.3
	Glycyl-L-proline	164	2.3	2.4	6.0
	L-alanine	166	1.8	1.9	5.5
	L-alanyl-glycine	167	1.6	1.8	5.3
	L-asparagine	169	–	2.4	5.5
	L-aspartic acid	170	1.9	2.1	5.3
	L-glutamine	172	8.9	18.0	9.5
	L-proline	181	–	10.0	5.3
	L-serine	183	1.6	1.6	5.0
Scleroproteins	L-alaninamide	189	11.0	16.8	8.4

Appendix 19 μ_{exp} for substrate use by NCTC12900 *luxS*$^{-}$ harvested during exponential phase (EP), stationary phase (SP) and starved state. Dash (–) indicates substrates tested but not utilised. Results are the average of duplicates.

Sub-class	Substrates	PM1 & PM2A	μ_{exp} ($A_{activity}$/hr)		
			EP	SP	Starved
Glycosides	α-methyl-D-glucoside	15	0.045	0.045	0.052
	β-methyl-D-galactoside	17	0.033	0.036	0.051
	β-methyl-D-glucoside	18	0.008	0.019	0.026
Monosaccharides	D-fructose	22	0.045	0.042	0.034
	D-galactose	24	0.043	0.045	0.048
	D-galacturonic acid	25	0.089	0.086	0.108
	D-gluconic acid	26	0.090	0.068	0.091
	Dihydroxy acetone	28	0.017	0.015	–
	D-mannose	30	0.047	0.048	0.057
	D-ribose	33	0.055	0.054	0.050
	D-xylose	35	0.054	0.048	0.055
	L-arabinose	36	0.035	0.038	0.023
	L-fucose	37	0.045	0.048	0.049
	L-lyxose	39	–	0.012	0.008
	L-rhamnose	40	0.037	0.038	0.039
	L-sorbose	41	0.032	0.058	–
	N-acetyl-D-galactosamine	43	0.045	0.041	0.058
	N-acetyl-D-glucosamine	44	0.029	0.030	0.032
	N-acetyl-neuramic acid	45	0.035	0.037	0.038
	N-acetyl-β-D-mannosamine	46	0.012	0.017	0.018
	α-D-glucose	48	0.032	0.032	0.028
	β-D-allose	50	0.026	0.041	0.045
Oligosaccharides	3-O-β-D-galactopyranosyl-D-arabinose	51	0.022	0.058	–
	D-melibiose	53	0.057	0.071	0.066
	D-raffinose	54	0.028	0.060	0.032
	D-trehalose	55	0.045	0.054	0.061
	Lactulose	57	0.038	0.040	0.032
	Maltose	59	0.048	0.057	0.058
	Maltotriose	60	0.046	0.060	0.063
	Sucrose	64	0.031	0.048	0.027
	α-D-lactose	66	0.051	0.050	0.038
Polysaccharides	Dextrin	67	0.041	0.025	0.035
Sugar alcohols	D-arabitol	77	0.037	0.042	0.048
	D-mannitol	78	0.048	0.067	0.058
	Dulcitol	80	–	–	0.025
	Glycerol	81	0.038	0.033	0.046
Sugar phosphates	D,L-α-glycerol-phosphate	87	0.052	0.043	0.054
	Fructose-6-phosphate	88	0.081	0.078	0.074
	Glucose-1-phosphate	89	0.085	0.077	0.132
	Glucose-6-phosphate	90	0.103	0.111	0.076
Acetic acids	Acetic acid	92	0.018	0.028	0.031
Aldehydic acids	Glyoxylic acid	93	–	0.022	0.011

Sub-class	Substrates	PM1 & PM2A	μ_{exp} ($A_{activity}$/hr)		
			EP	SP	Starved
Dicarboxylic acids	Bromo succinic acid	100	0.028	0.032	0.036
	D,L-malic acid	103	0.030	0.031	0.036
	Dihydroxy fumaric acid	104	0.042	0.040	0.058
	D-malic acid	105	–	–	0.011
	Fumaric acid	107	0.029	0.030	0.034
	L-malic acid	109	0.031	0.041	0.041
	Mono methyl succinate	112	0.035	0.045	0.043
	Succinic acid	117	0.036	0.032	0.036
Glycolates	Glycolic acid	119	–	0.028	0.014
Hydroxy acids	D-lactic acid methyl ester	122	0.032	0.037	0.037
	L-lactic acid	123	0.031	0.035	0.044
Keto acids	Methyl pyruvate	126	0.054	0.042	0.045
	Pyruvic acid	127	0.047	0.058	0.069
Propionates	Propionic acid	131	0.012	0.030	0.023
Sugar acids	D-glucuronic acid	134	0.088	0.066	0.105
	D-saccharic acid	135	0.063	0.058	0.067
	L-galactonic acid-γ-lactone	137	–	–	0.056
	Mucic acid	138	0.039	0.055	0.059
	β-methyl-D-glucuronic acid	139	0.031	0.040	0.038
Nucleosides	2-deoxy adenosine	147	0.072	0.071	0.076
	Adenosine	148	0.061	0.069	0.070
	Inosine	149	0.057	0.068	0.074
	Thymidine	150	0.053	0.060	0.066
	Uridine	151	0.046	0.063	0.077
Amino acids	D-alanine	156	0.025	0.025	0.028
	Glycyl-L-aspartic acid	162	0.020	0.047	0.031
	Glycyl-L-glutamic acid	163	0.046	0.021	0.038
	Glycyl-L-proline	164	0.040	0.038	0.039
	L-alanine	166	0.026	0.029	0.032
	L-alanyl-glycine	167	0.025	0.031	0.034
	L-asparagine	169	–	0.030	0.039
	L-aspartic acid	170	0.032	0.036	0.038
	L-glutamine	172	0.015	0.015	0.008
	L-proline	181	–	0.042	0.007
	L-serine	183	0.030	0.039	0.045
Scleroproteins	L-alaninamide	189	0.016	0.009	0.012